

The University of Nottingham

UNITED KINGDOM · CHINA · MALAYSIA

A Comparison Between Cyclin D1- and Cyclin D2-Expressing Myeloma Cell Lines in Terms of DNA Damage Response, Apoptosis Induction and Proteomic Profiling

A Thesis Submitted to the University of Nottingham, United Kingdom for the MD Degree

August 2022

Dr Firas Al-Kaisi

MBChB MSc FRCPath

Abstract

Multiple myeloma is a haematological malignancy with significant molecular heterogeneity. This heterogeneity reflects on the clinical side causing myeloma to be a disease with huge variability in clinical outcomes. Almost all myelomas are initiated from two mutually exclusive molecular events that arise during the premalignant MGUS (Monoclonal Gammopathy of Uncertain Significance) stage. These events involve either an immunoglobulin heavy chain translocation or a triploidy of an odd-numbered chromosome. The first group of events causes the upregulation of either cyclin D1 or cyclin D2. The type of translocation has been shown to have an impact on the prognosis such that the translocations causing a cyclin D2 upregulation have been implicated in an inferior prognosis. It is this group of initiating events that is the focus of this thesis, and our aim was to investigate if there was a differential response between cyclin D1- and cyclin D2- expressing myeloma cell lines following exposure to different stresses.

Ionising radiation (IR) was used to induce DNA damage that was compared between the myeloma cell lines. The effect of combining DNA damage with proteasome inhibition was also assessed. To examine the impact of the cyclin D-type on apoptosis induction, the BCL-2 inhibitor venetoclax and the MCL-1 inhibitor S63845 were used as single agents and in combination. The viability and targeted protein expression were analysed prior to full proteomic analysis by mass spectrometry.

We have shown the downregulation of cyclin D1 rather than cyclin D2 in response to DNA damage. Most of the DNA damage/DNA damage response happened at the earlier time points after exposure to irradiation and recovered to non-significant levels

with ongoing incubation. We have shown that there was no significant impact of the cyclin D-type on the response to proteasome inhibition as a single agent or in combination with IR. There was also no effect when a temporal variation of this combination was tried. The myeloma cell lines used in the project showed more sensitivity to MCL-1 than BCL-2 inhibition. The dual inhibition of both of these antiapoptotic proteins caused a significant synergistic apoptotic response that was generally associated with cyclin D1 and cyclin D2 downregulation. There was no clear differential impact of the cyclin D-type on apoptosis induction however the cyclin D2 cell lines used in this project appeared more sensitive to the dual BCL-2/MCL-1 inhibition. Finally, the proteomic analysis identified the inhibition of several pathways that are associated with protein translation and recycling. Although this project highlighted several interesting results, we were unable to identify a differential response that could be attributed to the underlying cyclin D type.

Acknowledgement

My gratitude and heartfelt thanks go to my supervisor (***Dr Claire Seedhouse***). Thank you for the opportunity to work in your group and under your supervision which I thoroughly enjoyed. Thank you for your ongoing guidance throughout this project and for supporting me during the height of the Covid pandemic when the clinical workload was immense. I also thank you for tolerating me during the protracted write-up phase of this project.

My thanks and gratitude also go to my clinical supervisor during this post (***Dr Dean Smith***) whom I thoroughly miss working with. Thank you for this opportunity and your ongoing guidance and kind support. The myeloma fellow post under your supervision was the highlight of my specialist training.

The same goes for ***Dr Cathy Williams*** who kindly supported and guided me during the initial phases of this project. It has been a great privilege working with you.

I have thoroughly enjoyed working with ***Dr Martin Grundy***. His calm and scientific approach speaks volumes about his dedication to his academic career. Thank you for showing me how to perform most of the lab assays in this project. You have always been there and answered my questions the silly and the meaningful with generous resolve.

Many thanks to ***Prof Stewart Martin*** for his kind guidance, support and for facilitating the use X-ray irradiation cabinet for the ionising radiation experiments. Many thanks

to ***Dr Radhika Ayippa*** and ***Richa Vasan*** for their time and help with the cell lines irradiation.

Thanks to ***Dr Graham Bailey*** for his support during the lifetime of this project. I will never forget your kindness and compassion during that tough time when I had to go to the hospital due to an accident in the lab. I sincerely miss working with you.

Many thanks to ***Dr Hayaa Alhuthali*** for her help and support during the lab work period. I wish her all the best in her future endeavours.

I would like to express my gratitude to ***Dr Amanda Miles*** (Nottingham Trent University). ***Dr Miles*** not only did the proteomics experiment in her lab but also provided altruistic support explaining the complex nature of data analysis, inviting us to her lab during the experimental work and providing very thorough answers to our questions. Many thanks to the ***Biosciences Department*** at ***Nottingham Trent University*** for facilitating the use of the Ingenuity Pathway Analysis software for the proteomics analysis.

I would like to express my deepest thanks and sincere gratitude to my wife (***Dr Zahraa Al-Ahmady***). Thank you for supporting me throughout the long life of this project. You looked after me at my lowest points, inspired and motivated me to finish this work and was always there for me when I needed help. This project would not have concluded without your loving care and support.

The same goes for my son ***Ahmed***. You have tolerated my unavailability due to the long hours I spent on this work like a champion. I hope I will now have more free time for you and your mother.

My everlasting gratitude goes to my parents ***(Prof Abdulhassan Al-Kaisi*** and ***Prof Basama Abbas***). Being raised by two hardcore academics meant that I was exposed to academia as far back as my memory goes. It also meant that following a scientific/academic path was always part of the plan. Thank you for your support during this project and the constant reminders to finish my writing!

Table of Contents

Chapter 1: Introduction and Review of Literature 1
1.1 Epidemiology of Multiple Myeloma 2
1.2 Myeloma Pathogenesis 3
1.2.1 Myeloma Initiating Events 6
1.2.2 Secondary Events 13
1.2.3 The Bone Marrow Microenvironment 25
1.2.4 Cell Cycle and DNA Damage Response Deregulation 27
1.2.4.1 DNA damage response in multiple myeloma 32
1.2.5 The Importance of the Cyclin D-type in Myeloma 34
1.2.5.1 Roles of cyclin D1 34
1.2.6 Apoptosis Derangement in Myeloma 35
1.3 Plasma Cell Dyscrasias from the Clinical Perspective 38
1.3.1 MGUS (Monoclonal Gammopathy of Uncertain Significance) 39
1.3.2 Multiple Myeloma Diagnostic Pathway 40
1.3.3 Management of Multiple Myeloma 42
1.4 The Rationale and the Aim of the Project 51
Chapter 2: Materials and Methods 54
2.1 Cell Culture 54
2.1.1 Cell Lines 54
2.1.2 Culture Method 54
2.1.3 Cell Lines Mycoplasma Testing 55
2.1.4 Cell lines verification 55
2.1.5 Cell Counting Using the Trypan Blue Exclusion Method 56
2.1.6 DNA Extraction and Cell Line Verification Testing 56
2.1.7 Primary Samples 58
2.2 Cell Lines Irradiation 59
2.3 Neutral Comet Assay 60
2.3.1 Comet Assay Principles 60
2.3.1.1 Application of comet assay in myeloma 61
2.3.2 Comet Slides Preparation 62
2.3.3 Comet Slides Analysis 63
2.4 γH2A.X Phosphorylation by Flow Cytometry 64

2.4.1 γH2A.X Phosphorylation principles 64
2.4.2 γH2A.X phosphorylation measurement by flow cytometry 65
2.5 Cytotoxic Molecules 66
2.6 Assessment of Synergy 66
2.7 Western Blotting 67
2.7.1 Preparation of the Lysis Buffer 67
2.7.2 Preparation of the Lamellae Buffer 67
2.7.3 Preparation of TBS-T 68
2.7.4 Preparing the Lysates 68
2.7.5 Determination of the Protein Concentration and Preparation of Aliquots for Gel Electrophoresis 68
2.7.6 Gel Electrophoresis and Protein Transfer 69
2.7.7 Probing with Primary and Secondary Antibodies 69
2.7.8 Membrane Development and Band Detection 70
2.7.9 Western Blot Results Data Analysis 71
2.8 Annexin V Binding 71
2.8.1 Annexin V Binding Assay Principles 71
2.8.2 Annexin V Assay 71
2.9 Alamar Blue Assay 72
2.9.1 The Alamar Blue Principles 72
2.9.2 The Alamar Blue Assay 73
2.10 Cytochrome c Release Assay 73
2.10.1 Cytochrome c Release Assay Principles 73
2.10.2 Cytochrome c Release Assay using Flow Cytometry 73
2.11 Mass Spectrometry 74
2.12 Statistical Analysis and Software 75
Chapter 3: DNA Damage Response Assessment in Cyclin D1- and Cyclin D2-Expressing Myeloma Cell Lines 78
3.1 Introduction 78
3.1.1 The Use of IR to Induce DNA Damage 78
3.2 The Aim of this Chapter 80
3.3 Results 80
3.3.1 IR Dose Optimisation 80
3.3.1.1 A pilot comparison between 5Gy and 10 Gy IR showed no difference in terms of the comet assay 80
3.3.2 Measurement of DNA Damage Following IR Using the Comet Assay 81

3.3.2.1 Cyclin D1-expressing cell lines (U266 and MOLP-8) showed a significant increase in tail moments immediately after IR 82
3.3.2.2 Cyclin D2-expressing cell lines (JJN3 and OPM-2) showed a significant increase in tail moments immediately after IR 85
3.3.3 γH2A.X Phosphorylation Results 86
3.3.3.1 Cyclin D1-expressing cell lines (U266, MOLP-8, KMS12-BM) showed a significant increase in γH2A.X phosphorylation after 4 h of IR. 86
3.3.3.2 Cyclin D2-expressing cell lines (JJN-3, OPM-2 and MM1s) showed a significant increase in γH2A.X phosphorylation 0 h and 4 h after IR 87
3.4 Discussion 88
Chapter 4: A Comparison of the Response to Proteasome Inhibition and DNA Damage between Cyclin D1- and Cyclin D2-Expressing Cell Lines 97
4.1 Introduction 97
4.1.1 The Proteasome Inhibitor Bortezomib in Multiple Myeloma 97
4.1.2 Mechanisms of Action of Bortezomib in Myeloma and Other Cancers 98
4.1.2.1 Unfolded protein response and NF-κB inhibition 98
4.1.2.2 The effect of bortezomib on apoptotic proteins 99
4.1.2.3 The effect of bortezomib on cyclins 99
4.1.3 The Rationale of Experimental Work and the Experimental Plan 100
4.2 The Aim of this Chapter 101
4.3 Results 102
4.3.1 Myeloma Cells Viability Assessment by Annexin V to IR and Bortezomib 102
4.3.1.1 Myeloma cell lines are sensitive to nanomolar bortezomib concentrations 102
4.3.1.2 IR had minimal impact on viability in 4 out of 6 myeloma cell lines 104
4.3.1.3 The combination of IR and bortezomib had a heterogenous effect on viability 105
4.3.2 The Effects of IR and Bortezomib on Cyclins D1 and D2 Expression 106
4.3.2.1 IR caused cyclin D1 rather than cyclin D2 downregulation 106
4.3.2.2 Bortezomib caused cyclin D downregulation in 2 out of the 6 myeloma cell lines 106
4.3.2.3 The combination of IR and bortezomib had a heterogenous effect on cyclin D expression 107
4.4 Discussion 107
Chapter 5: Assessment of Response to Apoptosis Induction via the Intrinsic Pathway in Cyclin D1- and Cyclin D2-expressing Myeloma Cell Lines 117
5.1 Introduction 117
5.1.1 The specific BCL-2 and MCL-1 Inhibitors Used 119
5.1.1.1 Venetoclax (ABT-199) 119

5.1.1.2 S63845 120
5.2 The Aim of this Chapter 120
5.3 Results 122
5.3.1 The Combination of MCL-1 and BCL-2 Inhibition was Synergistic in 5 out of 6 Myeloma Cell Lines 122
5.3.2 Annexin V Binding Confirms the Synergy from MCL-1/BCL-2 Inhibition is due to Apoptosis 125
5.3.3 Cytochrome c Release Assay was Predictive of Apoptosis in Response to BCL-2 and MCL-1 Inhibition and Correlated with the Annexin V and Alamar Blue Results 127
5.3.4 The Cytochrome c Release Assay was Suitable for Apoptosis Prediction in Primary Myeloma Patient Samples 128
5.3.5 Cyclin D, MCL-1, and BCL-2 Expression by Western Blotting 129
5.3.5.1 Western blotting showed no significant changes in protein expression in response to single-agent treatment. 130
5.3.5.2 Down-regulation of Cyclin D was associated with synergy to MCL-1 and BCL-2 inhibition 130
5.4 Discussion 131
Chapter 6: Proteomic Analysis of Myeloma Cell Lines Following Apoptosis Induction 140
6.1 Introduction 140
6.1.1 Mass Spectrometry and Data Analysis 141
6.2 The Aim of this Chapter 143
6.3 Results and Discussion 144
6.3.1 Individual Cell Line Analysis 144
6.3.1.1 The top five canonical pathways are implicated in the regulation of RNA translation 146
6.3.1.2 Causal and upstream pathway analysis 161
6.3.1.2.1 Upstream pathway analysis 161
6.3.1.2.2 Causal Pathways Analysis 169
6.3.2 Comparison Analysis 175
6.4 Conclusion 180
Chapter 7: Discussion and Conclusions 185
7.1 The Background and Rationale for this Experimental Work 185
7.2 Cyclins D1 and D2 and DNA Damage 189
7.3 Apoptosis Induction Through DNA Damage and Proteasome Inhibition 190
7.4 Apoptosis Induction via the Intrinsic Pathway 192
7.5 Assessing the Proteomic Profile of Myeloma Cell Lines 193
7.6 Conclusions and Future Work 195

Chapter 8: Appendix 199

8.1 Representative flow plots of Annexin V assay for KMS12-BM and JJN-3 cell lines after exposure to venetoclax and S63845 as single agents and in combinations 199

8.2 Discovering a predictive biomarker of venetoclax sensitivity and resistance in Multiple Myeloma-Short summary from C Ogden MSc Thesis done using fold change analysis of mass spectrometry data (295) 200

Chapter 9: References 204

List of Figures

Figure 1.1: The normal developmental journey of the B cell.. 4
Figure 1.2: The developmental spectrum of plasma cell dyscrasias..... 8
Figure 1.3: The interaction of primary events signified by hyperdiploidy and cyclin D translocations and secondary hits conspires to derive the pathogenesis of plasma cell myelom 12
Figure 1.4: Chromosome 1. 14
Figure 1.5 NF-κB pathway can be activated via a classical route through the tumour necrosis factor receptor or via an alternative pathway through CD40. 21
Figure 1.6: the interaction between MCL-1, BCL-2 the proapoptotic BIM and MCL-1 and BCL-2 inhibitors. 37
Figure 3.1: A pilot assay comparison of the tail moments of U266 cell line and JJN-3 cell line after exposure to 5Gy and 10Gy IR.. 81
Figure 3.2: Representative example of the JJN-3 comets as viewed under fluorescent microscope 82
Figure 3.3: Comet assay tail moments of cyclin D1 and cyclin D2 myeloma cell lines measured immediately, after 4 h and after 24 h of 10 Gy IR dose 83
Figure 3.4: The Trypan blue cell count after irradiation with 10 Gy at 0, 4 h and 24 h incubation 84
Figure 3.5: The percentage of γH2A.X phosphorylation by flow cytometry using a FITC conjugated Ab for the six human myeloma cell lines was measured immediately, after 4 h and after 24 h of irradiation with 10 Gy dose. 87
Figure 4.1: Dose-response to 24-hour treatment with bortezomib in the six myeloma cell lines as determined using the Annexin V assay 102
Figure 4.2: Viability of the myeloma cell lines as a percentage of control was assessed using Annexin V staining following IR 104
Figure 4.3: Viability of myeloma cell lines as a percentage of control was assessed using Annexin V after treatment with bortezomib in combination with IR 105
Figure 4.4: Representative individual Western blots for Cyclin D2 expression in JJN-3, OPM-2 and MM1s myeloma cell lines 4h/24h post 10Gy IR and 24h post Bortezomib treatment. . 110
Figure 4.5: Representative individual Western blots for Cyclin D1 expression in U266, KMS12-BM and MOLP-8 myeloma cell lines 4h/24h post 10Gy IR and 24h post Bortezomib treatment 110

Figure 4.6: Representative individual Western blots for Cyclin D2 expression in JJN-3, OPM-2 and MM1s myeloma cell lines following treatment with IR and Bortezomib under schedules 1 and 2 111
Figure 4.7: Representative Western blots for Cyclin D1 expression in U266, KMS12-BM and MOLP-8 myeloma cell lines following treatment with IR and Bortezomib under schedules 1 and 2 111
Figure 4.8: Densitometry analysis of the cyclin D expression in the myeloma cell lines following treatment with IR and bortezomib 112
Figure 5.1: The viability of the cyclin D1 myeloma cell lines and the cyclin D2 cell lines in response to treatment with fixed-ratio concentrations of venetoclax, S63845 and the combination of the two was assessed using the Alamar blue assay after 48 hours 124
Figure 5.2: Annexin V assay results for the 6 myeloma cell lines as percentages of the control 48 h following treatment with venetoclax, and S63845 as single agents and in combination. 126
Figure 5.3: Flow-cytometric cytochrome c measurement of the myeloma cell lines following a 4h treatment with venetoclax, S63845 and the combination of both. 128
Figure 5.4: Cytochrome c release was assessed by flow cytometry in 7 primary myeloma samples following treatment with venetoclax, S63845 and their combination for 4 hours.. 129
Figure 5.5: Representative MCL-1 and BCL-2 expression as assessed by Western blotting for Cyclin D2 cell lines (JJN-3, OPM-2 and MM1s) following treatment with venetoclax and S63845 as single agents and in combination 132
Figure 5.6: Representative MCL-1 and BCL-2 expression as assessed by Western blotting for Cyclin D1 cell lines (U266, KMS12-BM, and MOLP-8) following treatment with venetoclax and S63845 as single agents and in combination 132
Figure 5.7: Representative Cyclin D2 expression as assessed by Western blotting for Cyclin D2 cell lines (JJN-3 and OPM-2) following treatment with venetoclax and S63845 as single agents and in combination 133
Figure 5.8: Representative Cyclin D1 expression as assessed by Western blotting for Cyclin D1 cell lines (U266, KMS12-BM, and MOLP-8) following treatment with venetoclax and S63845 as single agents and in combination 133
Figure 5.9: Schematic summary of the levels of expression of cyclins D1 and D2, MCL-1 and BCL-2 in the 6 myeloma cell lines following treatment with venetoclax, S63845 and the combination of both agents 134

Figure 6.1: Schematic representation of the complex interactions between the eIF signalling and the mTOR pathway as generated by the IPA software 148
Figure 6.2: Schematic representation of the regulation of mRNA translation via eIF4 and p70S6K 151
Figure 6.3: Representative example of the BAG2 signalling pathway generated by the IPA software (U266 cell line treated with venetoclax and S63845 combination). 154
Figure 6.4: Representative example of the FAT10 signalling as generated by the IPA software (U266 cell line treated with venetoclax and S63845 combination) 157
Figure 6.5: Heat map based on hierarchical clustering of the canonical pathways in comparison analysis between all the conditions tested 177
Figure 6.6. Heat map based on hierarchical clustering of the diseases and functions in comparison analysis between all the conditions assessed 179
Figure 8.1 Representative Annexin V flow cytometry dot plots of KMS12-BM cell line treated with venetoclax, S63845 and the combination of both 199
Figure 8.2 Representative Annexin V flow cytometry dot plots of JJN-3 cell line treated with venetoclax, S63845 and the combination of both 200
Figure 8.3: Pathway analysis using Panther for KMS12-BM cell line. 202

List of Tables

Table 1.1: A summary of the main primary (initiating) and secondary genetic events in multiple myeloma. 7
Table 1.2: Secondary genetic events 18
Table 1.3: A list of different types of DNA damage together with their potential causes and the repair mechanisms. 27
Table 1.4: The diagnostic criteria of symptomatic multiple myeloma 41
Table 2.1: The human myeloma cell lines used in this project together with their cyclin D type properties, p53 status and some other features.. 57
Table 2.2 Primary samples characteristics 59
Table 2.3: A list of the primary and secondary antibodies used in this project together with the source and the concentration 70
Table 4.1: The concentrations chosen for the combination experiments with IR for each of the myeloma cell lines. Those did not result in more than a 30% drop in viability. 103
Table 5.1: A list of the venetoclax and the S63845 concentrations used for the single agent and the combination treatments 122
Table 5.2: The IC_{50} (μM) for single agent treatment with venetoclax and S63845 for each of the myeloma cell lines 123
Table 5.3: The combination index for each combination of the MCL-1 and the BCL-2 inhibitor obtained from data analysis using the Compusyn software ™ based on the Chou-Talalay method 123
Table 5.4: The concentrations (μM) of ABT-199 and S63845 used for Annexin V assay 125
Table 6.1: The concentrations (μM) of ABT-199 and S63845 used for Annexin V assay 144
Table 6.2: Tabulated summary of the significant pathway changes on individual cell lines analysis and comparison analysis following treatment with venetoclax, S63845 and their combination 145
Table 6.3: The activation pattern of EIF2 signalling across the myeloma cell lines in response to venetoclax and S63845 single agent and combination treatment 149
Table 6.4: The activation pattern of eIF4 and p70S6k across the myeloma cell lines in response to venetoclax and S63845 single agent and combination treatment 152
Table 6.5: The activation pattern of BAG2 across the myeloma cell lines in response to venetoclax and S63845 single agent and combination treatment 155

Table 6.6: The activation pattern of FAT10 across the myeloma cell lines in response to venetoclax and S63845 single agent and combination treatment 158
Table 6.7: The activation pattern of mTOR across the myeloma cell lines in response to venetoclax and S63845 single agent and combination treatment 160
Table 6.8: The activation pattern of c-myc across the myeloma cell lines in response to venetoclax and S63845 single agent and combination treatment 164
Table 6.9: The activation pattern of LARP1 across the myeloma cell lines in response to venetoclax and S63845 single agent and combination treatment 165
Table 6.10: The activation pattern of Torin-1 across the myeloma cell lines in response to venetoclax and S63845 single agent and combination treatment 167
Table 6.11: The activation pattern of 5-FU across the myeloma cell lines in response to venetoclax and S63845 single agent and combination treatment 168
Table 6.12: The activation pattern of p53 across the myeloma cell lines in response to venetoclax and S63845 single agent and combination treatment 169
Table 6.13: The activation pattern of PCGEM1 across the myeloma cell lines in response to venetoclax and S63845 single agent and combination treatment 171
Table 6.14: The activation pattern of CUL4B across the myeloma cell lines in response to venetoclax and S63845 single agent and combination treatment 172
Table 6.15: The activation pattern of PFU60 across the myeloma cell lines in response to venetoclax and S63845 single agent and combination treatment 173
Table 6.16: The activation pattern of SGI1776 across the myeloma cell lines in response to venetoclax and S63845 single agent and combination treatment 175
Table 8.1 Fold changes of myeloma cell lines 201

Covid Impact Statement

When the Covid pandemic hit the UK in March 2020, I have already finished the lab work for this project and was in process of the thesis write-up. I have also just been appointed as a haematology consultant and myeloma service lead at the Royal Derby Hospital. Under normal circumstances, the step up from a specialist trainee to a consultant is a challenge due to the steep increase in the responsibilities and workload. This challenge was further accentuated by the unprecedented pressure and the chaos imparted by the Covid pandemic. This eventually meant that any spare time that could have been used for the write-up was taken away by clinical work or by the need to wind down after a busy day at work. I have therefore had to apply for two extensions after discussion with my supervisor Dr Claire Seedhouse. This helped to ease of the pressure during that difficult period, however it extended the write-up period significantly.

Research Output

A short-term biomarker-based assay predicts apoptotic response to combined BCL-2/MCL-1 BH3 mimetic targeting in Myeloma cells.
Oral presentation. UKMF, Cavendish Conference Centre, London. Nov 2019

A short-term biomarker-based assay predicts apoptotic response to combined BCL-2/MCL-1 BH3 mimetic targeting in Myeloma cells.
Poster presentation. IMW Meeting, Sep 2019. Boston MA, USA

A same-day assay predicts apoptotic response to combined BCL-2 and MCL-1 BH3-mimetic targeting in multiple myeloma cells - Publication
Grundy, M, **Al-Kaisi, F**, Cull, J, Williams, C, Smith, D, Seedhouse, CH. A same-day assay predicts apoptotic response to combined BCL-2 and MCL-1 BH3-mimetic targeting in multiple myeloma cells. eJHaem. 2021; 2: 40– 47. https://doi.org/10.1002/jha2.133

Discovering a predictive biomarker of venetoclax sensitivity and resistance in Multiple Myeloma
Charlotte Ogden, MSc thesis. University of Nottingham, 10/8/2020

CHAPTER 1

INTRODUCTION AND REVIEW OF LITERATURE

Chapter 1: Introduction and Review of Literature

Multiple myeloma is an incurable haematological malignancy characterised by abnormal proliferation of immortalised plasma cells. It is a disease that is characterised by remarkable molecular and cytogenetic clonal and sub-clonal heterogeneity (1). This heterogeneity often manifests as significant and partially predictable variability in treatment response, rapidity of relapse and the velocity of disease progression with a direct impact on prognosis (2,3). This variability can originate, at least in part, from the initial pathogenetic primary events, the acquisition of which can predispose the evolving malignant clone to defined secondary events, which, in turn, exert their weight on the disease risk and prognosis (4).

The first account of multiple myeloma in the literature was probably in 1844. Samuel Soly described 'mollities ossium' in two cases in the Medico-Chirugical Transactions (5). He reported two cases with progressive skeletal deformities, broken and painful bones, mood changes and early deaths. In one of the patients, he described her thigh bone as 'divided, and in this, the disease had made such progress in the centre of it, that the whole osseous matter had been removed. Following the unsurprising failures of interventions such as rhubarb, quinine, and therapeutic venesections, melphalan was first used for the treatment of myeloma around 60 years ago. The first UK MRC trial (Myeloma I) found no difference between oral melphalan and oral cyclophosphamide (6). However, when the timeline of myeloma treatment development is examined, one can find a major expansion of the available therapeutics in recent history (7,8). Nevertheless, despite this remarkable progress,

myeloma remains an incurable disease and relapse is almost always inevitable. Moreover, research has shown that the progression-free survival (PFS) and the time to the next treatment get progressively shorter after each line of therapy, a likely reflection of the increasing genetic complexity of the disease and the acquisition of further sub-clonal hits (9).

1.1 Epidemiology of Multiple Myeloma

Multiple myeloma is the second most common haematological cancer and accounts for 2% of all new cancers. The number of new myeloma cases in the United Kingdom is estimated to be around 5,800 per annum. Myeloma is mainly a disease of the elderly with a median age at diagnosis of 74 years. There is a slight male preponderance (1.5:1). The incidence in African Americans is twice that of white Caucasians, but lower in people of Hispanic and Asian racial backgrounds (10). The incidence of multiple myeloma is higher in developed countries, reflecting probably the presence of better diagnostics. There is a degree of variability in the survival data, however there is no doubt that the median overall survival (OS) has increased significantly over time (10,11). Disease characteristics and patient-specific factors exert a significant effect in relation to survival. The median OS can range from 5 years in those over 75 years of age to more than 8 years in the fitter, transplant-eligible patients. As briefly alluded to above and will be explained in more detail below, several factors can partially predict the likely survival, such as those related to disease burden, cytogenetics and the sensitivity to therapy (12,13). It is important to mention that survival data, as one might expect, have the inherent downside of reflecting outcomes 5-10 years in the past and hence would not necessarily reflect the impact of newer therapeutics such

as monoclonal antibodies and other novel therapies such as antibody-drug conjugates, bispecific T-cell engagers, and CAR-T cells therapy.

1.2 Myeloma Pathogenesis

Myeloma propagating cells are essentially malignant plasma cells that have become immortalised, retained the molecular capability of cell cycling and are still able, in almost all cases, to synthesise, albeit dysfunctional, immunoglobulins. Those monoclonal, rather than their normal polyclonal counterparts, immunoglobulins (also known as paraproteins) serve no immune function. In addition, they mediate some of the pathogenic mechanisms that cause myeloma morbidity (14).

Before delving into the molecular pathogenesis of the myeloma cells, it is important to have a look at the process of the normal development of B cells. Not only does this lend to a better understanding of the disease itself but also as this process is fascinating in its own accord (Figure 1.1).

In essence, the developmental journey of B cells from a virgin B cell to a terminally differentiated plasma cell aims at creating a diverse repertoire of functional B cell receptors that can recognise and mount an immune response to a variety of antigens (15,16). This recognition power must tally with the expected diversity of antigens that can be potentially encountered by the immune system. Hence one can imagine the vastness of this repertoire. It is the ability to rearrange parts of the germinal DNA throughout this process that creates such diversity (17). The first step of B cell development occurs in the bone marrow (14).

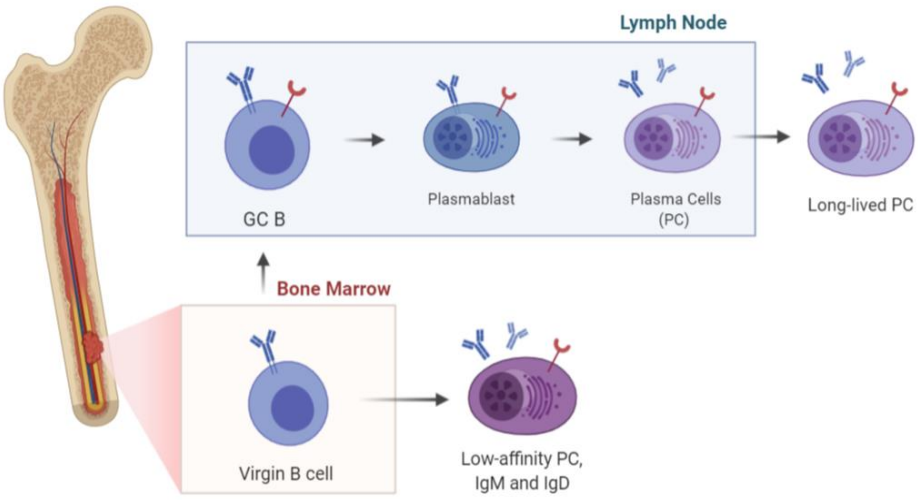


Figure 1.1: The normal developmental journey of the B cell. The B cell development starts in the bone marrow with VDJ rearrangement. Cells with a functional B cell receptor will leave the bone marrow and become low-affinity plasma cells. Upon encounter with their corresponding antigens, further development of B cells happens within the germinal centre (GC) where B cells undergo somatic hypermutation (SHM) to increase the antibody specificity. Class switch recombination (CSR) allows the production of different antibody isotypes. The long-lived plasma cells leave the lymph node and find their way into specialised niches in the bone marrow. Adapted from (14)**.**

The rearrangement of the VH (variable), DH (diversity) and JH (joining) heavy chain segments (located on Chromosome 14, 14q32) and the VL (variable) and the JL (joining) light chains segments (located on Chromosome 2p12 and Chromosome 22q11) is through regulated DNA double-strand breaks and re-joining these breaks. The heavy chain recombination happens first, in particular the rearrangement of the DH and the JH segments. If this is successful, this will be followed by a recombination step with the variable region (VH). The development of the light chain part of the B cell receptor takes place after that with a recombination process involving the kappa light chain variable (VL) and joining (VJ) on chromosome 2. Failure of this part results in the same process happening within the lambda light chain VH and VJ located on chromosome 22 with deletion of the redundant kappa light chain. This may explain

that kappa is almost one-third in excess of the lambda immunoglobulins (65% vs 35%) (15,17). When this procedure concludes with the production of a functional VDJ rearrangement and the assembly of the product on the surface of the B cell as the B cell receptor in association with CD79, a resultant IgM^+ virgin B cell departs from the bone marrow (14,16). These low-affinity B cells may encounter their kindred antigen and a whole new process of B cell development ensues but in the germinal centres of secondary lymphoid organs this time. Within the germinal centre, the activated B cells undergo a process called somatic hypermutation (SHM) and class switch recombination (CSR) (14). When activated B cells undergo SHM, intentional point mutations are created in the hypervariable regions of the B cell receptor while B cells proliferate, and high-affinity B cells are selected for survival. A further step in the B cell development in the germinal centre is the CSR. Following this step, the functionality of the B cell is increased further as it acquires the ability to secrete different antibody isotypes (IgA and IgG). This very last step is thought to be the culprit behind the majority of the genetic events that eventually cause the development of the immortalised monoclonal plasma cell. It follows that most myelomas are IgG or IgA, and pre-switched myelomas (IgD and IgM) are rare (15). SHM and CSR are possible through the generation, via activation-induced deaminase, and repair of dsDNA breaks. The hypermutated and switched plasma cell leaves the secondary immune organ's germinal centre and finds its way to the bone marrow. Here they reside within special locations and interact with the bone marrow microenvironment ready to produce specific antibodies when stimulated by the same antigenic process (14). The same process that provides the immune system with the diversity to repel foreign antigens, is the cause of an inherent weakness that can produce an oncogenic

potential. This happens when the dsDNA breaks are not repaired locally and instead the loose ends are fused with other dsDNA breaks in the genome. The danger of these errors is when they result in a survival advantage. Nevertheless, taking into account the high frequency of these 'error-prone' mechanisms and the comparable small risk of malignant transformation, it is no wonder that these mechanisms gained evolutionary survival advantage due to their benefit to the immune system.

1.2.1 Myeloma Initiating Events

As mentioned above, the normal processes that result in the ability of the immune system to deal with foreign antigenic diversity are the same creating an infrequent but important vulnerability. The main genetic events that underpin myeloma pathogenesis are summarised in Table 1.1.

Two main initiating events lead to the development of the immortalised myeloma propagating cell. Those clonal events are mutually exclusive in 90% of myelomas (18). Acquisition of one of those initiating events or the other can pre-determine which secondary genetic event the malignant clone will be more susceptible to acquire (4). It also follows that those primary events in the myeloma pathogenesis are consistent within the clone while the secondary genetic events that may be acquired later can be subclonal and hence may not be present among all the branching subclones (1,4). Moreover, the acquisition of the initiating events would not necessitate malignant transformation. Indeed, those initiating events are found in the premalignant MGUS phase and the majority of patients with this condition do not actually transform to develop a plasma cell dyscrasia (Figure 1.2) (19).

Table 1.1: A summary of the main primary (initiating) and secondary genetic events in multiple myeloma. Chromosomal translocation and trisomies of odd-numbered chromosomes lead to the upregulation of a cyclin D but are not sufficient on their own to derive the full malignant transformation and second hits are required. The progression from the pre-malignant and asymptomatic stages to the symptomatic stage involves the accumulation of more hits in one or more subclones and the expansion of those subclones. Adapted from (14).

Primary Genetic Events	
Chromosomal Translocation	**Hyperdiploides**
t(4;14): MMSET/FGFR3, cyclin D2	Trisomies of chromosomes
t(11;14): cyclin D1	3,5,7,9,11,13,15,19,21
t(14;16): MAF, cyclin D2	(cyclin D1 and D2 upregulation)
t(14;20): MAFB, cyclin D2	
t(6;14): cyclin D3	
13q del	
Secondary genetic events	
Chromosomal Gains/deletions and CNVs	**Epigenetics**
1q Gain/Amplification	DNA methylation
1p deletion	Histone acetylation
17p deletion	miRNA changes
c-myc	
11q gain	
16q del	
14q del	
8q gain	
12p gain	
Mutations	**Bone marrow microenvironment changes**
MAPK (***NRAS, KRAS, BRAF***)	
NF-κB (***TRAF3, CYLD, LTB***)	Osteoclast activation
DNA Damage (***ATM, ATR, p53***)	T regs
RNA metabolism (***FAM46C, DIS3***)	NK/cytotoxic T cells inertia
Plasma cell differentiation (*PRDM1, IRF4)*	VEGF/IL-6/RANKL

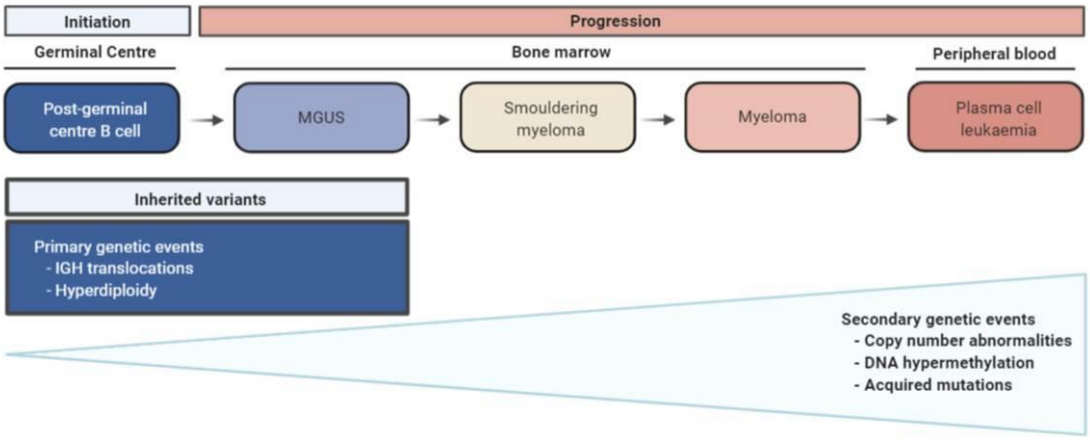


Figure 1.2: The developmental spectrum of plasma cell dyscrasias. The post germinal B cells become immortalised after acquiring initiating (primary) events such as trisomies and chromosomal translocation. It is the expansion of the abnormal clone and the acquisition of more (secondary) events over time in addition to the interaction with the bone marrow microenvironment that cause the progression into symptomatic myeloma. Plasma cell leukaemia is an aggressive plasma cell dyscrasia where the plasma cells are no longer adherent to the bone marrow and can be found in the peripheral blood. Adapted from (20)**.**

The two main myeloma initiating events are,

a. **Chromosomal translocations** mostly happen during the CSR phase of B cell development and they involve placing an oncogene next to the immunoglobulin heavy chain promoter (21). The collective outcome of this process is cyclin derangement leading, in eventuality, to the disruption of the physiological cell cycle arrest in normal plasma cells (22). The common genetic translocations are listed in Table 1.1.

t(11;14) is the most common translocation in myeloma and its frequency is even higher in AL amyloidosis (a plasma cell dyscrasia characterised by the presence of a small but dangerous light chain clone) (23). It is also the primary translocation found in mantle cell lymphoma (24). It causes the upregulation of cyclin D1 (CCND1) which

is not normally expressed in B cells, in contrast to cyclin D2 and cyclin D3 (25). The effect of this translocation on outcome has been a source of debate but is mostly classed as neutral (26). Interestingly, it was recently shown that patients harbouring this translocation have a higher level of the antiapoptotic protein, BCL-2. Venetoclax, an anti-BCL-2, was shown to be beneficial in this group of patients (27).

t(4;14) juxtaposes the *FGFR3* gene (in 70%) and the *MMSET* gene (in 100%) in chromosome 4 to the immunoglobulin heavy chain promoter on chromosome 14. The outcome of this translocation is the upregulation of cyclin D2 by relatively unknown mechanisms (21,28).

MMSET is a methyl-transferase and it may be the culprit behind the pathogenicity of this translocation rather than the FGFR3 given that the latter is not upregulated in all cases. The activation of MMSET induces methylation of several histones (such as H3K36 and H4K36) with a consequent impact on the translation of several genes and the recruitment of some factors to the DNA damage sites (29). The presence of this genetic translocation has been shown to impart a negative effect on prognosis, being one of the classical high-risk cytogenetic changes (30). Recently, however, this has been challenged and it may be that the negative effect of this translocation is intermediate rather than high. Indeed, bortezomib, a proteasome inhibitor that is considered a backbone of many myeloma-directed chemotherapy combinations, may abrogate the negative risk of this translocation (31). Recent evidence also suggests that the presence of additional genetic changes can modify the risk associated with this translocation. For example, the presence of trisomy 3 and trisomy 5 have been shown to mitigate the risk while the presence of trisomy 21 increases the risk (32).

Those two translocations are the most common. Other translocations in this context have been identified but are much less frequent.

c-MAF overexpression is the result of **t(14;16)** while MAFB is overexpressed with **t(14;20)**. *c-MAF* is an oncogene and is a splice variant of *MAF*. The latter can directly bind to and activate the cyclin D2 promoter (33). The gene expression profiles of *MAF* and *MAFB* are similar, hence, MAFB also has cyclin D2 as a downstream direct target similar to c-MAF (34).

APOBEC3A and APOBEC3B are two members of a family of cytidine deaminases comprised of 11 members in mammals. Those proteins serve important biological functions including in B cell development. APOBEC activity is increased in a variety of cancers and that increase contributes to an elevated mutational burden. APOBEC3 signatures can be detected through the presence of localised areas of genomic hypermutation characterised by the presence of dC>dT and dC>dG mutations (35).

The APOBEC signature was shown to be enriched in myelomas harbouring the t(14;16) and t(14;20) as a result of c-MAF and MAFB overexpression possibly through their binding to the APOBEC3A and B promoters and thereby myelomas with these translocations are associated with a heavy mutational burden (36).

t(6;14) results in the upregulation of *CCND3(cyclin D3)* and is not thought to have a negative impact on prognosis.

b. **Hyperdiploidy**, Trisomies of odd-numbered chromosomes contribute to around half of the initiating events in multiple myeloma. The culprit chromosomes are chromosomes 3, 5, 7, 9, 11, 15 and 21 (37). There is a positive correlation between

hyperdiploidy and translocations involving c-myc (36). Although hyperdiploidies exhibit a degree of heterogeneity in terms of the downstream deregulated pathways, they have been generally considered to be of good clinical risk compared to aneuploidy. It is worth mentioning, however, that this good risk can be modified by the presence of other adverse genetic events. Trisomies 3 and 5 are associated with a better prognosis while trisomy 21 is not. Moreover, trisomies can modify the risk of the t(4;14) translocation, such that the presence of trisomy 3 and 5 may abrogate the negative risk associated with this translocation (32,38). The origin of the trisomies is not related to the class-switch recombination process described earlier but is thought to stem from a catastrophic mitotic event that tends to precede chromosomal translocations if those are to exist together (1).

Hyperdiploid myelomas also overexpress cyclin D. The mechanism by which this happens is not clear, however cyclin D1 overexpression in hyperdiploid myelomas is thought to be secondary to bi-allelic overexpression due to the extra chromosome 11 where cyclin D1 resides (39). Cyclin D2 overexpression can also happen in this group of myelomas through poorly understood mechanisms. It has been postulated that certain miRNAs downregulation seen in hyperdiploid myelomas is responsible for creating a myeloma phenotype similar to that imparted by the effect of the immunoglobulin heavy chain translocations mentioned earlier. Therefore, this alteration may consequentially lead to similar dysregulations as those observed with the translocated myelomas including the overexpression of cyclin D (40). As mentioned above, those two primary genetic events are mutually exclusive in around 90% of myelomas and initiate the immortalisation of the affected plasma cells but

since they are present at the pre-malignant MGUS stage, they are not enough to be the sole aetiology of the malignant transformation and further 'secondary' events would need to be acquired (Figure 1.3).

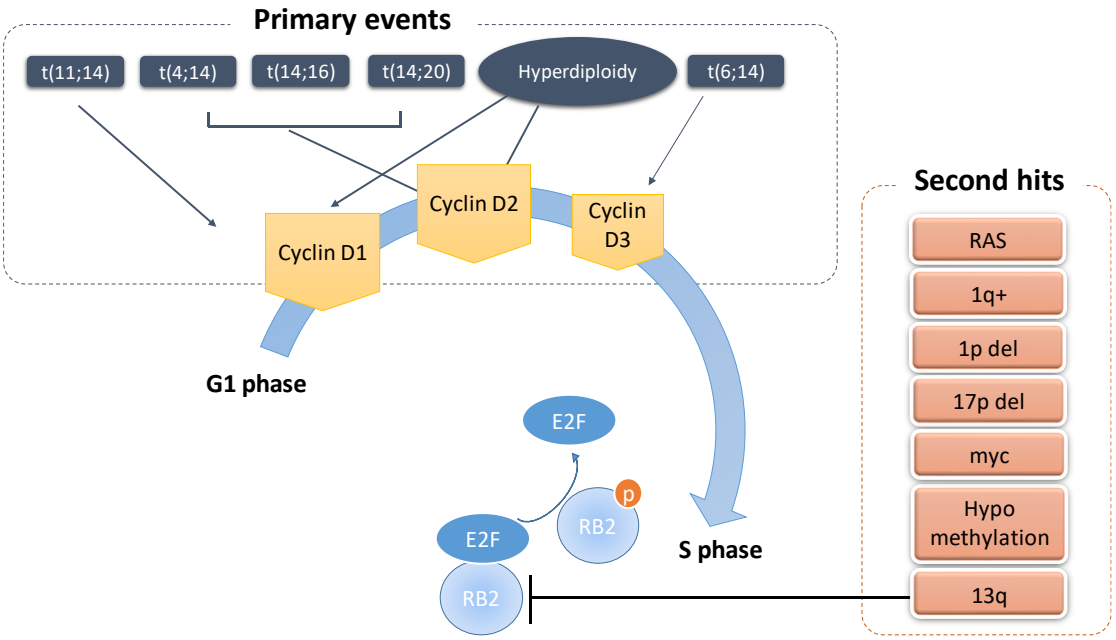


Figure 1.3: The interaction of primary events signified by hyperdiploidy and cyclin D translocations and secondary hits conspires to derive the pathogenesis of plasma cell myeloma. The cyclin D upregulation will indirectly lead to phosphorylation of RB2 and thus dissociating the E2F transcription factor with the resultant fast-forwarding of the cell cycle from G1 to S phases. Adapted from (41)**.**

13q deletion

This belongs to neither of the two classes above but is mentioned here as it has been found in patients with MGUS and thus may have a primary initiating role (42). This event, which is found in approximately half of the patients with myeloma, has been regarded in the past to be of a poor prognostic value however this view has changed. On its own, it has no prognostic impact and it is not a part of any of the cytogenetics risk scoring systems but is frequently associated with other high-risk changes (43). The

perceived high risk is thus only a reflection of these associations and not an independent effect of this deletion. An outcome of this deletion is the downregulation of RB1, a tumour suppressor and a negative regulator of the cell cycle, hence the oncogenic impact of this deletion (Figure 1.3) (43).

1.2.2 Secondary Events

Two main processes collaborate to fast forward the malignant transformation in the premalignant immortalised B cells. It is likely that not any one of these processes on its own is enough to cause the transformation of the plasma cell dyscrasia from the premalignant and asymptomatic entities to the symptomatic entity. The acquisition of secondary events and the interaction with the bone marrow microenvironment work hand in hand to initiate the malignant process.

A number of secondary events have been described in the literature. It is worthwhile to note that the development of some of the secondary events can be dependent on the specific primary event. For example, myc translocations are mainly seen in hyperdiploid myelomas and NRAS/KRAS mutations are seen in those with t(11;14) and those with hyperdiploidy.

A. Chromosomal gains, deletions, copy number variants (CNVs) and translocations

<u>1q gain</u>

The gain (up to 3 copies) and the amplification (4 or more copies) of the long arm of chromosome 1 can be detected in up to 40% of patients with myeloma and are associated with poor risk and reduced OS even with modern therapies (43,44). The exact culprit(s) conferring this negative impact are not fully elucidated, however, there

are a number of probable targets (Figure 1.4). CKS1B (CDC28 Protein Kinase Regulatory Subunit 1B), binds to and activates cyclin-dependent kinases (CDKs). It causes the degradation of the cell cycle negative regulator P27kip (45). Pro-survival STAT3, MEK/ERK and BCL-2 are also thought to be downstream targets of CKS1B (46).

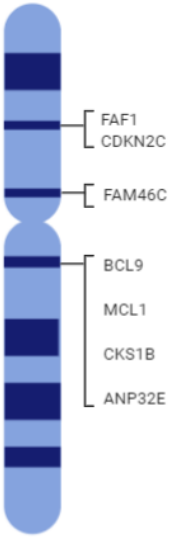


Figure 1.4: Chromosome 1. Chromosome 1q gain and 1p del are considered high-risk features in multiple myeloma. There are several genes on Chromosome 1 that are implicated. Some of those are denoted above.

Another gene of interest is the *ANP32E* (acidic leucine-rich nuclear phosphoprotein 32 family member E), the upregulation of which is associated with poor prognosis. ANP32E has a role in histone remodelling through the inhibition of histone acetylation and, therefore, may play a similar function to MMSET in patients with t(4;14) (43). Other genes that may be implicated include *BCL9*, which is involved in Wnt pathway overactivation (47) and *PDZK1*, involved in drug resistance to conventional chemotherapy (48). *MCL-1* is also located on chromosome 1q. MCL-1 and BCL-2 collaborate to prevent the activation of the intrinsic pathway of apoptosis by preventing caspase activation. Studies have shown that most myelomas are MCL-1 dependent rather than BCL-2 dependent, such that the inhibition of BCL-2 with agents such as venetoclax does not induce significant apoptosis (49,50). An exception to this

generalisation is in a subgroup of myelomas with t(11;14) which have over expression of BCL-2 and are more sensitive to treatment with venetoclax (27).

To highlight the negative impact of 1q gain, a recent study identified a group of the so-called 'double hit' myelomas, with either 1q amplification combined with an ISS (International staging system score) of III or biallelic TP53 inactivation. This group comprised 6 % of the myelomas and has a dismal PFS and OS of 15.4 months and 20.7 months respectively (3).

It is also worthwhile to mention that although 1q gain has universally been accepted as a high-risk cytogenetic marker, it has not made its way as yet to the revised international staging system (R-ISS) which predicts PFS and OS based on the combination of cytogenetics and disease burden (30), although other scoring systems that include chromosome 1q changes have been recently published but not yet fully adopted (51).

1p deletion

1p deletion is observed in just under a third of myelomas and is associated with an adverse outcome (43,52). Three genes on chromosome 1p are of interest (Figure 1.4). *FAF1* promotes apoptosis through the FAS ligand (extrinsic pathway of apoptosis) and when downregulated may play a role in the NF-κB pathway activation (53,54). *FAM46C (TENT5C)*, is a tumour suppressor that is involved in the stability of the endoplasmic reticulum-bound mRNA and the induction of apoptosis (see below) (55). *CDKN2C (cyclin-dependent kinase inhibitor 2C)* is involved in cell cycle arrest which is key in the terminal differentiation of normal plasma cells. Deletion of *CDKN2C* has been shown to have a negative impact on OS in myeloma (56).

17p deletion

The culprit gene is the *TP53* located on 17p13. The incidence is around 8-10% at diagnosis and this goes up with disease progression and relapse (57). As expected from the function of p53 as a major tumour suppressor with overarching roles in apoptosis, DNA damage response and cell cycle regulation, 17p deletion in myeloma is associated with an increase in the mutational burden and genomic instability. The percentage of del 17p increases in plasma cell leukaemia which is the most aggressive entity on the plasma cell dyscrasia spectrum. 17p deletion is also associated with an aggressive disease phenotype such as the presence of plasmacytomas (plasma cell tumours outside the bone marrow). 17p deletion is one of the high-risk cytogenetics and is associated with inferior survival (median OS of 40.9 months) (43,58). However, there is a role for the deletion burden. A recent study suggests a threshold of 55% for the adverse cytogenetic effect to manifest. p53 mutations have been identified in myeloma patients to be exclusively associated with 17p del thus causing a complete p53 inactivation (59). As mentioned above, bi-allelic *TP53* inactivation is part of the 'double-hit myeloma' entity and is associated with a significantly adverse OS (3).

c-myc rearrangement and overexpression

The role of c-myc in myeloma is discussed in detail in Chapter 6:. In brief, the incidence of *c-myc* rearrangement is much lower in the MGUS stage in comparison to symptomatic myeloma (4% vs 20%) hinting at it being a secondary event. Studies have found that the most common partner genes for those translocations are the IgH gene, t(8;14) and the Igλ light chain gene, t(8;22) (1,60). As mentioned earlier, *c-myc* translocation positively correlated with hyperdiploidy (36). c-myc upregulation can

also be the result of other mechanisms such as a focal gain in chromosome 8 (where the *c-myc* gene resides), the impact of IL-6 from the tumour microenvironment on STAT3 and CAP-dependent translation and MAPK activation (61–65).

Other chromosomal gains and losses

Some of those changes involve the gain or the loss of a whole arm in the affected chromosome while others are more focal. As one might expect, these, mainly secondary events, feature the loss of a tumour suppressor gene or the gain of pro-survival genes. The tumour suppressor genes *BIRC2* and *BIRC3* are located on Chromosome 11q and are lost in around 7%, whereas the gain of 11q13.2 causes upregulation of cyclin D1. Similarly, the deletion of 16q leads to the loss of the tumour suppressors CYLD and WWOX in around a third of myeloma patients and 14q deletion causes the loss of TRAF3 whereas c-myc upregulation is seen with 8q focal copy number gain and the gain of 12p upregulates LTBR (1,14,43).

B. Mutations

When compared to leukaemias, the mutational load in myeloma is considerably heavier, yet, it is less than that identified in epithelial cancers (14).

Studies addressing mutations in multiple myeloma have identified an increasing number of culprit mutated genes owing to the improvement of sequencing methodologies. When looking at the pattern of mutations in myeloma, two general patterns can be inferred. Firstly, unlike some of the other haematological conditions, not a single mutation can be regarded as the linchpin in multiple myeloma pathogenesis. Indeed, there are no equivalents of the Philadelphia chromosome or

BRAF7600E similar to what is found in CML and hairy cell leukaemia. This has obvious implications when it comes to the use of novel targeted molecular therapies (14). Secondly, certain mutations cluster within certain clones while others tend to be subclonal (14). A study has found subclonal variability by sampling different tumour sites within the same patient. Again, this has clear therapeutic implications If a drug is used to target a subclonal mutation, it can create a differential response by virtue of ineffectiveness against other subclones (Table 1.2) (4,36).

Table 1.2: Secondary genetic events tend to associate with certain primary genetic events. 17p del can arise in any clone and therefore was depicted without a primary event (1).

Primary Genetic event	Secondary Events
Hyperdiploidy	*BRAF, FAM46C, EGR1, CYLD* *NRAS* *c-myc* translocations *K-ras*
	17 p del
t(4;14)	*FGFR3/DIS3/PRDK2/PRDM1/KARS*/1q gain
t(11;14)	*KRAS* *NRAS* *CCND1/DIS3/IRF4*
t(6;14)	*MAF*
t(14;20)	*MAFB*

The most frequently mutated genes in myeloma include, *NRAS, KRAS, TRAF3, TP53, FAM46C, DIS3, BRAF, LTB, CYLD, RB1, HIST1H1E, IRF4, and MAX* (66).

It would be more informative to describe the important genetic mutations that have been identified in multiple myeloma in terms of their frequency and the pathways that become disrupted by those mutations.

1. **RAS/MAPK pathway**. The MAPK pathway has a pro-survival function and its inhibition in myeloma reduced plasma cell proliferation (67). This pathway is heavily mutated in myeloma indicating its importance for disease pathogenesis. Whole exome sequencing (WES) studies identified *KRAS* and *NRAS* mutations in multiple myeloma to be the commonest mutations (21% and 19% respectively). Both are upstream of BRAF which is mutated in up to 7% of myelomas (14,66). *NRAS* and *KRAS* mutations are mutually exclusive within clones in 98% of cases (66). *BRAF* and *NRAS* mutations tend to segregate in hyperdiploid myelomas while myelomas with t(11;14) translocation tend to segregate with *KRAS* mutations (66).

2. **mRNA homeostasis and function**

   FAM46c is mutated in around 10% of myelomas (2). *FAM46c* encodes a poly(A) polymerase that plays an important part in mRNA processing and translation. Most importantly, it has a tumour suppressor effect through its negative influence on the growth of B lymphocytes. The substrates of FAM46c are extensive but they share being enriched for Golgi/ER-targeted proteins. In myeloma, they may have a role in creating ER stress (55). Recurrent inactivating point mutations have been identified within FMA46c in myeloma

with the effect of mitigating its tumour suppressor anti-proliferative effect. However, despite this, there was no effect of FAM46c mutations on survival. FAM46c mutations are associated with hyperdiploid myelomas (68,69).

DIS3 is located on chromosome 13q and is mutated in 11% of myelomas (2). DIS3 is crucial for survival through the ribonuclease function of the protein that it encodes. DIS3 has widespread roles in terms of mRNA regulation, quality control and decay through its catalytic interaction with the exosome (70). Given its localisation, DIS3 can be affected by chromosome 13q del described above which may lead to loss of heterozygosity (2). DIS3 mutations are inactivating and they are associated with a negative impact on prognosis (71).

3. **NF-κB**. The NF-κB pathway has been demonstrated to be of significant importance for myeloma cell proliferation and survival (72). Mutations in the NF-κB pathway genes can be identified in around a fifth of myeloma patients (1). Two activation pathways govern NF-κB signalling (Figure 1.5). Signal transduction through the classical pathway is triggered through ligand binding to three main receptors, BCMA (B cell maturation antigen), TACI (transmembrane activator and calcium activator and cyclophilin ligand interactor) and TNF-R (tumour necrosis factor receptor). CD40 activates the alternative activation pathway [71]. The activation of the NF-κB results in a multitude of survival and proliferation processes such as increasing cell cycling (c-myc and cyclin D1), anti-apoptosis (BCL-2 and BCL-xL), cellular adhesion (ICAM-1) and cytokine production (IL-1 and IL-6) (73). BAFF and APRIL are

BCMA ligands that are produced by the tumour microenvironment such that their blockage results in reduced plasma cell survival (74).

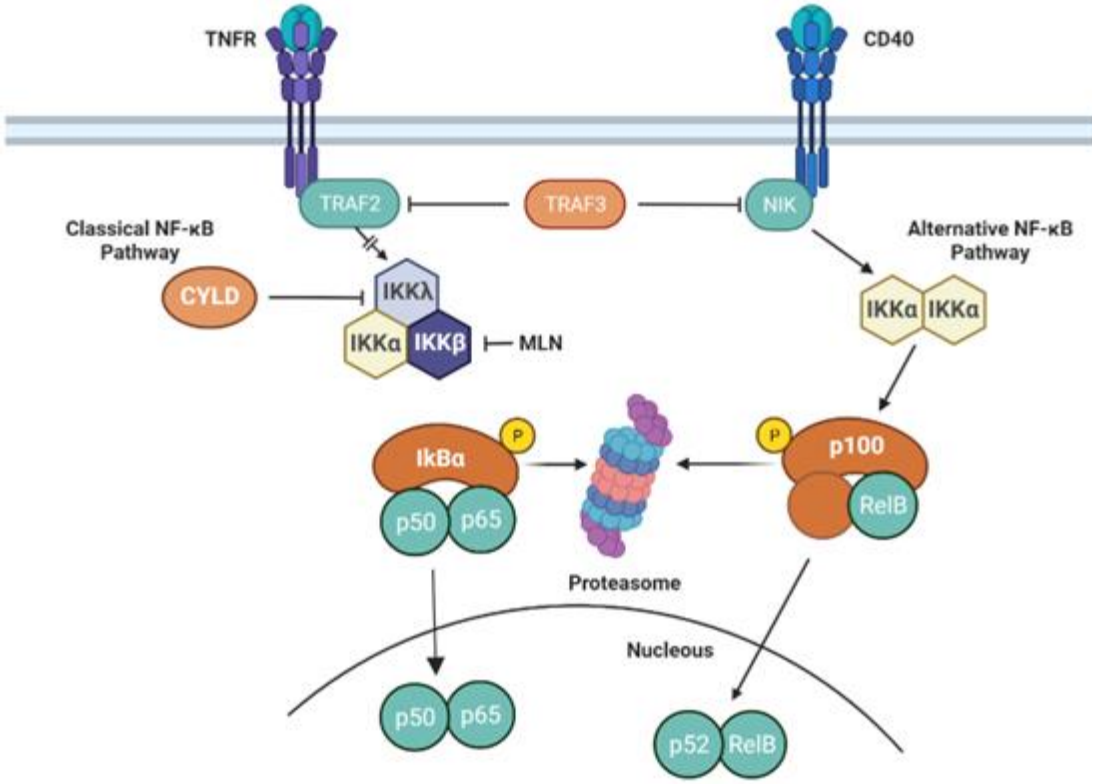


Figure 1.5 NF-κB pathway can be activated via a classical route through the tumour necrosis factor receptor or via an alternative pathway through CD40. Activation will result in the proteasomal degradation of IκB and p100 causing the release and nucleolar translocation of transcription factors p50/p65 and p52/RelB. Adapted from (72)**.**

Many of the frequently mutated genes in myeloma are related to the NF-κB pathway such as *TRAF3*, *CYLD* and *LTB* (66). Mutations in *TRAF3* and *CYLD* can cause constitutive activation of the NF-κB pathway through the loss of the inhibitory effect on both activation pathways with TRAF3 or on the classical

pathway with CYLD (73). Several other molecules are implicated in NF-κB activity in myeloma. NIK kinase can activate both NF-κB pathways and overexpression of NIK through translocations and increased mRNA stability has been identified in myeloma. CD40 overexpression has also been identified (72). *BIRC2/BIRC3* deletion, on the other hand, results in the loss of their inhibitory effect on the NF-κB pathway (72). LTB interacts with NF-κB through the alternative pathway. Mutations of this gene have been identified in 3% of myeloma cases and tend to associate with t(11;14) translocation (66,69).

4. **DNA damage response**. ATM (ataxia telangiectasia mutated) and ATR (ataxia telangiectasia and RAD3 related) sense DNA damage within minutes of it happening. Through a cascade of downstream events, phosphorylation of p53 plays a central role in the cellular response to DNA damage such that apoptosis happens when the quantity of damage is beyond repair or simply stalling of the cell cycle is triggered while the damage is repaired (75). *ATM, ATR* and *p53* mutations are detected in around 15% of multiple myeloma patients. *p53* mutations were found in 3% of cases and confer a negative impact on PFS and OS in myeloma patients (66). The frequency of *p53* mutations increases with disease progression. Some of those mutations were found to affect the DNA-binding domains (76). MDM2 and MDM4, the negative regulators of p53, are also upregulated in myeloma. *MDM4* is located on chromosome 1q, the gain of which is a frequent genetic event as mentioned earlier (76).

5. **Plasma cell differentiation**. PRDM1 is regarded as a tumour suppressor through its effect on transcription and B cell maturation. It represses the expression of the β-interferon gene(77). In myeloma, however, PRDM1 promotes the survival of myeloma cells. The knockdown of PRDM1 induced apoptosis through Bim induction and reduced MCL-1 expression (78). IRF4 is a transcription factor that plays a key role in lymphocyte and plasma cell development. An IRF4 downstream target is c-myc and it is also a transcription factor for PRDM1 (79). Moreover, IRF4 is inhibited through the action of the immunomodulatory drug (IMiD) lenalidomide on Cereblon (80). IRF4 knockdown induced apoptosis in myeloma cell lines. More than 300 enriched genes were downregulated when IRF4 was knocked down (79). IRF4 is mutated in just over 3% of myeloma and, counterintuitively, this mutation was found to have a positive impact on the OS (66). IRF4 mutations tend to associate with t(11;14) translocation.

Other important mutations

Mutations in the *CCND1* gene encoding for cyclin D1 tend to associate with the t(11;14) translocation and have a positive effect on the cell cycle. *RB1* is located on chromosome 13q and is a negative regulator of the cell cycle. Both of those mutations tend to be clonal and hence may have an initiating effect (1,43).

C. Epigenetic changes

Those involve, histone acetylation, histone methylation and micro-RNAs

1. **Histone acetylation**. It has been proposed that hypoacetylation of histones in myeloma can result in tumour suppressor downregulation. Histone deacetylase inhibitors (HDACi) have been approved as novel therapies for multiple myeloma. Vorinostat was used as one arm of the myeloma XI trial maintenance in combination with lenalidomide but was later dropped due to lack of efficacy (81,82). Vorinostat is thought to boost the expression of p53 (25) but it currently has no use in the treatment of myeloma. Another HDACi is Panobinostat which is currently licenced in combination with bortezomib after at least two lines of treatment (83).
2. **DNA methylation**. DNA methylation is an epigenetic modification where the methylation of the CpG-rich gene promoters causes repression of transcription. A study examined the methylation status in primary patient samples at various stages of MGUS/myeloma progression using methylation microarrays (84). Overwhelming loss of methylation was identified at the transition stage from MGUS to myeloma together with hypermethylation of specific genes that are associated with the regulation of transcription and cell cycle. Further hypermethylation of genes involved in cellular adhesion was identified at the transition to the plasma cell leukaemia stage. The same study also identified a methylation profile associated with hyperdiploid myelomas and myelomas with t(4;14) (84).
3. **miRNAs**. Several miRNAs can downregulate CDKN2A which is, as mentioned above, a negative down-regulator of the cell cycle. miRNA 106-25 and miRNA 32 alter certain inducers of p53 ultimately resulting in p53 downregulation.

Finally, MDM2 which binds to and inhibits p53 is downregulated by miRNA 192 which is downregulated in myeloma (25).

1.2.3 The Bone Marrow Microenvironment

The gene expression profiles of symptomatic myeloma and its precursor stages, MGUS and asymptomatic myeloma can be easily distinguishable from their healthy counterparts, however, may not be so from each other. This gives credence to the importance of the bone marrow microenvironment in deriving disease progression to the symptomatic stages. The interaction between the myeloma cells and the microenvironment is reciprocal and involves several feedback loops that consolidate the myeloma cell survival and resistance to apoptosis. The homing of the myeloma cells to the bone marrow niches is mediated through the CXC family of chemokines. Myeloma cells are attracted through their CXC4 receptors to the CXCL12 (also known as stromal cell-derived factor 1, SDF-1) in the bone marrow niches (85). When the myeloma cells reach the bone marrow they adhere to and interact with the bone marrow stromal cells. VCAM-1 (vascular cell adhesion molecule-1) on the bone marrow stromal cells binds to integrins on the myeloma cells to mediate this adherence. This interaction results in the production of several cytokines that further enhance the survival of the myeloma cells (86).

Angiogenesis is a key component of the tumour microenvironment. There is a defined role of angiogenesis in disease progression such that the microenvironment can be classified into an avascular stage (with MGUS and symptomatic myeloma after successful treatment) and a vascular stage (with active/progressive disease). VEGF (vascular endothelial growth factor) produced by the bone marrow stromal cells in

response to interactions from the myeloma cells plays a critical role in this process. VEGF is also produced by the myeloma cells in the bone marrow (87). In addition to VEGF, the bone marrow stromal cells also secrete a multitude of other cytokines in response to the close interaction with myeloma cells. These include, but are not limited to, IL-6, CXCL12, IGF-1 and matrix metalloproteinases (MMPs). The collective effect of those factors is the increase in myeloma cell survival, drug resistance and growth (87).

The reciprocal interaction between the myeloma cells and the bone marrow stromal cells also contributes to the activation of many pro-survival and pro-oncogenic pathways in the myeloma cells such as the MAPK, NF-κB, PI3K and the JAK/STAT pathways. The downstream effects of these activations are wide and include the upregulation of several BCL-2 antiapoptotic proteins, MCL-1 and cyclin D (87).

The interaction of the myeloma cells with the bone marrow microenvironment is a strong contributing factor to the pathogenesis of myeloma bone disease. The imbalance between the osteoblastic and the osteoclastic activities in favour of the latter is mediated through the production of several molecules, the most important of which is RANKL (receptor activator of NF-κB ligand) which interacts with the RANK receptor on the surface of the osteoclasts causing their activation and therefore bone resorption (88).

As has been illustrated above, primary genetic events occur at the MGUS stage but are, on their own, insufficient to derive the malignant process. Many of the second hit changes are also found at the MGUS stage but at a low level. It seems that the accumulation, overtime of secondary genetic events and the pro-survival interaction

of the myeloma cells with the bone marrow microenvironment allows for the malignant cells to gain a clonal advantage and initiate a malignant process.

1.2.4 Cell Cycle and DNA Damage Response Deregulation

The normal cellular mechanisms scramble to activate the DNA damage response almost immediately after DNA damage. These conservatory mechanisms aim at halting the DNA replication fork and the cell cycle while waiting for the damage to be repaired. If the damage is too severe or if the repair process becomes prolonged, apoptosis ensues. Consequently, the failure of this process will lead to the generation of double-strand breaks (DSBs) (75,89). DNA damage is repaired through several pathways, the activities of which depend on the type of the damage and the stage of the cell cycle (**Table 1.3**) (90).

Table 1.3: A list of different types of DNA damage together with their potential causes and the repair mechanisms. Different mechanisms are available at different stages of the cell cycle. The main two mechanisms for repairing DSBs are homologous recombination (HR) and nonhomologous end joining (NHEJ).

Type of DNA damage	Potential causes	Repair mechanisms
DSBs	IR	NHEJ, HR
SSBs	Oxidative damage, Topo I erroneous activity	Short and long patch SSB repair pathways
Protein DNA cross-links	Topo I and II inhibitors	PDC repair, NER, NHEJ, HR
ICL (inter and intra strand)	Alkylating agents	NER, HR, ICL repair
Bulky DNA adducts	Alkylating agents	NER
Base mismatch	Oxidation/deamination	MMR
Base modifications	Methylation	BER

A. **Base excision repair (BER)** is mainly active throughout the G1 phase of the cell cycle and is used to repair DNA damage resulting from base modifications when the helix structure is maintained. In other words, this form of repair is preferred when there are chemical changes (such as deamination and alkylation) that do not threaten the double helix structure of the DNA. A repair gap is created by mono- and bifunctional DNA glycosylases and endonucleases which is then tailored and repaired by the collaboration of several other factors such as POLβ, APE and DNA ligases (90).

B. **Nucleotide excision repair (NER)**, repairs mainly bulky lesions which distort the DNA helix. To initiate the process of nucleotide excision repair, access to the damaged area needs to be attained through chromatin remodelling. This is followed by the commencement of NER through two main pathways. The Xeroderma Pigmentosum complementation group C (XPC) senses the presence of DNA damage in the GG-NER (global genome NER). Following the binding of XPC to the sensed lesion, an incision step ensues that is mediated by the binding of various proteins such PCNA, various DNA polymerases and ligases. Those will carry out the process of gap filling and ligation. The transcription-coupled NER (TC-NER) is triggered by lesions that stall RNA-polymerase II. The process involves the recruitment of factors such as CSA, CSB UVSSA, USP7 and XAB2 to rewind the RNA polymerase which is then followed

C. by a series of steps similar to what is observed with the GG-NER (90).

D. **Mismatch repair (MMR)**, the activity of this high-fidelity pathway occurs mainly after the replication of the DNA and it is involved in the repair of base

mismatches and the insertion-deletion loops. This pathway is relevant to other important processes in B cell development such as CSR and SHM. The mismatches and the insertion-deletion loops are recognised by two MSH heterodimers, known as MutSα and MutSβ. This recognition step is followed by the recruitment of another heterodimer known as MutLα. PCNA helps with initial localisation of both MutS and MutL heterodimers. The excision of the mismatched base pairs is orchestrated by EXO1. The last step involves the synthesis of the correct base pairs and their ligation into the gap by the sequential functions of DNA polymerase POLδ and the ligase LIG1 (90).

E. **Interstrand cross-link (ICL) repair**, this pathway is concerned with the repair of lesions that result when two bases from complementary strands are cross-linked due to the effect of certain chemotherapeutic agents such as alkylators and platinum compounds. The Fanconi anaemia (FA) proteins are responsible for sensing and repairing those lesions. FA proteins assemble to the site of the lesion and a cascaded process of phosphorylation and ubiquination of various FA members is triggered also resulting in the activation of ATR and the phosphorylation of CHK1. The recruitment of endonucleases will mediate the excision of the lesioned DNA strand. Further on from this, the rest of the ICL repair process depends on whether the cell is replicating or not. If the cell in not replicating the NER repair pathway is involved and acts on both the leading and the lagging strands. In replicating cells, the process is more complicated. The replication fork is stalled. DNA polymerases use the leading strand for a template. The NER pathway is also involved as it excises the remnant ICL hook (90).

F. **<u>Translesion synthesis (TLS)</u>**, is a low-fidelity repair pathway that is mediated through the action of several TLS polymerases. This pathway of DNA repair can be error prone and its fidelity depends, in part, on the type of the lesion as well the TLS polymerase involved in the repair process. Although incorrectly repaired lesions may contribute to biological diversity, they can be a reason for mutational events that lead to neoplastic transformation or genetic diseases. TLS polymerases are structurally different in comparison to the high-fidelity DNA polymerases. They also miss the proofreading ability because they lack the exonuclease function. The TLS enzymes have an inserter function (putting repaired oligonucleotide opposite the DNA lesion) and an extender function, which, as the name implies, extends the inserted nucleotides after removing the inserter polymerases (90).

G. **Single strand breaks (SSBs) repair,** abasic sites and Topo I derangement can cause SSBs. When goes, unrepaired, SSBs can progress to DSBs, and may induce apoptosis through DNA replication stalling and the release of apoptosis inducing factors. PARP1 activity is crucial to the repair of those breaks. In the long patch repair pathway, SSBs are recognised by PARP1. This is followed by the action of endonucleases and FEN1 removing the damaged nucleotide and leaving a gap. This is later repaired by the action of a couple of DNA polymerases and ligases. The short patch repair follows the generation of SSBs after base excision repairs. This is followed by the action of a single DNA polymerase and ligase to fill in the gap (90).

The next two pathways are used for the repair of double-strand breaks (DSBs) and are discussed in more detail below.

H. Homologous Recombination (HR)

I. Non-homologous end joining (NHEJ).

DSBs are highly toxic and if left unrepaired cell death follows (75). Evidence has shown that DSBs can be a strong trigger of apoptosis. There is evidence that simpler DNA lesions can trigger apoptosis but only when that damage is converted to a DSB by the failure of repair mechanisms (91).

DNA damage is sensed through three main systems, ATM (ataxia telangiectasia mutated), ATR (ataxia telangiectasia and Rad3-related) and DNA-PK (DNA-dependent protein kinase) (75). It is thought that ATR is crucial to SSBs while ATM is mainly triggered by DSBs (92,93). These sensing proteins phosphorylate histone H2A.X at ser139 (γH2A.X) which then forms foci at the sites of DNA DSBs (94). They also trigger a downstream hold on the cell cycle progression and sanction the recruitment of DNA repair proteins to permit homologous repair (HR, where the sister chromatid is used as a template) and non-homologous end joining (NHEJ, the direct ligation of the two broken DNA ends) (75,93). It has been shown that H2A.X phosphorylation occurs within minutes of DNA DSBs formation (95). The phosphorylation co-localises with other factors that are involved in the formation of DNA repair foci such as Rad 50, Rad 51 and Brca 1. This supports the role of histone modification in DNA damage repair and permits the use of H2A.X phosphorylation as a marker of DNA damage site early before the recruitment of other DNA repair factors (94).

Whether HR or NHEJ are chosen for the repair of the DNA will depend on the cell cycle stage when the DNA damage has happened. NHEJ is active during the G1 phase. There is a lack of the sister chromatid to function as a template and the chromatin will be

compact during this stage hence the DSB repair will occur through NHEJ by joining the broken ends whether they come from the same chromosome or not (96,97). HR, on the other hand, is a high-fidelity process as it benefits from the presence of the sister chromatid during the S and G2-M phases (97). Through Chk1 and Chk2 respectively, ATM and ATR also phosphorylate p53, the sustained phosphorylation of which due to elevated levels of DNA damage can lead to cell death (75). NF-κB can be activated by double-stranded DNA damage. However, this process generates a pro-survival effect through the inhibition of mitochondrial and extrinsic apoptosis pathways (75).

The normal cellular responses to DNA damage in multiple myeloma are deranged in a plethora of ways, several of which are discussed.

1.2.4.1 DNA damage response in multiple myeloma

The basal DNA repair activity in multiple myeloma is elevated. Multiple myeloma cell lines showed a basal increase in γH2A.X foci even without DNA damaging treatment indicating the presence of endogenous DNA damage (98,99). After exposure to IR, the persistence of DSBs resulted in a prolonged G2/M arrest. Proteins involved in DNA damage repair such as Rad50, Rad51, XRCC4 and Artemis were upregulated in myeloma cell lines. DNA ligase IIIα, an enzyme implicated in the alternative non-homologous end joining (Alt-NHEJ) was also highly expressed (98). The efficiency of HR and NHEJ in myeloma cell lines tested through their ability to recirculate a plasmid was found to be increased and there is an overall increase in the activity of HR in primary myeloma samples (98).

The altered HR in myeloma arbitrated genomic instability. There was a significant increase in the transcript levels of genes that are involved in HR in myeloma cell lines

and primary samples such as, XRCC3, RAD50, HsRAD51, HsRAD52D, helicases and various endo- and exonucleases. Constitutive activation of HR was found to increase the chances of acquiring genetic mutations contrary to the notion of it being a high-fidelity DNA repair system. Acquisition of new mutations, assessed through genome-wide LOH, was higher with HR induction and lower when HR was inhibited (100). A recent study showed that the inhibition of HR was more toxic to myeloma cells than the inhibition of NHEJ (99).

DNA damage can activate the NF-κB pathway through the sumoylation and the nuclear localisation of the NF-κB essential modulator (NEMO). NEMO is also phosphorylated through ATM, a process that eventually causes the phosphorylation of IκB (101).

As mentioned previously, 17p del (where the p53 gene is located) and p53 mutations are important events in myeloma and confer a negative impact on prognosis. p53 is an important protein in the DNA damage response and can also be affected by the upregulation of its inhibitory proteins MDM2 and MDM4 and can be the subject of DNA methylation (75).

The DNA repair capacity of myeloma cells was found to affect their chemosensitivity and the clinical outcome. After a short melphalan exposure, a significantly higher number of DNA mono-adducts was found in patients who showed a response to melphalan therapy (102). Bone marrow plasma cells from responders to melphalan therapy showed lower rates of nucleotide excision repair and DSBs repair activities. There was a higher accumulation and slower removal of γH2A.X foci recruited to the DNA damage areas in responders compared to non-responders indicating a failure of DNA repair (102). Responders to melphalan therapy were also shown to have reduced

transcriptional activity and attenuated chromatin looseness as compared to non-responders (103).

1.2.5 The Importance of the Cyclin D-type in Myeloma

As mentioned earlier, the over expression of a D-type cyclin is almost a universal feature in MGUS, asymptomatic myeloma and symptomatic myelomas. This can be the direct result of a chromosomal translocation such as t(11;14) overexpressing cyclin D1, t(6;14) overexpressing cyclin D3, indirectly such as t(14;16) and t(14,20), whereby MAF and MAFB bind to the cyclin D2 promoter region or through relatively unknown mechanisms such as the overexpression of cyclin D2 as a result of MMSET/FGFR3 overexpression due to t(4;14) translocation. Even hyperdiploid myelomas can exhibit bi-allelic cyclin D1 over expression, possibly as an effect of trisomies affecting chromosome 11 (18). The segregation of certain secondary events within the pre-defined chromosomal translocations and trisomies and the associated variability in clinical risk scores and the chances of remission to chemotherapy hint toward the importance of those events from the outset.

1.2.5.1 Roles of cyclin D1

In addition to its established role in driving the cell cycle progression, cyclin D1 is an important player in the DNA damage response and the inhibition of apoptosis. Cyclin D1 is degraded by phosphorylation and then polyubiquitination after DNA damage leading to cell cycle arrest (104). It also interacts with proteins that participate in DNA damage repair such as BRCA1, BRCA2, RAD51 PCNA and replication factor C. The recruitment of RAD51 to DNA damage sites was reduced significantly in cells lacking cyclin D1 (105).

Several studies have shown that increased levels of cyclin D1 confer IR damage resistance (106,107). Some studies, however, showed increased radiosensitivity with cyclin D1 overexpression (105). These conflicting findings may be explained by the diversity in the biology of the cancers studied or may reflect a dual role for cyclin D1 in the response to DNA damage (105). More recently, the differential response to IR between myeloma cells that express cyclin D1 and those that express cyclin D2 has been investigated. Surprisingly, although only cyclin D1 was downregulated in response to IR, there was no difference in the cell cycle protein response or in the sensitivity to IR between those that expressed cyclin D1 and those that expressed cyclin D2. In both groups, cell cycle arrest happened at G2/S/M rather than in G1 (108).

Cyclin D1 also interacts with the mitochondrial apoptotic pathway. Cyclin D1 overexpression secondary to t(11;14) plays a major role in the pathogenesis of mantle cell lymphoma. It was found that cyclin D1 sequesters Bax in the cytoplasm thus imparting a pro-survival effect. When cyclin D1 was knocked down in mantle cells, Bax was released and sensitised cells to apoptosis (109).

1.2.6 Apoptosis Derangement in Myeloma

There are two main apoptotic signalling pathways. The extrinsic pathway involves the stimulation of the death receptors by ligands such as TNF leading to the formation of the death-inducing signalling complex (DISC). The BCL-2 family regulates the intrinsic (mitochondrial) pathway whereby various death stimuli can activate the pro-apoptotic members of the BCL-2 family (75,110). Both pathways can be activated by DNA damage (75). The BCL-2 family is comprised of the pro-survival members (such as BCL-XL, BCL-w, and MCL-1), the pro-apoptotic members (such as Bax and Bak) and the BH3-

only apoptosis initiators (such as Bad, Bim, Bid, PUMA and NOXA) (110). Those are also subdivided into activators (Bim, Bid and Puma) which bind to the effectors to initiate MOMP (mitochondrial outer membrane permeabilization) and the sensitisers (Noxa and Bad) which bind the antiapoptotic proteins to release the activators (110).

Inhibiting BCL-2 activity in haematological malignancies is an attractive therapeutic target. Venetoclax (ABT-199) is a potent and orally bioavailable selective BCL-2 inhibitor (111). This agent was shown to be most effective in myeloma cells harbouring the t(11;14) with little or no effect on those that are MCL-1 dependent (112). The BCL-2/MCL-1 ratio was found to be a strong predictor of response to venetoclax. Interestingly, venetoclax was effective in BCL-2-dependent cell lines even when there was a 17p deletion (112). Treatment of myeloma cell lines lacking the t(11;14) with venetoclax as a single agent yielded disappointing results, however. Bim released from BCL-2 following treatment with venetoclax was bound to MCL-1 and, thereby, was unable to activate the pro-apoptotic proteins Bax and Bak (113). A synergistic effect, however, was noticed when co-treating with dexamethasone (114). Dexamethasone treatment increased the levels of expression of Bim and BCL-2 and also increased the binding of Bim to BCL-2 such that upon treatment with venetoclax a greater amount of Bim is released to activate apoptosis. In other words, dexamethasone shifted MCL-1-dependent cells to become BCL-2-dependent for survival (114).

Many of the myeloma cell lines and primary samples, however, are MCL-1 dependent and thus insensitive to BCL-2 inhibition. BH3 profiling revealed heterogeneity among myeloma cell lines and primary samples in terms of BCL-2/MCL-1 dependence. One

study found that around 50% of the myeloma cell lines and 30% of the primary samples were MCL-1 dependent (113). In another study, using 25 myeloma cell lines, BCL-2 dependence was seen in 20% of the cell lines tested (115). Not all the sensitive cell lines, however, harboured t(11;14) with some demonstrating t(4;14). Significant cytotoxicity was noted when MCL-1 was targeted indicating that most of the myeloma cell lines are MCL-1 dependent and highlighting an attractive therapeutic potential (Figure 1.6) (115).

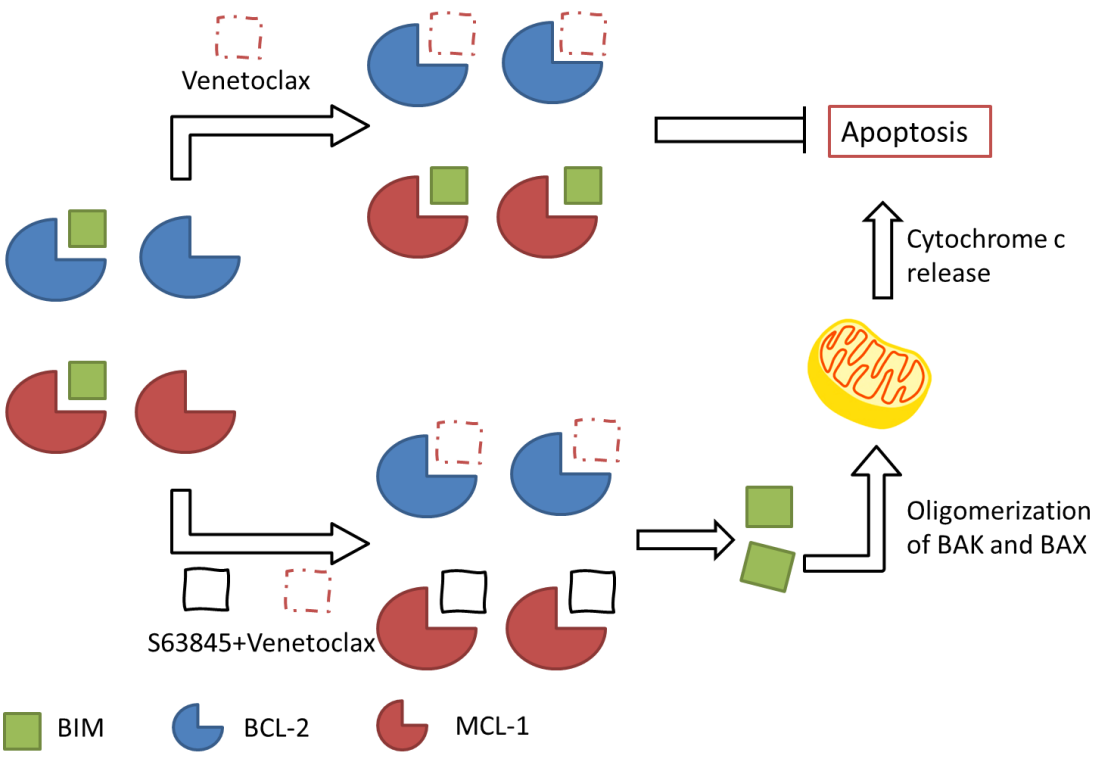


Figure 1.6: the interaction between MCL-1, BCL-2 the proapoptotic BIM and MCL-1 and BCL-2 inhibitors. When venetoclax binds to BCL-2 it displaces BIM however the extra MCL-1 binds to the free BIM and hence prevents the latter from initiating apoptosis. The combination of venetoclax and MCL-1 inhibitor causes the release of BIM, eventually followed by oligomerisation of BAK and BAX, and cytochrome c release from the mitochondria and apoptosis. Adapted from (114)**.**

The biological relationship between the t(11;14) translocation, BCL-2 dependence and sensitivity to venetoclax has been reflected clinically in the Bellini trial (116) [190]. In this randomised double-blind study, myeloma patients were assigned a combination of bortezomib and dexamethasone with or without venetoclax. Although the PFS was higher in the venetoclax arm, the overall survival was worse owing to a higher number of infection-related deaths in the venetoclax arm. The study did not stratify patients according to whether they had the t(11;14) translocation or not however when a subgroup analysis of this group of patients was done there was no negative impact from a higher infection risk. This indicated that venetoclax use in multiple myeloma should be restricted to patients with t(11;14) or those with BCL-2 dependence (116,117).

1.3 Plasma Cell Dyscrasias from the Clinical Perspective

Multiple Myeloma represents one, and the most common, of a number of plasma cell dyscrasia. Those conditions can occur separately, progress from one to another and/or co-exist in the same patient (86). Not all of these conditions require treatment (MGUS, low-risk asymptomatic myeloma) and there is an active debate on whether some require treatment (high-risk asymptomatic myelomas). Treatment usually involves a combination of various agents in a single line of treatment and sometimes the sequential combination of various treatments (118).

This section will focus on MGUS and multiple myeloma since both are the commonest encountered in clinical practice and the latter is the subject of this thesis.

1.3.1 MGUS (Monoclonal Gammopathy of Uncertain Significance)

Virtually all cases of multiple myeloma arise from the pre-malignant MGUS phase (19). As described earlier, there is a clonal expansion of immortalised plasma cells that have not yet accumulated enough genetic hits to allow for the progression to symptomatic disease (86). Most MGUS cases are detected incidentally and do not progress to the malignant stage (119). The incidence of MGUS increases with age. This is estimated to be just above 3% in those over 50 years of age and just over 5% in those over seventy (120). Diagnosis is achieved when serum protein electrophoresis and immunofixation identify the presence of a paraprotein and/or a free light chain imbalance with the absence of any diagnostic features of end-organ damage (collectively known as CRAB features), SLiM criteria and a plasma cell percentage of less than 10% (if a bone marrow examination was performed) (118). The risk of progression of MGUS is about 1% per year but certain biochemical characteristics can modify the risk of progression to make it range between 5% (when there are no risk factors) to 58% (all risk factors present) at 20 years. Those risk factors include the presence of non-IgG paraprotein, when the paraprotein level is more than 15 g/l or when the serum free light chain ratio is abnormal (120). Other risk factors that can predict the risk of progression include the bone marrow plasma cell percentage, the presence of an evolving increase in the paraprotein and the paraprotein subtype (19,119). MGUS does not require treatment since most cases do not progress. There is a suggestion that an evolving MGUS is an already developing myeloma but despite that, there is no evidence to suggest that an evolving MGUS should be treated (19). MGCS (monoclonal gammopathy of clinical significance), is being increasingly recognised as a clinical entity where the presence of the paraprotein is causing some clinical manifestations that are significant enough

to require attention but fall short of the diagnosis of symptomatic myeloma. These clinical manifestations can affect the kidneys (monoclonal gammopathy of renal significance such as immunoglobulin deposition disease, acquired Fanconi syndrome, etc.), the skin, the nervous system, and the cornea. Eradication of monoclonal paraprotein or the light chain is required sometimes to prevent (or reverse) further organ dysfunction and the therapies that are given mirror those that are available for the treatment of symptomatic myeloma (121,122).

The management in most cases of MGUS only requires regular monitoring in the primary care setting with clear referral criteria set in place to highlight any changes in the MGUS behaviour that may indicate the transformation to symptomatic disease (123).

1.3.2 Multiple Myeloma Diagnostic Pathway

The diagnosis of multiple myeloma requires the presence of more than 10% clonal plasma cells in the bone marrow or a biopsy-proven plasmacytoma (124). Malignant plasma cells have a distinct morphology and immunophenotype. When stained using MGG (May-Grünwald-Giemsa) stain and viewed under the light microscope, they are medium-sized cells with a peripheral nucleus and a perinuclear halo (reflecting an expanded Golgi apparatus). The cytoplasm is deep blue indicating active protein synthesis. The immunophenotype can be established using flow cytometry or immunohistochemistry on bone marrow or tissue samples. Malignant plasma cells are CD45-ve, CD38+ve, CD138+ve, CD20(+ve/-ve), CD56(+ve/-ve) and CD19-ve. Immunohistochemically, they express a light chain restriction and may show positivity for MUM1 and cyclin D (125).

The updated International Myeloma Working Group diagnostic criteria are summarised in Table 1.4. The presence of malignant plasma cells in excess of 10% makes the diagnosis of multiple myeloma, however, it is the differentiation between the symptomatic and the asymptomatic phases of myeloma that is of crucial importance since, with the former, treatment is required while with the latter, the management is mostly watch and wait (124).

Table 1.4: The diagnostic criteria of symptomatic multiple myeloma (124)

Clonal plasma cells of ≥10% in the bone marrow or biopsy-proven plasmacytoma with End-organ damage
Anaemia (a drop > 2 g/dl or Hb <10 g/dl)
Renal impairment (Creatinine Clearance < 40 ml/min or serum creatinine >177)
Hypercalcaemia (>2.75 mg/dl)
One or more lytic lesions on X-rays, CT, or PET
And/or Biomarkers (SLiM criteria)
Bone marrow plasma cell percentage of ≥ 60%
Involved : uninvolved light chain ratio > 100
More than one focal lesion (>0.5 cm) on MRI

There are two sets of criteria, the presence of any makes myeloma symptomatic. The first set reflects end organ damage. Collectively known as the CRAB criteria, they represent the insults imparted by the myeloma on the bone marrow (anaemia), the renal system and the bones (Hypercalcaemia, and lytic bone lesions). The second set of criteria (collectively known as the SLiM criteria) was added recently as the presence of any indicates a very high-risk disease with a danger of progression to end organ damage such that it would be reasonable to start treatment. These include a high

serum free light chain ratio, MRI focal lesions and the presence of more than 60% plasma cells in the bone marrow (124).

It is recommended that patients undergo whole body imaging with low dose CT, PET scan or MRI. It is also recommended to establish the cytogenetics by FISH analysis on the bone marrow sample. The latter is not part of the diagnostic criteria however it offers prognostic information and can influence treatment options. Assessing the cytogenetics is also part of the R-ISS score (in addition to the LDH, albumin and β2microglobulin) which give prognostic information with regards to the PFS and OS (118).

1.3.3 Management of Multiple Myeloma

The management landscape of multiple myeloma is in a state of constant change. As the understanding of the disease molecular pathology deepens, there is a steady flux of new therapeutics which reflects a prolongation of survival. Many of the novel therapies are expensive and the availability is largely guided by what is reimbursed in each country and by what is available through clinical trials.

This section will not list all the available treatment regimens as these keep changing but will list some of the available drug classes focusing on the agents used in this project.

A. Proteasome inhibitors (PIs)

The proteasome is a cellular digestive mechanism that recycles proteins tagged by ubiquitin. This process serves an important regulatory function for cellular activities such as cell cycling, apoptosis, and proliferation. The proteasome is a cylindrical structure made of two 19s subunits that sandwich 4 catalytic rings (2α outer rings

capping 2β inner rings). The β subunits have chymotrypsin-like, trypsin-like, and caspase-like activities. A polyubiquitinated protein marked for degradation gains access to the proteasome through the 19s subunits to be acted on by the catalytic subunits in the β chains emerging from the other end as smaller, digested oligopeptides (126).

The first PI to be approved was bortezomib in 2003 by the FDA and then in 2004 by EMEA. This is a boronic acid peptide that inhibits the chymotrypsin-like activity of the β subunits. Several other proteasome inhibitors have since been approved or in clinical trials (Carfilzomib, Ixazomib, Oprozomib, Marizomib) (127).

Bortezomib can induce toxicity in myeloma through various mechanisms related to the inhibition of the proteasome. As mentioned earlier, it has been established that the NF-κB pathway plays an important role in myeloma pathogenesis. IκB, is a suppressor of the NF-κB pathway and is degraded through the proteasome. Hence inhibition of the proteasome will cause the restoration of IκB and the suppression of NF-κB. Bortezomib also blocks a mechanism by which TNF-α secreted by the myeloma cells causes the upregulation of NF-κB. This, however, is not the major pathway of how PIs cause cytotoxicity since specific inhibitors to IκB degradation do not produce the same cytotoxicity as PIs (127,128). Myeloma cells have a highly active protein synthesis machinery since, in most cases, they make copious amounts of monoclonal proteins. They rely on the proteasome function to get rid of misfolded and unfolded proteins. It has been shown that the inhibition of the proteasome leads to the accumulation, in the endoplasmic reticulum (ER), of these proteins which eventually causes ER stress and the activation of the unfolded protein response (UPR). When the

accumulation of those proteins becomes too much for the ER to handle, the proapoptotic mechanisms in the UPR pathways are activated resulting in cell death (127–129).

Bortezomib can also induce apoptosis via the activation of JNK which causes mitochondrial cytochrome c release and the activation of caspase 8. Bortezomib also stabilises p53 and other proapoptotic factors such as BAX, BID and NOXA (thereby increasing apoptosis) and the cyclin-dependent kinase inhibitors p21 and p27 (thereby reducing proliferation). By reducing the levels of activated Caveolin-1, through VEGF inhibition, bortezomib reduces myeloma cell migration (128).

Several combinations of PIs are used in clinical practice such as those with immunomodulators (IMiDs), monoclonal antibodies, HDACi, alkylators and steroids (118,130).

B. <u>Immunomodulatory agents and Cereblon modifiers</u>

Thalidomide, lenalidomide and pomalidomide IMiDs have been in clinical use long before their direct mechanism of action had been elucidated. IMiDs bind to the Cereblon (CRL4-CRBN), an E3 ubiquitin ligase adapter. The binding causes the ubiquitination of two transcription factors (Aiolos and Ikaros, also known as IKZF1 and IKZF3). IZKF3 is regulatory for IRF4 which is an important transcription factor in myeloma and exerts an upstream positive effect on myc, which, as discussed earlier, plays a particularly important role in myeloma pathogenesis (80,131). IMiDs, as the name implies, have immunomodulatory effects. At least part of this is due to the upregulation of IL-2 mediated by the ubiquitination of IKZF3. IL-2 restores some of the natural killer cell function. Other immunomodulatory effects observed with IMiDs

include the suppression of the T-regulatory effect, the co-stimulation of CD4 and CD8 lymphocytes, the suppression of angiogenesis and the downregulation of TNFα, IL-6 and RANKL (132). A new generation of the so-called Cereblon modulators have shown excellent efficacy in clinical trials but are still not yet licenced. Iberdomide (CC220) is an example. It binds strongly to the Cereblon at significantly lower concentrations when compared to the other IMiDs (133). IMiDs use in clinical practice is usually in combination with bortezomib, monoclonal antibodies, alkylators, or steroids (130).

C. Alkylating agents and conventional chemotherapy

Melphalan was one of the first agents used in the treatment of myeloma that made a meaningful difference in prognosis in the 1960s followed by cyclophosphamide. Interestingly, those drugs are still in clinical use. Cyclophosphamide is given in combinations with dexamethasone and/or lenalidomide, pomalidomide and bortezomib, while high dose melphalan is still universally the induction of choice before stem cell rescue. Melphalan is also used in combination with bortezomib and steroids (134–136). Doxorubicin and cisplatin have limited use nowadays but are still part of some of the intensive chemotherapy combinations used to rescue patients with aggressive myelomas and those with plasma cell leukaemias (137).

D. Monoclonal Antibodies

Those are relatively new to the clinical practice. Daratumumab and Isatuximab target CD38 on the malignant plasma cells but can also modulate the immune response to the tumour through their effect on the natural killer cells, complement activation and antibody-dependent cell cytotoxicity. They are more effective in combinations with bortezomib, carfilzomib, lenalidomide and pomalidomide.

Elotuzumab targets SLAMF7 receptor on the myeloma cells. SLAMF7 is also expressed on normal immune cells. Soluble SLAMF7 is a growth factor for myeloma cells. Targeting SLAMF7 by elotuzumab exerts its main cytotoxic effect, however, via the activation of the immune cells such as the NK cells and the macrophages against myeloma cells. Elotuzumab has no value as a single agent and is used in combination with IMiDs (138).

E. Novel Therapies

Three categories of novel therapies have gained attention recently and are likely to gain licencing as standard treatments in the near future.

CAR T cells (chimeric antigen receptor T cells). CAR T cells are engineered T lymphocytes that can recognise a target antigen on the myeloma cells (most commonly the BCMA) through a chimeric receptor. Following recognition, the CAR T cell mounts an attack against the myeloma cells. Many are in late clinical trials, and the two CAR T cell for myeloma therapy has recently been approved in Europe and in the States (139). Cilta-cel (Ciltacabtagene autoleucel) employs double BCMA targeting antibodies. The CARTITUDE 1 clinical trail is a single arm phase 1b/2 clinical trial of heavily pre-treated myeloma patients. The overall response rate was impressive at 97%. The median PFS and the median duration of response were 34.9 and 33.9 months respectively. The outcome of this study resulted in the approval of this CAR-T cell therapy (140,141). In CARTITUDE 4 trial patients were randomised between cilta-cel and standard of care as per the physician's choice. The median PFS was not reached vs 11.9 in favour of the cilta-cel arm and the probability of PFS at 12 months was 75% vs 48.6% in the standard arm (142). Ide-cel (Idecabtagene vicleucel) is another

approved BCMA-targeting CAR-T cell therapy. The KarMMa-1 clinical trial is a single-arm phase 2 clinical trial in which patients treated with ide-cel showed a median PFS of 8.8 months (143). In the KarMMa-3 trial, 386 patients were randomised to have ide-cel vs standard of care. The median PFS was 13.3 versus 4.4 months in favour of the ide-cel arm(144). BCMA is not the only target employed in the CAR-T cells designed for myeloma therapy. CAR-T cells targeting GPRC5D are in development. A phase 1 dose escalation study reported 71% overall response rate following GPRC5D CAR-T cell therapy (145).

ADCs (Antibody-drug conjugates). Belantamab mafodotin contains an anti-BCMA antibody attached to a tubulin toxin called MMAF (monomethyl-auristatin F). Once the antibody is bound to the myeloma cells it will be internalised and the MMAF can exert its cytotoxic action in a targeted fashion. Several trials are investigating the safety and efficacy of belantamab mafodotin combinations with other chemotherapeutic agents such as bortezomib (146,147). The DREAMM-2 trial was a phase 2 single agent comparison between two doses of belantamab mafodotin. An overall response was seen in a third of patients and in those who achieved the very good partial response or better the median PFS was 14-16.8 months (148). The combination of Belantamab mafodotin with VRD (bortezomib-lenalidomide-dexamethasone) was explored in the phase 1 DREAMM-9 trial. The results of this trial are still awaited (149). The DREAMM-3 trial compared a single agent treatment with belantamab mafodotin to Pomalidomide and dexamethasone. Although the PFS was numerically longer in the belantamab arm, this was not statistically significant. The interim overall survival analysis also did show a difference between the two arms

(150). Belantamab mafodotin is available in the United Kingdom through the named patient programme route.

BiTEs (Bispecific T cell engagers) are antibodies that are engineered to bring T cells into close vicinity of myeloma cells. Activated T cells then mount an immune response against the myeloma cells. They do this by targeting CD3 on the T cells on one end and targeting the BCMA on the myeloma cells on the other end. Several are in clinical trials and have shown impressive results (151). Teclistamab is a BCMA T cell engager that is approved for myeloma treatment. In the phase 1/2 MajesTEC-1 trial, teclistamab overall response rate was 63% with a median PFS and a median duration of response of 11.3 and 18.4 months. Just over a quarter of patients achieved MRD negativity (151). In the phase 1b TRIMM-2 trial, teclistamab in combination with daratumumab (152). The MajesTEC-3 trial is a randomised comparison between teclistamab and daratumumab and physician's choice (daratumumab-velcade-dexamethasone or daratumumab-pomalidomide-dexamethasone) in patients with 1-3 prior lines of therapy is currently underway (153).

Elranatamab is another BCMA targeting T cell engager. In the phase I Magnetismm-1 clinical trial, elranatamab induced an overall response rate of 70%. The complete remission rate was 30% (154,155). The ongoing MagnetisMM-4 clinical trial is a a phase 1b/2 clinical trial exploring the safety and efficacy of elranatamab in combination with lenalidomide and dexamethasone(156).

Not all T cell engagers target BCMA on the myeloma cells. Talquetamab is another novel T cell engager that targets the GPRC5D receptor on the myeloma cells. The phase 1/2 MonumenTAL-1 clinical trial demonstrated a median PFS of 7.5 months with

an overall response rate in excess of 70% (156). The MonumenTAL-3 is a phase 3 randomised clinical trial of Talquetamab-Daratumumab with or without Pomalidomide versus Pomalidomide-Daratumumab-Dexamethasone that is still ongoing (157).

F. Radiotherapy

Gamma irradiation causes SSBs and DSBs. Cells with defective DNA repair mechanisms will be unable to reverse the effect of radiotherapy and will engage their apoptotic mechanisms causing cell death. In clinical practice, the use of radiotherapy in myeloma is limited to local treatment to reduce pain and lessen organ compromise (such as skeletal fractures). It is used with a curative intent to treat solitary plasmacytomas, where there is no evidence of systemic disease or significant bone marrow involvement (158).

Ionising radiation generates reactive oxygen species which mediate various types of DNA damage. Reactive hydroxyl radicals can cause oxidation of DNA bases, the formation of inter- and intrastrand cross-links, the formation of SSBs and DSBs and DNA-protein cross-links (159).

G. Other therapies

HDACi (Histone Deacetylase Inhibitors). Panobinostat is licenced for the treatment of myeloma in the UK in combination with bortezomib. The rationale for using this class of agents has been detailed earlier.

XPO1 inhibitors (Exportin 1 Inhibitors). XPO1 is a nuclear transport protein that is thought to be responsible for shuttling more than two hundred molecules. Those range from tumour suppressors (p53, Rb), cell cycle regulators (p21, p27), proliferative

and immune regulators (NF-κB, IκB), and chemotherapeutics. XPO1 inhibitors in myeloma were found to selectively activate caspases-3, -7, and -9 and induce apoptosis through various mechanisms including the reduction in cell cycle promoters such as cyclin D1, cyclin E and CDK2/4/6, downregulating BCL-xl, MCL-1 and c-myc, inhibiting NF-κB activation and activating p21 and p27 (160,161). Selinexor (an XPO1) inhibitor was recently approved for use in multiple myeloma by the FDA following the results of the STORM trial (162).

Venetoclax. This BCL-2 inhibitor has been in clinical practice for the management of CLL (chronic lymphocytic leukaemia), especially in those patients with p53 deletion (163). It was recently licenced for the treatment of AML (acute myeloid leukaemia) in combination with azacitidine (164). The role of BCL-2 and MCL-1 in apoptosis induction in myeloma was discussed earlier. BCL-2 inhibition shifts the malignant cells towards apoptosis. The binding of venetoclax to BCL-2 causes the release of BIM (a proapoptotic protein) that is kept from initiation of apoptosis by BCL-2. Free BIM causes oligomerization of BAK and BAX and the initiation of apoptosis through mitochondrial cytochrome c. Most myeloma cells, however, are MCL-1 dependent for survival such that any free BIM released as a result of binding of venetoclax to BCL-2 is mopped up by the excess of MCL-1 and hence apoptosis does not follow (114). In a small minority of patients with myeloma (those with the t(11;14) translocation), there is over expression of BCL-2 and venetoclax was found to be effective in this subgroup of patients (27,112).

1.4 The Rationale and the Aim of the Project

Due to its genetic heterogeneity, multiple myeloma can be viewed as a collection of closely related pathological entities that share in common the malignant transformation of plasma cells but can vary considerably when it comes to the clinical manifestations of this malignant transformation. Indeed, the OS of patients in the ISS 1 risk score was not reached whilst those with double hit myeloma had an OS of less than 2 years (3,165). As explained above, two main pathways have been identified to be behind the initiation of the malignant transformation. The first is the acquisition of a primary chromosomal translocation that causes the upregulation of a D-type cyclin. Even within this group, which represents nearly half of all myelomas, heterogeneity is prominent. Patients who have a chromosomal translocation that causes the upregulation of cyclin D2 tend to have more aggressive disease, shorter remissions and eventually a poorer prognosis. It is logical, hence, to hypothesise that myeloma entities with different D-type cyclins as a consequence of a different initiating event would also behave differently in response to DNA damage, apoptosis and response to novel agents.

To put this hypothesis to test, myeloma cell lines used for this project were chosen based on their underlying cyclin D-type expression. These cell lines were then differentially compared following the induction of DNA damage, proteasome inhibition and apoptosis via mitochondrial pathways. Proteomic analysis comparison was also done following apoptosis induction to examine the underlying pathways changes and to attempt to find out if there is a discernible differential pattern on the molecular level based on the cyclin D-type expression.

Although cyclin D upregulation seems to be almost universal in multiple myeloma, it is however important to note that the chromosomal translocations that lead to cyclin D upregulation happen early during the myeloma genesis path as they can be encountered in the premalignant MGUS stages and in the asymptomatic myeloma stage. This may indicate, as mentioned earlier, that the acquisition of these changes may not be enough to assume a full malignant potential and further downstream second hits are required. These second hits may provide redundancy to the malignant effect of the cyclin D upregulation and maybe more pathogenetic in terms of generating a symptomatic disease. It is therefore plausible that although there is a clear early and mutually exclusive distinction between the initiating events that generate different types of upregulated cyclins, the behaviour of myeloma cells in the malignant stage will rely on the underlying secondary, rather than the initiating genetic events and that those will shape how myeloma cells will respond to events such as cytotoxic stress, DNA damage or apoptosis induction. The focus of this thesis revolves on exploring the impact of cyclin D on those events rather than the ensuing secondary events benefiting from the universality of the initiating events and the fact that secondary events would only happen within specific primary initiating events.

CHAPTER 2:

MATERIALS AND METHODS

Chapter 2: Materials and Methods

2.1 Cell Culture

2.1.1 Cell Lines

JJN3 and U266 were a kind donation by Dr Alex Thompson (University of Nottingham), MM1s cell line was bought from ATCC (Virginia, USA) and OPM-2, MOLP-8 and KMS-12BM were bought from DSMZ (Braunschweig, Germany). The myeloma cell lines were chosen for this project based on their cyclin D-type translocation and p53 status (Table 2.1). The six human myeloma cell lines were put in two groups: three with a cyclin D1 translocation (U266, KMS12-BM and MOLP-8) and three with a cyclin D2 translocation (JJN-3, OPM-2 and MM1s). Within each group, there is one cell line with a p53 wild-type status (MOLP-8 and MM1s respectively). Cytogenetic testing for all myeloma cell lines was facilitated through the courtesy of the Cytogenetics Department at Nottingham City Hospital and confirmed the underlying translocations.

2.1.2 Culture Method

The KMS-12BM and MOLP-8 were maintained by splitting three times a week in RPMI 1640 (Sigma-Aldrich, Dorset, UK) with 20% FCS (Foetal calf serum, First link UK Ltd., Birmingham, UK) and 0.1% Glutamine (200 mMol, Sigma-Aldrich, Dorset, UK). The JJN-3, OPM-2, U266 and MM1s were maintained by splitting three times a week in RPMI 1640 with 10% FCS and 0.1% Glutamine.

The MM1s is an adherent cell line and cell scrapers (TPP, Trasadingen, Switzerland) were used to detach the adherent cells. The OPM-2, U266 and MOLP-8 can be semi-adherent. Cells were detached by firm tapping on the flasks' underside. All cell lines were incubated at 37◦C with 5% CO2 (HeraCell 150I, ThermoFisher Scientific, MA,

USA). Cells were grown from an early passage stocks and cell lines were discarded after three months of passaging and replaced with new batches from previously frozen cells. After the new cell lines are established, aliquots from each cell line were frozen to replenish the frozen cell lines stores.

Seeding density for various experiments was chosen based on advice from Dr Martin Grundy based on previous experience with leukaemia cell lines. The seeding frequency depended on the anticipated incubation period required (lower density for longer incubation periods) and whether protein extraction (such as for Western blots experiments) was required in which case, a higher cell volume was used. Specific experiments using the myeloma cell lines for the sole purpose of assessing the seeding concentrations were not carried out in this project.

2.1.3 Cell Lines Mycoplasma Testing

All cell lines were subjected to regular testing for mycoplasma infection using the MycoAlert kit (Lonza, Basel, Switzerland) and were found to be consistently mycoplasma negative.

2.1.4 Cell lines verification

Earlier during this project, it became apparent to us the OPM-2 cell line was not behaving as expected based on the literature. Discrepancies included its rapid doubling time and its lack of cyclin D2 expression on Western blot analysis. STR analysis confirmed that this indeed was not an OPM-2 cell line. Further experiments using this cell line were discontinued and the early results were discarded. It is worth noting that this cell line was sent to us as a gift. Therefore, we acquired a genuine

OPM-2 cell line from DSMZ and this was used thereafter in the project. Subsequent STR analysis of all the six cell lines used confirmed that they are genuine.

2.1.5 Cell Counting Using the Trypan Blue Exclusion Method

Cells in suspension were agitated briefly to ensure uniform distribution within the flasks then a 10 µl aliquot was taken and mixed with 10 µl of Trypan Blue (Sigma-Aldrich, Dorset, UK). 10µl of the mixture was then taken and loaded into the loading notch of a haemocytometer (Sigma-Aldrich, Dorset, UK) covered by a coverslip until the counting chamber is full. Viable cells (with no Trypan blue uptake) were counted in at least two opposing squares of the haemocytometer under a light microscope (Olympus, Tokyo, Japan). As the volume that can be contained by any of the haemocytometer's squares is 0.1 mm^3, the number of viable cells can be calculated from the following equation:

$$Number\ of\ cells\ per\ ml = \frac{Number\ of\ viable\ cells\ \times Dilution\ factor}{Number\ of\ squares\ counted} \times 10^4$$

Where, the dilution factor would be 2 for 1:1 mix with Trypan Blue.

2.1.6 DNA Extraction and Cell Line Verification Testing

DNA extraction from all the myeloma cell lines was performed using Qiagen DNA extraction kit (Qiagen, Hilden, Germany). Cells in suspension were counted using the Trypan Blue Exclusion method outlined in section 2.1.4 and 1 x 10^6 cells were taken

Table 2.1: The human myeloma cell lines used in this project together with their cyclin D type properties, p53 status and some other features. The other genetic changes and the doubling time data were obtained from the manufacturer's product information.

Cell line	IGH translocation	P53 Status	Other Genetic Changes	Doubling time	Culture medium
U266	t(11;14) (D1)	Loss	RB-1 null, hypodiploid, 1q gain, 1p gain ATM/ATR/PKC expressing	55 h	RPMI 1640+10% FCS+ 0.1% Glutamine
MOLP-8	t(11;14) (D1)	WT	Near diploid, 1q amplification, 1p gain	40 h	RPMI 1640+20% FCS+ 0.1% Glutamine
KMS12-BM	t(11;14) (D1)	Mutated	Hyperdiploid, 1q (3-4 copies)	60 h	RPMI 1640+20% FCS+ 0.1% Glutamine
MM1s	t(14;16) (D2)	WT	Dex sensitive, 1q gain ATM/ATR/PKC expressing	72 h	RPMI 1640+10% FCS+ 0.1% Glutamine
JJN-3	t(14;16) (D2)	No expression	C-myc (8;14), Hypotriploid, 1q amplification, 1p gain, ATM/ATR expressing	20-35 h	RPMI 1640+10% FCS+ 0.1% Glutamine
OPM-2	t(4;14) (D2)	Mutated	1q amplification, c-myc (8;14), hyperdiploid, 1p gain PKC expressing	50-60 h	RPMI 1640+10% FCS+ 0.1% Glutamine

and spun down at 300g for 5 minutes. After discarding the supernatant, the pellet was re-suspended in 200 µl of PBS (Oxoid, Basingstoke, UK) and 20 µl of proteinase K and 200 µl of Buffer AL were added followed by incubation at 56◦C in a heat block for 10 minutes. Following that, 200 µl of absolute ethanol (Honeywell Research Chemicals, Germany) was added and the mixture was transferred to QIAmp Mini spin column and spun down at 6000g for 1 min. After discarding the filtrate, 500µl of AW1 buffer were added and spun down as in the previous step. The filtrate was discarded and 500 µl of AW2 buffer were added after which the samples were spun down again at 20,000g for 3 minutes. Finally, 200µl of distilled water was added to the supernatant then the DNA was spun down at 6000g for 1 minute and stored at -20◦C. The extracted DNA was used to authenticate the cell lines using multiplex short tandem repeat analysis (Promega, UK). STR analysis was done regularly throughout the life of this to maintain the confirmation of the identity of the cell lines used. This process was kindly done by Dr Claire Seedhouse.

2.1.7 Primary Samples

Primary patient samples were obtained from excess bone marrow material after informed consent. Histopaque 1077 (Sigma-Aldrich, Dorset, UK) was used for density gradient separation of mononuclear cells before the plasma cells were isolated using CD138 magnetic beads as per the manufacturer's protocol (Miltenyi Biotec, Germany) (166). This work was performed by Dr Martin Grundy (Academic Haematology, University of Nottingham).

Table 2.2 Primary samples characteristics			
Sample ID	**Gender**	**Age (years)**	**Cytogenetics**
MM2	Female	69	t(4;14) FGFR3-IGH rearrangement
MM4	Male	85	Normal
MM5	Female	71	1q gain
MM18	Male	75	ATM gain
MM19	Male	41	Normal
MM22	Male	67	1p and 1q gain, TP53 gain, IGH gain
MM23	Male	52	1q gain

2.2 Cell Lines Irradiation

Cell lines were counted the day before irradiation using the Trypan Blue Exclusion assay. 4 ml of cells at 5 x 10^5 cells/ml per condition were incubated in T25 Corning flasks (Corning Inc., New York, USA) to allow for exponential growth. The small volume in each flask was to ensure adequate and uniform penetration of the X-ray beams. On the day of the experiment, the flasks were transferred on ice for irradiation at the Clinical Oncology Department (Nottingham City Hospital, Nottingham, UK). Irradiation was done using RS225 Xstrahl X-ray cabinet irradiation system (Xstrahl Limited, Surrey, UK). The use of this machine was kindly facilitated by Prof Stewart Martin (Head of Translational and Radiation Biology Research Group, Clinical Oncology, Nottingham City Hospital). The irradiator has a rotating plate to allow for even distribution of the X-ray beams. Controls were left on the bench for the same amount of time taken to

irradiate the experimental flasks. At the end of irradiation, all flasks were transferred quickly back on ice and processed/incubated immediately.

The irradiation dose used was 10 Gy and the incubation time post-irradiation was 0 hours, 4 hours, and 24 hours. Controls were treated exactly as the experimental flasks (except with no radiation). The 10 Gy dose and the time points choices were based on previous work and also the results of pilot experiments (3.4).

2.3 Neutral Comet Assay

2.3.1 Comet Assay Principles

As means of assessing DNA damage, this assay was first reported in 1984, by Ostling and Johanson (167), who migrated irradiated then lysed mammalian cells through an agarose gel cast on a microscope slide using a small electric current. The nucleoids, after staining with a DNA binding agent, showed proportional increases in the degree of migration according to the dose of irradiation used (167). This single cell gel electrophoresis technique, subsequently termed the comet assay, underwent several modifications to allow for more DNA migration. The neutral version of the comet assay is considered to be more sensitive to DSBs compared to the alkaline version which is more useful to assess SSBs (168). A fixed number of treated cells is mixed with a low melting point agarose gel in a liquid state and allowed to solidify on a glass slide. The choice of lysis used is dependent on whether SSB detection is also needed as the latter would require double-stranded DNA unwinding using an alkaline pH lysis buffer. A neutral lysis buffer is sufficient for the detection of DSBs but may not be very sensitive to SSBs. As damaged DNA is migrated out of the nucleoid it leaves a trail behind thereby producing a comet-like shape (See Figure 3.2B). The degree of migration and

the amount of DNA in the tail are proportional to the degree of DNA damage after efficient lysis (168). The product of DNA fraction in the tail and the tail length, the tail moment, is popularly used to evaluate the comets. Various software is available for analysis and capture of the comets (168).

This method, though, is not without its challenges and limitations. Technical dexterity is required when combining the washed cells with the molten gel as delay in smearing the mixture over the slides can result in the gel solidifying before or very shortly after the smearing processes with a potential loss of the sample. The positioning of the slides in the electrophoresis tank needs to be done at an identical level since any slanting or misorientation will affect the direction of the comets on the slides and this will subsequently affect the scoring.

An adequate number of comet cells also needs to be scored to combat any heterogeneity. The degree of migration of the DNA-damaged cells can vary according to their position within the slide since the gel tends to be thinner at the edges. Therefore, it is a good practice to count cells from the centre and to avoid edges to reduce heterogeneity and increase accuracy (169).

2.3.1.1 Application of comet assay in myeloma

The comet assay has previously been used to assess DNA damage in multiple myeloma. Supiot al used the alkaline comet assay to establish synergy between doxorubicin and alpha radioimmunotherapy (170). There was an increase in DNA strand breaks with the combination compared to single agents alone in the RPMI 8226 cell line but not in LP-1 or U266 cell line. Another study used the decrease in the tail moment in irradiated myeloma primary samples due to inter-strand crosslinking after

exposure to melphalan as a surrogate for DNA damage repair. When exposed to gamma irradiation, melphalan naïve patients samples showed a reduction in the tail moment that remained stable after 40 hours of incubation while cells from patients who relapsed following melphalan exposure showed an increase in the tail moments back to the baseline indicating the repair of DNA damage (171). In another study, the combination of doxorubicin and Selinexor in resistant myeloma cell lines increased the degree of DNA damage measured through the neutral comet assay as compared to both single agents alone (172).

The assay was done based on the Trivegen Comet Assay protocol.

2.3.2 Comet Slides Preparation

Cells were irradiated as described above and processed immediately or incubated for 4 hours and 24 hours to allow potential resolution of DNA damage before processing. LMAgarose Gel (Cat #4250-050-02, Trivegen, Gaithersburg, Maryland, USA) was heated to 92◦C for 10 minutes in a water bath then transferred in a liquid state and maintained at 42◦C in another water bath. Viable cells were counted using the Trypan Blue Exclusion Assay as described above and 2 x 10^4 cells/ml were harvested into 1.5 ml labelled Eppendorf tubes (Starstedt Ltd., Numbrecht, Germany) and centrifuged at 400g for 5 minutes. All processing thereafter was done on ice. The supernatant was discarded, and the pellets were washed with 50 µl of ice-cold PBS and spun down at 400g for 5 minutes. The supernatant was removed and 50 µl of ice-cold PBS was added. Following that, 450µl of the molten LMAgarose gel at 42◦C was added to each sample and 75µl of the mixture was taken off immediately and spread on labelled CometSlides (Trivegen, Gaithersburg, Maryland, USA). The slides were then incubated

at 4◦C in the dark on a flat surface for 10 minutes and immersed in lysis buffer (Cat#4250-050-0, Trivegen, Gaithersburg, Maryland, USA) and kept refrigerated at 4◦C in the dark overnight.

The next day, the slides were washed in cold 1x TBE buffer (ThermoFisher Scientific, MA, USA) and then aligned in an electrophoresis tank (Geneflow Ltd., Lichfield, UK) at equidistance from the electrodes, immersed in 2 litres of cold 1xTBE and incubated in the dark for 30 minutes. The electrophoresis was done for 30 minutes at 1V/cm (22 Volts) using Power Pack 300 Electrophoresis Unit (Biorad, California, USA) after which the slides were washed with ddH20 three times and then fixed with 70% ethanol for 5 minutes. The slides were then left to air dry in the dark until analysis.

2.3.3 Comet Slides Analysis

100 µl of Sybr Gold working solution (1 µl Sybr Gold (10,000 x in DMSO), Invitrogen, ThermoFisher Scientific, MA, USA) in 30 ml of 1x Tris EDTA buffer (Sigma-Aldrich, Dorset, UK) at pH 7.5) was added to each dried agarose spot on the CometSlides and incubated for 30 minutes in the dark then washed with ddH20 and incubated at 37◦C in the dark until completely dry. A fluorescence microscope (Olympus BX40 fluorescence microscope, Tokyo, Japan) was used to view the slides and the comets were captured using Comet Assay IV analysis software (Perceptive Instruments, Bury Saint Edmunds, UK). Two slides were made for each condition and at least 100 comets were captured for each slide. Scoring was done in a dark room to avoid rapid fading of the Sybr Gold stain. Overlapping and peripheral comets were avoided for scoring as recommended (168). The averages of the scored Tail moments were taken and used

for analysis. Unless indicated in the results section, each experiment was repeated independently at least two times.

2.4 γH2A.X Phosphorylation by Flow Cytometry

2.4.1 γH2A.X Phosphorylation principles

The organisation of the DNA double helix into nucleosomes each composed of DNA genetic material intertwined with 4 types of highly conserved proteins, called histones, is what allows the packaging of phenomenal lengths of DNA into the human cells (173). In addition to geometric stability, histones affect transcription and DNA damage repair. One component, histone H2A plays a central role in the double-stranded DNA damage response. H2A.X is a variant of H2A that has a variable abundance within the histone pool, the phosphorylation of which at position Serine-139 (γH2A.X) by ATR correlates with the presence of DSBs in a temporal, numerical and spatial fashion and may drive the focal recruitment of various proteins that are implicated in the DNA damage response such as Rad50, MDC1, NBS1 and MRE11 (173).

It is no wonder, therefore, that the detection of the phosphorylated γH2A.X by specific anti γH2A.X antibodies using flow cytometry or immunohistochemistry has been considered a sensitive methodology for the identification of DNA damage (174). The effect of IR as a cause of γH2A.X phosphorylation has been established (94). Foci can be detected after exposure to doses as low as 1.2 mGy (159). Several established cytotoxic and experimental agents have been shown to induce γH2A.X phosphorylation (175–177).

2.4.2 γH2A.X phosphorylation measurement by flow cytometry

Cells were counted and irradiated as described earlier (sections 2.1.5 2.2). $5x10^5$ cells were then harvested, spun down and washed with PBS then fixed with 2% paraformaldehyde (ThermoFisher Scientific, MA, USA) and 1% methanol (Honeywell Research Labs, Germany) in PBS and incubated on ice for 20 minutes. Thereafter, the cells were spun down and washed with PBS three times. The cells were then permeabilised using 100 µl of 1X permeabilisation solution (10x permeabilisation solution contains 5% saponin (Sigma-Aldrich, Dorset, UK), 100mM HEPES (1M, Gibco, Life Technologies, ThermoFisher Scientific, MA, USA), 1.4M NaCl (ThermoFisher Scientific, MA, USA), 25mM CaCl2 (ThermoFisher Scientific, MA, USA) in PBS filtered in 0.2µl sterile filters and diluted 1:10 in ddH2O before use).

The fixed and permeabilised cells were then incubated on ice for 20 minutes with Anti-Phospho H2A.X (ser139) FITC conjugated (#16-202, Merck Millipore, MA, USA) at a working concentration of 4µg/ml. After that, the samples were washed with 1% saponin in PBS (diluted 1:10 in ddH2O before use) then the tubes were spun down and washed with PBSAA containing 1% BSA (Sigma-Aldrich, Dorset, UK) and 0.1% Sodium Azide (Sigma-Aldrich, Dorset, UK) in PBS before re-suspending in 300µl of PBSAA. The samples were kept in the dark at 4◦C before analysis on the BDFACS Canto II flow cytometer (BD Biosciences, New Jersey, USA). Debris was gated out based on the forward and side scatter plot and FITC positive cells were gated versus cell count. At least 10,000 cells were captured and the percentage of FITC-positive cells was analysed. Analysis was done using BDFACS Diva flow cytometry software (v6.1.3, 2009, BD Biosciences, New Jersey, USA).

2.5 Cytotoxic Molecules

Venetoclax (ABT-199) was obtained from Bioquote Limited (York, UK), S63845 from Active Biochem (Kowloon, Hong Kong) and bortezomib from Sigma-Aldrich (Dorset, UK). Stock solutions were prepared in DMSO and stored in -20°C. Dilutions to desired concentrations were done in RPMI 1640 medium.

2.6 Assessment of Synergy

Two methods were used to assess synergy in this project. For the Alamar Blue experiments done to assess the combination effect of MCL-1 and BCL-2 inhibition, the Chou-Talalay method was used. In this method, the combination index (CI) was used to indicate the presence of synergy, antagonism or additive effect (CI values <1, >1 or =1 respectively) (178). The Chou-Talalay method uses the mass-action law principle to derive a median-effect equation, the output of which is the CI. In order to be able to use this method to obtain the CI at multiple drug concentrations using the Compusyn software, the authors recommend constant-ratio drug combinations (equal ICx_1/ICx_2 values at all drug combination points, where ICx_1 and ICx_2 are the inhibitory concentrations for a value x for drug 1 and 2 respectively). Using Compusyn with constant-ratio drug combination will enable the use the automated median-effect calculation. The authors of this method assert that non-constant drug ratios can also be used to assess for synergy, however the calculations will have to be done for each specific combination point (178). To benefit from the simulated, software-based CI calculations, the concentrations used for venetoclax and S63845 were, therefore, of a constant ratio.

When the Annexin V binding assay was used to examine the effect of MCL-1 and BCL-2 inhibition, The Bliss independence model was used to assess for synergism. Synergism is perceived if the observed effect from combination treatment is higher than the anticipated additive effect from single agent treatment as per the equation (179):

*Bliss Independence additive effect = Fa + Fb - (Fa*Fb)*

Where, Fa and Fb are the single agent fractional effects of drugs a and b respectively. As shown in Figure 5.2, the combination treatment was synergistic in all of the six myeloma cell lines.

2.7 Western Blotting

2.7.1 Preparation of the Lysis Buffer

Lysis buffer stock was prepared in ddH2O by adding 50mM Tris pH6.8 (0.605%), 150mM NaCl (0.876%), Triton X-100 (1%), SDS (0.1%), 10mM EDTA (0.372%) and Deoxycholic acid (0.5%) and stored at 4°C. Protease inhibitors stored at -20°C were added just before use to ensure stability as follows; 1mg/ml Leupeptin, 2mg/ml Aprotinin, 1mg/ml Pepstatin, 200nM NaF, 100mM Sodium Orthovanadate and 200mM PMSF.

2.7.2 Preparation of the Lamellae Buffer

4x Lamellae buffer was prepared by mixing 0.5M Tris HCl (pH 6.8), Glycerol (100%), SDS (10%), and Bromophenol Blue (0.2%). 60 µl/ml of β Mercaptoethanol (Sigma-Aldrich, Dorset, UK) was added before use.

2.7.3 Preparation of TBS-T

10x TBS-T was prepared in ddH2O by adding Tris base (2.42%) and NaCl (8.76%). The pH was adjusted to 7.4-7.6 before adding Tween 20 (1%) (ThermoFisher Scientific, MA, USA).

2.7.4 Preparing the Lysates

The cell concentration used for Western blots was 2 x 10^6 cells/ml. Cells were obtained after treatment with radiation or drugs in 8 well plates or T25 flasks. Processing was done on ice for the steps below. The cells were spun at 400g for 5 minutes at 4°C then the pellets were washed twice with 10 ml of ice-cold PBS before transferring the pellets into previously autoclaved Eppendorf tubes on ice. 1 ml of lysis buffer was added per pellet then the samples were left on a shaker at 4°C for 30 minutes. Sonication was done after this step for 10 seconds per sample before a further 200nM of PMSF was added to each sample. A further incubation step on the shaker at 4°C was conducted before a centrifugation step at 10,000g at 4°C which was done for 10 minutes. The lysates were transferred to pre-cooled previously autoclaved Eppendorf tubes and stored at -80°C.

2.7.5 Determination of the Protein Concentration and Preparation of Aliquots for Gel Electrophoresis

Protein concentration from lysates was determined using Nanodrop (ThermoFisher, MA, USA). A blanking step was done at the beginning using lysis buffer. The protein concentration used for each well was 50µg/µl. The volume was made up to a total volume of 40µl/well using lysis buffer and 10µl of 4x Lamellae buffer with Mercaptoethanol.

2.7.6 Gel Electrophoresis and Protein Transfer

Gel electrophoresis and protein transfer steps were done using Invitrogen Mini Gel Tank and Mini Blot Module (Invitrogen, ThermoFisher Scientific, MA, USA) as described by the manufacturer's product information. Briefly, ready-made gels were washed 3 times with 1x running buffer and then immersed in 1x running buffer in the Mini Gel tank. Samples were loaded into the wells in the Mini Gel. Rainbow recombinant molecular weight marker (Amersham, Sigma-Aldrich, Dorset, UK) was used to mark progress and identify the molecular weights of the bands. This was loaded at a volume of 10 µl in at least one well per gel. The Mini Gel Tank was connected to a Power Pack and run at 200V for 20-30 minutes.

The Mini Blot Module was used for transfers. Briefly, the freed gels after electrophoresis were aligned against PVDF membrane (washed briefly in 100% Methanol) and sandwiched in between sponges and filter papers soaked in 1x transfer buffer with 10% Methanol. The module was then fixed inside the Mini Gel Tank and connected to a power pack. The transfer was done for 1h at 20V.

Following the transfer, the membranes were washed with ddH2O and then blocked with 5% non-fat milk (BioRad, California USA) in 1xTBS-T for 1 hour on the shaker at room temperature.

2.7.7 Probing with Primary and Secondary Antibodies

Membranes were washed x3 with 1x TBS-T then incubated with primary antibodies in 1% non-fat milk in 1x TBS-T with agitation either overnight at 4°C or for 2 hours at room temperature. A washing step with 1xTBS-T was done as above before the membranes were incubated with agitation with the appropriate secondary antibody

in 1% non-fat milk in TBS-T. For a list of the primary and secondary antibodies used and the working concentration, please see Table 2.3.

Table 2.3: A list of the primary and secondary antibodies used in this project together with the source and the concentration

Antibody	Primary / Secondary	Category Number/Source	Concentration (1% milk in TBS-T)
Mouse anti-actin (loading control)	Primary	ab8226 (Abcam, Cambridge, UK)	1:2500
Lamin anti-rabbit (loading control)	Primary	ab133645 (Abcam, Cambridge, UK)	1:2500
Rabbit anti-cyclin D1	Primary	ab134175 (Abcam, Cambridge, UK)	1:2000
Rabbit anti-cyclin D2	Primary	ab207604 (Abcam, Cambridge, UK)	1:2000
Rabbit anti-MCL-1	Primary	SC-819 (Santa Cruz Biotechnology, Texas, USA)	1:500
Mouse anti-BCL-2	Primary	SC-7382 (Santa Cruz Biotechnology, Texas, USA)	1:2000
Goat anti-rabbit	Secondary	ab26721 (Abcam, Cambridge, UK)	1:10 000
Rabbit anti-mouse	Secondary	ab6728 (Abcam, Cambridge, UK)	1:10 000

2.7.8 Membrane Development and Band Detection

Following incubation with the secondary antibody, the membranes were washed with TBS-T as above then incubated for 1 minute in ECL Chemiluminescence Buffer (GE Healthcare Life Sciences, Chicago, USA) at room temperature and developed by incubation in the dark with Hyperfilm (GE Healthcare Life Sciences, Chicago, USA) before washing in a developer then a fixer solution.

2.7.9 Western Blot Results Data Analysis

Bands obtained after membrane development were quantified using the ImageJ software (NIH, USA, version 1.8.0_311). The band densities were converted to a numerical representation and represented as averages of the control.

2.8 Annexin V Binding

2.8.1 Annexin V Binding Assay Principles

Cells undergoing apoptosis feature a cell membrane molecular change that probably acts as a beacon to alert macrophages to the presence of the dying cell. Phosphatidyl serine, which is normally located facing the cytosol, flips side and becomes exposed to the exterior. More phosphatidyl-serine becomes exposed as the process of apoptosis progresses. Annexin V is a calcium-dependent protein that belongs to the phospholipid-binding protein family. It has been shown that Annexin V binds with very high affinity to the exposed phosphatidyl-serine and may play an important role in the phagocytosis process. The detection of Annexin V binding by flow cytometric analysis has thus been used as a sensitive marker for cells committed to apoptosis. For the purpose of the Annexin V assay, a FITC-conjugated anti-annexin V antibody is used to stain the cells undergoing apoptosis, often in combination with a nuclear stain such as propidium iodide to exclude necrotic cells.

2.8.2 Annexin V Assay

The Annexin V Assay for apoptosis detection was done using the TACS Annexin V kit by Trivegen (Gaithersburg, Maryland, USA) using the manufacturer's protocol. Briefly, treated cells and controls were collected by centrifugation at 400g for 5 minutes then

washed with PBS. The pellets were then incubated with an incubation reagent containing 1% Annexin V-FITC conjugated Antibody and 10% Propidium iodide in ddH2Ofor 15 minutes in the dark at room temperature. Following this step, 1x binding buffer was added and the samples were assayed on a flow cytometer within one hour for maximal signal.

2.9 Alamar Blue Assay

2.9.1 The Alamar Blue Principles

The Alamar Blue assay exploits the reducing capabilities of living cells carried out by enzymes, such as NADH and NADPH to induce a chemical change in a substance called resazurin. This non-toxic, water-soluble and cell membrane-permeable compound is the active ingredient in the Alamar blue assay. In its oxidised form, resazurin is blue in colour and non-fluorescent. The action of reducing machinery, in viable, actively metabolising cells causes the change of resazurin to a pink, fluorescent compound. This colour change is utilised as a surrogate for cell viability and can be detected using colourimetric or fluorometric assays (180).

The Alamar Blue assay was founded by Alamar biosciences in the early 90s and has been evaluated as a measure for viability, apoptosis and chemosensitivity. The Alamar Blue assay is simple, rapid, and reproducible. Since resazurin is non-toxic, it allows for an ongoing evaluation of cells in culture. These properties are not shared by other assays commonly used for assessing viability and cytotoxicity such as the MTT assay.

In the experiments within this chapter, the Alamar Blue assay was used to create a dose-response evaluation for MCL-1 and BCL-2 inhibition and to assess for synergy with dual inhibition.

2.9.2 The Alamar Blue Assay

Cells were seeded at a concentration of $2.5x10^6$/ml in triplicates in 96-well plates in exponential growth phase and incubated with drugs for 48 hours in an incubator. At the end of this incubation period, 10µl of Alamar Blue (ThermoFisher Scientific, MA, USA) were added to each well. Following a 4h incubation with Alamar Blue, the plates were assayed for absorbance at 570nm using a plate reader.

2.10 Cytochrome c Release Assay

2.10.1 Cytochrome c Release Assay Principles

As mentioned in the introduction chapter (1.2.6), the induction of apoptosis via the mitochondrial pathway requires the release of factors such as BIM and BAD. Those agents will promote the oligomerisation of BAK and BAX leading to the permeabilization of mitochondrial outer membrane. This in turn releases cytochrome c and the latter causes caspases activation and therefore commitment to apoptosis. The detection of the release of the cytochrome c, is therefore considered to be indicative of cells commitment to apoptosis and has been developed to allow a rapid detection of apoptosis without the need for prolonged incubation otherwise required for conventional methods.

2.10.2 Cytochrome c Release Assay using Flow Cytometry

Myeloma cell lines in exponential growth phase and primary samples were incubated for 4 h with venetoclax, S63845 or the combination of both agents then fixed and permeabilised with 2% paraformaldehyde and saponin before staining with AlexFluor 647 Anti-Cytochrome c Antibody (Abcam, Cambridge, UK). The cells were then acquired on BDFACS Canto II flow cytometer and analysed using BDFACS Diva flow

cytometry software (166). This work was performed by Dr Maritn Grundy (Academic Haematology, University of Nottingham).

2.11 Mass Spectrometry

The same lysates prepared for Western blots were used in 50ug aliquots for the mass spectrometry experiments. Mass spectrometry analysis was performed at the Van Geest Lab (Nottingham Trent University, Nottingham, UK) by Dr Amanda Miles. Briefly, 4 µl lysate volume was injected into YMC Triart-C18 pre-column (0.3 x 5 mm, 300 µm ID) (YMC, Kyoto, Japan) before gradient elution onto the YMC Triart-C18 analytical column. Samples were then analysed using the SWATH (sequential window acquisition of all theoretical fragment ion spectra) and then SWATH data were analysed using Sciex OneOmics software (AB Sciex LLC, MA, USA) extracted against the locally generated library using bottom-up proteomics. Normalised protein data were first generated, followed by a calculation of the fold changes in the protein levels accompanied by the peptide confidence percentage. Bottom-up proteomics is used to quantify the protein levels in the samples through the quantification of the peptides from the trypin-digested proteins. The Assembler application determines changes in protein expression from digested proteomics samples when analysing SWATH® Acquisition data. Before protein fold changes are determined, a normalisation step is required. A normalised peak area for every sample along with a reproducibility metric (MLRw-most likely ratio reproducibility weight) is calculated. An MLR value threshold of 0.15 is used to ensure stringent filtering and increase the confidence in the data. The outcome of the normalisation step is a peptide ratio and confidence for each experimental condition relative to the control for all of the

peptides in the SWATH acquisition data. Protein fold changes are then calculated in the up and down directions. The peptides showing a unidirectional change between experimental conditions are assembled and their median ratios are calculated together with a confidence value in the unidirectionality of those changes. The final reported protein fold change is that of the direction with the most confidence.

Further analysis of the mass spectrometry data was done using the Ingenuity Pathway Analysis Software (IPA) from Qiagen. First, a regression analysis was performed using each replicate within the treatment group against the control and the absolute values of the standard residuals were taken and averaged for each treatment condition. Then, a Student t-distribution analysis was done using the values obtained in the first step. The Bonferroni P-value was calculated from the product of the Student t-distribution and the number of proteins in each condition. The results were then ranked in ascending order. The ranked P-value was obtained by dividing the Bonferroni P-value by the corresponding rank. Following that, to reduce the false discovery rate, the Benjamini-Hochberg P-value is calculated from the ranked P-value.

The four values calculated above (averages of protein expression, the Student t-distribution values, the Benjamini-Hochberg P-values and the proteins fold changes) were analysed using the IPA to generate, heat maps and pathway analysis data.

2.12 Statistical Analysis and Software

Unless otherwise specified, the data in this thesis were plotted from the means of independent experiments. Error bars were plotted from the standard deviations. Unpaired T-test and 2-way ANOVA were used for statistical analysis. P values <0.05 were considered to be significant. Graphs and statistical analysis were done using

GraphPad Prism (v 7.04, GraphPad Software Inc., California, USA). The IC_{50} data and the combination indices were calculated using Compusyn (v 1.0, PD Science LLC, USA). The analysis of the proteomics data was performed using the IPA (Ingenuity Pathway Analysis software, Qiagen, Hilden, Germany).

CHAPTER 3:

DNA DAMAGE RESPONSE ASSESSMENT IN CYCLIN D1- AND CYCLIN D2-EXPRESSING MYELOMA CELL LINES

Chapter 3: DNA Damage Response Assessment in Cyclin D1- and Cyclin D2-Expressing Myeloma Cell Lines

3.1 Introduction

The molecular pathogenesis of the initiating events in myeloma was discussed in depth in Chapter 1 (Section 1.2). In around half of the myelomas, the initiating event involves a chromosomal translocation that causes the upregulation of a D-type cyclin (14). It was previously shown that, in response to DNA damage by ionising radiation (IR), cyclin D1 was downregulated while there was no effect on cyclin D2 (108).

To investigate the effect of DNA damage induced by IR on myeloma cell lines, two well-established methods have been used, the comet assay and the detection of γH2A.X phosphorylation.

3.1.1 The Use of IR to Induce DNA Damage

IR tips the balance between reactive oxygen species and the body's defensive antioxidant system towards the former. It can directly cause damage to the DNA through a process called one-electron oxidation or indirectly by the generation of highly reactive hydroxyl radicals (159). The latter accounts for around two-thirds of the damage. The outcome of these processes are different types of DNA damage such as base oxidation, DNA-protein cross-links, SSBs and DSBs. The latter are highly toxic and occur when the DNA is severed on one or more sites on both DNA strands within two helix loops.

A single Gy of IR is expected to cause up to 40 DSBs, around 30 DNA-DNA cross-links and around 150 DNA-protein cross-links per cell (159). The effect of IR can vary

depending on the phase of the cell cycle at the time of exposure. Cells in G0 are radioresistant due to the lack of DNA replication. In contrast, the M-phase is the most sensitive to IR. G1 and G2 radiosensitivity are more than that observed with the S-phase (181).

We envisaged the use of IR to induce DNA damage rather than standard DNA damaging chemotherapeutics. The rationale for this was the easy applicability of IR and to bypass the heterogeneity imparted by chemoresistant cellular mechanisms (such as PgP pumps) that would have been encountered if a chemical DNA damaging agent was used instead. There were two points to consider when choosing a working dose of IR for this project. First, the dose should not be lethal but enough to cause sufficient DNA damage to allow for direct comparison and, second, the dose of irradiation to be used needed to be sufficient to downregulate cyclin D1.

Previous research has demonstrated the downregulation of cyclin D1 using IR. Exposure to SK-MEL-28 cells to 20 Gy caused downregulation of cyclin D1 due to DSBs (182) while another study demonstrated phosphorylation-dependent proteolysis of cyclin D1 using Gamma Irradiation from a 137 Cs source (104). Similarly, cyclin D1 downregulation was observed as early as 10 minutes after exposing cell lines to doses of 6-20 Gy of gamma irradiation (183). The impact of IR on cyclin D2 is less clear. There is no downregulation of cyclin D2 following DNA strand breaks (104,183). 10 Gy of IR was recently used to study the effect of the cyclin D type on the cell cycle response to DNA damage in myeloma cell lines (108). We elected to use that dose for this project given the similarities in the experimental conditions.

3.2 The Aim of this Chapter

The experiments in this chapter aimed at investigating if there is a differential response between the cyclin D1- and the cyclin D2-expressing myeloma cell lines in response to DNA damage induced by IR. This differential response was investigated by the direct assessment of DNA damage using the comet assay, by measuring the cellular response to DSBs using the γH2A.X phosphorylation and by assessing the effect of IR on cell count.

3.3 Results

3.3.1 IR Dose Optimisation

3.3.1.1 A pilot comparison between 5Gy and 10 Gy IR showed no difference in terms of the comet assay

As mentioned in the introduction of this chapter, the dose of IR chosen for this project was 10Gy and this was based on previous work (108). However, initial pilot experiments were done using the comet assay to establish if there is a difference in the tail moments between 5Gy and 10Gy of IR in two cell lines.

The comet assay did not show a difference in terms of tail moments between the two doses of IR (Figure 3.1). Hence, to ensure uniformity and confidence in D1 downregulation a dose of 10 Gy was used in all subsequent experiments.

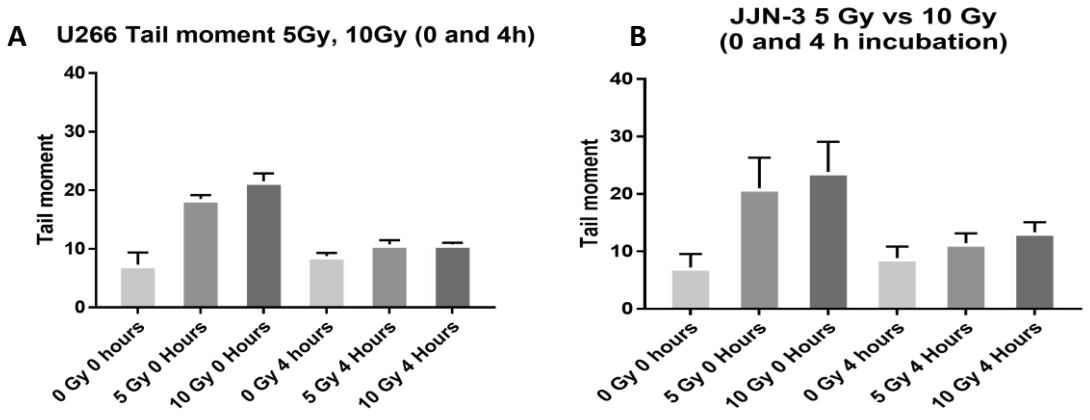


Figure 3.1: A pilot assay comparison of the tail moments of (A) U266 cell line and (B) JJN-3 cell line after exposure to 5Gy and 10Gy IR. Analysis was done immediately following IR and after 4 h incubation. Tail moments at 0 h time point have increased as compared to the baseline but there was no significant difference between 5Gy and 10Gy. Bars represent averaged tail moments from three independent experiments; error bars represent the standard deviation.

3.3.2 Measurement of DNA Damage Following IR Using the Comet Assay

The six myeloma cell lines were seeded at a concentration of 5 x 10^5 cells/ml and exposed in the exponential growth phase to 10Gy of IR. Controls were treated in exact steps apart from the irradiation process. To assess the dynamics of DNA damage/repair in the cell lines, irradiated cells were either processed immediately for the comet assay or incubated for 4 h and 24 h then processed. The time points were chosen based on previous literature that suggested D1 down-regulation occurring as early as 1 hour after exposure to DNA damage (108). All cell lines, treated and controls, were transported on ice in between irradiation and processing or incubation to slow down the process of DNA damage repair. Trypan blue assay was used to check viability, cell count and to select a fixed number of cells to be assessed for DNA damage

using the neutral Comet assay (2.3). A representative example of the comets in the JJN-3 cell line as observed under a fluorescent microscope is shown in (Figure 3.2).

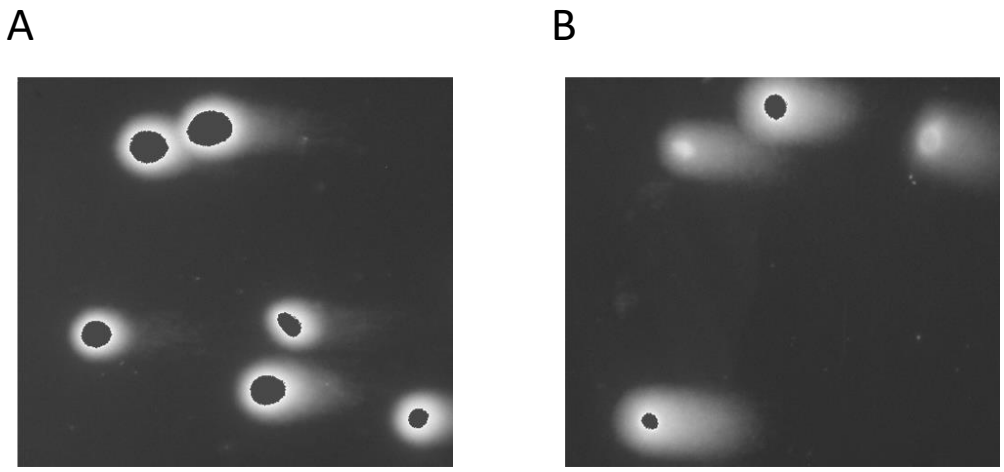


Figure 3.2: Representative example of the JJN-3 comets as viewed under fluorescent microscope (A) without treatment and (B) immediately after 10Gy of IR. The cells appear rounded in the controls as most of the genetic material is in the nucleoid. Visible tails are seen after irradiation due to the differential movement of the dsDNA fragments in agarose gel. 50x magnification.

3.3.2.1 Cyclin D1-expressing cell lines (U266 and MOLP-8) showed a significant increase in tail moments immediately after IR

After irradiation and immediate processing (0 h) both the U266 and the MOLP-8 cell lines saw their tail moments significantly increasing from 7.8 to 20 and from 11.5 to 21 respectively ($P < 0.001$) (Figure 3.3). This effect was not observed at the same time point in the third cyclin D1 cell line, KMS12-BM, (12.3 to 17.6, $p=0.45$). When the cell lines were incubated for 4h, there was a reduction in the tail moments as compared to the first time point. However, the tail moments at this time point were still higher

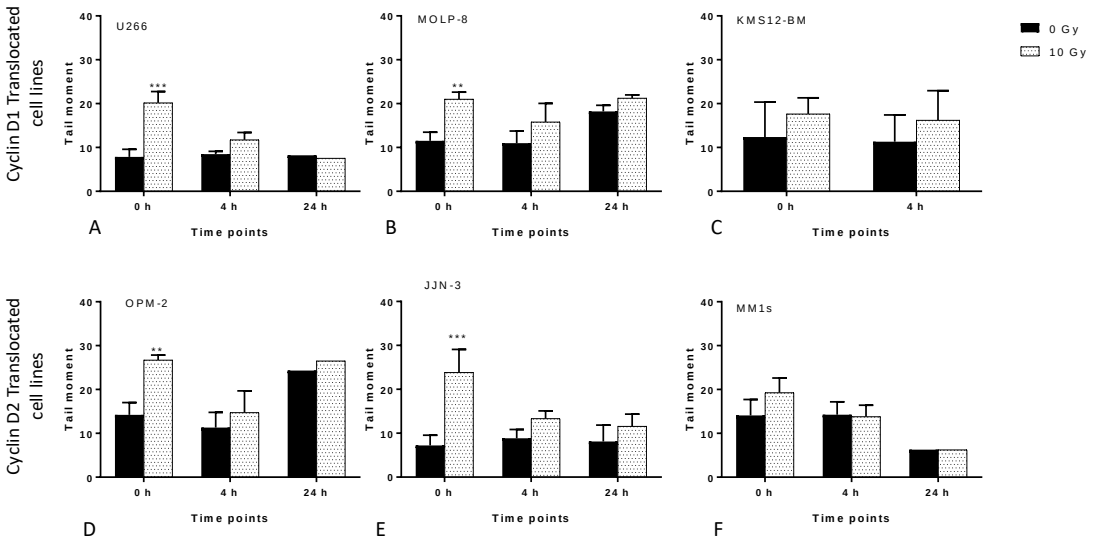


Figure 3.3: Comet assay tail moments of cyclin D1 and cyclin D2 myeloma cell lines measured immediately, after 4 h and after 24 h of 10 Gy IR dose. U266, MOLP-8, OPM-2, and JJN-3 (A, B, D and E respectively) showed a significant increase in tail moments immediately after irradiation while a trend towards higher tail moments was seen with KMS12-BM (C) and MM1s (F). A trend towards the restoration of the tail moments was seen in subsequent time points in all the cell lines. The MOLP-8 (B) and the MM1 (F) have a p53 wild-type status. * represents P<0.05, ** represents P<0.01 and * represents P<0.001. Within a single experiment, each condition was done in a duplicate. The bars represent the mean of at least two independent experiments; error bars represent the standard deviations. All experiments were repeated independently at least twice unless indicated by the lack of error bar where those conditions were done once.**

than the control but this was not statistically significant (u266 p=0.056, MOLP-8 p=0.044, KMS12-BM p =0.48). After 24 hours of incubation, the U266 tail momentshave decreased further and are now comparable to the controls. The tail moments of the MOLP-8 cell line, at the 24h time point, were still high and comparable to the 0h and 4h incubation results, however, there was a similar increase in the tail moments of the control at this time point and the difference between the control and the treated was not significant (Figure 3.3). We acknowledge the lack of 24h results for the KMS12-BM cell line. This was unforeseen and was due to the agarose gel falling

off the comet slides unexpectedly during storage rendering them unsuitable for analysis.

When the cell count was assessed using the trypan blue assay, there was no difference between the controls and the irradiated U266 and KMS12-BM samples at all the time points assessed. There was a significant drop in the cell count of MOLP-8 samples after irradiation and incubation as compared to the controls (17.35% drop at 4 hours, p=0.006 and 50.7% at 24 hours, p <0.0001) (Figure 3.4).

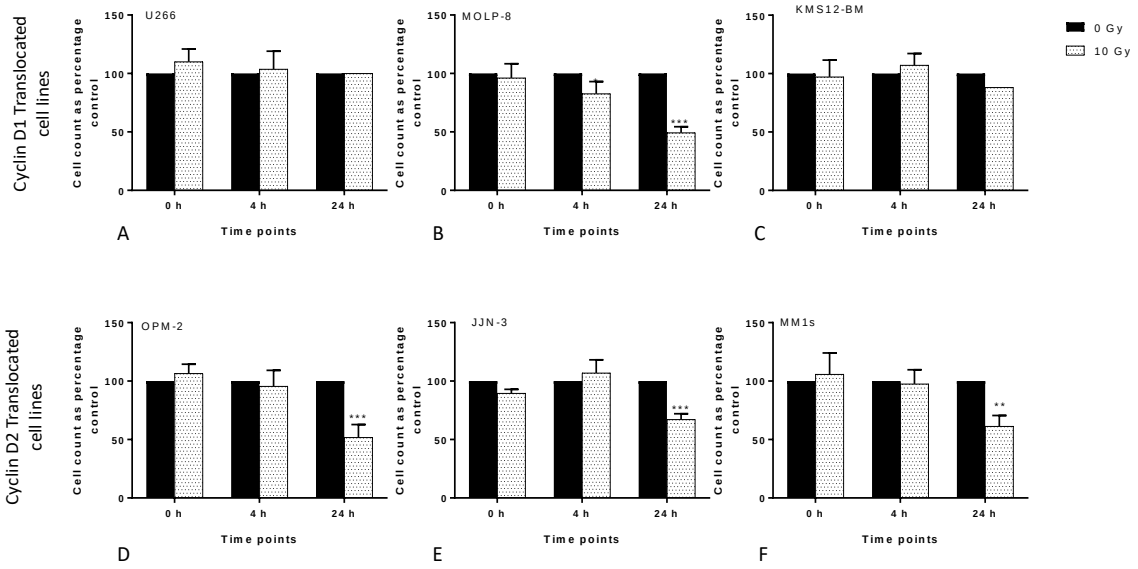


Figure 3.4: The Trypan blue cell count after irradiation with 10 Gy at 0, 4 h and 24 h incubation. The cyclin D2 cell lines (D-F) all showed a significant drop in the cell count as compared to controls after 24 hours of irradiation while only the MOLP-8 of the cyclin D1 cell lines showed a time-dependent decrease in the cell count after irradiation. MOLP-8 (B) and MM1s (F) have a wild-type p53. * represents P<0.05, ** represents P<0.01 and represents P<0.001. Within a single experiment, each condition was done in a duplicate. The bars represent the mean of at least two independent experiments; error bars represent the standard deviations. All experiments were repeated independently at least twice unless indicated by the lack of error bar where those conditions were done once.

3.3.2.2 Cyclin D2-expressing cell lines (JJN3 and OPM-2) showed a significant increase in tail moments immediately after IR

The JJN-3 cell line tail moments almost tripled after exposure to 10Gy of IR (7.2 to 23.8, p=0.0001), however the tail moments reduced at the rest of the time points and became comparable to the controls (p=0.29 at 4 hours and p=0.5 at 24h) (Figure 3.3). Irradiation did not cause a significant increase in the tail moments in the MM1s at all time points assessed, however, there was a trend towards higher tail moments at the 0h time point (tail moment increased from 14 to 19, p=0.078). The tail moments reduced at the 4 h time point and reduced even further at the 24 h time point. The OPM-2 cell line tail moments increased significantly from 14.2 to 26.7 at the 0 h time point after exposure to IR (p=0.002). At the 4 h time point, the tail moment has reduced to become comparable to the controls. Similar to what was observed with the MOLP-8 cell line, the tail moments increase again at the 24 h time point but a similar increase was observed in the controls and therefore the difference was not significant (Figure 3.3). As far as the cell count is concerned, all the cyclin D2 cell lines showed a significant drop in the cell count after 24h of 10 Gy IR (Figure 3.4).

Overall, the largest increase in the tail moments was observed in the OPM-2 and JJN-3 cell lines (both are cyclin D2-expressing) at the earliest time point following irradiation. This is not enough to infer, however, that the pattern of increase in the tail moments can be attributed to the cyclin D type translocation. When an increase in the tail moment was significant, this was only observed at the first time point following irradiation (4 of 6 cell lines). Subsequent time points generally showed a pattern of a gradual reduction in the tail moments indicating resolution of the DNA damage caused

by IR. The patterns observed did not conform to whether a cell line was D1 or D2 translocated or whether it had a mutated or wild-type p53 status.

It is also worthwhile to note that although there was a drop in cell count when assessed with Trypan Blue mainly at 24 hours in 4 of 6 cell lines (MOLP-8, JJN-3, OPM-2 and MM1s), the viability was consistently above 90% (as assessed by Trypan Blue exclusion). Similar to what was observed with the tail moments, this pattern was unrelated to the cyclin D type translocation or the p53 status (Figure 3.4).

3.3.3 γH2A.X Phosphorylation Results

3.3.3.1 Cyclin D1-expressing cell lines (U266, MOLP-8, KMS12-BM) showed a significant increase in γH2A.X phosphorylation after 4 h of IR.

The γH2A.X phosphorylation in response to gamma irradiation was heterogenous across the three cyclin D1 cell lines. Consistently, however, there was a significant increase in γH2A.X phosphorylation after 4 hours of 10 Gy IR in all the cyclin D1 cell lines (U266, MOLP-8 and KMS12-BM) as compared to the controls (14.8%-p=0.001, 17.9%-p=0.0013 and 13.8%-p=0.039 respectively) (Figure 3.5). Only the KMS12-BM cell line showed a significant increase in the γH2A.X phosphorylation after 24 h of gamma irradiation (31.1%, p=0.0008). The largest increase was observed with the KMS12-BM cell line immediately after irradiation (0h) (55%, p=0.00003). A significant, albeit a smaller increase, was also seen at this time point with the MOLP-8 cell line (17.9%, p=0.0032) which stayed at a similar level after 4 hours. In contrast, there was no increase in phosphorylation immediately after irradiation in the U266 cell line (Figure 3.5).

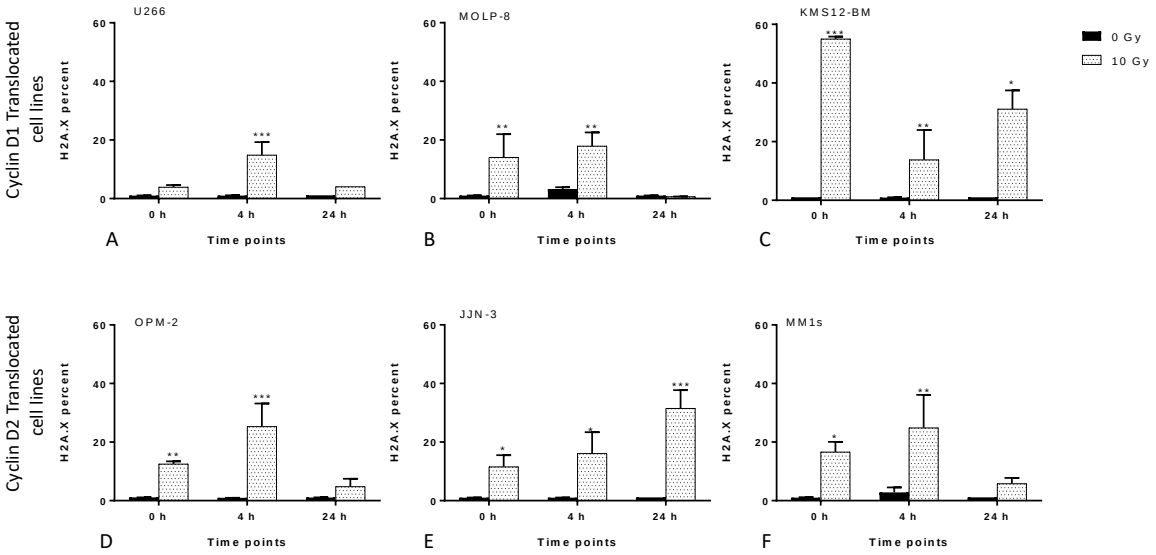


Figure 3.5: The percentage of γH2A.X phosphorylation by flow cytometry using a FITC conjugated Ab for the six human myeloma cell lines was measured immediately, after 4 h and after 24 h of irradiation with 10 Gy dose. The 4 h time point was significant in all cell lines tested. Apart from KMS12-BM (C) and JJN-3 (E), all cell lines managed to dephosphorylate γH2A.X after 24 hours of incubation. The MOLP-8 (B) and the MM1 (F) have a p53 wild-type status. Statistical analysis was performed using an unpaired t-test where * represents P<0.05, ** P<0.01 and *** P<0.001. Within a single experiment, each condition was done in a duplicate. The bars represent the mean of three independent experiments; error bars represent the standard deviations.

3.3.3.2 Cyclin D2-expressing cell lines (JJN-3, OPM-2 and MM1s) showed a significant increase in γH2A.X phosphorylation 0 h and 4 h after IR

There was a gradual and significant increase in the γH2A.X phosphorylation observed with cyclin D2 cell lines at 0 and 4 h after 10 Gy of IR before the γH2A.X phosphorylation returned to almost normal after 24 h (except in the JJN-3 cell line) (Figure 3.5). The phosphorylation levels approximately doubled in the OPM-2 cell line between the first and the second time points (12.5% and 25.5% respectively). The increase was less pronounced in the MM1s cell line at those time points but remained significant (16.6% and 24.8%, p=0.005 and p=0.0005 respectively). The JJN-3 cell line

showed a steady increase in the phosphorylation levels of γH2A.X at all the three time points tested which was significant as compared to the controls. Immediately after irradiation, γH2A.X levels were 11.5% (p=0.03) before increasing to 16.1% (p=0.006) after 4 hours. The γH2A.X phosphorylation levels then doubled after 24h to 31.5% (p=0.0006) (Figure 3.5).

Overall, all the cell lines (cyclin D1 or cyclin D2 expressing) showed a significant increase in the phosphorylation levels of γH2A.X after 4 hours of IR. The increase was also significant immediately after irradiation in all cell lines apart from U266. MOLP-8, U266, OPM-2 and MM1s phosphorylation levels almost dropped to normal after 24 h of irradiation. However, the largest increase in the γH2A.X levels was seen in the KMS12-BM cell line directly after irradiation, while both the JJN-3 and the KMS12-BM cell lines had the highest and almost equal increase in the phosphorylation levels at the 24 h time point.

3.4 Discussion

In this chapter, two methods were used to assess the differential response between the myeloma cell lines to DNA damage induced by IR. The comet assay measures DNA damage directly while γH2A.X phosphorylation measurement assesses the cells immediate response to DNA damage. Although both methods have been used to assess the degree of DNA DSBs, differences in results may occur as they look at DNA damage from different angles. The comet assay measures the degree of unwinding of the DNA due to DNA strand breaks while the γH2A.X phosphorylation quantifies DNA damage indirectly by measuring one of the very first steps in the cellular response to the damage. The degree of DNA damage in the comet assay is depicted by the increase

in the tail moment after exposure to IR. When a nucleoid is severely DNA damaged, most of the DNA will be in the tail with very little in the head. It could be misconceived that the damage in those cells is irreversible and hence those cells will undergo apoptosis. However, experiments have shown that many of those cells can still repair their DNA. In addition, during the process of apoptosis, the DNA fragments into oligomers and those can be lost during the lysis process and thus would not be visible on the comet slides. Moreover, the comet assay cannot determine the size of the DNA fragments rather the tail of the comet increases in size as a result of the relaxation of the DNA supercoil imparted by the increase in the number of DNA breaks (169,184,185). It is important to note that the comet assay is not a surrogate for viability. Cells with large comets can repair themselves back to normal and dead necrotic cells can have comet tails when visualised.

As with regards to γH2A.X phosphorylation, apoptotic cells that uptake anti-γH2A.X Ab are gated out during flow cytometry analysis and similar to what has been mentioned above, phospho-γH2A.X positive cells can repair their DNA and so would not necessarily undergo apoptosis.

In order to establish the optimum dose of IR to be used for the experiments in this chapter, two cell lines (U266 and JJN-3) were exposed to 5Gy and 10Gy of IR and a comet assay was done at the 0-hour and 4-hour time points. Although there was no significant difference between the two doses at both time points with regards to the tail moments, the latter increased slightly with the increase in the dose of IR. It is plausible that a more prominent dose effect would have been observed if the analysis was done after a longer period of time (for example after 24 hours of incubation). This

time point was not done during the pilot experiments. Similarly, a dose response effect could have been observed if lower doses of IR were tested. Given that previous work has shown that the 10Gy IR was capable of downregulating cyclin D1 and given that there was no significant difference between the two doses in the pilot study at the earlier time points when it came to the tail moments, the 10 Gy IR dose was chosen for subsequent experiments. Moreover, the 10 Gy dose did not cause a significant impact on viability. A more comprehensive approach would have been to perform the pilot experiment in more cell lines with longer time points using various doses of IR, however, for the reasons mentioned above, it was felt that this was not required.

A common theme observed in most of the cell lines in this chapter was the increase in DNA damage at the earlier time points after exposure to IR as compared to controls. This is consistent with the published research (108). We noticed a significant increase in the tail moments, compared to the controls, immediately after IR indicating the induction of DNA DSBs. This was the only time point where the increase in the tail moments was significant. Subsequent time points showed a reversal of this pattern such that there was no difference between the irradiated cells and the controls (Figure 3.3). This could be explained by either the apoptosis of the damaged cells or the possibility that those cells have managed to repair their damaged DNA. The latter may be more plausible given that the trypan blue results showed no significant drop in cell numbers compared to controls at 0h and 4h after IR (Figure 3.4). Moreover, in Chapter 4:, we showed that there was no significant increase in apoptosis after 4h of 10Gy IR when apoptosis was assessed by the annexin V assay (Figure 4.2). Therefore, the reduction in the tail moments at this time point cannot be fully explained by apoptosis and DNA damage repair is likely to be at play. As a side point, the results also meant

that the dose of irradiation that was used for those experiments met the objective of causing DNA damage without actually causing significant cell death so as to degrade the measurable data at the later time points. A significant increase in the tail moments was observed at the first time point in four out of the 6 cell lines tested. The KMS12-BM and the MM1s cell lines in which this effect was not observed have a longer doubling time (>60 hours) as compared to the other four and this could explain the presence of a trend towards the increase in the tail moments rather than this difference being significant. Another possible explanation is the potential need for a higher IR dose to induce significant DNA damage in those two cell lines. In a study by Herrero et al (98), 40 Gy of IR were used to induce DNA damage in multiple myeloma cell lines (including MM1s) that was assessed by the comet assay after a shorter incubation time compared to what we used in this project. They found a significant increase in the tail moments at the 0 h time point that gradually reduced at the later time points. Although the 4 h time point was not tested, the 6 h time point tail moments were close to the baseline. We are unaware of data from literature examining the tail moments of the KMS12-BM cell line after exposure to IR. We acknowledge that the lack of 24 h tail moment data for the KMS12-BM cell line is unfortunate and it prevents drawing firm conclusions about how this cell line would have responded to IR after longer incubation. Also, It was not possible to deduce from the basic molecular characteristics in the product literature for the KMS-12BM and the MM1s cell lines why they would appear to behave in radioresistant fashion with regards to the tail moments. As mentioned earlier, the neutral comet assay we used in this chapter is sensitive to double- rather than single-stranded DNA damage and

therefore a different behaviour could have been observed if the alkaline comet assay was used instead.

Some of the cell lines showed a slightly higher tail moment results in the controls at the 24 h time as compared to the earlier treated time points. This was the case for the MOLP-8 and the OPM-2 cell lines but not the rest. This can appear counterintuitive; however, it would make more sense to review the results at each time point as a comparison between the treated and the controls rather than a timeline comparison between treated and untreated cell lines across multiple time points. There are two main reasons why this viewpoint maybe more informative. Firstly, due to the basal DNA damage observed in myeloma cell lines, it is possible that those cells will accumulate more DNA damage spontaneously after long incubation in culture anyway. This would apply to both treated and untreated cell lines and therefore it would make more sense to compare treated and untreated conditions at each time point rather than across different time points. Secondly, and supporting the first point, there was no significant difference at the 24 h time point between the treated and the untreated conditions.

The trypan blue data showed no significant drop in cell count after IR and 24 h incubation in the KMS12-BM and the U266 cell lines. This cannot be fully explained by the underlying cyclin D translocation, p53 status or indeed the other secondary genetic changes such as chromosome 1q. One limitation of our data is that the results of this time point is from one experiment and therefore statistically meaningful data could not be obtained. However, Herrero et al (98) also demonstrated relative IR resistance in the U266 cell line. Cell death was only around 10% after 48 h of exposure

to IR. Their panel did not include the KMS12-BM cell line so similar conclusion regarding chemoresistance could not inferred. Doubling time may be a factor as discussed above but would not explain the findings fully. It should also be noted that the U266 was found to be the most resistant cell line after treatment with BCL-2 and MCL-1 inhibitors (Chapter 5). This is not true of the KMS-12BM cell line, however and therefore there may be other factors at play.

The dephosphorylation of γH2A.X after DNA repair is mediated by phosphatase 2A (PP2A), the kinetics of which are unknown in myeloma cell lines. All the cell lines showed a significant increase in the γH2A.X phosphorylation at the 4 h time point. This significance was not mirrored in the tail moments at the same time point. This could indicate two possibilities. There is evidence from the literature that there can be persistence of γH2A.X phosphorylation even after DNA repair (98). In the absence of significant cell death at the 4h time point from the Trypan blue data, the restoration of the tail moments coupled with the persistence of γH2A.X phosphorylation could indicate either delayed dephosphorylation or, most likely, the presence of DNA damage that is under the limit of detection by the comets assay. This left-over damage was not enough to induce apoptosis and may have been more challenging to repair.

Looking at cell lines individually, the pattern of γH2A.X phosphorylation was different in the JJN-3 and the KMS12-BM cell lines as compared to the rest of the cell lines. In the JJN-3, there was a gradual increase in the percentage of γH2A.X phosphorylation while a more erratic pattern was observed in the KMS12-BM cell line. A similar pattern with JJN-3 was previously described (98). It may be inferred that those two cell lines

are more tolerant of DNA damage and the genetic instability imparted by the failure to repair some of the DNA breaks.

It has been demonstrated previously that myeloma and other cancer cell lines exhibit a degree of basal γH2A.X phosphorylation that may reflect a background of DNA damage and genetic instability (98). In this experiment, the degree of γH2A.X phosphorylation was compared to the controls of the same cell line and thus the measurements are additional to any basal H2A.X phosphorylation present in those cell lines.

When a possible differential response in response to DNA damage depending on the D-type cyclin overexpressed was assessed, there was no pattern to the tail moments or the γH2A.X phosphorylation. As mentioned above, cyclin D1 quickly undergoes downregulation in response to DNA damage by IR, a feature that is not observed with cyclin D2. We, therefore, hypothesised that sensitivity to DNA damage could differ as a consequence of this variability. This was not demonstrated in our data. There was no discernible pattern that could have been attributed to whether cell lines expressed cyclin D1 or cyclin D2. Moreover, apart from increased cell death at 24 hours for the p53 wild-type cell lines (MOLP-8 and MM1s), no attributable pattern to the p53 status of the cell lines was observed in the comet assay and the γH2A.X phosphorylation data. One caveat of the latter statement is that a firm conclusion with regards to the role of p53 in this process cannot be assumed as we only had once cell line in each of the cyclin D groups with a wild-type p53 status. This is obviously not enough to investigate the role of p53 with regards to cyclin D variation, however the equal number of cell lines with similar p53 status between the two groups is useful to reduce imbalance.

Smith et al, studied the effect of DNA damage by IR on the cell cycle in myeloma cell lines according to their underlying cyclin D expression (108). Cyclin D1 downregulation was seen in response to IR but a similar effect was not observed with the cyclin D2 cell lines. Counter-intuitively, cell cycle arrest did not happen in G1 as one might expect from the effect of the downregulation of cyclin D1 but rather happened in the G2/S phase. Despite the downregulation of cyclin D1 with DNA damage, significant levels of it were still bound to CDK4/6; enough to keep pushing the cell cycle through G1. In subsequent chapters, we also show the downregulation of cyclin D1 rather than cyclin D2 with IR in agreement with previously published research (see Chapter 4). To conclude this chapter, a differential response to DNA damage induced by IR according to the underlying cyclin D type was not identified.

CHAPTER 4:

A COMPARISON OF THE RESPONSE TO PROTEASOME INHIBITION AND DNA DAMAGE BETWEEN CYCLIN D1 AND CYCLIN D2 EXPRESSING CELL LINES

Chapter 4: A Comparison of the Response to Proteasome Inhibition and DNA Damage between Cyclin D1- and Cyclin D2-Expressing Cell Lines

4.1 Introduction

As discussed in depth in the Introduction chapter, chromosomal translocations that involve the immunoglobulin heavy chain on chromosome 14 are observed as initiating events in approximately 50% of multiple myelomas. Those translocations upregulate cyclin D1 or cyclin D2. There has been an established association between the translocation subtype and the prognostication and response to treatment. Translocations that are associated with an upregulated cyclin D2, t(4;14) and t(14;16), tend to be associated with an adverse revised international staging system (R-ISS) score with a consequent inferior overall and progression-free survival. Therefore, another aspect of assessing if the underlying cyclin D type imparts a differential effect in myeloma cell lines is to compare the responses to standard myeloma chemotherapy between our D1-expressing cell lines (U266, KMS12-BM and MOLP-8) and D2-expressing cell lines (JJN-3, OPM-2 and MM1s).

4.1.1 The Proteasome Inhibitor Bortezomib in Multiple Myeloma

The proteasome inhibitor bortezomib (Velcade®, previously PS-341) represents an integral constituent of modern myeloma therapy. Since its inception in 2003, it has advanced the outcomes of patients with plasma cell dyscrasias and has also been trialled in other haematological cancers (126,127).

Triplet and quadruplet combinations of bortezomib with immunomodulatory agents, steroids, alkylators or monoclonal antibodies are frequently used regimens for

multiple myeloma treatment. The combinations of bortezomib and dexamethasone with thalidomide and daratumumab are the most commonly used induction treatments for transplant-eligible multiple myeloma patients in the UK. Bortezomib is also an important first-line therapy in combination with melphalan when autologous stem cell transplant is not an option (118,130).

4.1.2 Mechanisms of Action of Bortezomib in Myeloma and Other Cancers

4.1.2.1 Unfolded protein response and NF-κB inhibition

As discussed in chapter 1 (1.3.3), bortezomib acts through the inhibition of the proteasome, the cellular mechanism for recycling unwanted and defective proteins. The accumulation of large numbers of misfolded/unfolded proteins, as a result of the proteasome dysfunction and the consequent triggering of ER stress, is thought to be the prime mechanism of toxicity of bortezomib in myeloma (128,129). In addition, various products that are normally ushered for ubiquitinylation and degradation by cancer cells due to their undesired antineoplastic effect accumulate due to proteasome inhibition with the subsequent restoration of their anti-proliferative/pro-apoptotic functions. A major example of this process that is of relevance to myeloma cells is the way NF-κB is activated following the proteasomal degradation of its inhibitor (IκB). The resultant nuclear translocation of NF-κB causes the upregulation of pro-inflammatory, antiapoptotic and proliferative pathways with an obvious consequential pro-malignant effect (186–188). As previously mentioned, the NF-κB activity in myeloma cell lines and primary samples is increased, thus lending to the role of proteasome inhibition in the treatment of myeloma (189). It follows that chemo-resistant myeloma cell lines with high NF-κB activity were more sensitive to bortezomib treatment compared to their chemo-sensitive counterparts (189).

4.1.2.2 The effect of bortezomib on apoptotic proteins

NOXA, a BH3-only member of the BCL-2 family and a pro-apoptotic protein was found to be induced in multiple myeloma cell lines that were sensitive to treatment with bortezomib probably through the inhibition of its proteasomal degradation. The accumulation of NOXA causes an increment in MCL-1/NOXA complexes together with the dissociation of BIM from MCL-1. MCL-1 cleavage was also induced by bortezomib in sensitive cell lines. The obvious consequence of this accumulation of events is the induction of apoptosis (190). In another study, proteasome inhibitor treatment caused the induction of apoptosis through NOXA upregulation in myeloma and melanoma cell lines. The blocking of NOXA caused the reduction of apoptosis by a third to a half (191). A similar effect was observed in mantle cell lines (192). The preclinical evaluation also showed a significantly increased chemosensitivity to melphalan, mitoxantrone and doxorubicin in previously resistant myeloma cell lines to these agents when combinations with non-cytotoxic concentrations of bortezomib were used (189).

4.1.2.3 The effect of bortezomib on cyclins

The effect of bortezomib on cyclins and other molecular targets may vary depending on the type of tumour studied. In a breast cancer model, the stabilisation of cyclin D1 due to reduced proteasomal degradation was observed after treatment with bortezomib. Since cyclin D1 can sequester STAT3, a transcription factor and a signal transduction molecule for cancer inflammation and promotion of tumour microenvironment, stabilisation of cyclin D1 lead to more STAT3 sequestration and consequently more anti-tumour effect (193). Malignant fibroblasts treated with bortezomib showed an increase in the levels of p27, which eventually led to apoptosis (194). In Ewing sarcoma cell lines, treatment with bortezomib caused apoptosis

induction through cell cycle arrest at G2/M phase in addition to the upregulation of p27 (195). In colorectal and hepatocellular cancer cell lines, G0/G1 arrest was induced by bortezomib with associated suppressed expression of cyclin D1 thereby reducing cyclin D1/CDK4 expression. A proapoptotic effect was observed through increased FOXO3 and inhibited CTNNB1 (196).

4.1.3 The Rationale of Experimental Work and the Experimental Plan

Given the common use of bortezomib in clinical practice, it was worthwhile to investigate whether there was a differential response between cyclin D1 and cyclin D2 expressing myeloma cell lines when treated with bortezomib in a combination that mimicked what is commonly used in clinical practice. Indeed, it is not unreasonable to hypothesise different response profiles according to the underlying cyclin D status given the mutual exclusivity of those initiating molecular events and the resultant prognostic impact. Velcade (bortezomib)-Cyclophosphamide-Dexamethasone (VCD) is a common first-line induction treatment for transplant-eligible patients with multiple myeloma in the UK. To imitate this combination, myeloma cell lines were treated with bortezomib but instead of cyclophosphamide, IR was used to induce DNA damage. This was done to ensure uniformity and to circumvent any possible variability in myeloma cell line intrinsic chemoresistance to alkylators. In addition, some evidence suggests that pre-treatment with bortezomib will arrest myeloma cells in the G2/M phase and thus render them more susceptible to damage by IR (197). IR increases NF-KB activity as a cellular pro-survival feedback, however, this increase was completely abrogated by pre-treatment with bortezomib before IR (197). Similarly, pre-treatment with bortezomib of LOVO, a colorectal cancer cell line, prevented the upregulation of

NF-KB and rendered that cell line more susceptible to apoptosis by IR (198). A Japanese study demonstrated the prolongation of the S-phase and an increase in TRAIL receptors in myeloma cell lines transfected to overexpress cyclin D1. Those changes were suggested to be the reason behind the increased cytotoxic effect of some anti-myeloma agents when cyclin D1 is overexpressed (199).

4.2 The Aim of this Chapter

The experiments in this chapter aimed to investigate if there is a differential response between cyclin D1 and cyclin D2 myeloma cell lines in response to bortezomib combined with IR. This combination attempts to mimic the combination of bortezomib and alkylators that is commonly used in clinical practice. We also examined the effect of variation in the temporal administration of bortezomib and IR. This is to investigate, as a secondary aim, whether DNA damage imparts a different degree of chemotoxicity depending on when this is introduced following treatment with bortezomib. In routine clinical practice, it is fair to say that when bortezomib is combined with an alkylator, little concern is paid towards when those agents are given in relation to each other. VCD can be given with once or twice weekly bortezomib while cyclophosphamide is almost always given on a weekly basis.

To determine the effect of temporal variation when combining bortezomib with IR, cell lines were treated with bortezomib for a total of 24 hours then IR was introduced either 4 hours or 20 hours after treatment with bortezomib. The annexin V assay was used to assess apoptosis following bortezomib and IR treatment as single agents and in combination. The level of expression of cyclins D1 and D2 was assessed using Western blotting. The concentrations of bortezomib chosen for these experiments

were based on results from single-agent treatment where no more than 30% reduction in the viability was seen to allow for a meaningful assessment of protein expression.

4.3 Results

4.3.1 Myeloma Cells Viability Assessment by Annexin V to IR and Bortezomib

4.3.1.1 Myeloma cell lines are sensitive to nanomolar bortezomib concentrations

All six myeloma cell lines were treated with increasing nanomolar concentrations of bortezomib then assessed for apoptosis after 24 hours using the Annexin V assay (Figure 4.1).

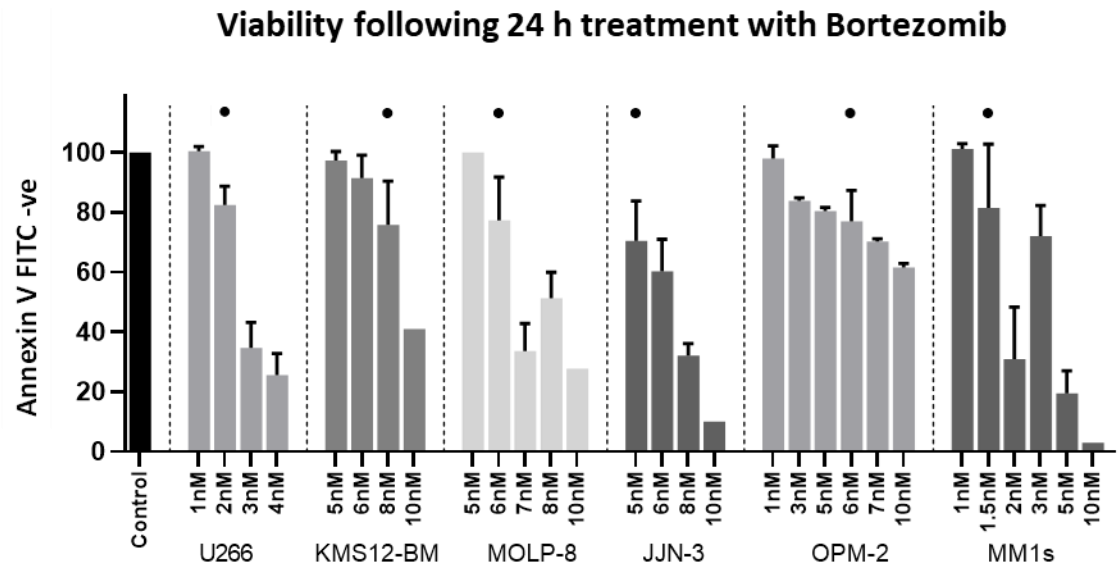


Figure 4.1: Dose-response to 24-hour treatment with bortezomib in the six myeloma cell lines as determined using the Annexin V assay. The concentrations of bortezomib that were chosen for the bortezomib-IR combination experiments are denoted by the black circles. The bars represent the mean of at least three independent experiments; error bars represent the standard deviations.

All the cell lines were sensitive to nanomolar concentrations of bortezomib. The most sensitive cell lines were the MM1s and the U266 whereby concentrations of 5nM and 4nM, respectively caused a 30% loss of viability.

The most resistant cell line was the OPM-2, the treatment of which with 10nM of bortezomib caused only around 40% loss of viability. Whereas the same concentration caused more than 60% loss of viability in the rest of the cell lines. There was no pattern to the sensitivity of the cell lines that could have been predicted from their underlying cyclin D status. Concentrations of bortezomib specific to each cell line causing no more than 30% reduction in the viability were taken forward for the combination experiments with IR (Table 4.1)

Table 4.1: The concentrations chosen for the combination experiments with IR for each of the myeloma cell lines. Those did not result in more than a 30% drop in viability.

	Cell lines	Bortezomib concentration (nM)
cyclin D1 cell lines	U266	2
	KMS12-BM	8
	MOLP-8	6
cyclin D2 cell lines	JJN-3	5
	OPM-2	6
	MM1s	1.5

4.3.1.2 IR had minimal impact on viability in 4 out of 6 myeloma cell lines

The myeloma cell lines were irradiated with 10Gy of IR. This dose was chosen based on previous experiments (See Chapter 3:). Apoptosis using Annexin V staining was determined following 4 hours and 24 hours of incubation.

There was no significant change in the viability following 4 hours of IR treatment. This is similar to the results of the Trypan Blue count following IR in Chapter 3. After 24

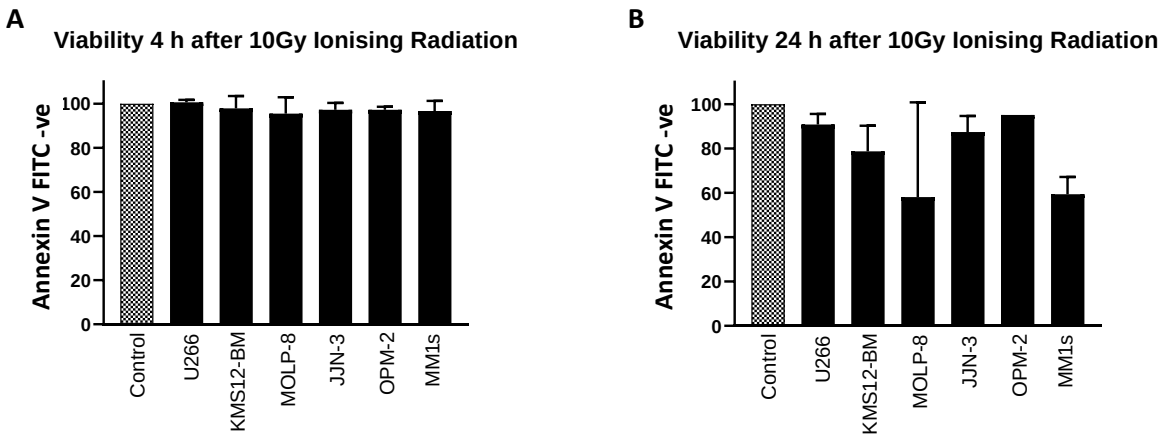


Figure 4.2: Viability of the myeloma cell lines as a percentage of control was assessed using Annexin V staining following IR and incubation for (A) 4h and (B) 24h. The bars represent the mean of at least three independent experiments; error bars represent the standard deviations.

hours, however, the viability of the MOLP-8 and the MM1s cell lines dropped by approximately 50%. These two cell lines showed a significant drop in the cell count at 24h time-point after irradiation in chapter 3. All the other cell lines maintained their viabilities above 75% (Figure 4.2).

4.3.1.3 The combination of IR and bortezomib had a heterogenous effect on viability

To assess the impact of combining IR and bortezomib on apoptosis and cyclin D expression, two schedules that involved a total of 24-hour treatment with bortezomib were evaluated,

Schedule 1: 24-hour treatment with bortezomib; IR introduced 4 hours after initiation of bortezomib treatment.

Schedule 2: 24-hour treatment with bortezomib; IR introduced 20 hours after initiation of bortezomib treatment.

When the cell lines were treated under schedule 1, the reduction in the viability of five

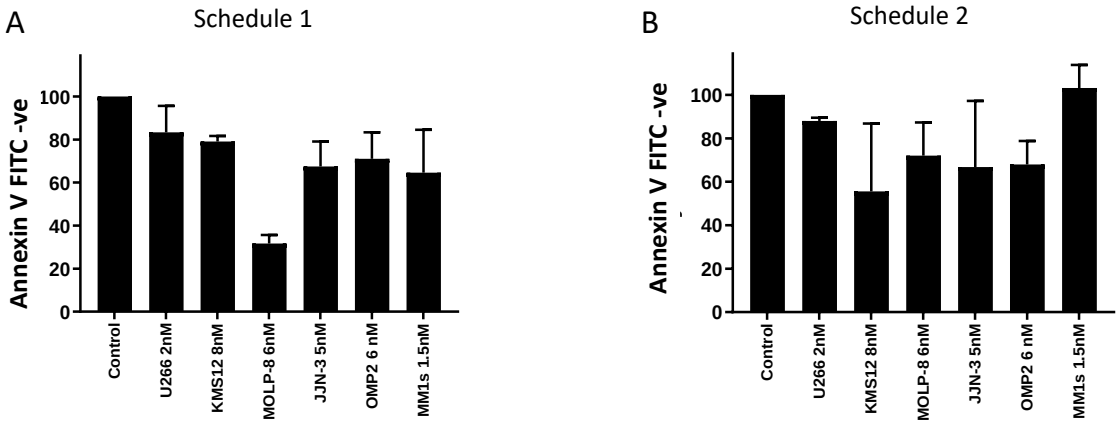


Figure 4.3: Viability of myeloma cell lines as a percentage of control was assessed using Annexin V after treatment with bortezomib in combination with IR introduced 4 hours after bortezomib treatment (Schedule 1, A) and 20 hours after bortezomib treatment (Schedule 2, B). The bortezomib concentrations used are indicated next to each cell line name. The bars represent the mean of at least three independent experiments; error bars represent the standard deviations.

of the cell lines was limited when compared to the control and ranged between 20-30% which was similar to what was observed after single agent treatment with

bortezomib. The MOLP-8 cell line did not follow this trend and viability decreased to 35% (Figure 4.3A).

When treated under schedule 2, the viability of the U266, MOLP-8, JJN-3 and OPM-2 ranged between 60-80%. The most sensitive cell line was the KMS12-BM (50% viability), and the least sensitive cell line was the MM1s (near 100% viability) (Figure 4.3 B).

4.3.2 The Effects of IR and Bortezomib on Cyclins D1 and D2 Expression

4.3.2.1 IR caused cyclin D1 rather than cyclin D2 downregulation

Cyclin D1 levels were reduced after 4 hours of treatment with IR and this reduction was generally maintained after 24 hours (except in the U266 cell line), confirming the results of previous research indicating the down-regulation of cyclin D1 in response to DNA damage [105]. Conversely, there was no significant change to cyclin D2 at either time point after IR (Figure 4.5, Figure 4.4 and Figure 4.8A and C).

4.3.2.2 Bortezomib caused cyclin D downregulation in 2 out of the 6 myeloma cell lines

Following a 24-hour treatment of the six cell lines with bortezomib, there was a reduction in cyclin D1 expression in the U266 cell line and a reduction in the cyclin D2 expression in the JJN-3 cell line. There was no significant change in the cyclin D1 expression in the KMS12-BM and the MOLP-8 cell lines nor the cyclin D2 expression in the OPM-2 and the MM1s cell lines (Figure 4.5, Figure 4.4 and Figure 4.6 A and C).

4.3.2.3 The combination of IR and bortezomib had a heterogenous effect on cyclin D expression

Next, the impact of combining DNA damage, mediated through IR, and proteasome inhibition on D-type cyclin expression was assessed. Analysis for cyclin D expression by Western blotting was done 24 hours after bortezomib treatment in both schedules.

The cyclin D1-expressing cell lines generally showed a uniform reduction in the expression of cyclin D1 with both schedule 1 and schedule 2 except for the KMS12-BM cell line (Figure 4.7 and Figure 4.8 B). With the cyclin D2 expressing cell lines, cyclin D2 was reduced in the JJN-3 cell line when treated under schedule 1. The OPM-2 cell line showed a slight reduction in both schedules. In contrast, there was no change in the MM1s cell line. The MM1s cell line, showed an unexpected restoration of the cyclin D2 expression under Schedule 2, coinciding with viability approaching 100% as assessed by Annexin V (Figure 4.3 B, Figure 4.6, and Figure 4.8 D).

4.4 Discussion

The experiments in this chapter attempted to explore if there was a pattern to the impact of commonly used chemotherapeutics in the treatment of multiple myeloma depending on whether myeloma cell lines expressed cyclin D1 and cyclin D2. IR was used to induce DNA damage and was combined with bortezomib to try to mimic myeloma therapy in real-life. As mentioned previously, IR was used as a uniform and guaranteed way of inducing DNA damage and its impact on cyclin D1 has been previously established. DNA-damaging agents such as cyclophosphamide and melphalan are relatively old therapies that are still being used nowadays despite the advent of new molecular and novel therapies. Alkylators can often be used in

combination with other agents such as bortezomib, lenalidomide and pomalidomide and/or with steroids. More recently however, such DNA-damaging agents have been replaced in earlier lines of treatment by more modern combinations such as those involving bortezomib, steroids immunomodulatory agents and monoclonal antibodies. Since the main aim of this project was to see the impact of cyclin D and that we already know that DNA damage causes the downregulation of cyclin D1, we sought to investigate the impact of a relatively older combination (bortezomib and DNA damaging agents) rather than a combination of entirely novel therapies. Rather than using cyclophosphamide or melphalan to induce DNA damage and risk a probably inherent variability in the chemosensitivity of the myeloma cell lines to those agents, a more direct (and guaranteed) approach of causing DNA damage was employed with ionising radiation. Obviously, this approach is not a like for like comparison for the use of alkylators in clinical practice and it does not address the observed clinical variability in the response to those agents. It is however the approach we adopted to investigate the impact of DNA damage (regardless of what is causing that) in combination with bortezomib in view of the underlying cyclin D translocation. We also acknowledge that this combination lacked the impact of steroids which is a departure from many chemotherapy combinations used in clinical practice. The use of steroids would have introduced a more complete picture in terms of clinical relevance however it would have potentially added significant variability and may have complicated this in vitro approach and therefore two agents were used instead of three. Moreover, we are unaware of any studies addressing the effect of steroids on cyclin D. This means that using steroids in those experiments could have been potentially interesting but would have added another layer of complexity to the experimental work.

There was a uniform reduction in cyclin D1 following exposure to IR. This was not statistically significant when assessed by densitometry. A similar reduction was not observed with cyclin D2 Bortezomib on the other hand caused the downregulation of the corresponding cyclin D in the U266 and the JJN-3 cell lines. Again, this did not reach statistical significance when assessed using densitometry. No pattern was attributable to the underlying cyclin D type in terms of downregulation or chemosensitivity. Similarly, when the cyclin D1 expressing cell lines were treated with a combination of IR and bortezomib, this caused the downregulation of cyclin D1 regardless of the schedule used, whereas nonuniformity was observed again with cyclin D2. Although two out of the three cyclin D2 expressing cell lines showed downregulation of cyclin D2, restoration of cyclin D2 was observed when the MM1s cell line was treated under schedule 2.

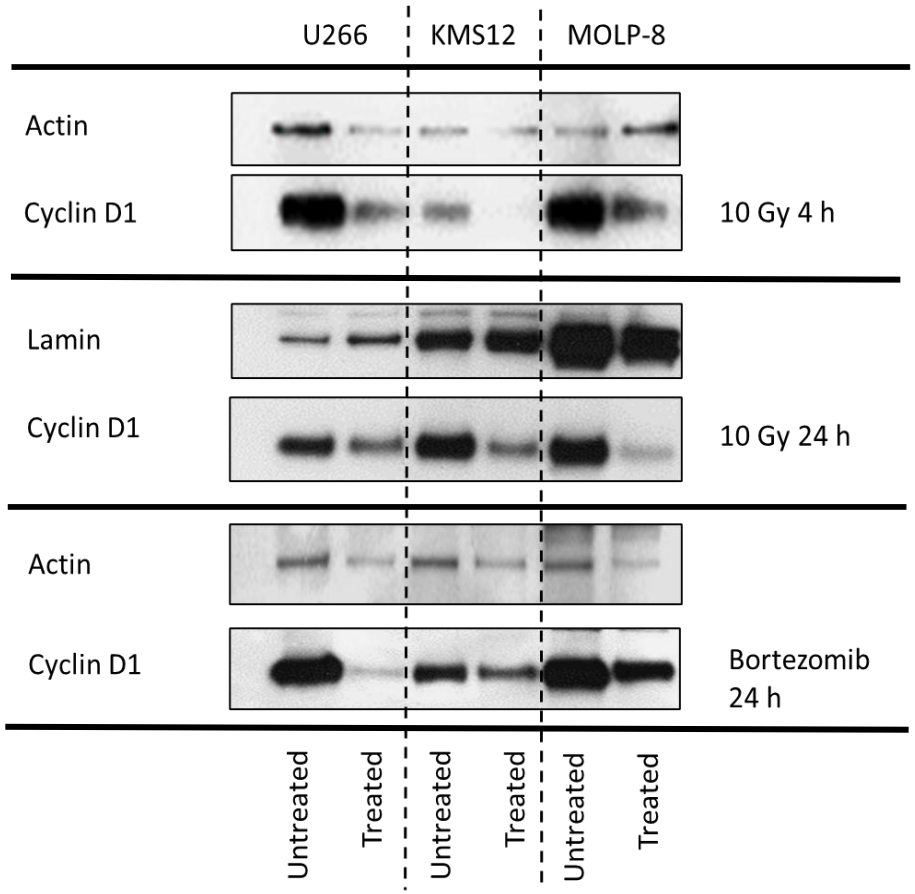


Figure 4.5: Representative individual Western blots for Cyclin D1 expression in U266, KMS12-BM and MOLP-8 myeloma cell lines 4h/24h post 10Gy IR and 24h post Bortezomib treatment. Actin and Lamin were used as housekeeping proteins for loading control. N=2-3

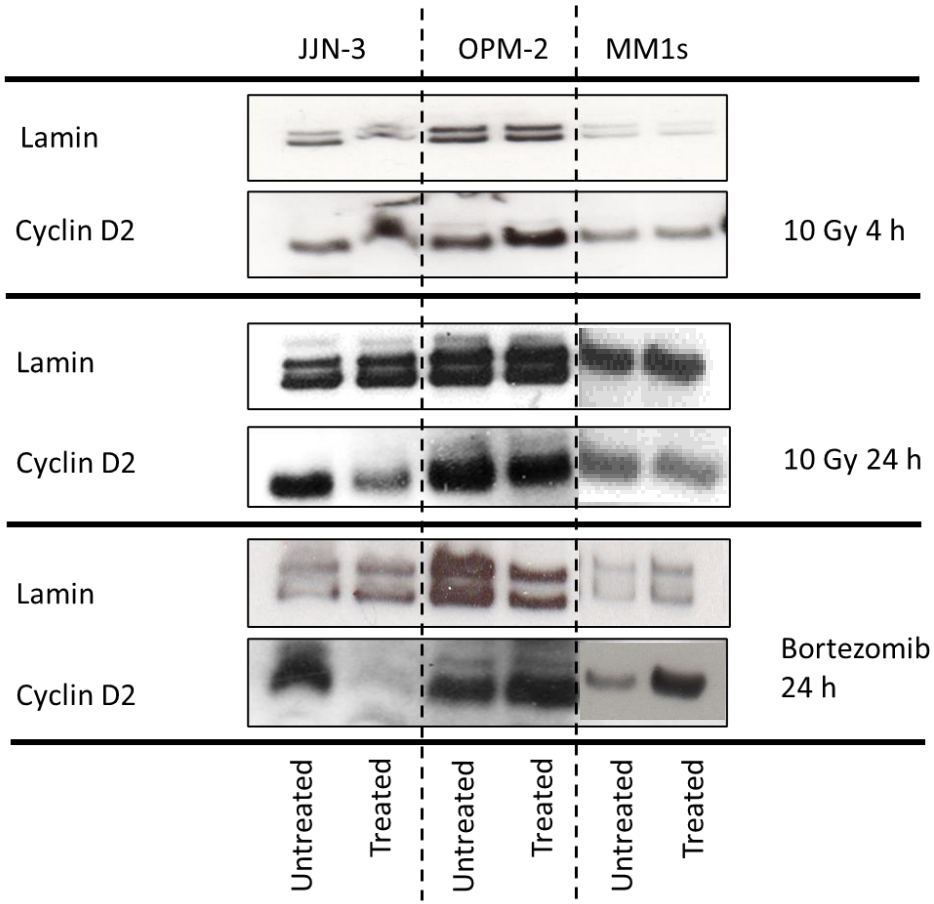


Figure 4.4: Representative individual Western blots for Cyclin D2 expression in JJN-3, OPM-2 and MM1s myeloma cell lines 4h/24h post 10Gy IR and 24h post Bortezomib treatment. Lamin was used as housekeeping protein for loading control. N=2-3

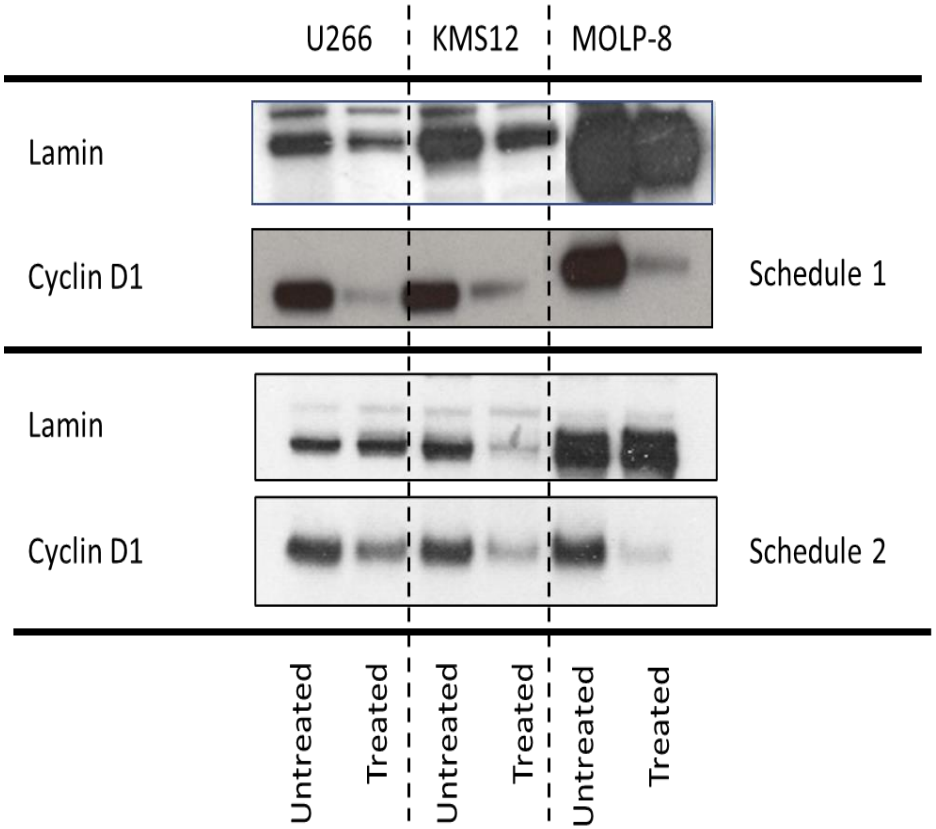


Figure 4.7: Representative Western blots for Cyclin D1 expression in U266, KMS12-BM and MOLP-8 myeloma cell lines following treatment with IR and Bortezomib under schedules 1 and 2. Lamin was used as housekeeping protein for loading control. N=2-3

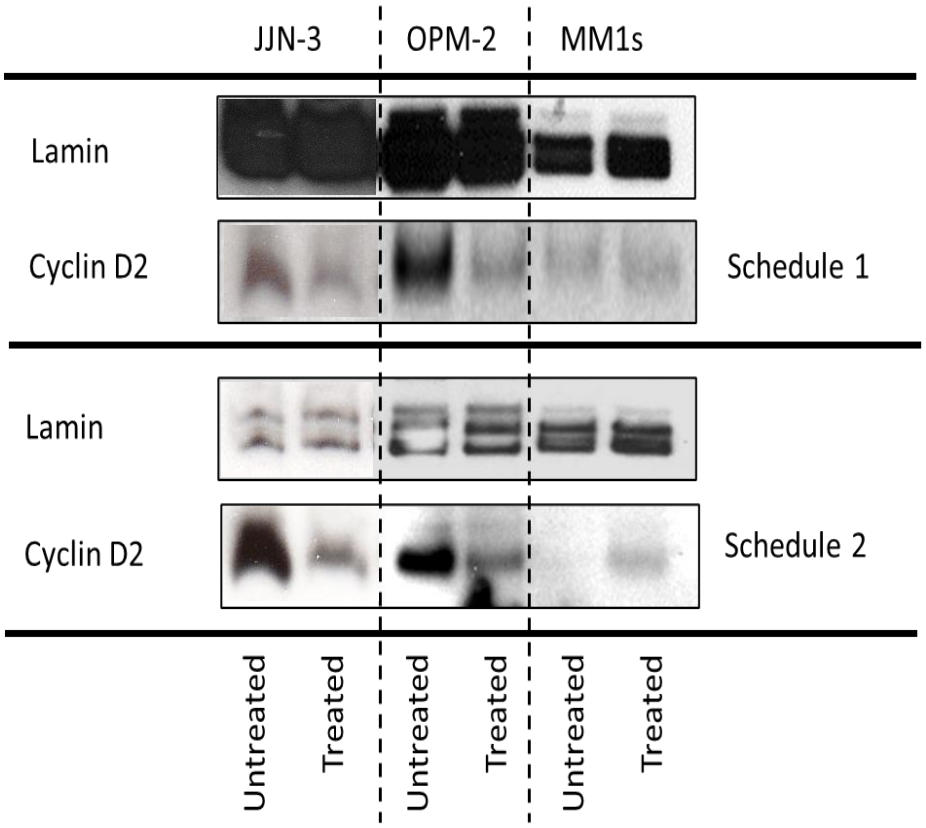


Figure 4.6: Representative individual Western blots for Cyclin D2 expression in JJN-3, OPM-2 and MM1s myeloma cell lines following treatment with IR and Bortezomib under schedules 1 and 2. Lamin was used as housekeeping protein for loading control. N=2-3

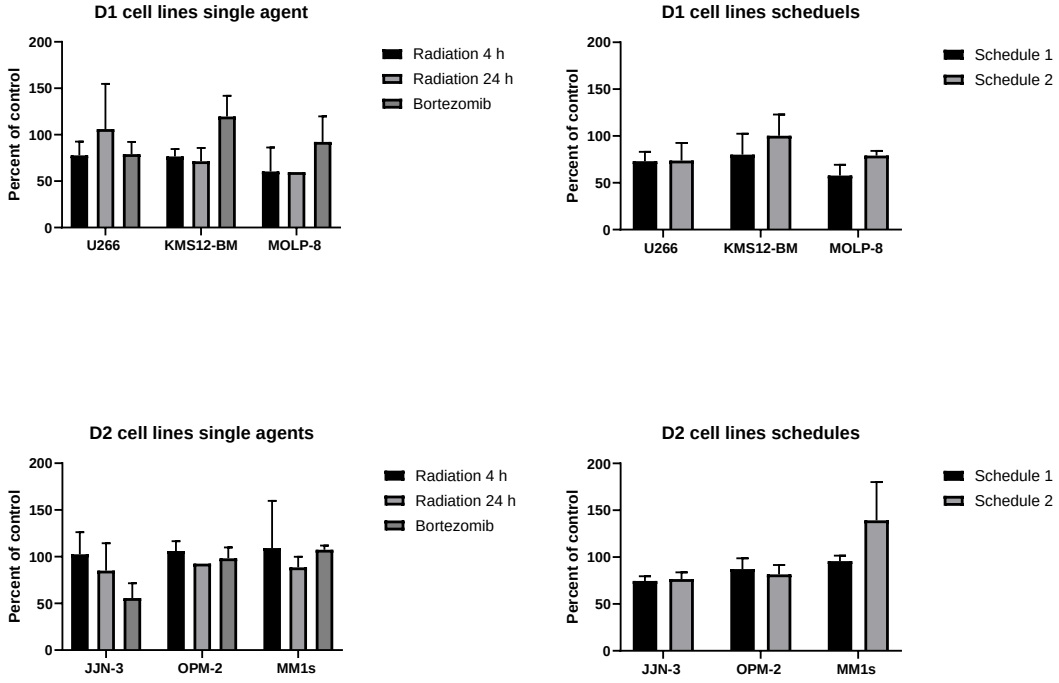


Figure 4.8: Densitometry analysis of the cyclin D expression in the myeloma cell lines following treatment with IR and bortezomib as single agents (A and C) and in combinations (B and D). The bars represent the mean of at least three independent experiments; error bars represent the standard deviations. The control bar (100%) is not plotted. Although there were numerical differences in all the graphs in comparison to the controls, the changes were not statistically significant.

The myeloma cell lines used in this project were sensitive to nanomolar concentrations of bortezomib. This was expected and has been established previously in the literature (197,200). The IC_{50} of U266 and MM1s using the MTT assay was found to be 3 and 1.5 nM respectively (200).

A study by Ngo et al found an association between cyclin D1 levels and good response to treatment with bortezomib. In addition, longer remission was observed than in those patients with cyclin D2 or cyclin D3 overexpression. The study suggested the use of cyclin D1 as a predictive marker for response to treatment (201). As this study was

conducted more than 10 years ago, combinations of bortezomib were not as mature and the standard cytogenetic assessments were not done (apart from 13q deletion).

The concentrations of bortezomib used for the treatment of the six myeloma cell lines were chosen based on the induction of a modest degree of apoptosis of around 30% as assessed by the annexin V assay. The reason for this is two-fold; first, concentrations that would cause a significant reduction in viability would make the assessment of any additivity or synergy when combining bortezomib with IR difficult due to the dominant effect of bortezomib at higher concentrations, and, two, a lower number of viable cells would also jeopardise the assessment of cyclin D changes especially that bortezomib was toxic at nanomolar concentrations and that cyclin D levels have changed even when using these low concentrations. Therefore, it was not possible to assess, within these limits, whether a higher concentration of bortezomib would have had a different impact on the three cell lines (KMS12-BM, OPM-2 and MM1s) in terms of any changes to the relevant cyclin D expression. There was a noticeable variability in the sensitivity of different cell lines to bortezomib which is not unexpected. The bortezomib concentrations chosen for the combination experiments with IR were based on the observed reduction in viability (as assessed by the annexin V assay) of 20-30%. A better way of choosing those concentrations would have been to calculate the IC70 or IC80 using non-linear regression. We acknowledge that this would have been a better model and would have introduced more uniformity to our data.

The reduction in cyclin D1 expression in the relevant cell lines with schedule 1 and schedule 2 is expected given that the effect of IR in all of the three cell lines and the

effect of bortezomib in all but the KMS12-BM cell line was the downregulation of cyclin D1 expression.

Although a previous study by Goel et al examined the impact of combining bortezomib and IR and showed synergy when those were combined in sublethal doses (197), the four cell lines in that study were treated for a longer duration (16 hours with bortezomib in addition to assessment 72 hours after IR). This makes a direct comparison between that study and the results of this chapter difficult. It is also possible that the duration of bortezomib treatment used in schedules 1 and 2 was not long enough to downregulate NF-κB.

It does give credence, however, to the approach used in this chapter where bortezomib was used as a pre-treatment before IR. Goel et al used cell lines with different cyclin D expressions (ARH-77 expresses cyclin D1 (202), RPMI 8662 does not express cyclin D (203) and JJN-3 and MM1s are cyclin D2 expressors). The presence of synergy, although, not detected using the experiments in this chapter, was not associated with or attributed to the variation in the cyclin D type status.

There was significant heterogeneity in terms of responses to the bortezomib and radiation in combination, especially in the cyclin D2-expressing cell lines. Whilst cyclin D1 was downregulated with radiation and with bortezomib singly or in combination, the cyclin D2 status did not follow a uniform course. In the JJN-3, bortezomib caused the downregulation of cyclin D2 that persisted with schedule 1 whereas in the OPM-2 cell line, cyclin D2 downregulation only happened with the combination treatment. More interesting, however, was the increase in the cyclin D2 in the MM1s when the cell was treated with schedule 2 as compared to the control. This was also associated

with an improvement in viability as compared to schedule 2 and the monotherapy treatments. Although, explaining this mechanistically would require further experiments, these findings may suggest that cyclin D2 can be associated with chemoresistance. Nevertheless, the densitometry results for this observation does not hold statistical significance. Moreover, the heterogeneity of the cyclin D2 responses observed indicates that a mechanistic explanation solely based on the cyclin D type status is not possible and therefore cyclin D use as a predictive biomarker to response may not be appropriate. It does not deviate, however, from the clinical observation of a worse myeloma phenotype seen with myeloma cells exhibiting cytogenetic changes associated with cyclin D2 overexpression. It is also not difficult to imagine a positive impact on survival and proliferation when a protein associated with driving the cell cycle forward is overexpressed and is congruent to previously mentioned research associating cyclin D with a negative impact on prognosis. Perhaps the only feasible way to investigate this observation is to replicate the experiments before and after cyclin D2 induction in a cyclin D2 negative cell line. Such isogenic comparison will remove almost all confounding factors and an ideal for future work.

In conclusion, the experiments undertaken in this chapter did not reveal a direct relationship between cytotoxicity due to DNA damage and proteasome inhibition and the underlying D-type cyclin in the myeloma cell lines used in this project. While the cyclin D1 downregulation in response to DNA damage was demonstrated, the cyclin D2 response to the same treatment was more heterogenous and did not follow a discernible pattern. The upregulation of cyclin D2 in the MM1s cell line and the apparent reduced cell death in response to the combination treatment may hint toward a survival role for cyclin D2, however, this would require further confirmation.

CHAPTER 5:

ASSESSMENT OF RESPONSE TO APOPTOSIS INDUCTION VIA THE INTRINSIC PATHWAY IN CYCLIN D1- AND CYCLIN D2-EXPRESSING MYELOMA CELLS

Chapter 5: Assessment of Response to Apoptosis Induction via the Intrinsic Pathway in Cyclin D1- and Cyclin D2-expressing Myeloma Cell Lines

5.1 Introduction

Apoptosis is a complex multistep active process. Central to the initiation of apoptosis is the action of caspases. These cysteine-aspartate proteases prepare the cells for apoptosis by macrophages as they fragment the DNA and other cellular structures. The externalisation of phosphatidyl serine on the surface of apoptotic cells serves as a signpost for macrophages. Two main pathways converge to activate caspases, the extrinsic and the intrinsic (mitochondrial) pathways.

The process of mitochondrial outer membrane permeabilisation (MOMP) lies at the heart of cell death via the intrinsic pathway of apoptosis. This process, which leads to the release of cytochrome c, among other factors, from the space between the inner and the outer mitochondrial membranes hinges on the oligomerisation of BAK and BAX. This is followed by caspase activation and the streamlined process to cell death. The event of MOMP is considered the point of no return and the affected cell at this stage is considered to be at the event horizon of apoptosis (204,205) (Figure 1.6). Detecting the release of cytochrome c (such as by flow cytometry) has been demonstrated to be an early predictor of commitment to apoptosis (166,206). Under physiological/steady state, a balance is kept between the pro-apoptotic sensitisers/activators of the BH3-only family of proteins (BIM, BID, BAD, BIK, BMF,

HRK, PUMA and NOXA) and the anti-apoptotic BCL-2 family proteins (BCL-2, BCL-xL, BCL-W, BFL1 and MCL-1). The pro-apoptotic activators, BIM, BID and PUMA, are capable of mainly activating BAK and BAX, while the rest (the sensitisers) are less efficient at this function and are mainly inhibitors of the anti-apoptotic proteins. When a process is significant enough to initiate apoptosis, the equilibrium is lost and the balance tips towards pro-apoptosis whereby the activators/sensitisers over-saturate their counterparts leading eventually to the activation of BAK and BAX and the chain of events as described above (205).

As stated in Chapter 1 (Section 1.2.6), BCL-2 and MCL-1 are at interplay in terms of myeloma cell survival with a dominant effect of MCL-1 over BCL-2 in the majority of myeloma cell lines and myeloma primary samples. MCL-1 plays a critical survival role in multiple myeloma such that the inhibition of this protein by an anti-sense oligonucleotide has been shown to induce apoptosis (49,207). MCL-1 expression is induced by IL-6 from the bone marrow and can also be BCMA (B cell maturation antigen)-mediated. Patients with a relapsed disease were also found to have higher levels of MCL-1 dependency and MCL-1 expression as compared to levels at diagnosis (208).

MCL-1 is located on chromosome 1q, the gain of which is an important prognostic event (Chapter 1, Section 1.2.2). There is evidence that primary myeloma samples from patients with 1q gain were more sensitive to MCL-1 inhibition (50), however, this was not replicated in other studies (209).

A detailed account of apoptosis derangement in multiple myeloma is found in the introduction (Section 1.2.6). In brief, BCL-2, and MCL-1 both play an important antiapoptotic effect in myeloma. BCL-2 binds to BIM, inhibiting its interaction with BAK and BAX and

therefore preventing apoptosis. BCL-2 inhibition (such as with venetoclax) was ineffective in the majority of myelomas. The reason is that any released BIM from BCL-2 inhibition was taken up by MCL-1 thereby preventing the initiation of apoptosis. It follows that most myelomas are MCL-1 dependent. The exception is those myelomas with t(11;14) translocation that tend to be dependent on BCL-2 rather than MCL-1 (Figure 1.6). Simultaneous inhibition of BCL-2 and MCL-1 is therefore an attractive target and is synergistic in multiple myeloma (112–115,210). Our group has shown the synergistic effect of BCL-2/MCL-1 inhibition in myeloma cell lines and primary samples. The synergy was confirmed through the detection of cytochrome c release in response to dual BCL-2 and MCL-1 inhibition (166).

5.1.1 The specific BCL-2 and MCL-1 Inhibitors Used

5.1.1.1 Venetoclax (ABT-199)

This is a selective BCL-2 inhibitor that is a successor of navitoclax which inhibits BCL-xL in addition to BCL-2 and caused thrombocytopenia in clinical trials. Venetoclax does not inhibit BCL-xL. Although the main licenced indications in clinical practice for venetoclax are in the treatment of CLL and AML, it has also been used in the treatment of myeloma (163,164,211). Early-phase clinical trials showed efficacy in combination with dexamethasone that correlated with the level of expression of BCL-2. Notably, this was seen, although not exclusively, in patients with t(11;14) (27). In the Bellini trial, venetoclax, bortezomib and dexamethasone were compared to bortezomib and dexamethasone in patients with multiple myeloma. Although the PFS was higher in the experimental arm, a rather unsuspected inferior OS (probably due to increased infections) was observed with the venetoclax arm. The maximum

benefit was seen in patients with t(11;14)/high BCL-2 expressors and, interestingly, this group did not suffer an inferior OS (116).

5.1.1.2 S63845

S63845 is a thienopyrimidine-based compound that was shown to be a highly selective and potent inhibitor of MCL-1 in multiple haematological cancers (211). It has been shown to be effective in apoptosis induction in many myeloma cell lines. Sensitive cell lines were shown to have low BCL-xL levels with no impact on the underlying level of expression of BCL-2 (212). It is worthwhile to note that deletion of MCL-1 was actually found to be lethal on account of the development of dilated cardiomyopathy and mitochondrial dysfunction (213) and, therefore, intermittent inhibition as a goal in clinical translation is suggested (212). S63845 has not been reported in any clinical trials as far as we are aware. However, other MCL-1 inhibitors have been used in early phase clinical trials (PRT1419 and S64315) but those trials are either still recruiting, not reported or withdrawn/terminated.

5.2 The Aim of this Chapter

This work investigated whether there is a differential response in terms of apoptosis between the cyclin D1 and the cyclin D2 myeloma cell lines. The intrinsic (mitochondrial) pathway was interrogated for this purpose and to ensure induction of apoptosis via this pathway without the need to implicate DNA damage, inhibitors to the main anti-apoptotic culprits in myeloma were used. BCL-2 and MCL-1 inhibition also mitigates the impact of p53 status variability between cell lines since apoptosis induction through this route is p53-independent. We also wanted to examine the possible synergistic response to dual BCL-2/MCL-1 inhibition, whether

there is a differential response for this synergy in terms of the underlying cyclin D translocation and the impact of the dual inhibition on cyclin D1 and cyclin D2 expression.

To be able to examine the process of cooperative inhibition of MCL-1 and BCL-2 and the effect of that on viability and induction of apoptosis, two assays were used. The Alamar Blue is a metabolic assay that is fast, reproducible, and easy to use. The Alamar Blue assay was used as a surrogate to assess the viability after exposing the myeloma cell lines to BCL-2 and MCL-1 inhibitors as single agents and in combinations. The points of apparent maximum synergy with the combination treatment were then interrogated with the Annexin V assay to confirm that the observed drop in the viability as inferred by the Alamar Blue assay is indeed a reflection of apoptosis.

As mentioned in the introduction, our group has shown a synergistic effect of simultaneous BCL-2 and MCL-1 inhibition through the release of cytochrome c. The cytochrome c release assay provides a quick and reliable flow-cytometric way of assessing cytotoxicity. The attractiveness of this assay comes from the short incubation period of only 4h after drug addition to establish whether there is a cytotoxic effect or not. This is useful since it provides a rapid read-out of cytotoxicity especially when assessing primary samples that are known to have poor survival in vitro. As a second aim of this chapter, we sought to confirm that the cytochrome c release assay indeed mirrored the results of conventional apoptosis assays (Alamar Blue and Annexin V).

5.3 Results

5.3.1 The Combination of MCL-1 and BCL-2 Inhibition was Synergistic in 5 out of 6 Myeloma Cell Lines

Cell lines were treated with the BCL-2 inhibitor, venetoclax and/or with the MCL-1 inhibitor S63845 using fixed-ratio micromolar concentrations as detailed in Table 5.1 for 48 hours before analysis. The Alamar Blue assay was used as described above to assess viability and to deduce if there was synergy from the combination treatment.

Table 5.1: A list of the venetoclax and the S63845 concentrations used for the single agent and the combination treatments. All concentrations are in µM

U266, JJN-3, MM1s		KMS12-BM, MOLP-8, OPM-2	
Venetoclax	**S63845**	**Venetoclax**	**S63845**
0.1	0.01	0.01	0.001
0.5	0.05	0.05	0.005
1	0.1	0.1	0.01
5	0.5	0.5	0.05
10	1	1	0.1

The IC_{50} data for the single agent treatment of the myeloma cell lines showed that the U266 cell line was the most resistant to treatment with venetoclax and S63845 (Table 5.2). The cell lines were generally more sensitive to single agent treatment with the MCL-1 inhibitor (S63845) judging by the IC_{50} micromolar concentration with the MOLP-8 being the most sensitive. The KMS12-BM cell line was the most sensitive to venetoclax. The combination treatment appeared synergistic in all the cell lines apart from the MOLP-8 where the combination treatment effect on the viability appeared to be similar to that of the S63845

single agent treatment with no contribution from the venetoclax treatment (Figure 5.1). Synergy was identified in the rest of the cell lines by a combination index < 1 as per the Chou-Talalay method 194 (Table 5.3). The MOLP-8 combination index results were very close to 1. Similar to the single agent treatment, the U266 cell line appeared to be the least sensitive to the combination treatment. There was no defined pattern in terms of drug sensitivity or synergy that could have been attributed to the underlying cyclin D-type.

Table 5.2: The IC_{50} (µM) for single agent treatment with venetoclax and S63845 for each of the myeloma cell lines. This is based on the Alamar Blue assessment of viability. NE=Not evaluable.

	U266	KMS12-BM	MOLP-8	JJN-3	OPM-2	MM1s
Venetoclax	NE	3.44	NE	3.821	NE	8.167
S63845	1.02	0.098	0.035	0.1047	0.05	0.345

Table 5.3: The combination index for each combination of the MCL-1 and the BCL-2 inhibitor obtained from data analysis using the Compusyn software ™ based on the Chou-Talalay method. A combination index <1 indicates synergy

Conc. (µM)		Combination Index			**Conc. (µM)**		Combination Index		
Ven+S63845		U266	JJN-3	MM1s	**Ven+S63845**		MOLP-8	KMS12	OPM-2
0.1	0.01	>1500	0.296	0.4	0.01	0.001	>1500	1.2	0.61
0.5	0.05	0.37	0.07	0.43	0.05	0.005	0.09	0.64	0.58
1	0.1	0.45	0.13	0.22	0.1	0.01	0.8	0.7	0.04
5	0.5	0.245	0.68	0.133	0.5	0.05	0.898	0.005	0.04
10	1	0.48	1.4	0.271	1	0.1	0.99	0.011	0.09

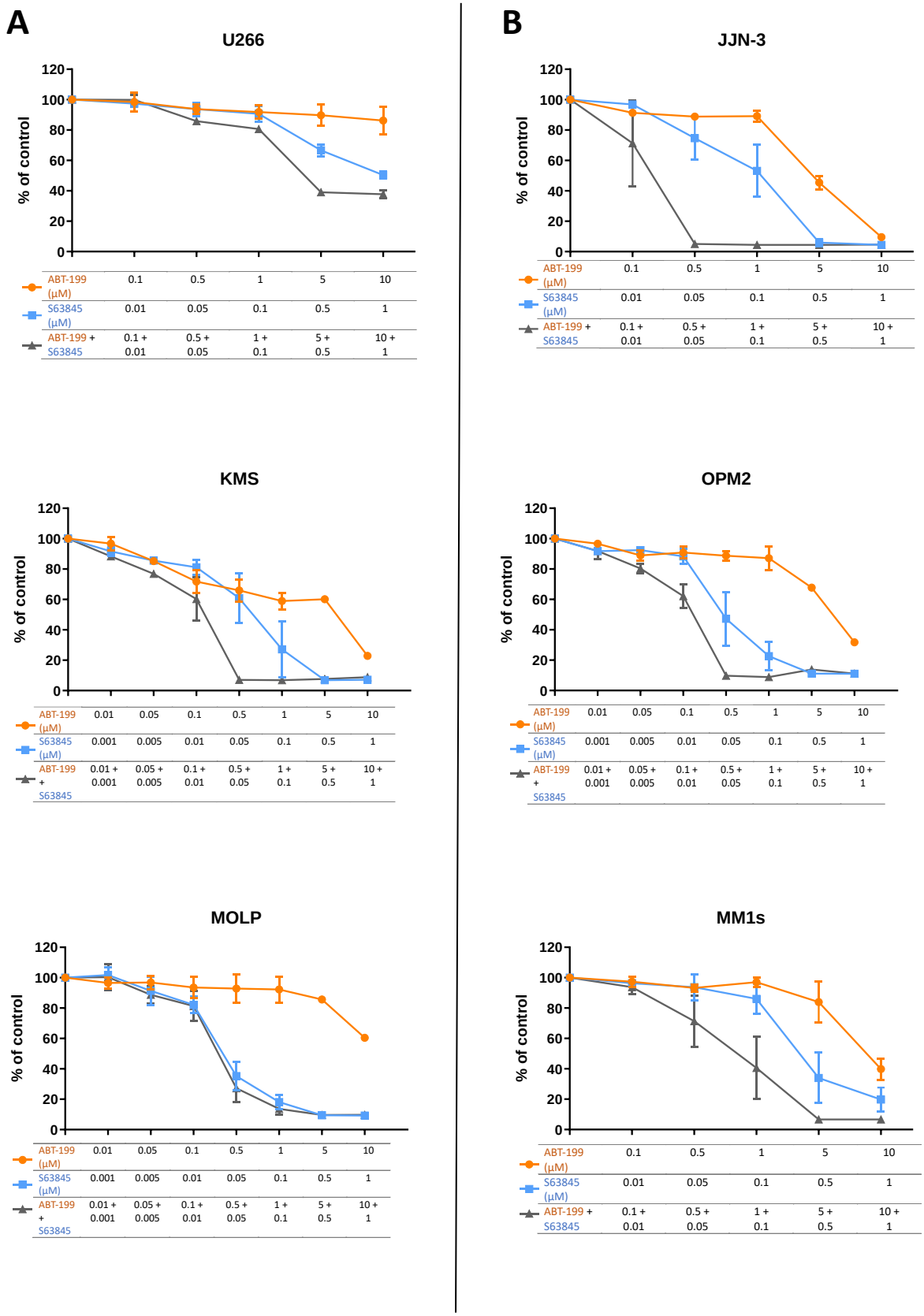


Figure 5.1: The viability of the cyclin D1 myeloma cell lines (A) and the cyclin D2 cell lines (B) in response to treatment with fixed-ratio concentrations of venetoclax, S63845 and the combination of the two was assessed using the Alamar blue assay after 48 hours. The results were expressed as mean percentages of the control of three independent experiments. Error bars represent the standard deviation

5.3.2 Annexin V Binding Confirms the Synergy from MCL-1/BCL-2 Inhibition is due to Apoptosis

Since the Alamar blue assay does not measure apoptosis directly, the next step was to confirm that the observed synergistic effect of the combined BCL-2 and MCL-1 inhibition is due to apoptosis induction. For that purpose, Annexin V binding quantification was used as the next step as this is a more specific assay for apoptosis. The concentrations chosen for this experiment are as in Table 5.4 and were inferred from the results of the Alamar Blue assay at the points of perceived maximum synergy. Cell lines were treated with the chosen concentrations for 48 hours and assayed using flow cytometry for Annexin V binding. Cells that stained with anti-annexin V antibody and those that stained with propidium iodide were counted as apoptotic.

Similar to the results obtained from the Alamar Blue experiments, the impact of single-agent treatment with venetoclax and S63845 was minimal in terms of the percentage of apoptotic cells as compared to the controls. In addition, the myeloma cell lines appeared to be less sensitive to single agent treatment with venetoclax (<20% apoptosis) as compared to single agent treatment with S63845.

Table 5.4: The concentrations (μM) of ABT-199 and S63845 used for Annexin V assay

	U266	KMS12-BM	MOLP8	JJN-3	OPM-2	MM1s
ABT-199 (μM)	5	0.5	0.5	0.5	0.5	1
S63845 (μM)	0.5	0.05	0.05	0.05	0.05	0.1

Synergy with the combination treatment was assessed using the Bliss independence model as detailed in Chapter 2 (2.6). The combination treatment produced an impressive increase in apoptosis indicating that the synergistic effect observed with the Alamar Blue assay was indeed due to apoptosis (Figure 5.2).

The OPM-2 and U266 synergistic effect for the combination treatment, was slightly less pronounced than that observed with the other cell lines.

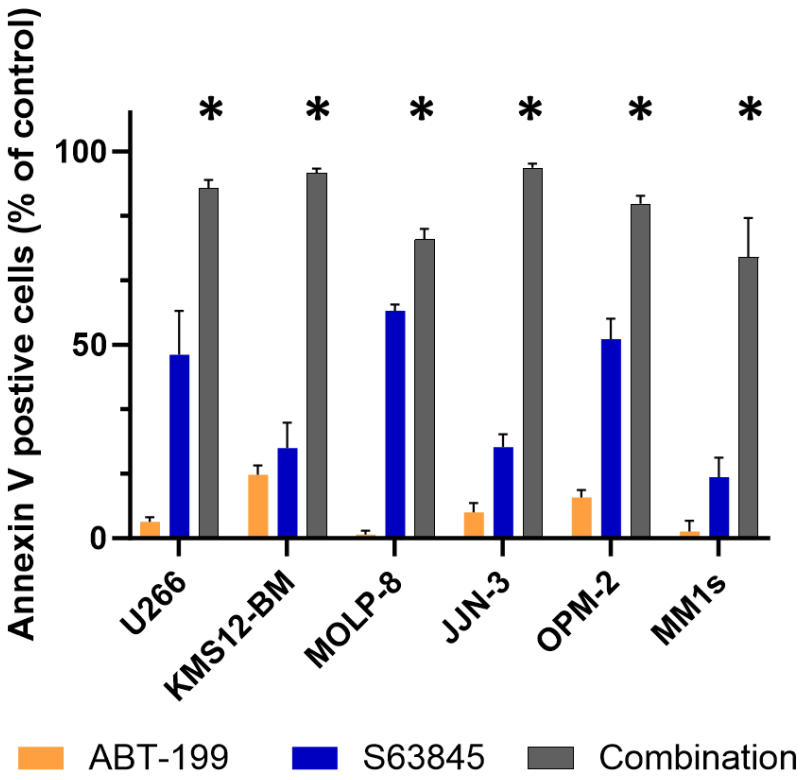


Figure 5.2: Annexin V assay results for the 6 myeloma cell lines as percentages of the control 48 h following treatment with venetoclax, and S63845 as single agents and in combination. * indicates synergism as per the Bliss independence model. The bars represent the mean of at least three independent experiments; error bars represent the standard deviations.

Again, there was no apparent pattern of apoptosis that could have been attributed to the underlying cyclin D type terms of their response to venetoclax and S63845 treatment as single agents.

With the combination treatment, all the cell lines with cyclin D2 over-expression showed synergy. Within the cyclin D1 translocated group, the U266 cell line, despite showing a synergistic effect with the combination, was generally the least sensitive cell line while border line/ no synergy was observed with the MOLP-8 cell line.

The p53 status had no apparent impact on whether the cell lines are more sensitive to the single agent treatment or the combination treatment.

5.3.3 Cytochrome c Release Assay was Predictive of Apoptosis in Response to BCL-2 and MCL-1 Inhibition and Correlated with the Annexin V and Alamar Blue Results

The cytochrome c release assay was performed by a project MSc student (Joanna Cull) under my co-supervision. The project aimed at investigating the BCL-2 / MCL-1 combination synergy using the cytochrome c release assay. The cytochrome c results demonstrated, similar to the Annexin V and the Alamar Blue results above, the lack of appreciable single agent responses at the concentrations used whereas the combination treatment led to a significant cytochrome c release indicating a significant synergistic response in all the myeloma cell lines. The synergy was most pronounced with the cyclin D2 cell lines (JJN-3, OPM-2 and MM1s). Again, the p53 status had no bearing on the degree of synergy observed (Figure 5.3).

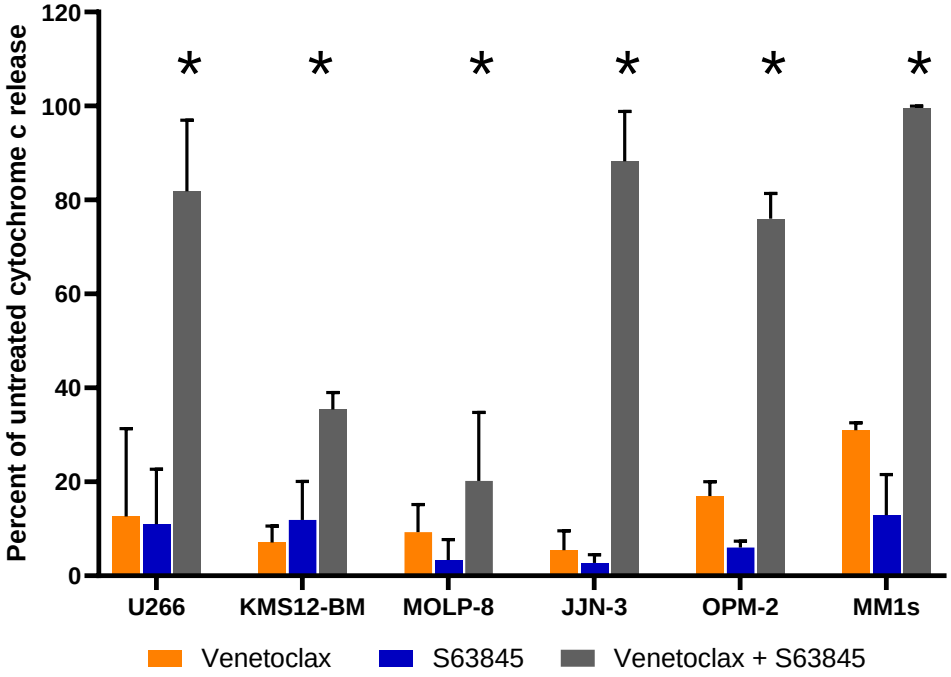


Figure 5.3: Flow-cytometric cytochrome c measurement of the myeloma cell lines following a 4h treatment with venetoclax, S63845 and the combination of both. *=synergy as per the Bliss independent model. The bars represent the mean of at least three independent experiments; error bars represent the standard deviations.

5.3.4 The Cytochrome c Release Assay was Suitable for Apoptosis Prediction in Primary Myeloma Patient Samples

Primary myeloma samples from seven patients were incubated with 1µM of each of venetoclax and S63845 as single agents and in combination for 4 hours then cytochrome c release was assessed. Like the cell line results, impressive synergy was demonstrated with the combination treatment in all the samples indicating the utility of the cytochrome c release assay use in apoptosis prediction in primary samples after a short period of incubation and therefore mitigating the need to keep the primary

myeloma samples in culture in vitro for a long period to assess apoptosis using conventional assays such as Annexin V binding (Figure 5.4).

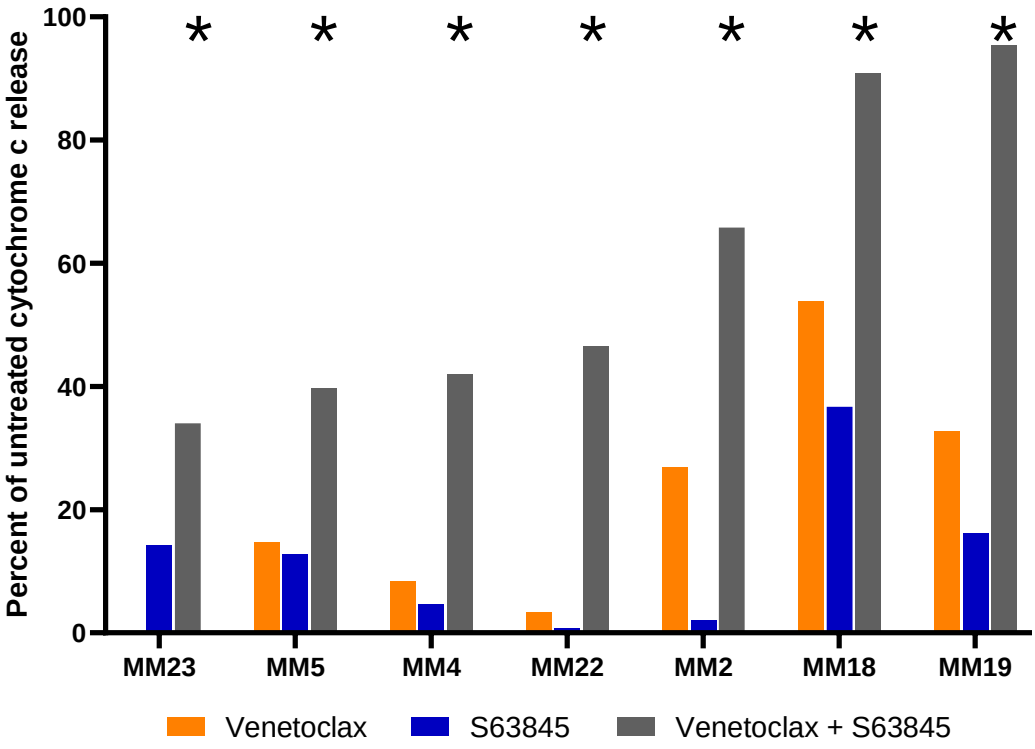


Figure 5.4: Cytochrome c release was assessed by flow cytometry in 7 primary myeloma samples following treatment with venetoclax, S63845 and their combination for 4 hours. *=synergy as per the Bliss independent model. The cytogenetic characteristics of those patients have been described previously in Table 2.2.

5.3.5 Cyclin D, MCL-1, and BCL-2 Expression by Western Blotting

After assessing the impact of BCL-2 and MCL-1 inhibition on the myeloma cells viability, the next step was to assess the impact of this inhibition on actual protein expression. Changes to the expression of cyclins D1 and D2, MCL-1 and BCL-2 in response to venetoclax and S63845 single-agent and combination treatment were assessed using Western blotting. Figure 5.9 is a schematic representation of the

Western blot results to allow easier comparison across the myeloma cell lines. Unfortunately, the blots for the MM1s cell line were not clear, however, there was a concurrent MSc project in our lab investigating the BCL-2/MCL-1 targeting in myeloma cell lines using the same inhibitor in this project. The comments on and the images of the MM1s Western blotting results were referenced to that project [195].

5.3.5.1 Western blotting showed no significant changes in protein expression in response to single-agent treatment.

Cell lines were treated with venetoclax and S63845 using the concentrations in Table 5.4 and Western blotting for MCL-1, BCL-2, and cyclins D1 and D2 was done. The single agent treatment whether with venetoclax or S63845 did not cause appreciable changes to the protein expression of cyclins D1 and D2, MCL-1 and BCL-2 in 5 out of the 6 cell lines tested. There was a slight reduction in the cyclin D2 band in the MM1s cell line following the single-agent treatment (Figure 5.5, Figure 5.6, Figure 5.7, Figure 5.8 and Figure 5.9).

5.3.5.2 Down-regulation of Cyclin D was associated with synergy to MCL-1 and BCL-2 inhibition

There was a clear down-regulation with the combination treatment in all the cell lines apart from the MOLP-8 (Figure 5.7, Figure 5.8 and Figure 5.9). As mentioned above, the MOLP-8 cell line where synergy was doubtful with the combined MCL-1 and BCL-2 inhibition. MCL-1 expression was also reduced with the combination treatment in two of the cyclin D2 cell lines (JJN-3 and MM1s) (Figure 5.5) and one of the cyclin D1 cell lines (U266) (Figure 5.6).

5.4 Discussion

In this chapter, the effect of inhibition of major pro-survival proteins in the apoptotic pathway in multiple myeloma (BCL-2 and MCL-1) was examined to elucidate if there was an observable difference in terms of apoptosis induction via the mitochondrial pathway depending on whether cell lines expressed cyclin D1 or cyclin D2. Synergism due to dual BCL-2/MCL-1 inhibition in multiple myeloma has been reported previously [186,187]. We wanted to see if that synergy varied according to the underlying cyclin D translocation. Venetoclax and S63845 are established BCL-2 and MCL-1 inhibitors, respectively. The myeloma cell lines were treated with venetoclax and S63845 as single agents and in combination. The concentrations used for the combination treatment were based on the data from the single agent treatment and were in fixed ratios. As mentioned in Materials and Methods (section 2.6), the use of Fixed drug concentration ratio allows an automated analysis of synergy using the median-effect equation via Compusyn software rather than using a separate analysis for each combination point. Our myeloma cell lines were generally more sensitive to MCL-1 inhibition as compared to BCL-2 inhibition, confirming their dependence on MCL-1 rather than BCL-2 for survival (49,207). It has been shown that BCL-2 over-expression, and thereby sensitivity to venetoclax, was seen in myelomas with t(11;14) (112,214,215). Despite this, there is no complete biological explanation for this association and there is a group of myelomas that over-express BCL-2 without necessarily having a t(11;14) (214). Our data from the single agent treatment with venetoclax did not suggest higher cytotoxicity in the cyclin D1 group of cell lines however, the concentrations of venetoclax used were relatively small.

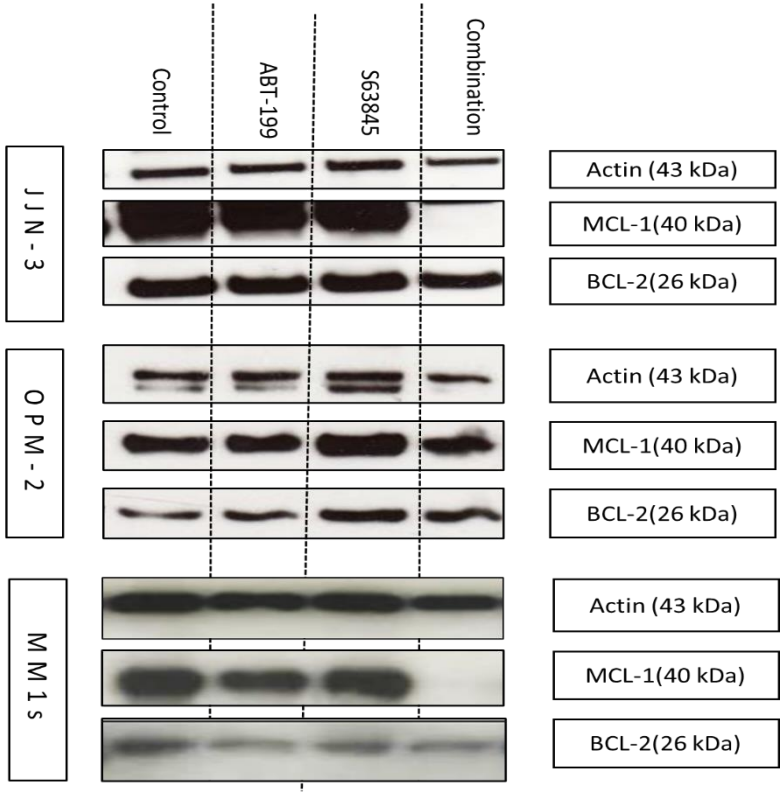


Figure 5.5: Representative MCL-1 and BCL-2 expression as assessed by Western blotting for Cyclin D2 cell lines (JJN-3, OPM-2 and MM1s) following treatment with venetoclax and S63845 as single agents and in combination. Actin was used as a housekeeping control. N=2-3. MM1s Western blots were done by an MSc project student

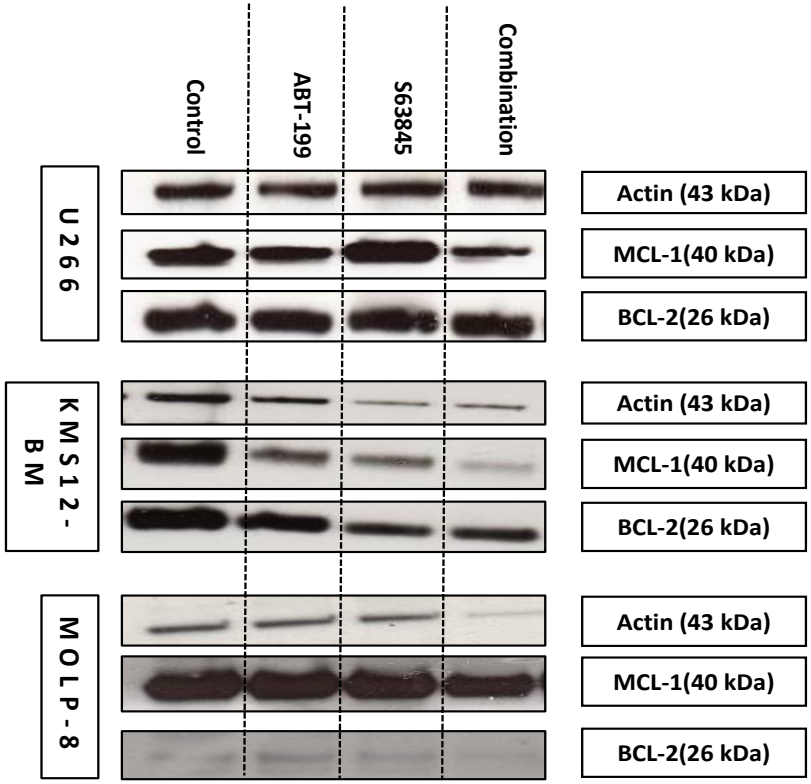


Figure 5.6: Representative MCL-1 and BCL-2 expression as assessed by Western blotting for Cyclin D1 cell lines (U266, KMS12-BM, and MOLP-8) following treatment with venetoclax and S63845 as single agents and in combination. Actin was used as a housekeeping control. N=2-3.

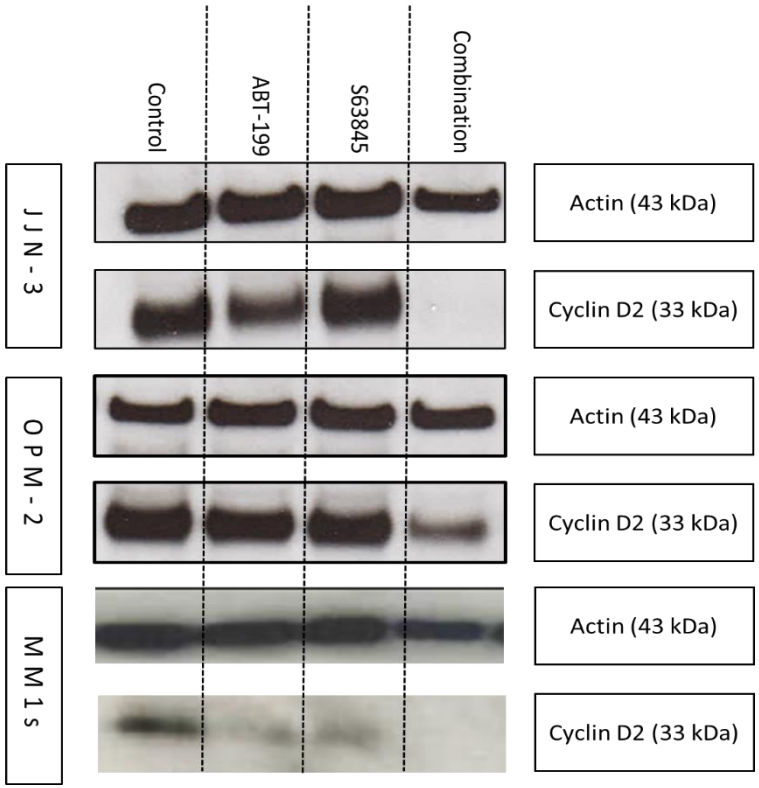


Figure 5.7: Representative Cyclin D2 expression as assessed by Western blotting for Cyclin D2 cell lines (JJN-3 and OPM-2) following treatment with venetoclax and S63845 as single agents and in combination. Actin was used as a housekeeping control. N=2-3. MM1s Western blots were done by an MSc project student[195]

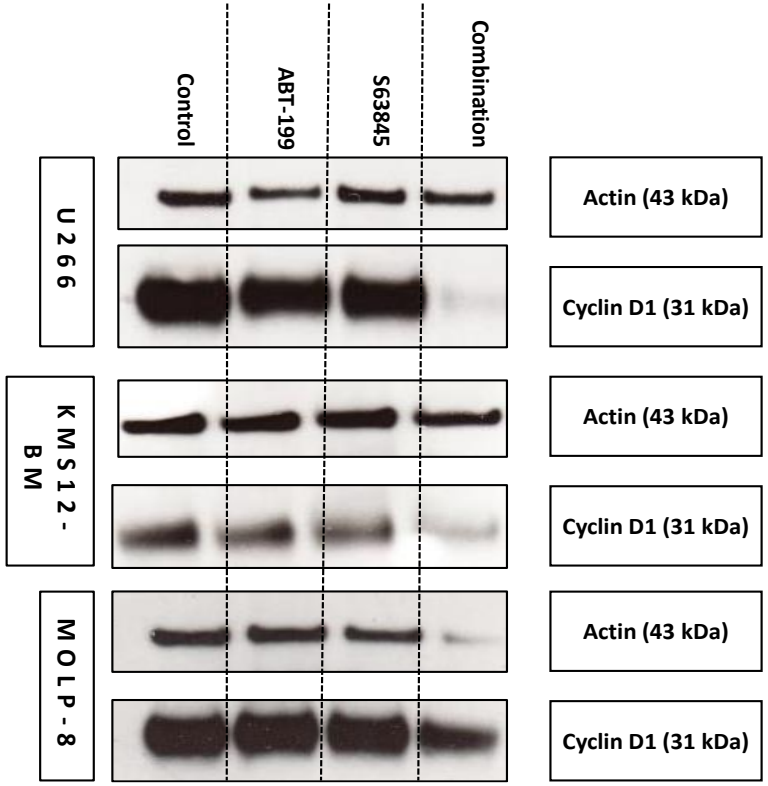


Figure 5.8: Representative Cyclin D1 expression as assessed by Western blotting for Cyclin D1 cell lines (U266, KMS12-BM, and MOLP-8) following treatment with venetoclax and S63845 as single agents and in combination. Actin was used as a housekeeping control. N=2-3

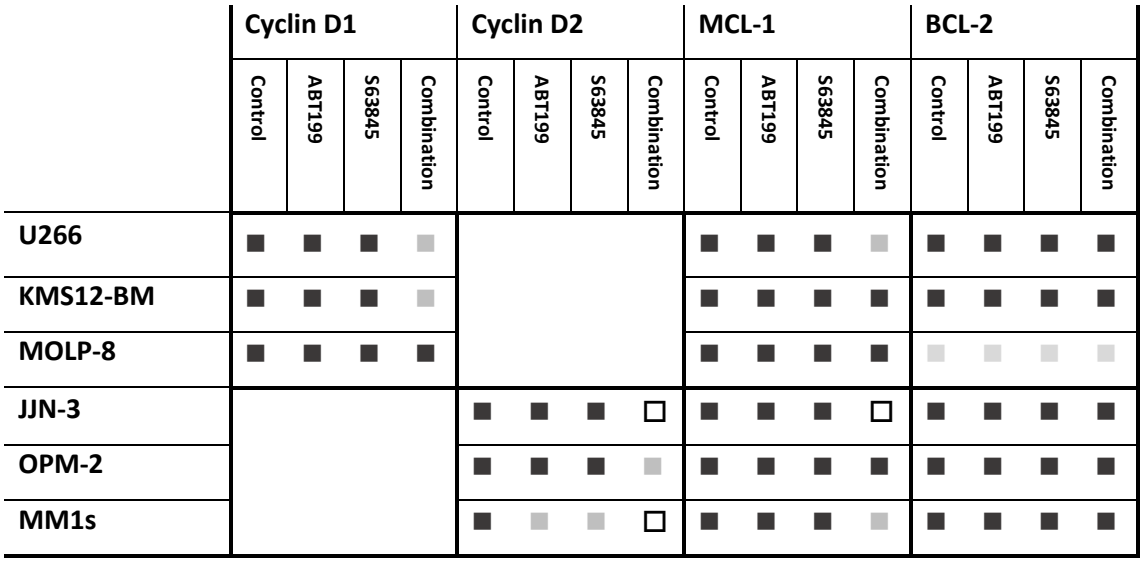


Figure 5.9: Schematic summary of the levels of expression of cyclins D1 and D2, MCL-1 and BCL-2 in the 6 myeloma cell lines following treatment with venetoclax, S63845 and the combination of both agents. Each experiment was repeated independently at least twice. ■ = normal expression, ■ = reduced expression, □ = no expression)

Moreover, cell lines have inherently more genetic dysregulation than primary myeloma cells and it is not difficult to imagine that the acquisition of other changes due to the cytogenetic instability in those cell lines can confer resistance to BCL-2 inhibition even in cell lines with the t(11;14). As mentioned above, the sensitivity of the myeloma cells to venetoclax was associated with t(11;14) but this was no exclusive. Given the that number of cell lines we used is relatively small, it is possible that this lack of exclusivity to the t(11;14) could play a role in the lack of sensitivity to venetoclax that we observed. MCL-1 sensitivity is not associated with an underlying chromosomal translocation, however, there is some evidence that it can correlate with the level of 1q gain load (50) although not all studies confirmed this (216). Although the myeloma cell lines used in this project all had 1q gain, they varied in the

gain load (6-8 copies in MOLP-8 and OPM2 and 3-4 copies in KMS12-BM and JJN-3). This did not have an impact on the sensitivity to single agent S63845 at the concentrations we used.

Consistent with the reports in the literature, the combination of MCL-1 and BCL-2 inhibition in the myeloma cell lines demonstrated synergy at multiple concentrations when tested using the Alamar Blue assay. To confirm that this observed effect was due to apoptosis induction, the annexin V assay was used at the points of maximum observed synergy. The results of the annexin V assay confirmed the results observed with the Alamar Blue assay. They also confirm our previous results showing synergy with cytochrome c release following simultaneous venetoclax and S63845 treatment (166). All the cyclin D2 (JJN-3, OPM-2 and MM1s) cell lines showed a synergistic effect. MOLP-8 which is a cyclin D1 cell line border line/ no synergy and the U266 cell line was generally more resistant to treatment with single agents and the combination treatment. A firm conclusion, however, regarding the sensitivity being related to the underlying cyclin D-type cannot be deduced.

The cytochrome c release assay has been demonstrated to provide a rapid assessment of sensitivity after only a short incubation with drugs (206). This has clear benefits when assessing the cytotoxicity in more vulnerable cells in vitro such as primary patient samples. It is well known that primary myeloma cells are notoriously difficult to maintain in culture. We have shown a significant increase in apoptosis in primary myeloma samples after 24h incubation in vitro and without cytotoxic agents (166). The use of cytochrome c assay can undercut this shortfall and provide a rapid and predictive apoptosis assessment within only 4 hours of incubation with the drugs of

interest. We have demonstrated the feasibility of this assay for this purpose and confirmed, in myeloma cell lines and primary samples, that the results of the assay mirrored the results of the conventional (longer incubation) assays such as the annexin V assay.

Cyclins D1 and D2 downregulation mirrored the synergy observed with the apoptosis assays. The downregulation of cyclin D with the combination treatment was seen in all the cell lines except the MOLP-8. The inter-relationship between cyclin D and BCL-2/MCL1 is complex and probably not fully elucidated. In two previous studies, the use of the pan-BCL-2 inhibitor, Obatoclax, in colorectal cancer cell lines caused the downregulation of cyclin D1 with a resultant cell cycle arrest at G1. The downregulation of cyclin D1 was associated with the upregulation of p21 and p27 (217,218). Another study using TW-37, a small molecule inhibitor of BCL-2, showed the downregulation of cyclin D1, cell cycle arrest during the S-phase and upregulation of phosphorylated Chk1 (219). Silencing BCL-2 in a mantle cell lymphoma *in vivo* model was shown to cause the downregulation of cyclin D1. Some of the suggested mechanisms were attributed to the additional role of BCL-2 as a docking protein and include the ubiquitylation and degradation of cyclin D1 and p27 through extranuclear transport and the degradation of cyclin D1 by phosphorylation through p38 and GSK3b (220). As far as we are aware, the association between cyclin D2 downregulation and BCL-2/MCL-1 inhibition has not been described previously in the literature.

There were no significant changes to BCL-2 or MCL-1 expression following single agent treatment with their corresponding inhibitors, confirming that the effect of the inhibitor is mainly to displace the pro-apoptotic BIM. The effect of the combination

was different. The expression levels of MCL-1 went down in half of the cell lines (U266, JJN-3 and MM1s). This did not correlate with the degree of synergy, the level of cytotoxicity and whether cell lines belonged to the D1 or the D2 groups. As this is not consistent in all the myeloma cell lines, a unified cause-effect cannot be assumed. Nevertheless, this may have clinical applicability since the complete abolition of expression of MCL-1 has a lethal effect, an approach that involves intermittent inhibition may have a role in clinical translation.

There was no pattern to the synergy that could have been attributed to the underlying D-type cyclin translocations. This observation is also true of the effect of venetoclax and S63845 as single agents.

In conclusion, this set of experiments has demonstrated again synergy as a consequence of apoptosis induction through the intrinsic pathway from the dual inhibition of BCL-2 and MCL-1. The cell lines were less sensitive to single agent treatment with venetoclax consistent with their MCL-1 dependence on survival. Although the cell lines with cyclin D2 expression were perceived to be more sensitive to the combination treatment, this cannot be taken to suggest a causal relationship due to the possible number of confounding factors. To reduce the effect of those factors and verify this hypothesis would be to repeat the same experiment in a larger number of cell lines that. Another, and potentially better way to verify if cyclin D2 cell lines are more sensitive to dual BCL-2/MCL-1 inhibition is to create an isogenic cell line that only differs in the underlying cyclin D type status and rerunning the experiments in this chapter. Any statistically significant difference at that point can then be attributed to the cyclin D variation. There was a consistent downregulation of both

types of cyclins in the sensitive cell lines to the combination, however. The p53 status had no impact on the sensitivity as expected from the mechanism of action of the inhibitors. The same can be said about the degree of 1q gain where MCL-1 is located. The findings although showed significant synergy that may have a great translational potential in the future did not suggest a clear differential response to apoptosis induction between cyclin D1 and cyclin D2 cell lines. It is also important to note that the results from this chapter contributed to a publication (166). We showed that the cytochrome c release assay is applicable in myeloma cell lines and primary samples and it provides a predictive read-out for apoptosis induction after a very short incubation period that mirrors other apoptosis assays that require a longer incubation period.

CHAPTER 6:

PROTEOMIC ANALYSIS OF MYELOMA CELL LINES FOLLOWING APOPTOSIS INDUCTION

Chapter 6: Proteomic Analysis of Myeloma Cell Lines Following Apoptosis Induction

6.1 Introduction

We attempted to dissect another layer of the molecular complexity in myeloma that has not been explored previously within this thesis. Therefore, in this chapter, we explored if there was a differential response following BCL-2 and/or MCL-1 inhibition between the cyclin D1- and cyclin D2-expressing cell lines at the proteomic level using mass spectrometry. After studying the impact of conventional chemotherapy, DNA damage and apoptosis induction on the myeloma cell lines, a further attempt was made in this chapter to assess the molecular differences at the proteomic level and whether those differences had any correlation with the sensitivity of the myeloma cell lines to apoptosis induction that was observed in Chapter 5:

The proteomic analysis becomes useful as it can look at the proteins as end products and thereby bypasses the variability due to epigenetics and post-translational modifications that may be encountered at the translational and post-translational stages. Nevertheless, due to the complex nature of the proteomic analysis, definitive causalities may not be easy to discern. Pathway activation and inhibition based on the activity of individual proteins can be deduced through bioinformatics, but this is limited by the available knowledge of the functions and contributions of individual proteins which may not be fully accurate or complete.

Protein extracts obtained from the treatment of the myeloma cell lines with venetoclax (ABT-199, BCL-2 inhibitor), S63845 (MCL-1 inhibitor) and the combination

of those two agents at concentrations shown to produce synergy in Chapter 5: were used for the experiments in this chapter. Quality control measurements demonstrated enough protein extracts to perform mass spectrometry for all the myeloma cell lines apart from the OPM-2 cell line which was then excluded from further analysis in this chapter. Three replicates of each condition were analysed.

We are incredibly grateful to Dr Amanda Miles at Nottingham Trent University who altruistically conducted the mass spectrometry runs in her lab and supplied us with the results together with an elaborate and generous explanation of the scientific basis of those results, how the assays worked and how to analyse the data further. Without her help and support, the conception of this chapter would not have been possible.

6.1.1 Mass Spectrometry and Data Analysis

The method for the mass spectrometry and the subsequent data analysis was detailed in Chapter 2:Materials and Methods. Treated cells lines (single agents venetoclax and S63845 and combination) were compared to DMSO controls. To avoid unnecessary repetition, the main points are summarised below. After protein lysates were injected into the columns, the data generated following mass spectrometric analysis were analysed using Sciex OneOmics Software. Two types of data were generated, the normalised protein data and the protein fold changes with the peptide confidence levels. Further statistical analysis was done on the obtained data as detailed previously in Chapter 2 and the generated data was further analysed using the IPA (Ingenuity Pathway Analysis software, Qiagen, courtesy of Nottingham Trent University). Heat maps were generated using a hierarchical analysis according to the z-scores comparing

all the cell lines tested. Individual cell lines (and conditions) were also analysed to establish the enriched canonical pathways, the causal networks and the upstream regulators. The p-value for significance used by the IPA was 0.05.

The data analysis was done in two main sections. Individual cell lines in each condition were analysed separately. Individual proteins were ranked according to their p values then the top canonical pathways were identified based on the p values of individual component proteins. Those proteins were mapped to their relevant canonical pathways using the IPA internal data set. The determination of whether a certain pathway was activated or inhibited was based on the proportion of individual proteins in that pathway that was considered to be activated or inhibited based on their z scores. Next, the IPA software was able to predict, based on the pathway and individual protein analysis, the upstream effect on those proteins. Upstream network activation or inhibition was based on the direct collaboration of the individual proteins whereas causal network determination was identified when the collaboration was indirect. It is also worthwhile to note that the upstream analysis could also include the anticipated effect of a certain compound or chemotherapeutic that is predicted to yield comparable results in terms of protein/pathway activation and inhibition.

As a standard, heatmaps using z-score hierarchical clustering were also generated for each individual cell line in all three treatment conditions. The most significant proteins were displayed at the top.

A combined analysis of all the conditions in all the cell lines was also done. Heatmaps were generated as described above based on z score hierarchical clustering of individual proteins. In addition, using the disease and function analysis method in the

IPA software, heat maps were generated based on the z score contribution of individual proteins to pre-determined pathways that are involved in cellular functions such as survival, proliferation, and apoptosis. The contribution of those proteins to the activation or the inhibition of a given disease and function pathway was based on their individual z scores which were combined to determine the overall effect on that specific pathway in terms of activation or inhibition.

Due to the nature of the results in this chapter, it was decided that it would be more informative to present and discuss the results together in combination with a background literature review rather than in dedicated sections. It is hoped that this approach would allow a more jointed and coherent presentation of the data and the relationships between the proteins of interest.

6.2 The Aim of this Chapter

The primary aim of performing the experiments in this chapter was to elucidate if there was a differential proteomic profile between cyclin D1 and cyclin D2 myeloma cell lines in response to apoptosis induction achieved through dual BCL-2 and MCL-1 inhibition. We wanted to identify the significantly changed pathways and the status of activation or inhibition of those pathways. In addition, we aimed to identify if there was a specific proteomic profile pattern that would predict or be associated with sensitivity or exposure to MCL-1/BCL-2 inhibition.

6.3 Results and Discussion

Proteomic analysis using mass spectrometry was conducted on the myeloma cell lines following treatment with venetoclax and S63845 as single agents and in combination. The concentrations used are as mentioned in Chapter 5: and are included below (Table 6.1) for easier reference.

Table 6.1: The concentrations (µM) of ABT-199 and S63845 used for Annexin V assay

	U266	KMS12-BM	MOLP8	JJN-3	OPM-2	MM1s
ABT-199 (µM)	5	0.5	0.5	0.5	0.5	1
S63845 (µM)	0.5	0.05	0.05	0.05	0.05	0.1

These concentrations were shown to induce synergism (Chapter 5:). Data from all the myeloma cell lines were included in the analysis apart from OPM-2 cell line as explained above. Combined as well as individual cell line analysis was done using the IPA Software.

A summary of the significantly affected pathways observed with individual cell lines analysis and with comparison analysis between all the cell lines is found in Table 6.2. Each individual pathway will be reviewed in depth below in terms of the literature and the results obtained in this chapter.

6.3.1 Individual Cell Line Analysis

Although the cell lines were analysed individually, the top pathways that were found to be of significance were consistent among all the cell lines tested. This may appear surprising in the first instance however on a deeper inspection it is congruous to the

myeloma cells pathophysiology. Since most of the individual component proteins for those pathways are implicated one way or another in protein synthesis and protein synthesis regulation and myeloma cells have a very active protein synthesis machinery. The individual pathways, however, differed in their activation / inhibition status as described below.

Table 6.2: Tabulated summary of the significant pathway changes on individual cell lines analysis and comparison analysis following treatment with venetoclax, S63845 and their combination. All the pathways listed were significantly changed in response to venetoclax and S63845 combination. The individual cell lines analysis includes the top changed canonical pathways and the predicted upstream pathway changes whether directly or indirectly. The top affected pathways on comparison analysis of all the cell lines after the combination treatment are included in the bottom panel of the table. Those pathways were consistent across all the cell lines tested.

Individual Cell Lines Analysis	**Canonical Pathway**	**Upstream Pathways Analysis**	**Causal Pathway Analysis**
	1. EIF2 signalling 2. Regulation of eIF4 and P70s6K 3. BAG2 signalling 4. FAT10 signalling 5. mTOR signalling	1. MYC 2. LARP1 3. Torin1 4. Fluorouracil (5-FU) 5. TP53	1. PCGEM1 2. CUL4B 3. PUF60 4. SGI 1776 5. LARP1
Comparison Analysis	1. EIF2 signalling 2. Granzyme B signalling 3. Spliceosomal cycle 4. Ephrin B signalling 5. tRNA charging 6. synaptogenesis signalling pathway	7. Glutathione-mediated detoxification 8. Reelin Signalling 9. fMLP signalling 10. CD28 signalling 11. RAC and RhoA signalling	

6.3.1.1 The top five canonical pathways are implicated in the regulation of RNA translation

Pathway analysis was done based on mapping of the significantly up or downregulated proteins in each treatment condition to corresponding pathways using an internal bioinformatics database to the IPA software. The pathway was judged to be activated or inhibited based on the z scores of the component proteins. The p and the z values for each pathway are included the in the tables below.

The top five canonical pathways in order of significance were

1. EIF2 signalling
2. Regulation of eIF4 and P70s6K
3. BAG2 signalling
4. FAT10 signalling
5. mTOR signalling

1. <u>EIF2 signalling pathway</u>

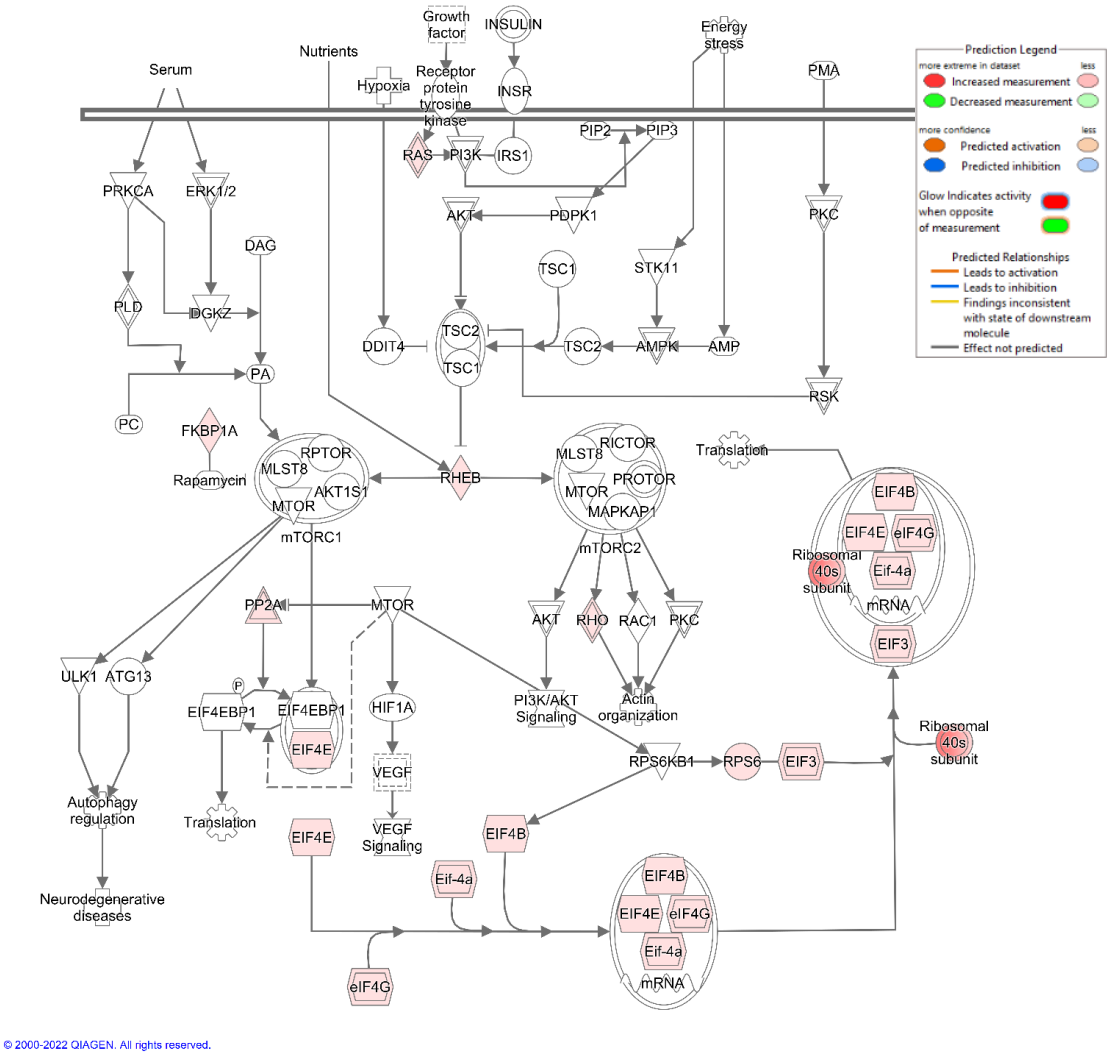
Protein synthesis in the eukaryotic cells is a complex process that involves four consecutive steps; the initiation, the elongation and the termination of the peptide synthesis followed by the recycling of the ribosome (221).

Protein translation in eukaryotic cells is mediated through the recruitment of the ribosomal translatory machine to the mRNA via two main mechanisms. In the first, and the most common, the translational machinery scans the mRNA and is then recruited to the mRNA cap sequence (5’ methyl-7 guanosine moiety). The association of the eIF4F heterodimer with mRNA initiates cap-dependent translation of mRNA. The complex has three subunits, a cap-binding component (eIF4E), an RNA helicase component (eIF4A) and a scaffolding subunit (eIF4G). eIF4B significantly enhances the

helicase function of the eIF4A. This process is dependent on the eIFs and is regulated through mTOR (Figure 6.1). In the second, cap-independent mechanism, there is a direct interaction of the translational complex with the mRNA near or at the initiation codon through the IRES (internal ribosomal entry site) located within the mRNA (222,223). This process is independent of mTOR and the eIF proteins but happens through ITAF (IRES-associated trans-acting factors). Cap-independent translation thus can be regarded as an escape mechanism to maintain protein production crucial to cellular survival when the cap-dependent pathway is inhibited (64).

In the 'standard' cap-dependent translation and during the initiation phase of the translational process, the eIF proteins work to assemble the 80S ribosome and initiate polypeptide translation. This is a complex process that involves at least a dozen eIF proteins.

The interplay mediated by the phosphorylation/dephosphorylation of several proteins in the eIF2 signalling pathway, in addition to interaction from mTORC1 (see below), governs the activation and inhibition of this pathway. Certain stresses can negatively regulate protein translation. This regulation is a conserved cellular process and is crucial as a response mechanism to stress or nutrient deficiencies (Figure 6.1) (224,225). The process has the phosphorylation of eIF2α at its core and results in a halt in protein synthesis initiation. If the phosphorylation of eIF2α becomes sustained, apoptosis happens (221). The unfolded protein response (UPR) due to proteasome inhibition, for example, further adds to this protein synthesis slow down through the phosphorylation and inhibition of eIF2α (65).



© 2000-2022 QIAGEN. All rights reserved.

Figure 6.1: Schematic representation of the complex interactions between the eIF signalling and the mTOR pathway as generated by the IPA software

Dysregulation of various eIF components has been observed in several types of cancers and several of those proteins were postulated to be useful anti-cancer targets (221). It was found that myeloma cells surviving bortezomib treatment enter a quiescent state of G0-G1 arrest by ameliorating the phosphorylation status of eIF2α. This, in addition, to the upregulation of ER chaperone proteins and the downregulation of cyclin D1 are coping mechanisms to deal with the increased pressure from the accumulation of unfolded proteins resulting from the inhibition of

the proteasome (226,227). The reversal and therefore the eradication of those quiescent cells was achieved by combining bortezomib treatment with salubrinal, a phosphatase inhibitor that maintained eIF2 phosphorylation (227,228). Proteomic analysis of patients samples who achieved a very good partial response or better to bortezomib combinations identified a prominent enrichment of the eIF2 signalling pathway suggesting a role for this pathway to be a marker of response to bortezomib treatment (229).

The results from the individual cell lines analysis and the comparison analysis showed that the EIF2 signalling pathway was the most significantly affected in all the conditions (Table 6.3). While the effect of individual treatments on this pathway in terms of activation or inhibition was heterogenous and did not follow a specific pattern, the overall effect of the combination treatment was the inhibition of this pathway in all the cell lines evaluated. This is consistent with the general theme anticipated from the above review of the literature and can probably be explained by the initiation of a global slow-down of protein production as a survival mechanism

Table 6.3: The activation pattern of EIF2 signalling across the myeloma cell lines in response to venetoclax and S63845 single agent and combination treatment. P=4e-38 (■ = activation, ■ = inhibition, ■ = no activation pattern discerned)

	U266			KMS12-BM			MOLP-8			JJN-3			MM1s		
	Venetoclax	S53845	Combination	Venetoclax	S53845	Combination	Venetoclax	S53845	Combination	Venetoclax	S53845	Combination	Venetoclax	S53845	Combination
EIF2 Signalling	■	■	■	■	■	■	■	■	■	■	■	■	■	■	■
Z score	1.5	-2.3	2.6	0.4	3.15	-3.4	-2.8	1.2	3.15	2	5	-2	-4.8	-4.5	-5.3

when the cells are undergoing stress (apoptosis induction in this situation). Supporting this, it was found that the levels of phosphorylated eIF2α were found to be associated with a better prognosis in triple-negative breast cancer (230).

In addition, dexamethasone resistance in the MM1R and U266 myeloma cells line was overcome with the increased phosphorylation of eIF2α through stimulation of the upstream heme-regulated eIF2a kinase (HRI) (231).

Taking a closer look at the individual components of this pathway, there was a global predicted inhibition of the eIF2 components in all the cell lines with the combination treatment (Table 6.3). Most of the eIF proteins in this pathway were downregulated and although the changes in terms of their p-value were not significant, the trend was that of a generalised downregulation of most of the eIF proteins in this pathway. This data suggests that the downregulation of the eIF pathway can be indicative of cellular stress due to apoptosis induction.

2. <u>Regulation of eIF4 and P70S6K pathway</u>

This pathway is closely related to the previous, and whilst there is a degree of overlap with the eIF2 signalling pathway, it can be regarded as the regulatory component of the previous pathway (Figure 6.2). Several pro-survival and proliferative pathways that feature in malignant transformation such as the PI3K and the MAPK pathways converge on the eIF signalling pathway through the mTOR pathway (221). This is mediated through the action of the mTORC1 component of the mTOR pathway on the 4E-BPs and S6K regulatory proteins.

Dephosphorylated 4E-BP proteins compete with eIF4G for binding to eIF4E and thereby inhibit protein translation by preventing the formation of the eIF4F complex

(221). The phosphorylation of 4E-BP abrogates their negative effect on the formation of the eIF4F complex that is required for the initiation of the peptide translation.

S6K, on the other hand, regulates the peptide translation process through a number of downstream substrates such as eIF4B, rpS6, eEF2 kinase, and PDCD4. As mentioned above eIF4B potentiates the helicase activity of the eIF4F complex (221). S6K1 and S6K2 are the two variants of S6K. Each has two isoforms and the P70S6K1 is the most abundant of the S6K1 variant (Figure 6.2). The phosphorylation of P70SK1 by mTORC1 causes activation of the former (221).

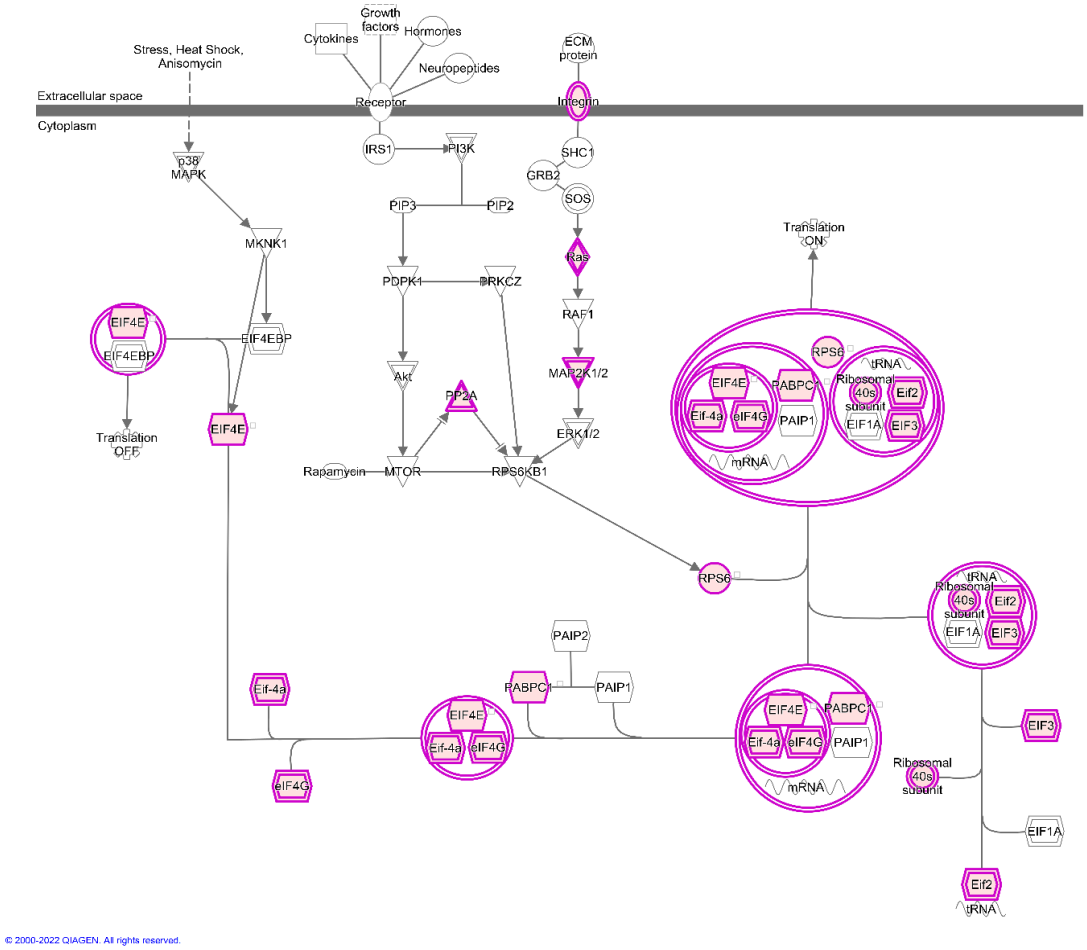


Figure 6.2: Schematic representation of the regulation of mRNA translation via eIF4 and p70S6K

In addition to its role as the cap-binding component, eIF4E, through its nuclear localisation, can have a nuclear transport function. Contribution to leukemogenesis from raised eIF4E levels has been attributed to blocking the differentiation of monocytes and granulocytes (232). Tissue microarray of multiple tumours showed eIF4E elevation (233) and siRNA inhibition of eIF4E inhibition was associated with reduced tumour growth (234).

Table 6.4: The activation pattern of eIF4 and p70S6k across the myeloma cell lines in response to venetoclax and S63845 single agent and combination treatment. P=4.4e-39 (■ = inhibition , ■ = activation)

	U266			KMS12-BM			MOLP-8			JJN-3			MM1s		
	Venetoclax	S53845	Combination	Venetoclax	S53845	Combination	Venetoclax	S53845	Combination	Venetoclax	S53845	Combination	Venetoclax	S53845	Combination
Regulation of eIF4 and p70S6K	■	■	■	■	■	■	■	■	■	■	■	■	■	■	■
z-score	0.3	1	0.3	-1	-1	0.3	1	-0.3	0.3	0.3	-0.3	-0.3	0.3	-0.3	-1

Our data suggest that the regulation of eIF4 and P70S6K canonical pathway was generally activated with the combination of BCL-2 and MCL-1 inhibition in the cell lines that expressed cyclin D1 (U266, MOLP-8 and KMS12-BM) but was inhibited in the rest (Table 6.4). It is difficult to draw a definite conclusion from this pattern, especially because the viability results obtained in Chapter 5 from the venetoclax and the S63845 combination treatment showed synergy across both the cyclin D1 and the cyclin D2 cell lines (Section 5.3.1). However, previous studies have identified a close relationship between eIF4E and cyclin D1. eIF4E increases the cyclin D1 protein levels

in the cytoplasm through preferential translation and increased nuclear export of cyclin D1 mRNA (65,232). Moreover, physical co-localisation of eIF4E with the cyclin D1 mRNA in nuclear bodies was also identified (235). Our results showed a reduction in the eIF4E expression levels in the U266 and KMS12-BM (but not in the MOLP-8) cell lines and an opposite effect in the JJN-3 and the MM1s cell lines indicating a possible differential effect. As per the results from the previous chapter, we have shown a downregulation in the cyclin D1 levels with the combination treatment in the U266 and KMS12-BM cell lines (where the eIF4E expression was reduced) which may hint that the cyclin D1 reduction could be in part related to eIF4E reduction. However, those changes were not significant, and one should be careful in drawing conclusions from this observation due to the relatively small sample size.

3. BAG2 signalling

BAG2 belongs to the family of BAG proteins (BCL-2 associated athanogene). Those proteins have an antiapoptotic function through their interaction with BCL-2 and Hsp70. They also interact with various other proteins involved in cell survival, cell death and cell division. BAG2, through its interaction with Hsp70, increases protein refolding, promotes ubiquitin-independent degradation, and inhibits CHIP-mediated ubiquitination and substrate degradation through the proteasome. BAG2 induction was observed in the cell lines that were more sensitive to proteasome inhibition (236). The role of BAG2 in cancer may be differential and contradictory. One study found that c-myc inhibition caused an upregulation of BAG2. Moreover, BAG2 induction whether artificial or through c-myc knockdown was associated with senescence in a p21cip1/p53 dependent fashion (237). On the contrary, BAG2 overexpression was observed in several cancers such as oesophageal and hepatocellular cancers and was

associated with inferior outcomes. Moreover, the knockdown of BAG2 induced apoptosis and reduced proliferation (238,239).

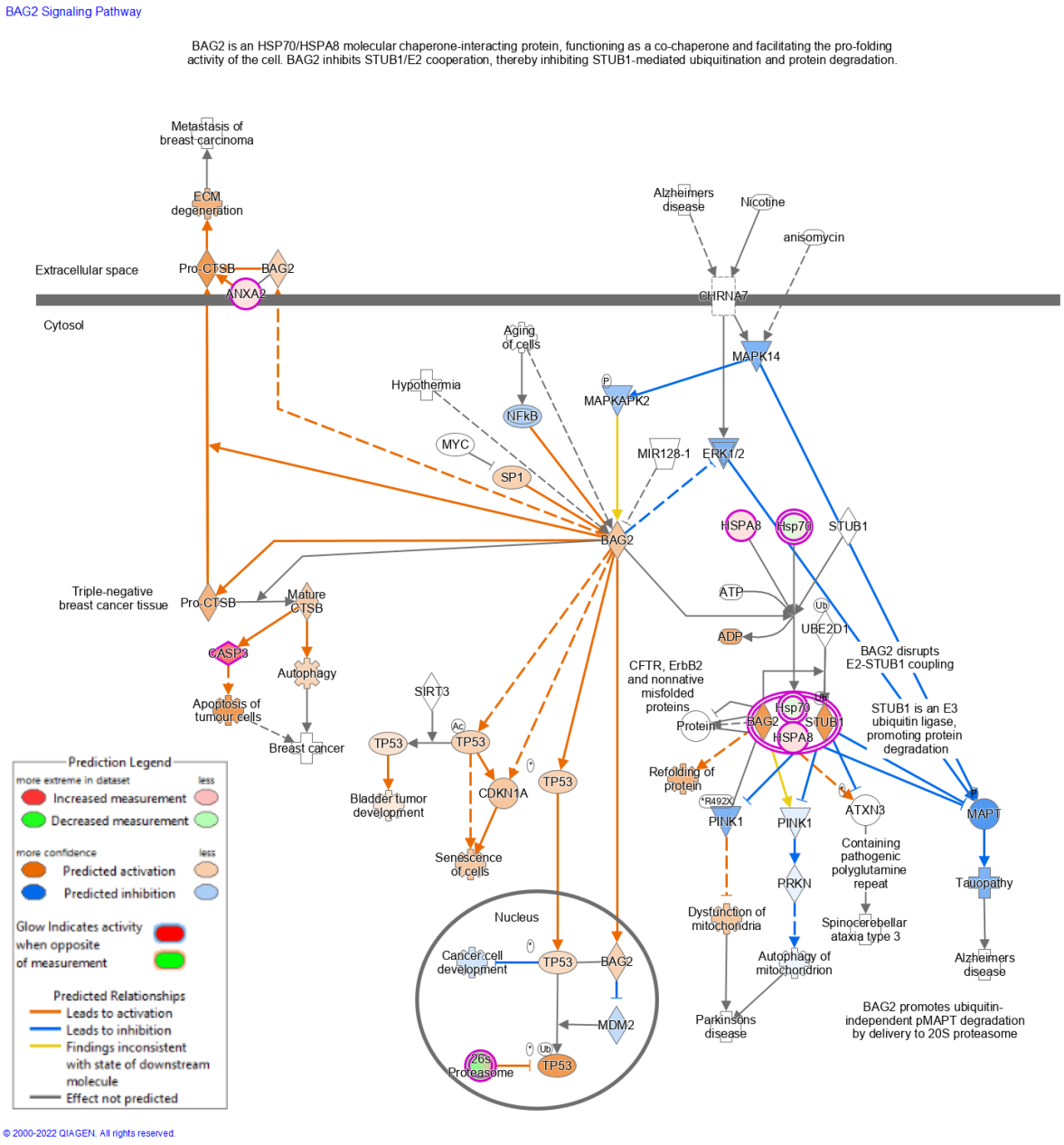


Figure 6.3: Representative example of the BAG2 signalling pathway generated by the IPA software (U266 cell line treated with venetoclax and S63845 combination).

Similar results were observed with breast and colorectal cancers. BAG2 was also overexpressed in T-ALL patient samples as compared to healthy donors and in T-ALL cell line, the knockdown of BAG2 induced apoptosis (240). As mentioned above, the Hsp proteins are an important part of this pathway. Hsp70 chaperone protein has an important function in multiple myeloma as part of the unfolded protein response and to combat ER stress induced by treatment with proteasome inhibitors (241,242). MCL-1 levels would increase in response to proteasome inhibition in part through the stabilising effect of Hsp70. It follows that the combination of bortezomib and Hsp70 inhibitor synergistically reduced myeloma cells viability and caused the downregulation of BCL-2 and BCL-xl without a compensatory increase in MCL-1 (242–244).

Our data from the combination treatment of BCL-2 and MCL-1 inhibitors were heterogeneous in terms of the degree of activation of this pathway (Table 6.5, Figure 6.3). There was an overall predicted increase in activity noted with U266 and MOLP-8 cell lines and a predicted reduced activity with KMS12-BM and JJN-3.

Table 6.5: The activation pattern of BAG2 across the myeloma cell lines in response to venetoclax and S63845 single agent and combination treatment. P=4.6e-34 (■ = activation, ■ = inhibition, ■ = no activation pattern discerned)

	U266			KMS12-BM			MOLP-8			JJN-3			MM1s		
	Venetoclax	S53845	Combination	Venetoclax	S53845	Combination	Venetoclax	S53845	Combination	Venetoclax	S53845	Combination	Venetoclax	S53845	Combination
BAG2 signalling	■	■	■	■	■	■	■	■	■	■	■	■	■	■	■
Z-score	0	1.26	1.26	0.6	-0.63	0.6	-1.89	0.6	1.26	0.6	-0.63	-2.5	-0.6	-0.63	0

On the other hand, the z score for this pathway with the MM1s cell line was zero and therefore activity could not be discerned. Inspecting the Hsp part of the pathway, changes in those proteins featured heavily however there was a degree of variability and heterogeneity with the various proteins that precluded drawing a meaningful conclusion other than the fact that changes in this pathway are important for apoptosis induction and that although certain Hsp members were slightly upregulated, this did not prevent apoptosis induction with the combination treatment.

4. <u>FAT10 signalling</u>

This ubiquitin-like modifier is implicated in the promotion of cancer development. FAT10-bound proteins are directed towards the proteasome for degradation with the help of another mediator called NUB1L (245). FAT10 protein binding was as effective as ubiquitin in ushering those proteins for proteasomal degradation (246). It has been established that FAT10 has pro-oncogenic properties, is upregulated in various types of cancers and its level of expression has been linked to disease severity and prognosis. FAT10 has a pro-inflammatory effect being a downstream mediator for interferon-gamma and TNF alpha (245). The NF-κB signalling pathway is regulated through FAT10 which induced the proteasomal degradation of IκB (245,247). Moreover, it has been found that FAT10 activation is mediated through STAT3 and NF-κB itself in a positive feedback fashion (248). Free MAD2 targeted by FAT10 causes the reduction of the former's availability during mitosis resulting in early separation of the sister chromatids and consequent aneuploidy. Furthermore, FAT10 overexpression reduced the transcriptional activity of activated p53, thereby, inducing resistance to apoptosis (245). p53, on the other hand, has a negative impact on FAT10 expression (249).FAT10

also contributes to wnt signalling pathway activity through the inhibition of β-catenin ubiquitination and degradation and through the activation of Akt which eventually leads to the stabilisation of β-catenin (245).

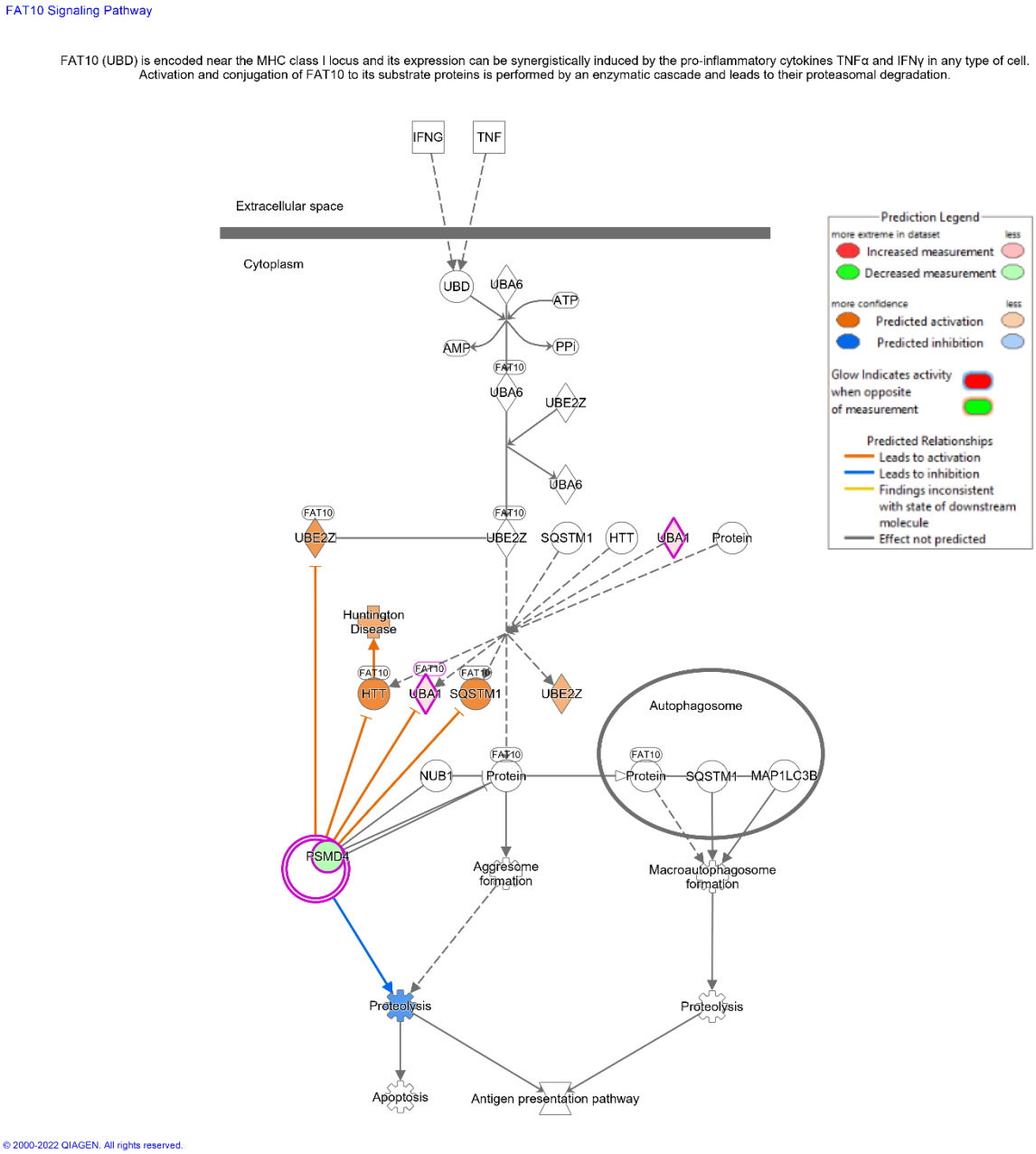


Figure 6.4: Representative example of the FAT10 signalling as generated by the IPA software (U266 cell line treated with venetoclax and S63845 combination)

The z score for this pathway in all the conditions was zero in our data (Figure 6.4, Table 6.6). Taking a closer look at the component proteins, many of those scored by the IPA software were related to the proteasome 20s and 26s subunits and some other factors such as HTT, UBA1, UBE2Z to which FAT10 binds to with variable degrees of expression changes and with no significance in terms of P-values. Again, one can only infer the already established importance of the function of the proteasome and alternative pathways for proteasomal degradation in myeloma cell lines, but the data does not predict a certain pattern that can be attributed to BCL-2 inhibition, MCL-1 inhibition, their combination, or the underlying cyclin D translocation.

Table 6.6: The activation pattern of FAT10 across the myeloma cell lines in response to venetoclax and S63845 single agent and combination treatment. P=3e-33 (■ = no activation pattern discerned)

	U266			KMS12-BM			MOLP-8			JJN-3			MM1s		
	Venetoclax	S53845	Combination	Venetoclax	S53845	Combination	Venetoclax	S53845	Combination	Venetoclax	S53845	Combination	Venetoclax	S53845	Combination
FAT10 signalling	■	■	■	■	■	■	■	■	■	■	■	■	■	■	■
z-score	0	0	0	0	0	0	0	0	0	0	0	0	0	0	0

5. mTOR pathway

The mTORC1 and mTORC2 complexes mediate the vast biological functions of the mTOR pathway. Through its serine-threonine kinase activity, mTOR has an important regulatory function and mediates the effect of growth factors and other positive signals to impact a large array of cellular functions (250). The two mTOR complexes

differ functionally and structurally, for example, mTORC1 is sensitive to rapamycin and is closely involved in the protein translation control through its downstream targets (4E-BPs and S6K) while mTORC2 is insensitive to rapamycin and activates a different set of downstream targets such as AKT and PKC (Figure 6.1) (221). In multiple myeloma, global slow-down of protein production as a protective mechanism from the consequences of ER stress happens as a result of mTORC1 inhibition. mTOR targeting in multiple myeloma with rapamycin induced G1 arrest through the phosphorylation of p70SK6 and was found to downregulate cyclins D2 and D3 in myeloma cell lines. Dexamethasone sensitisation was also seen as a result of rapamycin treatment (251,252). Downregulation of several pro-survival factors such as XIAP, BAG-3, and HSP27 was also noted (252). There have been several early phase clinical trials involving the use of the rapamycin analogues everolimus and temsirolimus either alone or in combination with lenalidomide or bortezomib with modest results (250). Interestingly, there is a differential effect from the mTORC1 and mTORC2 on Akt where it is inhibited by the former and activated by the latter. This differential effect may explain the lack of therapeutic impact of the rapamycin analogues since they only inhibit mTORC1 (253). DEPTOR is a component of both mTORC1 and 2 complexes where mTOR and DEPTOR both negatively regulate each other. When DEPTOR was overexpressed, this caused an unexpected PI3K/Akt hyperactivity imitating mTORC2 activation probably due to the loss of the inhibitory effects of mTORC1 on PI3K/Akt signalling (253). The levels of DEPTOR mRNA were found to be elevated in a third of the human myeloma cells tested and, more interestingly, this overexpression of DEPTOR was mostly observed in IgH translocated myelomas (non-hyperdiploid) and in particular with t(11;14), t(14;16) and t(14;20)

(253). As mentioned previously, the inhibition of mTORC1 can be the result of proteasome inhibition as cellular survival mechanism during ER stress. This was associated with a remarkable increase in c-myc translation that was IRES-dependent (65).

Looking at the overall activity pattern in our datasets (Table 6.7), the total z scores with the combination treatment predicted mTOR signalling inhibition in the U266 and the JJN-3 cell lines, mTOR signalling activation with the MOLP-8 cell lines and no activity pattern in the MM1s and the KMS12-BM cell lines. However, probing specific changes within the pathway, there was a predicted activation in both mTORC1 and mTORC2 complexes with the combination treatment with all cell lines except the JJN-3. This may appear unexpected given the strong apoptosis induction with the combination treatment so one would expect downregulation of that pathway. However, this pattern may alternatively indicate that the mitochondrial pathway of apoptosis which is activated through the combination treatment is independent of mTOR activity.

Table 6.7: The activation pattern of mTOR across the myeloma cell lines in response to venetoclax and S63845 single agent and combination treatment. P=3.4e-32 (■ = activation, ■ = inhibition, ■ = no activation pattern discerned)

	U266			KMS12-BM			MOLP-8			JJN-3			MM1s		
	Venetoclax	S53845	Combination	Venetoclax	S53845	Combination	Venetoclax	S53845	Combination	Venetoclax	S53845	Combination	Venetoclax	S53845	Combination
mTOR signalling	■	■	■	■	■	■	■	■	■	■	■	■	■	■	■
z-score	-0.57	0.57	-0.57	-0.57	-1.5	0	0.57	0	0.57	1.5	0.57	-0.57	-0.57	-0.57	0

Supporting this suggestion was the inhibition of both mTORC1 and 2 with the JJN-3 cell line despite the strong synergistic effect of the combination treatment and activation of both complexes in most of the single agent treatment in the other cell lines when the concentrations used did not result in apoptosis. Nevertheless, the activation of the mTORC1 and mTORC2 was a true finding in most of the conditions as compared to the controls and this may indicate that this activation was, directly or indirectly, induced by the treatment possibly as a survival feedback mechanism. The other finding was the increased expression of eIF4B (which potentiates the helicase effect of the eIF4F complex). This was most pronounced with the KMS12-BM and the MM1s cell lines. This, however, did not translate into increased protein translation probably due to the downregulation, as mentioned above, of the other eIFs.

6.3.1.2 Causal and upstream pathway analysis

As mentioned above, the IPA software allows the prediction, based on the patterns of activation and inhibition of significantly changed proteins in the treated samples and the controls, of upstream and causal pathways that could have been changed based on the 'downstream' changes seen in the experimental samples. As stated above, an upstream or a causal prediction could be a drug or a therapeutic molecule, the downstream effect of which may produce the same pattern of activation/inhibition witnessed in our data set. As those predictions were inferred by the IPA database there were no specific individual p and z values on IPA.

6.3.1.2.1 Upstream pathway analysis

The top five predicted upstream pathway/molecules changes based on direct collaboration between the significantly changed proteins in the tested samples included,

1. MYC
2. LARP1
3. Torin1
4. 5-Fluorouracil (5-FU)
5. TP53

1. <u>c-myc in multiple myeloma</u>

Although the role of c-myc in myeloma was mentioned in the introduction of this thesis, the frequent convergence and interaction of many of the proteins and factors mentioned in this chapter on c-myc make it worthwhile to visit its role in multiple myeloma again.

myc proteins are major transcription factors that are believed to regulate more than 15% of the genome. Their regulatory function involves genes implicated in a wide variety of cellular processes from cell growth to protein translation (254). Many signal transduction pathways converge on myc, such that its level is tightly regulated in normal conditions and its dysregulation is featured in three-quarters of human cancers (255). Given the plurality of its function, contribution to oncogenesis in the event of its dysregulation is not difficult to imagine and is mediated through myc effects on cellular functions such as cell cycle regulation, resistance to apoptosis, the alteration of the tumour microenvironment and its effect on angiogenesis (254).

Perhaps the clearest role of myc in haematological cancers is observed in Burkitt's lymphoma whereby translocations involving chromosome 8 (where myc is located) and the immunoglobulin heavy chain (on chromosome 14), the kappa light chain (on chromosome 2) or the lambda light chain (chromosome 22) lead to increased levels of myc by virtue of adjacency to these active promoters. These translocations are

diagnostic of Burkitt's lymphoma. Myc overexpression (without these translocations) can also be seen in diffuse large B cell lymphoma (256).

As mentioned previously, the incidence of c-myc rearrangement is around 20% in multiple myeloma. This rearrangement happens mostly due to translocations involving the immunoglobulin heavy chains or light chains promoter with chromosome 8. c-myc upregulation can also be the result of focal chromosome 8q gain (61). c-myc overexpression in multiple myeloma may also be mediated through the stimulatory effect of IL-6 from the tumour microenvironment on the STAT-3 pathway (62). A further mechanism of c-myc overexpression may occur through cap-independent translation (63) which could also be mediated through IL-6 (64) or through MNK1 (MAPK-interacting serine/threonine kinase 1) activation (65). This mechanism allows survival under ER stress without causing a further burden from protein translation (65). As mentioned previously, c-myc overexpression in myeloma is generally regarded as a secondary event. A gene expression profile signature related to myc (myc activation signature) was found to be differentially present in multiple myeloma patient samples but not in MGUS. Interestingly, there was a close correlation between the presence of RAS mutation and that signature and it was also more common in hyperdiploid myelomas as compared to IgH-translocated myelomas (257).

The chemotherapeutic effect of bortezomib may be more pronounced when myc is upregulated. Patients who were treated with single-agent bortezomib did better when they had the myc activation signature than those who did not (257). Lenalidomide, and other immunomodulatory agents, interact with the Cereblon causing the ubiquitination and the proteasomal degradation of two proteins, Aiolos and Ikaros.

Both can activate c-myc through IRF4 (80). Analysis of primary myeloma cells from bone marrow samples of lenalidomide refractory patients revealed a decrease in the Cereblon and an increase in c-myc (258).

Table 6.8: The activation pattern of c-myc across the myeloma cell lines in response to venetoclax and S63845 single agent and combination treatment (■ = activation, ■ = inhibition, ■ = no activation pattern discerned)

	U266			KMS12-BM			MOLP-8			JJN-3			MM1s		
	Venetoclax	S53845	Combination	Venetoclax	S53845	Combination	Venetoclax	S53845	Combination	Venetoclax	S53845	Combination	Venetoclax	S53845	Combination
c-myc	■	■	■	■	■	■	■	■	■	■	■	■	■	■	■

Overexpression of c-myc is associated with a shorter OS (259). This was regardless of the degree of proliferation of the myeloma (257). In our data set, there was an overall inhibition of c-myc in all of the combination and most of the single agent treatments. This can probably be traced back to the overall reduction in global protein synthesis due to the eIF2 signalling pathway inhibition mentioned earlier (Table 6.8).

2. LARP1

La-related protein 1 (LARP1) is an important downstream target of mTORC1. LARP1 overexpression has been shown to impart a negative prognostic impact in non-small cell lung cancer probably through its effect on cell migration and invasion (260). Similarly, and through its interaction with anti-apoptosis proteins, LARP1 has been found to promote resistance to apoptosis of ovarian cancer cell lines through a differential effect of its binding to BCL-2 and BIK where it stabilises the former and destabilises the latter (261). In colorectal cancer human tissue samples, LARP1 was

overexpressed in comparison to adjacent normal tissue and this was associated with increased proliferation and reduced survival (262). LARP1 may also be increased in multiple myeloma and has a similar oncogenic effect (263) however the literature is scarce when it comes to the role of LARP1 in myeloma. mRNAs containing the 5'terminal oligopyrimidine (5'TOP) motif encode ribosomal proteins and are regulated through LARP1 and eIF4G. There is a competitive and inverse relationship between the latter two, where LARP1 binding causes 5'TOP translation repression and eIF4G binding causes its activation. It is through LARP1 that mTORC1 exerts a negative downstream inhibitory effect on 5'TOP mRNA translation (264).

There was a predicted activation of LARP-1 in most of the conditions in this experiment (Table 6.9). This was an unexpected finding given the antiapoptotic role of LARP1 via its pro-BCL-2 function, but it could be compensatory. Characterizing the role of LARP1 in myeloma would therefore be an interesting idea for a future project especially if synthetic lethality can be created from the inhibition of LARP1 together with MCL-1.

Table 6.9: The activation pattern of LARP1 across the myeloma cell lines in response to venetoclax and S63845 single agent and combination treatment (■ = activation, ■ = inhibition, ■ = no activation pattern discerned)

	U266			KMS12-BM			MOLP-8			JJN-3			MM1s		
	Venetoclax	S53845	Combination	Venetoclax	S53845	Combination	Venetoclax	S53845	Combination	Venetoclax	S53845	Combination	Venetoclax	S53845	Combination
LARP1	■	■	■	■	■	■	■	■	■	■	■	■	■	■	■

3. Torin 1

Torin1 is an ATP competitive blocker that has established pre-clinical use as an mTOR inhibitor, similar to Rapamycin, however, it can inhibit both mTORC1 and mTORC2. In a study by Park et al, Torin 1 was shown to induce apoptosis in the RPMI-8226 myeloma cell line and reduced BrdU uptake in several leukaemia cell lines (265). As previously discussed, there is a close collaboration between the NF-κB pathway and mTOR pathway such that the latter can cause activation of the former through Akt. In the same study mentioned above, NF-κB activity was reduced through impaired phosphorylation of p65 in acute lymphoblastic leukaemia (ALL) cells following Torin1 treatment. Several genes encoding pro-apoptotic proteins such as PUMA and BIM were overexpressed in T-ALL cell lines treated with Torin1 (265). A more potent inhibitor of mTORC1 and mTORC2 has been developed (Torin2) (266). Torin 2 induced cell cycle arrest in ALL cell lines at the G0/G1 phase, induced LC3A/I and II indicating promotion of autophagy and caused PARP cleavage indicating apoptosis (267).

Another mTOR inhibitor, pp242, was evaluated in myeloma cell lines, a xenograft model, and primary patient samples. In contrast to rapamycin, which was ineffective against mTORC2, and similar to Torin1 and Torin2, this compound was effective against both mTORC1 and 2, induced apoptosis, and was synergistic with bortezomib. INK128 is another novel mTORC1 and mTORC2 inhibitor that was found to be more effective than rapamycin as an inhibitor of mTOR in myeloma cell lines and primary cell lines. Annexin V assessment showed increased apoptosis and cell cycle analysis showed G2 arrest (268). Since the IPA software tries to predict the activation/inhibition patterns that can also be attributed to compounds and chemicals, Torin 1 was highlighted. Nevertheless, the activation pattern was only

observed in the U266 and the MM1s cell lines with no discernible specific pattern while the z score in the rest of the conditions was below the threshold to indicate activity or inhibition (Table 6.10). The fact that Torin1 features here is unsurprising since it seems that the regulatory pathways for protein translation featured heavily in this analysis and the heterogeneity in the activation could be the combination of the observed global protein translation slow down combined with the rather unexpected mTORC1 and 2 activations noted earlier.

Table 6.10: The activation pattern of Torin-1 across the myeloma cell lines in response to venetoclax and S63845 single agent and combination treatment (■ = activation, and ■ = no activation pattern discerned)

	U266			KMS12-BM			MOLP-8			JJN-3			MM1s		
	Venetoclax	S53845	Combination	Venetoclax	S53845	Combination	Venetoclax	S53845	Combination	Venetoclax	S53845	Combination	Venetoclax	S53845	Combination
Torin-1	■	■	■	■	■	■	■	■	■	■	■	■	■	■	■

4. 5-Fluorouracil (5-FU)

5-FU is an antimetabolite and a uracil analogue. Its active metabolites incorporate heavily into the RNA and disrupt its homeostasis on multiple levels. It also disrupts the function of the thymidylate synthase enzyme and therefore sanctions the production of thymidine nucleotides resulting in nucleotide supply shortage for DNA synthesis. The downstream effects of thymidylate synthase inhibition are complex and may not have been fully elucidated. A DNA microarray analysis of the downstream effects of 5-FU identified several genes of interest. Among those is FAS, which is implicated in the extrinsic pathway of apoptosis (269). 5-FU is integral in the treatment of colon cancer

but has no role in the treatment of myeloma. The prediction of 5-FU as an upstream effector in this data analysis is unsurprising given the treatments used in this experiment. Supporting this is the predicted 5-FU activation with all the combination conditions where synergy in apoptosis induction was observed (Table 6.11).

Table 6.11: The activation pattern of 5-FU across the myeloma cell lines in response to venetoclax and S63845 single agent and combination treatment (■ = activation, ■ = inhibition, ■ = no activation pattern discerned)

	U266			KMS12-BM			MOLP-8			JJN-3			MM1s		
	Venetoclax	S53845	Combination	Venetoclax	S53845	Combination	Venetoclax	S53845	Combination	Venetoclax	S53845	Combination	Venetoclax	S53845	Combination
5-FU	■	■	■	■	■	■	■	■	■	■	■	■	■	■	■

5. p53

p53 is a major tumour suppressor gene and it has been regarded as the guardian of the genome. Various cell stresses will cause the activation of p53 via the disruption of its binding to its inhibitor MDM2. Phosphorylation of p53 induces a plethora of downstream effects. For example, p53 will halt cell cycling in the event of DNA damage. If the damage is severe or the repair is taking a prolonged time then p53 will mediate the activation of apoptosis (75,270). p53 acts as a transcription factor for many of the genes involved in the apoptosis pathway whether this is via the extrinsic or the mitochondrial pathways (270). The role of p53 in the pathogenesis of myeloma has been discussed extensively in Chapter 1. 17p (where p53 is located) del is one of the cellular events in the immortalised plasma cells that may herald the transformation to a symptomatic disease (1). This is unsurprising since disruption of

p53 features in half of human cancers (76). p53 disruption in myeloma is considered to be a high-risk event and has been associated with an inferior outcome whether as a stand-alone or through association with other genetic events such as 1q deletion (3,43,58).

Although the data set analysis features p53 as one of the top predicted upstream effectors, no specific activation pattern was possible. This could be potentially due to the fact that apoptosis induction via the combination of venetoclax and S63845 is p53 independent (Table 6.12).

Table 6.12: The activation pattern of p53 across the myeloma cell lines in response to venetoclax and S63845 single agent and combination treatment (■ = no activation pattern discerned)

	U266			KMS12-BM			MOLP-8			JJN-3			MM1s		
	Venetoclax	S53845	Combination	Venetoclax	S53845	Combination	Venetoclax	S53845	Combination	Venetoclax	S53845	Combination	Venetoclax	S53845	Combination
p53	■	■	■	■	■	■	■	■	■	■	■	■	■	■	■

6.3.1.2.2 Causal Pathways Analysis

Causal Pathways activation or inhibition was predicted based on the indirect collaboration of the significantly changed proteins in the experimental samples. The top five causal pathways/molecules included (**Table 6.2**),

1. PCGEM1
2. CUL4B
3. PUF60
4. SGI 1776
5. LARP1

1. PCGEM1

Prostate cancer gene expression marker 1 belongs to the long non-coding RNA (lncRNA) group. Members of this group are generally over 200 nucleotides and they do not encode a peptide. Instead, they exert an epigenetic influence, modulating functions such as apoptosis and proliferation (271) partly through interacting with microRNAs (272).

PCGEM1 was identified through comparative Northern blot analysis of prostate tissue versus other tissues (273). In prostate primary patients samples, PCGEM1 overexpression was associated with advanced and more invasive disease (274). PCGEM 1 can increase the activation of myc and exert a positive effect on metabolic gene activation through recruiting myc (275). Although PCGEM1 is specific to prostate tissue and may not have an effect in haematological tissues, another lncRNA (NEAT1), was associated with dexamethasone resistance in human primary myeloma cells and myeloma cell lines. Moreover, lncRNA NEAT1 was associated with increased MCL-1 expression and was correlated with poor survival (276).

A pattern of predicted inhibition was observed across all the cell lines with the combination treatment with a rather heterogenous pattern of activation and inhibition with the single agent treatments (Table 6.13). Given that PCGEM1 does not feature in myeloma or indeed other haematological cancers as far as the literature is concerned, it may be possible to dismiss this observation being specific to PCGEM1 and attribute it to the software prediction based on the pattern observed in the data elsewhere. Nevertheless, it is not difficult to imagine that effect from other lncRNA

with a similar function such as NEAT1. However, this hypothesis would still require experimental proof since NEAT1 did not feature in the data analysis.

Table 6.13: The activation pattern of PCGEM1 across the myeloma cell lines in response to venetoclax and S63845 single agent and combination treatment (■ = activation, ■ = inhibition, ■ = no activation pattern discerned)

	U266			KMS12-BM			MOLP-8			JJN-3			MM1s		
	Venetoclax	S53845	Combination	Venetoclax	S53845	Combination	Venetoclax	S53845	Combination	Venetoclax	S53845	Combination	Venetoclax	S53845	Combination
PCGEM1	■	■	■	■	■	■	■	■	■	■	■	■	■	■	■

2. CUL4B (cullin4B)

CUL4B is one of the nine members of the Cullins family of proteins. They function as scaffolds to E3 ubiquitin ligases and play a key role in certain protein degradation. CUL4B was found to be overexpressed in several solid cancers and this overexpression was found to correlate negatively with prognosis. CUL4B exerts a repressive effect on transcription through DNA methylation and histone deacetylation (277). CUL4B is also implicated in the regulation, through proteasomal degradation and transcription repression, of several cell cycle proteins. CUL4B can induce cyclin E degradation, suppresses p21 and positively regulates CDC6. All these processes are implicated in cell cycle progression and DNA replication (277). In ovarian cancer patient samples, overexpression of CUL4B was associated with cell cycle progression evidenced by more cells in the S phase. Moreover, through repression of miR-732, CUL4B causes the upregulation of cyclin D1 and CDK2 with a further positive impact on cell cycle progression (278). The IMiDs group of drugs used for the treatment of myeloma are

substrates of the Cereblon which is part of the E3 ubiquitin ligase complex. As mentioned above CUL4B is part of that complex and CUL4B mutations have been identified in myeloma patients resistant to IMiDs (279).

Our data (Table 6.14) showed that CUL4B was predicted to be activated in most of the conditions and in all the combination conditions. This finding obviously goes against the observed cytotoxicity due to the pro-survival effect for CULIN4B. One explanation

maybe a feedback loop that was caused by the observed myc suppression that was mentioned earlier. c-myc suppression may result in a compensatory feedback loop that would cause the CULIN4B to go up. Another plausible explanation for our data would be the independence of the CUL4B-myc axis from apoptosis induction via the mitochondrial pathway although that would not necessarily explain the activation pattern observed with the combination treatment and the heterogeneity observed with the single agent treatment.

Table 6.14: The activation pattern of CUL4B across the myeloma cell lines in response to venetoclax and S63845 single agent and combination treatment (■ = activation, ■ = inhibition, ■ = no activation pattern discerned)

	U266			KMS12-BM			MOLP-8			JJN-3			MM1s		
	Venetoclax	S53845	Combination	Venetoclax	S53845	Combination	Venetoclax	S53845	Combination	Venetoclax	S53845	Combination	Venetoclax	S53845	Combination
CUL4B	■	■	■	■	■	■	■	■	■	■	■	■	■	■	■

3. PUF60

Mature mRNA production involves splicing out the correct introns then connecting the exons. A mature mRNA could be one of many splice-variants of a single pre-mRNA due

to alternative splicing thereby diversifying the functional capabilities of the translated mRNA. The process of intron excision is mediated by a complex of ribonucleoproteins called the spliceosome. PUF60 (poly(U) binding splicing factor 60) is a splicing factor that is implicated in the recognition of splice sites. A collaboration between PUF60 and another factor called U2AF65 is found to mediate alternative splicing (280). PUF60 splice variants can exert different cellular functions. For example, the splice variant FIR which lacks exon 5 can regulate c-myc and cell cycle protein transcription (281). FIR has been shown to be a transcriptional repressor of c-myc. FIR also monitors DNA damage repair. FIR lacking exon 2 negatively represses FIR and therefore causes c-myc overexpression. A study found that bleomycin-induced DNA damage caused the up-regulation of FIR lacking exon 2 which monitors DNA damage repair (282). Because of the upregulation of this alternative splicing form of FIR in many cancer cells, DNA damage may indirectly cause the up-regulation of c-myc (283).

Table 6.15: The activation pattern of PFU60 across the myeloma cell lines in response to venetoclax and S63845 single agent and combination treatment (■ = activation, ■ = inhibition, ■ = no activation pattern discerned)

	U266			KMS12-BM			MOLP-8			JJN-3			MM1s		
	Venetoclax	S53845	Combination	Venetoclax	S53845	Combination	Venetoclax	S53845	Combination	Venetoclax	S53845	Combination	Venetoclax	S53845	Combination
PUF60	■	■	■	■	■	■	■	■	■	■	■	■	■	■	■

Anti-FIR antibodies have been detected in the serum of patients with colorectal and oesophageal cancers, reflecting c-myc overexpression (284). To our knowledge, FIR/PUF60 has not been studied in myeloma. The pattern observed in our dataset was

that of activation which can be explained through the global transcriptional suppression observed throughout this chapter, possibly combined with c-myc suppression (

Table 6.15).

4. **SGI 1776**

This is an ATP competitive inhibitor of the Pim group of kinases (pro-viral insertion site for the Moloney Murine Leukaemia Virus). The Pim kinases are constitutively active and are overexpressed in several types of cancers including myeloma, acute myeloid leukaemia and certain types of lymphomas (285). Microarray analysis identified Pim2 in a subset of 52 genes that were differentially expressed in myeloma as compared to non-myeloma cells (286). Pim-2 causes the stabilisation, through ser 329, of c-myc, increases c-myc levels and enhances its oncogenic effect (287). Phosphorylation of 4E-BP1 which is involved in cap-dependent translation was an indirect effect of Pim-2 kinase activity (288). Pim also induced BAD phosphorylation which causes its dissociation from BCL-2. The increased availability of BCL-2 imparts apoptosis resistance (285).

SGI 1776 inhibits the three isoforms of Pim. SGI 1776 treatment of U266 and MM1s myeloma cell lines produced only limited toxicity and a similar minimal effect was observed in primary myeloma samples (289). There is no room for SGI 1776 in the current treatment pathway for multiple myeloma and indeed other haematological and non-haematological cancers. Phase I clinical trials were prematurely suspended due to cardiac toxicity (290). AZD1208 was developed by AstraZeneca as another Pim kinase inhibitor. Similar to SGI 1776, prolonged incubation was required to

demonstrate cytotoxicity in myeloma cell lines. The combination of AZD1208 with bortezomib was synergistic in three myeloma cell lines (U266, KMS-12BM and MM1s) (291).

Although the preclinical activity of this compound was demonstrated in AML cell lines and xenograft model (292), a phase I clinical trial showed no clinical benefit and failed to demonstrate the maximum tolerated dose (MTD) (293). An activated pattern was observed in most of the conditions in this dataset. This is mechanistically predictable from the effect of Pim inhibition on BCL-2 and from what we have observed in terms of c-myc downregulation and thereby becomes consistent with the literature findings above (Table 6.16).

Table 6.16: The activation pattern of SGI1776 across the myeloma cell lines in response to venetoclax and S63845 single agent and combination treatment (■ = activation, ■ = inhibition, ■ = no activation pattern discerned)

	U266			KMS12-BM			MOLP-8			JJN-3			MM1s		
	Venetoclax	S53845	Combination	Venetoclax	S53845	Combination	Venetoclax	S53845	Combination	Venetoclax	S53845	Combination	Venetoclax	S53845	Combination
SGI1776	■	■	■	■	■	■	■	■	■	■	■	■	■	■	■

6.3.2 Comparison Analysis

Heat maps were generated using hierarchical clustering of the z values of the significantly changed proteins compared across all the myeloma cell lines Comparison analysis through IPA generates heat maps. Those heat maps can be obtained by comparing any number of cell lines (and any treatment condition). The analysis that is presented in this section is based on the comparison between all five myeloma cell

lines exposed to the combination treatment rather than single agent treatment. Comparison analysis across the myeloma cell lines exposed to single agent treatment is not presented. The reason this approach to data analysis was adopted relates to the results presented in the previous chapter. While single agent treatment produced variable results in terms of apoptosis induction, the combination treatment of the MCL-1 and BCL-2 inhibition led to apoptosis consistently. As mentioned previously, it was not possible to ascertain a specific pattern of sensitivity with the single agent treatments to whether cell lines were cyclin D1 or cyclin D2 translocated. Therefore, presenting a comparison analysis of the myeloma cell lines exposed to the combination rather than the single agent treatment appears more reasonable given the uniformity of the combination approach in apoptosis induction across all cell lines.

Two types of heat maps were generated; in the first (Figure 6.5), significantly changed proteins were clustered according to their corresponding pathways and activation or inhibition of those pathways was based on the total z scores of the individual proteins. The association of the proteins to the displayed pathways is based on an internal database in the IPA software. Although no specific pattern could be deduced from this type of heat map analysis based on whether the cell lines were cyclin D1 or D2 expressing, on a close inspection of the generated heat map, it is clear that the significantly changed pathways showed an increased degree of inhibition, based on the z scores, with the combination treatment. This was most pronounced in the KMS12-BM and the MM1s myeloma cell lines. It is unclear, however, from the data that we have, why these two cell lines appeared similar on the heat map analysis as they express different cyclin D type and although they both showed synergy with the combination treatment, this did not stand different from the other cell lines (except

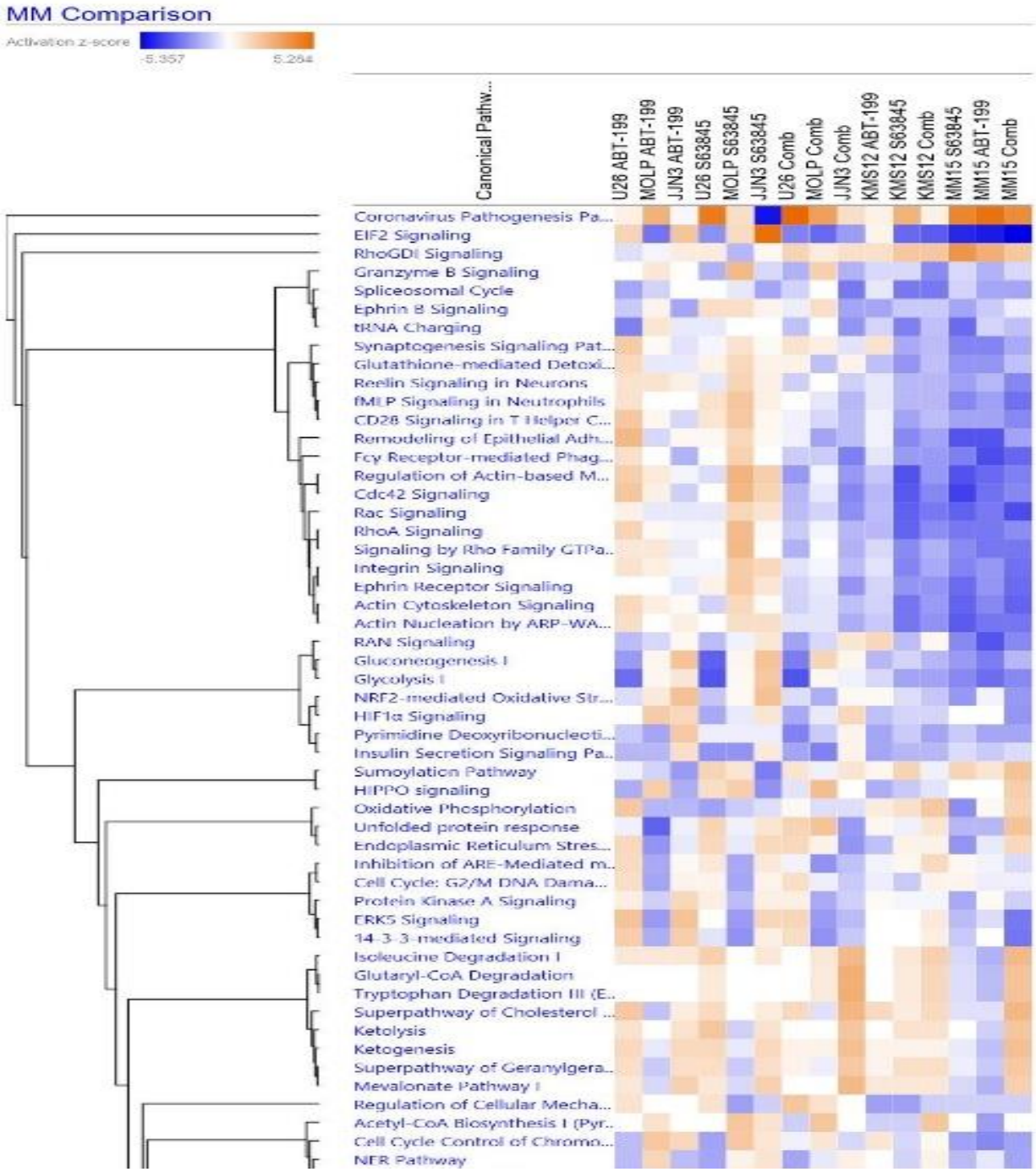


Figure 6.5: Heat map based on hierarchical clustering of the canonical pathways in comparison analysis between all the conditions tested. The visualisation is based in the z-score values.

The second type of heat maps generated from the comparison analysis was based on the association of the significantly changed proteins to cellular functions. This disease and function analysis (Figure 6.6) was again based on the internal database within the IPA software and, similar to canonical pathway analysis, uses hierarchical clustering to generate the heat maps.

On a close inspection of this heat map, it is possible to deduce that pathways and functions that are associated with cell death and apoptosis were activated with the S63845 and venetoclax combination and most of the single agent treatments. In addition, pathways that are associated with DNA repair and survival were inhibited with the combination and single agent treatments.

Moreover, even when the above pattern was not observed with the single agent treatment (such as with JJN-3 and MOLP-8 treatment with S63845), the combination treatment restored the above effect. In other words, the combination treatment was able to enforce the activation of pathways that were associated with cell death and apoptosis with an opposite effect on pathways associated with survival, proliferation, and various forms of DNA repair even when the single agent treatment was unable to produce that effect.

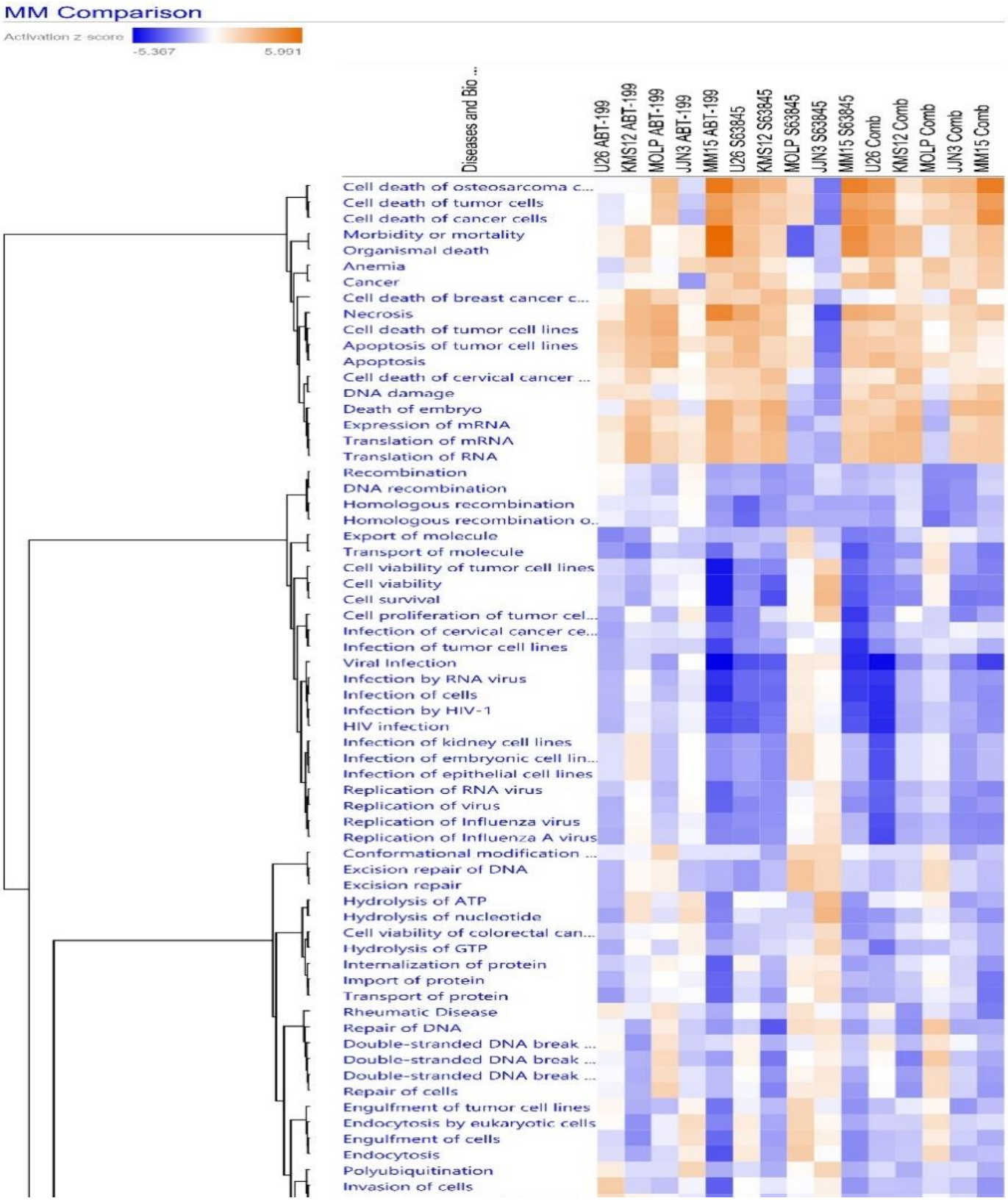


Figure 6.6. Heat map based on hierarchical clustering of the diseases and functions in comparison analysis between all the conditions assessed. The visualisation is based on the z-score value.

6.4 Conclusion

In this chapter, we attempted to explore if there is a differential effect of cyclin D1 or D2 expression on the proteomic profile of the myeloma cell lines following apoptosis induction. Following the general theme in this thesis, the underlying D cyclin did not seem to impart a discernible pattern. One must take into consideration the potential effect of the small sample size and the fact that only the mitochondrial pathway of apoptosis was interrogated. There was also an apparent lack of concordance between the data obtained from this proteomic analysis and the Western blot data obtained in Chapter 5. For example, cyclins did not appear in the list of proteins identified through this analysis. This, however, is not unusual and there could be several reasons behind this apparent lack of concordance. Certain proteins are not digestible by trypsin due to not enough lysine-arginine residues. Moreover, if the digestion creates a massive peptide then this will not be detectable by mass spectrometry. The detection of proteins also relies on the column properties. Certain properties will preclude the detection of certain proteins using MS. Certain typsin-digested peptides will fail to ionise efficiently and therefore may not fly in the mass spectrometer. Finally, the detection of the peptides relies on the SWATHE library and proteins that are not present in the library will not be identified.

Nevertheless, there were still some interesting findings to note. Given the synthetic nature of the myeloma cells in general, pathways related to mRNA translation and the regulatory mechanisms behind this process featured heavily in the canonical pathway analysis of the datasets. We have noted a global reduction in translation probably due

to the downregulation of several important eIF2 proteins and potentiation of the negative regulators of the protein translation such as eIF4 and P70S6K, especially in the cyclin D1 expressing cell lines. This was the only differential effect observed and although previous work did suggest a collaboration between eIF4 and cyclin D1 through the nuclear transport function of the former, it would be difficult to draw definite conclusions in terms of the effect of the underlying cyclin type from our data. c-myc inhibition also featured heavily and may also reflect the global translation slow-down. This also hints that the inhibition of cap-dependent translation did not cause the upregulation of myc through a compensatory cap-independent mechanism. This proteomic analysis was unable to show the presence of specific biomarkers or a proteomic profile that can predict sensitivity to MCL-1 inhibition, BCL-2 inhibition or indeed their dual inhibition. The proteomic signatures identified in this set of data heavily feature the inhibition of protein turn-over, protein recycling and protein synthesis. All are points of vulnerability in myeloma cells and are targets for commonly used drugs in myeloma treatment such as proteasome inhibitors and IMiDs. Our data may indicate that the dual BCL-2/MCL-1 inhibition maybe ultimately exploiting such vulnerabilities. It would be interesting to see the effect of this dual inhibition in myeloma cells that have developed resistance to one or more of these features such as in bortezomib-resistant myeloma cells. The data from the combination analysis showed the inhibition of pathways related to survival, proliferation and DNA damage repair and the activation of pathways associated with cell death and apoptosis. This was most pronounced in the combination setting and corroborates the findings from the previous chapter in terms of the effect of the combination treatment on apoptosis induction and cytotoxicity.

The results from this chapter, although did not achieve the set aim of identifying a differential proteomic pattern between the myeloma cell lines based on whether they have a cyclin D1 or D2 translocation, highlighted a prominent role of pathways related to protein translation. The combination treatment of MCL-1 and BCL-2 inhibition that was shown to induce apoptosis in the previous chapter also appeared to show a slowdown in the regulatory pathways related to mRNA translation in the cyclin D1 cell lines. There was a degree of granularity probably exaggerated by the small sample size and the need for more replicates. This granularity will prevent drawing a firm conclusion regarding a clear correlation with whether cyclin D1 overexpression was present or not.

The data analysis in this chapter took the approach of identifying which pathways are heavily affected through the changes in the individual component proteins. The focus was thus mainly on pathways rather single proteins. A different approach would have been to look at individual proteins fold changes. Validating the pathways activation or inhibition requires further dedicated experimentation. The analysis could have been extended to see if there are any commonalities between this approach and the data analysis that would have been obtained from fold-change analysis. The identification of some common ground proteins through such analysis would have increased the robustness of the data. Furthermore, if this analysis led to the identification of a certain protein or group of proteins of interest, then further interrogation of their impact could be attempted. Protein expression could be checked through Western blotting or flow cytometry for example. The impact of those proteins could be tested through inhibition/induction of their expression using RNAi or transfection, and the impact of this on viability could be tested. Due to the complexity of those proposed

experiments however, such approach would not have been possible during the short lifetime of this project and further work in that direction would benefit from a dedicated research project.

CHAPTER 7:

FINAL DISCUSSION AND CONCLUSION

Chapter 7: Discussion and Conclusions

7.1 The Background and Rationale for this Experimental Work

The underlying molecular heterogeneity that is observed in multiple myeloma is initiated at the point of creation of the immortalised plasma cell at the MGUS stage and follows a pattern whereby further events accumulate throughout the process of disease progression.

Those events (or hits) play a significant role in the likelihood of development of symptomatic disease, the rate of progression, the development of aggressive disease, and the likelihood of response to a specific type of treatment whether conventional or novel. The heterogeneity created by those events lends to the accepted notion that plasma cell myeloma is not necessarily a single disease but can vary from one patient to another. Not only that but this heterogeneity has been established within the same patient and can generate multiple subclones and those can have a differential response to chemotherapy (1,4,14) .

The initiating genetic events in myeloma are divided into two main categories that are mutually exclusive except in around a tenth of cases. These events are either the hyperdiploidy of odd-numbered chromosomes or translocations involving the immunoglobulins heavy chains (18,21,28,61).

The chromosomal translocations result in the placement of the active immunoglobulin heavy chain promoter located on chromosome 14 next to partner genes, the accelerated transcription of which leads to the overexpression of a D-type cyclin either directly or through a series of downstream events. Cyclin D1 overexpression is seen

with the t(11;14) whereas t(4;14), t(14;16), and t(14;20) lead, eventually to overexpression of cyclin D2 through MMSET, MAF and MAFB respectively (21).

The focus of this thesis was the cyclin D over-expressing myeloma cell lines. We sought to explore if a specific pattern would emerge that could be attributed to the underlying overexpressed cyclin D when those cells were subjected to DNA damage (alone or in combination with proteasome inhibition), apoptosis induction (via intrinsic pathways) or when the proteomic analysis was attempted.

There are several reasons why this research question is of interest. There is a clear impact of the underlying cyclin D-type translocation on prognosis. For example, the cyclin D1 expressing t(11;14) is considered, with some dispute, to be a standard risk cytogenetic change as compared to the cyclin D2 expressing t(4;14) or t(14;16) which are considered to be high-risk cytogenetic changes in the revised international staging system with a clear impact on the PFS and the OS (30,38). In addition, there is a proven effect of the underlying cytogenetic change on the therapeutic approach, whether through treating high-risk cytogenetics more aggressively (for example with a tandem autologous stem cell transplant) (118) or through the higher sensitivity of certain translocations to specific treatments such as the higher sensitivity of t(11;4) translocated myelomas to BCL-2 inhibition with venetoclax (26).

Fortifying the concept that multiple myeloma is not necessarily a single disease given the variance by which it behaves clinically between patients, secondary genetic events can segregate within specific initiating events as the disease develops. For example, the KRAS and NRAS mutations tend to segregate within hyperdiploid myelomas and

those with t(11;14) and c-myc translocations are mostly found within hyperdiploid myelomas (69).

The biological roles of the different types of cyclins may also extend beyond their canonical function in terms of cell cycle progression. There is a defined role for cyclin D1 in the DNA damage response. Cyclin D1 is quickly downregulated following DNA damage (as compared to cyclin D2 which does not) and cyclin D1 was also found to sequester BAX thereby exerting an anti-apoptotic effect (104,105,193,199,286).

The thesis attempted to investigate if there is a differential response according to the underlying cyclin D. From the clinical perspective, the thesis addressed the question of differential response to standard chemotherapy, combination chemotherapy and the cytotoxicity and the synergy of novel agents. From the biological aspect, we have explored the effect of cyclin D on DNA damage, proteasome inhibition and apoptosis induction through the mitochondrial route and the effect of the latter on the proteomic profile of the myeloma cell lines.

To carry out the objectives set out for this thesis, six myeloma cell lines were chosen based on their underlying D-type cyclin such that three were known to express cyclin D1 (U266, KMS12-BM and MOLP-8) and the rest were known to express cyclin D2 (JJN-3, OPM-2 and MM1s). The choice of the cell lines for this project was done with the aim of establishing uniformity when comparing the effect of cyclin D status on DNA damage, response to chemotherapy, apoptosis response and mass spectrometry analysis. There are many human myeloma cell lines available for clinical research and it goes without saying that various other cell lines could have been used for the purpose of this project however those potential other choices were not expected to

introduce additional uniformity for two main reasons. Firstly, although human myeloma cell lines were found to be genetically uniform within each cell line (294), they vary significantly between each other and it would not be feasible to find myeloma cell lines that are only differ in terms of their underlying cyclin D status. Secondly, even if such cell lines existed, further yet uncharacterized molecular differences between those cell lines could still exist. A logical approach would have been, if there was a differential response found, to explore that in more detail in other cell lines to confirm its attribution to the cyclin D status. This, however, was not done within the lifetime of this project as no such differential response was found.

The cyclin D1 cell lines all had the same initiating translocation, t(11;14). This was not the same for the cyclin D2 cell lines. Two cell lines exhibited the *MAF* translocation (t(14;16) in JJN-3 and MM1s), the OPM-2 cell line had a t(4;14) translocation. While this can be viewed as a point for nonuniformity, it actually allows the study of the impact of cyclin D2 translocation as an end result regardless of the underlying initiating event that caused its upregulation in the first place. A potentially different approach would involve the use of two cell lines with t(4;14) such as OPM-2 and LP-1 and two cell lines with t(14;16) such as JJN-3 and MM1s but this would create an imbalance in terms of the overall cell line numbers and may have potentially complicated the experimental work. We have chosen two cell lines with a wild type p53 status. Again it could be argued that it would have been better to use cell lines with a similar p53 status for the sake of uniformity. However, the same discussion points mentioned above would still apply and comparing the impact of the p53 status on the investigative methods used in this thesis was an attractive research question.

7.2 Cyclins D1 and D2 and DNA Damage

We sought to explore the dynamics of DNA damage in cyclin D1- and cyclin D2-expressing myeloma cell lines. To induce DNA damage, IR was used. This method avoids the individual cell lines variability of response to DNA-damaging chemotherapy. Moreover, IR is relatively quick and reproducible. To observe the effect of IR on DNA damage induction, a direct metric was used through the neutral comet assay, whereas the cellular response to DNA damage was assessed using the γH2A.X phosphorylation. This assessment was done immediately, at the 4h and at the 24h time points after irradiation.

What we have observed from the comet assay is a clear increase in the tail moments immediately after IR indicating the induction of DNA damage. This was the only time point where the increase was significant (Figure 3.3). γH2A.X phosphorylation was significant immediately and/or at the 4h time point (Figure 3.5). The reduction in the tail moments significance at the subsequent time points could have indicated either the apoptosis of the irradiated cells or that they have managed to repair their DNA. The fact that the γH2A.X phosphorylation changes did not mirror the changes observed with the tail moments may indicate the presence of residual DNA damage that could not be repaired and/or that which the cell lines could tolerate without having to go through apoptosis. There was a drop in the cell count in most of the cell lines at 24h but not at the 4h time-points (Figure 3.4). When the apoptosis was assessed using the annexin V assay subsequently, that was not increased at the 4h time point after IR (Figure 4.2). Therefore, we stipulated that the reduction in the tail moments was due to the repair of the damaged DNA rather than due to the apoptosis

of the irradiated cells. The results, however, did not show a differential response between the D1 and the D2 cell lines. We have subsequently confirmed the rapid downregulation of cyclin D1 following irradiation, but this was not enough to result in differential response. This was attributed previously to the presence of enough cyclin D1 bound to CDK4/6 to enable the cell cycle to carry on (108). Assessment after longer incubation, therefore, may be required following irradiation to confirm this effect.

7.3 Apoptosis Induction Through DNA Damage and Proteasome Inhibition

To address the research question from a different angle, the next step was to examine the impact of clinically relevant therapeutics on the induction of apoptosis while assessing the levels of cyclins D1 and D2. To tackle this objective, it was sensible to interrogate the two main components of the apoptotic pathway (the extrinsic and the intrinsic pathways) separately.

The proteasome inhibitor, bortezomib was used alone and in combination with IR as a DNA-damaging agent. As documented previously, bortezomib was cytotoxic at nanomolar quantities. The concentrations chosen for bortezomib for subsequent experiments were unique to each cell line and were those that induced an approximate 30% drop in viability so as not to erode the Western blot analysis for the cyclin D. Confirming previous research, DNA damage due to IR caused a reduction in cyclin D1 levels but no impact on cyclin D2 (Figure 4.8), whereas bortezomib treatment only caused a reduction in the cyclin D1 and cyclin D2 levels in the U266 and the JJN-3 cell lines respectively. The impact of single treatments on apoptosis was assessed using the annexin V assay. Apoptosis was not significant after 4h of IR but increased

mainly in the MOLP-8 and the MM1s cell lines after 24h (Figure 4.2A). It is worth mentioning that both of those cell lines had a wild-type p53.

Given that cyclin D1 reduction was observed as early as 4 hours after IR but apoptosis seemed to increase with longer incubation, we have attempted a temporal variation of when IR (or DNA damage) was introduced during a 24h treatment with bortezomib. Since DNA damaging agents (such as cyclophosphamide or melphalan) are frequently used in combination with bortezomib in clinical practice, it would be interesting to see if this temporal variation can produce variable results based on when DNA damage happens during bortezomib treatment. There was no significant impact of changing the time when the DNA damage was induced during the course of bortezomib treatment generally on cyclin D expression but the impact was rather an additive of the single agent effect (Figure 4.3 B, Figure 4.6, Figure 4.7). There was a non-significant increase in the cyclin D2 level with the combination treatment in the MM1s cell line which was unexpected (Figure 4.8). Whether this finding may indicate that cyclin D2 increase can confer an anti-apoptotic effect or not is difficult to establish, and, since this observation was only noticed in only one out of the three cyclin D2 expressing cell lines, a reasonable inference cannot be made. There was no significant impact of changing the time of exposure to IR on the cyclin D1 expression in the cyclin D1 cell lines. As far as the aim of the thesis, and apart from the observed downregulation of cyclin D1 associated with IR, there was no differential response to extrinsic apoptosis induction via IR alone or in combination with bortezomib treatment. The observed downregulation of cyclin D1 did not have a measurable effect on apoptosis.

7.4 Apoptosis Induction via the Intrinsic Pathway

The next step was to see the effect of apoptosis induction via the intrinsic (mitochondrial) pathway. In addition to being DNA damage-independent, apoptosis induction via this pathway is free from any possible impact from the p53 status of the cell lines used in this project. As mentioned in the introduction, previous research demonstrated that most myelomas are MCL-1 dependent for survival such that when BCL-2 is inhibited any released BIM would not be able to trigger apoptosis as it will be mopped up by MCL-1 (49). A small group of myelomas are BCL-2 dependent and those tend to be mostly sequestered within the t(11;14) translocation. Those myelomas were the most sensitive to venetoclax (the BCL-2 inhibitor) in clinical practice (27,114). To be able to induce apoptosis effectively, the BCL-2 inhibitor (venetoclax) and the MCL-1 inhibitor (S63845) were used as single agents and in combination. The focus was on the achievement of synergy given that through this, apoptosis via the mitochondrial pathway was induced. Our cell lines appeared to be more sensitive to MCL-1 inhibition than BCL-2 inhibition judging by the micromolar quantities required to achieve the same cytotoxicity (Figure 5.1), therefore confirming previous research that most myelomas are MCL-1 dependent for survival. The cyclin D1 cell lines were not found to be more sensitive to BCL-2 inhibition with venetoclax at the concentrations used, but the establishment of venetoclax sensitivity was not part of the aims of this section. Of note, our data do not support variability in the sensitivity to S63845 based on the degree of 1q gain (MCL-1 is located on chromosome 1q).

Five out of the six cell lines showed clear synergy with BCL-2 and MCL-1 dual inhibition and in all of those cell lines, there was a reduction of the relevant cyclin D as assessed

by Western blotting (Figure 5.1, Figure 5.2, Figure 5.7, and Figure 5.8). The MOLP-8 cell line did not show clear synergy or cyclin D1 reduction and the cytotoxicity that was observed was attributed to the effect of MCL-1 inhibition by S63845. Cyclin D levels were not affected by the single agent treatment with either venetoclax or S63845 in all the cell lines at the sublethal concentrations used except in the MM1s where there was a slight reduction in the cyclin D2 expression. This indicates that apoptosis induction via the mitochondrial pathway is associated with cyclin D1 and cyclin D2 reduction as compared to DNA damage which only caused a reduction in cyclin D1 levels. Several studies have demonstrated the downregulation of cyclin D1 with BCL-2 inhibition in multiple cancers, but the impact of the dual inhibition on cyclin D2 has not been demonstrated previously as far as we are aware. Nevertheless, no emerging pattern was identified in terms of the expression of cyclin D, MCL-1, or BCL-2 or in terms of cytotoxicity that could be attributed directly to the underlying cyclin D type.

We have established the utility of the cytochrome c release assay with its advantageous short drug incubation time as a predictor of cytotoxicity. After only 4 hours of incubation with drugs, this assay was as accurate as the longer incubation assays in predicting apoptosis (Figure 5.3).

7.5 Assessing the Proteomic Profile of Myeloma Cell Lines

The assessment of the proteomic profile of the myeloma cell lines using mass spectrometry was a further attempt to identify if there is an underlying proteomic signature that could be attributed to the underlying D-type cyclin. Protein extracts from the BCL-2 and MCL-1 synergy experiments were used for the proteomic analysis.

The top canonical pathways that were identified through this analysis (Table 6.2) were those concerned with mRNA translation (the eIF2 signalling pathway), the regulation of protein translation (eIF4, P70S6K and mTOR pathways), apoptosis (BAG2 signalling) and ubiquitination (FAT10 signalling). We have observed a generalised slowdown of protein translation manifested as the inhibition of the eIF2 signalling pathway with the MCL-1/BCL-2 combination. The inhibition of this pathway with the combination treatment happened even if the single agent treatment showed activation. The differential effect that was observed with the cyclin D1 expressing cell lines compared to the cyclin D2 cell lines was the activation of the eIF4 and P70S6K pathway in the former and its inhibition with the latter. There is a close relation between eIF4E and cyclin D1 through the nuclear export function of the former. The same cell lines that showed downregulation of cyclin D1 (U266 and KMS12-BM) showed the reduction of the eIF4E.

c-myc, which plays a key role in myeloma progression, was identified in the causal network analysis and was predicted to be inhibited with the combination treatment and with most of the single-agent treatments. The comparison analysis between all the conditions showed the upregulation of pathways associated with cell death and apoptosis with the combination treatment and downregulation of survival and DNA repair pathways. Despite those interesting findings, the dataset analysis did not show a proteomic expression signature that was specific to the underlying cyclin D type. This conclusion, however, is specific to the treatment conditions selected for this analysis in this thesis and would not necessarily negate the presence of a cyclin D type-related signature if other conditions are tried. It would be interesting, for example, to carry out the same experimental analysis following cyclin D1 and cyclin D2 silencing to see

if different pathways become enriched. Similarly, running a proteomic profile in bortezomib-resistant cells may be interesting given that many of the pathways identified in this exercise are related to protein synthesis and recycling.

7.6 Conclusions and Future Work

To summarise, the results of this project did not support the presence of a prominent differential response between cyclin D1- and cyclin D2-expressing myeloma cells under the various experimental conditions explored. Weather, the variation of those experimental conditions would lead to different results is yet to be explored. We have not explored the effect of other therapies that may converge, through their own mechanisms of action, on the pathways highlighted in this thesis. Such therapies include the IMiDs (lenalidomide, pomalidomide), hypomethylating agents or exportin inhibitors (XPO1 inhibitors such as Selinexor). However, there remains the possibility that although there is a clear distinction in the developmental pathology of myeloma cells in terms of cyclin D expression, this may not turn out to be the culprit mechanism behind the differences by which those myelomas behave.

It is well known that the genesis of primary (initiating) events (cyclin D translocation included) happen at the MGUS stage. This premalignant process will need to acquire secondary hits in addition to bone marrow microenvironment dysfunction before any transformation to symptomatic myeloma. It is, therefore, possible that the acquisition of a cyclin D translocation would only result in the immortalisation of the pre-malignant plasma cells and the subsequent events that would initiate the malignant transformation are the true biological and clinical culprits. As mentioned previously, the segregation of secondary events can be dependent on the primary initiating

events, although this segregation is not necessarily unique and may be shared between different primary events.

There is also the possibility of downstream redundancy. The fact that the downregulation of cyclin D1 as compared to cyclin D2 that was observed did not result in differential toxicity may suggest the presence of downstream mechanisms that would compensate for the downregulation of cyclin D1. After all, previous work has shown that the cell cycle arrest in cyclin D1 and cyclin D2 cell lines happened at the G2/S phase rather than the expected G1 phase.

Nevertheless, there may be other ways of exploring if there is a differential response between cyclin D1 and cyclin D2 expressing myelomas. A direct approach that involves silencing the overexpressed immunoglobulin heavy chain partner genes or targeting the upregulated proteins downstream of those translocations (such as the H3K36 methyltransferase or SETD2 downstream of MMSET) in combination with proteasome inhibition or DNA damage may reveal a differential response or highlight novel mechanisms that may be explored for therapeutic purposes.

The potential impact of the molecular heterogeneity between cell lines remains a limitation and may have had an important effect on the results. Indeed, the only way, perhaps, to overcome this heterogeneity is by rerunning the experimental work using cyclin D1 and D2 knockout models of the same cell lines. The creation of such isogenic cell lines would be the only way to study the impact of cyclin D while removing any confounding factors that may arise because of the molecular variability between cell lines. This can be a suggestion for future work on this project.

One must also not forget the crucial effect of the bone marrow microenvironment on the pathogenesis of symptomatic myeloma and its contribution to drug resistance. Studying if there is an impact of the bone marrow microenvironment on the impact of the genetic architecture of multiple myeloma can be more representative of the in vivo behavior of myeloma cells.

In a final conclusion, although several interesting findings were uncovered throughout this thesis, the presence of a differential response to DNA damage, proteasome inhibition or apoptosis induction or the presence of a specific proteomic signature could be attributed to the underlying cyclin D type in multiple myeloma cell lines could not be established within the experimental work set out in this thesis.

CHAPTER 8:APPENDIX

Chapter 8: Appendix

8.1 Representative flow plots of Annexin V assay for KMS12-BM and JJN-3 cell lines after exposure to venetoclax and S63845 as single agents and in combinations

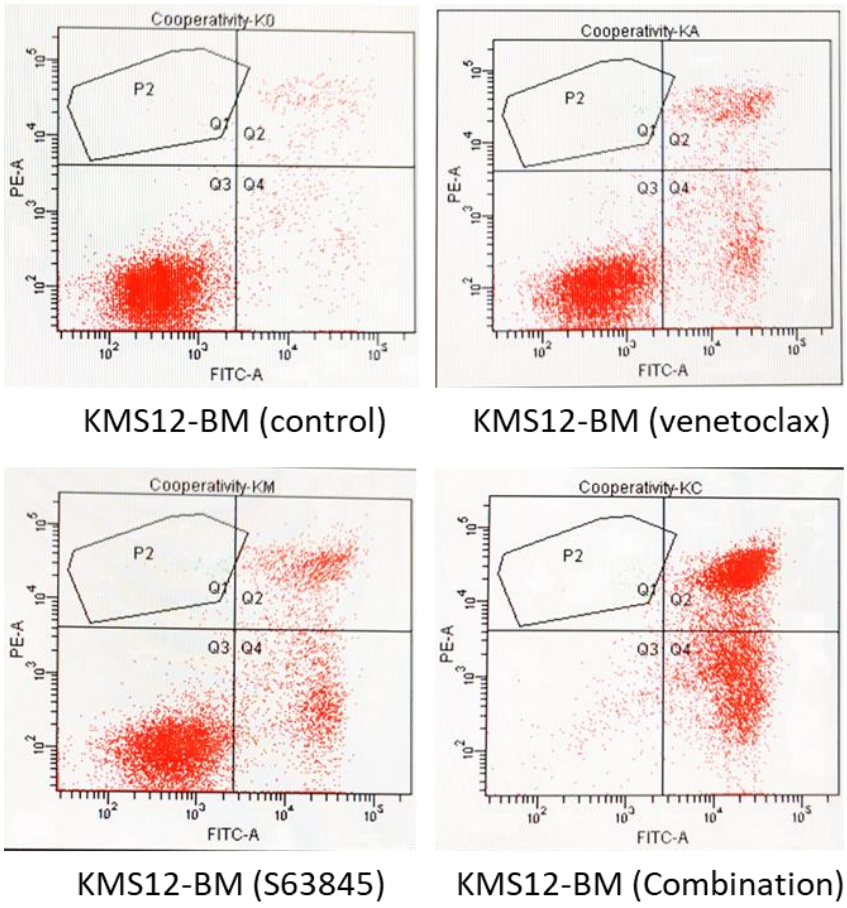


Figure 8.1 Representative Annexin V flow cytometry dot plots of KMS12-BM cell line treated with venetoclax, S63845 and the combination of both. The upper left plot is the control untreated sample. Viable cells are in Q3 gate (Annexin V-ve and Propidium Iodide -ve). Cells in Q2 and Q4 are Annexin V +ve (apoptotic). Cells in Q2 are also Propidium Iodide +ve. Single agent treatment caused a slight increase in Annexin V positivity while with the combination treatment, most cells became Annexin V +ve. Debris is gated out (P2 Gate)

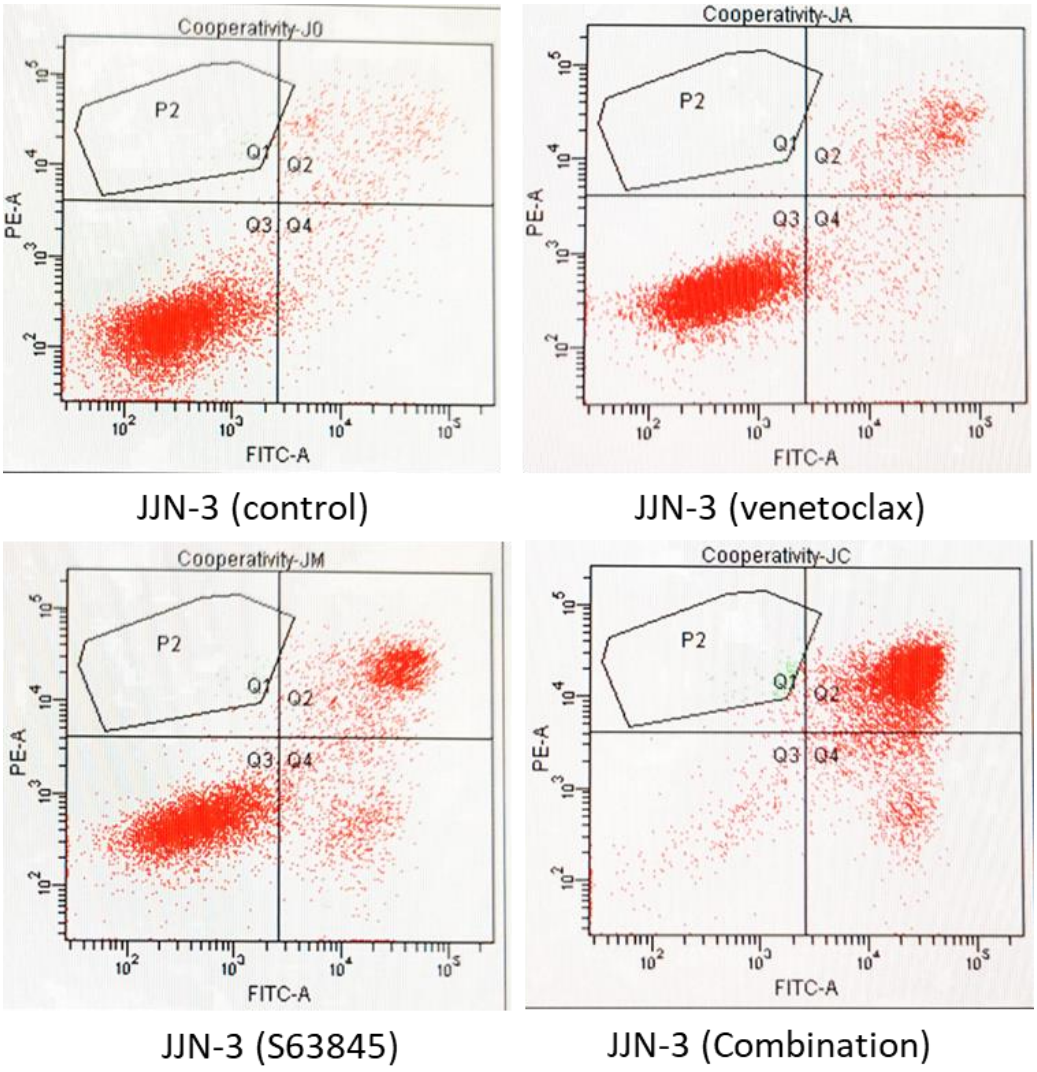


Figure 8.2 Representative Annexin V flow cytometry dot plots of JJN-3 cell line treated with venetoclax, S63845 and the combination of both. The upper left plot is the control untreated sample. Viable cells are in Q3 gate (Annexin V-ve and Propidium Iodide -ve). Cells in Q2 and Q4 are Annexin V +ve (apoptotic). Cells in Q2 are also Propidium Iodide +ve. Single agent treatment caused a slight increase in Annexin V positivity while with the combination treatment, most cells became Annexin V +ve. Debris is gated out (P2 Gate)

8.2 Discovering a predictive biomarker of venetoclax sensitivity and resistance in Multiple Myeloma-Short summary from C Ogden MSc Thesis done using fold change analysis of mass spectrometry data (295)

The mass spectrometry data generated from this project were analysed in a collateral project by MSc student Charlotte Ogden. The aim of the analysis was to look for

potential biomarkers for sensitivity / resistance to venetoclax. Since the KMS-12 cell line was found to be the most sensitive to venetoclax using the cytochrome c assay (166), fold change data from this cell line were compared to those from the other cell lines. This analysis identified, based on differential expression, 13 proteins. See **Table 8.1**.

Table 8.1 Fold changes of myeloma cell lines

Upregulated	KMS-12	MOLP-8	U266	JJN3	MM.1S
Acyl-CoA dehydrogenase 9	40.27	-34.15	-	2.07	-2.80
Cystatin-B	33.73	-	-	-1.65	2.54
Scribble	32.43	-	-	-	-
Protein disulphide-isomerase A3	29.55	1.21	-2.60	1.38	-1.73
Protein disulphide-isomerase TMX3	26.94	-2.20	-	-3.69	-5.27
Downregulated					
Heterogeneous nuclear ribonucleoprotein D0	-22.47	-3.23	-2.15	3.22	-2.02
Estradiol 17-beta-dehydrogenase 11	-21.12	-	-	-15.19	4.78
ATP-dependent RNA helicase DDX42	-20.85	-	3.33	-1.93	-
ERO1-like protein alpha	-17.85	-3.47	-	-1.54	-3.20
Ras-related protein Rab-10	-17.79	-	3.12	-1.90	-

Further pathway enrichment analysis using Panther for the upregulated protein showed over-representation in 7 pathways and for the downregulated proteins in 14 pathways. Those are shown in Figure 8.3.

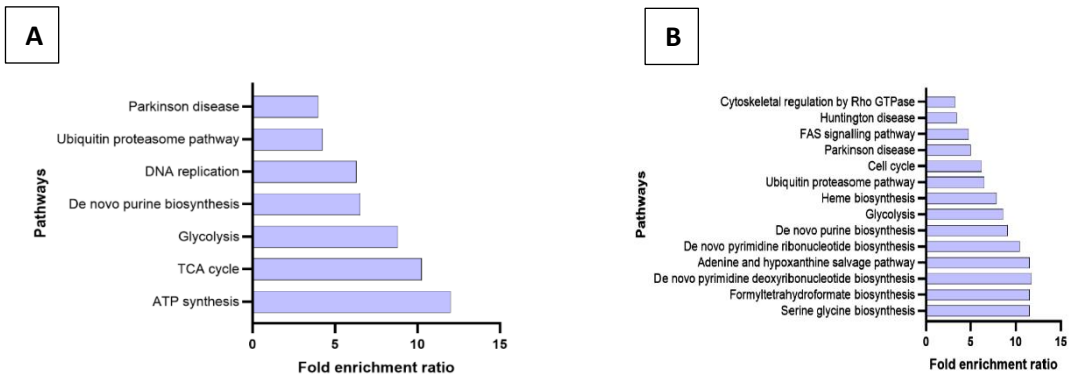


Figure 8.3: Pathway analysis using Panther for KMS12-BM cell line. Upregulated pathways are shown in A and downregulated pathways in B.

CHAPTER 9:

REFERENCES

Chapter 9: References

1. Manier S, Salem KZ, Park J, Landau DA, Getz G, Ghobrial IM. Genomic complexity of multiple myeloma and its clinical implications. Nat Rev Clin Oncol [Internet]. 2017;14(2):100–13. Available from: https://doi.org/10.1038/nrclinonc.2016.122

2. Lohr JG, Stojanov P, Carter SL, Cruz-Gordillo P, Lawrence MS, Auclair D, et al. Widespread Genetic Heterogeneity in Multiple Myeloma: Implications for Targeted Therapy. Cancer Cell. 2014;25(1):91–101.

3. Walker BA, Mavrommatis K, Wardell CP, Ashby TC, Bauer M, Davies F, et al. A high-risk, Double-Hit, group of newly diagnosed myeloma identified by genomic analysis. Leukemia [Internet]. 2019;33(1):159–70. Available from: https://doi.org/10.1038/s41375-018-0196-8

4. Rasche L, Chavan SS, Stephens OW, Patel PH, Tytarenko R, Ashby C, et al. Spatial genomic heterogeneity in multiple myeloma revealed by multi-region sequencing. Nat Commun [Internet]. 2017;8(1):268. Available from: https://doi.org/10.1038/s41467-017-00296-y

5. Solly S. Remarks on the pathology of mollities ossium; with cases. Med Chir Trans. 1844;27:435-498.8.

6. Rivers SL, Patno ME. Cyclophosphamide vs Melphalan in Treatment of Plasma Cell Myeloma. JAMA [Internet]. 1969 Feb 17;207(7):1328–34. Available from: https://doi.org/10.1001/jama.1969.03150200094011

7. San Miguel JF, Mateos MV, Ocio E, Garcia-Sanz R. Multiple myeloma: treatment evolution. Hematology [Internet]. 2012;17(sup1):s3–6. Available from: https://doi.org/10.1179/102453312X13336169154971

8. Shah UA, Mailankody S. Emerging immunotherapies in multiple myeloma. BMJ [Internet]. 2020;370:m3176–m3176. Available from: http://www.bmj.com/content/370/bmj.m3176.abstract

9. Yong K, Delforge M, Driessen C, Fink L, Flinois A, Gonzalez-McQuire S, et al. Multiple myeloma: patient outcomes in real-world practice. Br J Haematol [Internet]. 2016;175(2):252–64. Available from: https://doi.org/10.1111/bjh.14213

10. Cancer Research UK. https://www.cancerresearchuk.org/health-professional/cancer-statistics/statistics-by-cancer-type/myeloma#heading-Two [Internet]. 2022. Available from: https://www.cancerresearchuk.org/health-professional/cancer-statistics/statistics-by-cancer-type/myeloma#heading-Two

11. HMRN. HMRN. 2022. HMRN. Available from: https://hmrn.org/statistics/quickstats

12. Bergsagel PL, Mateos MV, Gutierrez NC, Rajkumar SV, San Miguel JF. Improving overall survival and overcoming adverse prognosis in the treatment of cytogenetically high-risk multiple myeloma. Blood [Internet]. 2013;121(6):884–92. Available from: https://doi.org/10.1182/blood-2012-05-432203

13. Nandakumar B, Binder M, Dispenzieri A, Kapoor P, Buadi F, Gertz MA, et al. Continued improvement in survival in multiple myeloma (MM) including high-risk patients. Journal of Clinical Oncology [Internet]. 2019;37(15_suppl):8039. Available from: https://doi.org/10.1200/JCO.2019.37.15_suppl.8039

14. Morgan GJ, Walker BA, Davies FE. The genetic architecture of multiple myeloma. Nat Rev Cancer [Internet]. 2012;12(5):335–48. Available from: https://doi.org/10.1038/nrc3257

15. González D, van der Burg M, García-Sanz R, Fenton JA, Langerak AW, González M, et al. Immunoglobulin gene rearrangements and the pathogenesis of multiple myeloma. Blood [Internet]. 2007;110(9):3112–21. Available from: https://doi.org/10.1182/blood-2007-02-069625

16. Radbruch A, Muehlinghaus G, Luger EO, Inamine A, Smith KGC, Dörner T, et al. Competence and competition: the challenge of becoming a long-lived plasma cell. Nat Rev Immunol [Internet]. 2006;6(10):741–50. Available from: https://doi.org/10.1038/nri1886

17. Tonegawa S. Somatic generation of antibody diversity. Nature [Internet]. 1983;302(5909):575–81. Available from: https://doi.org/10.1038/302575a0

18. Chesi M, Bergsagel PL. Molecular pathogenesis of multiple myeloma: basic and clinical updates. Int J Hematol [Internet]. 2013;97(3):313–23. Available from: https://doi.org/10.1007/s12185-013-1291-2

19. Bladé J, Rosiñol L, Cibeira MT, de Larrea CF. Pathogenesis and progression of monoclonal gammopathy of undetermined significance. Leukemia [Internet]. 2008 Sep 31;22(9):1651–7. Available from: https://www.nature.com/articles/leu2008203

20. Kumar SK, Rajkumar SV. The multiple myelomas — current concepts in cytogenetic classification and therapy. Nat Rev Clin Oncol [Internet]. 2018;15(7):409–21. Available from: https://doi.org/10.1038/s41571-018-0018-y

21. P. Leif B, Marta C, Elena N, Leslie A. B, Suzanne L. K, W. Michael K. Promiscuous translocations into immunoglobulin heavy chain switch regions in multiple myeloma. Proceedings of the National Academy of Sciences [Internet]. 1996;93(24):13931–6. Available from: https://doi.org/10.1073/pnas.93.24.13931

22. Bergsagel PL, Kuehl WM, Zhan F, Sawyer J, Barlogie B, Shaughnessy Jr J. Cyclin D dysregulation: an early and unifying pathogenic event in multiple myeloma. Blood [Internet]. 2005;106(1):296–303. Available from: https://doi.org/10.1182/blood-2005-01-0034

23. Merlini G, Dispenzieri A, Sanchorawala V, Schönland SO, Palladini G, Hawkins PN, et al. Systemic immunoglobulin light chain amyloidosis. Nat Rev Dis Primers [Internet]. 2018;4(1):38. Available from: https://doi.org/10.1038/s41572-018-0034-3

24. Jares P, Colomer D, Campo E. Genetic and molecular pathogenesis of mantle cell lymphoma: perspectives for new targeted therapeutics. Nat Rev Cancer [Internet]. 2007;7(10):750–62. Available from: https://doi.org/10.1038/nrc2230

25. Roccaro AM, Ghobrial IM. Plasma Cell Dyscrasias. Roccaro AM, Ghobrial IM, editors. Vol. 169. Cham: Springer International Publishing; 2016.

26. Durie BG, Goldschmidt H, Mateos MV, Gonzalez V, Du J, Kim K, et al. Outcomes of patients with t(11;14) multiple myeloma: An International Myeloma Working Group (IMWG) multicenter study. Journal of Clinical Oncology [Internet]. 2019;37(15_suppl):8015. Available from: https://doi.org/10.1200/JCO.2019.37.15_suppl.8015

27. Kaufman JL, Gasparetto C, Schjesvold FH, Moreau P, Touzeau C, Facon T, et al. Phase I/II Study Evaluating the Safety and Efficacy of Venetoclax in Combination with Dexamethasone As Targeted Therapy for Patients with t(11;14) Relapsed/Refractory Multiple Myeloma. Blood [Internet]. 2019 Nov 13;134(Supplement_1):926. Available from: https://doi.org/10.1182/blood-2019-125871

28. Fonseca R, Barlogie B, Bataille R, Bastard C, Bergsagel PL, Chesi M, et al. Genetics and Cytogenetics of Multiple Myeloma: A Workshop Report. Cancer Res [Internet]. 2004;64(4):1546–58. Available from: https://doi.org/10.1158/0008-5472.CAN-03-2876

29. Martinez-Garcia E, Popovic R, Min DJ, Sweet SMM, Thomas PM, Zamdborg L, et al. The MMSET histone methyl transferase switches global histone methylation and alters gene expression in t(4;14) multiple myeloma cells. Blood [Internet]. 2011 Jan 6;117(1):211–20. Available from: https://doi.org/10.1182/blood-2010-07-298349

30. Palumbo A, Avet-Loiseau H, Oliva S, Lokhorst HM, Goldschmidt H, Rosinol L, et al. Revised International Staging System for Multiple Myeloma: A Report From International Myeloma Working Group. Journal of Clinical Oncology [Internet]. 2015 Aug 3;33(26):2863–9. Available from: www.r-project.org

31. Avet-Loiseau H, Moreau P, Mathiot C, Charbonnel C, Facon T, Attal M, et al. Use of bortezomib to overcome the poor prognosis of t(4;14), but not del(17p), in young patients with newly diagnosed multiple myeloma. Journal of Clinical Oncology [Internet]. 2010 May 20;28(15_suppl):8113. Available from: https://doi.org/10.1200/jco.2010.28.15_suppl.8113

32. Chretien ML, Corre J, Lauwers-Cances V, Magrangeas F, Cleynen A, Yon E, et al. Understanding the role of hyperdiploidy in myeloma prognosis: which trisomies really matter? Blood [Internet]. 2015 Dec 17;126(25):2713–9. Available from: https://doi.org/10.1182/blood-2015-06-650242

33. Hurt EM, Wiestner A, Rosenwald A, Shaffer AL, Campo E, Grogan T, et al. Overexpression of c-maf is a frequent oncogenic event in multiple myeloma that promotes proliferation and pathological interactions with bone marrow stroma. Cancer Cell [Internet]. 2004;5(2):191–9. Available from: https://www.sciencedirect.com/science/article/pii/S1535610804000194

34. Zhan F, Huang Y, Colla S, Stewart JP, Hanamura I, Gupta S, et al. The molecular classification of multiple myeloma. Blood [Internet]. 2006 Sep 15;108(6):2020–8. Available from: https://doi.org/10.1182/blood-2005-11-013458

35. Rebhandl S, Huemer M, Greil R, Geisberger R. AID/APOBEC deaminases and cancer. Oncoscience [Internet]. 2015 Apr 28;2(4):320–33. Available from: https://www.oncoscience.us/lookup/doi/10.18632/oncoscience.155

36. Walker BA, Wardell CP, Murison A, Boyle EM, Begum DB, Dahir NM, et al. APOBEC family mutational signatures are associated with poor prognosis translocations in multiple myeloma. Nat Commun [Internet]. 2015;6(1):6997. Available from: https://doi.org/10.1038/ncomms7997

37. Smadja NV, Fruchart C, Isnard F, Louvet C, Dutel JL, Cheron N, et al. Chromosomal analysis in multiple myeloma: cytogenetic evidence of two different diseases. Leukemia [Internet]. 1998;12(6):960–9. Available from: https://doi.org/10.1038/sj.leu.2401041

38. Perrot A, Lauwers-Cances V, Tournay E, Hulin C, Chretien ML, Royer B, et al. Development and Validation of a Cytogenetic Prognostic Index Predicting Survival in Multiple Myeloma. Journal of Clinical Oncology [Internet]. 2019 May 15;37(19):1657–65. Available from: https://doi.org/10.1200/JCO.18.00776

39. Kuehl WM, Bergsagel PL. Early Genetic Events Provide the Basis for a Clinical Classification of Multiple Myeloma. Hematology [Internet]. 2005 Jan 1;2005(1):346–52. Available from: https://doi.org/10.1182/asheducation-2005.1.346

40. Rio-Machin A, Ferreira BI, Henry T, Gómez-López G, Agirre X, Alvarez S, et al. Downregulation of specific miRNAs in hyperdiploid multiple myeloma mimics the oncogenic effect of IgH translocations occurring in the non-hyperdiploid subtype. Leukemia [Internet]. 2013;27(4):925–31. Available from: https://doi.org/10.1038/leu.2012.302

41. Pawlyn C, Morgan GJ. Evolutionary biology of high-risk multiple myeloma. Nat Rev Cancer [Internet]. 2017 Sep 24;17(9):543–56. Available from: https://www.nature.com/articles/nrc.2017.63

42. Kaufmann H, Ackermann J, Baldia C, Nösslinger T, Wieser R, Seidl S, et al. Both IGH translocations and chromosome 13q deletions are early events in monoclonal gammopathy of undetermined significance and do not evolve during transition to multiple myeloma. Leukemia [Internet]. 2004;18(11):1879–82. Available from: https://doi.org/10.1038/sj.leu.2403518

43. Walker BA, Leone PE, Chiecchio L, Dickens NJ, Jenner MW, Boyd KD, et al. A compendium of myeloma-associated chromosomal copy number abnormalities and their prognostic value. Blood [Internet]. 2010 Oct 14;116(15):e56–65. Available from: https://doi.org/10.1182/blood-2010-04-279596

44. Shaughnessy J. Amplification and overexpression of CKS1B at chromosome band 1q21 is associated with reduced levels of p27 Kip1 and an aggressive clinical course in multiple myeloma. Hematology [Internet]. 2005 Sep 1;10(sup1):117–26. Available from: https://doi.org/10.1080/10245330512331390140

45. Zhan F, Colla S, Wu X, Chen B, Stewart JP, Kuehl WM, et al. CKS1B, overexpressed in aggressive disease, regulates multiple myeloma growth and survival through SKP2- and p27Kip1-dependent and -independent mechanisms. Blood [Internet]. 2007 Jun

1;109(11):4995–5001. Available from: https://doi.org/10.1182/blood-2006-07-038703

46. Shi L, S W, M Z, H X, TM C, C X, et al. Over-expression of CKS1B activates both MEK/ERK and JAK/STAT3 signaling pathways and promotes myeloma cell drug-resistance. Oncotarget. 2010;1(1).

47. van Andel H, Kocemba KA, Spaargaren M, Pals ST. Aberrant Wnt signaling in multiple myeloma: molecular mechanisms and targeting options. Leukemia [Internet]. 2019;33(5):1063–75. Available from: https://doi.org/10.1038/s41375-019-0404-1

48. Inoue J, Otsuki T, Hirasawa A, Imoto I, Matsuo Y, Shimizu S, et al. Overexpression of PDZK1 within the 1q12-q22 amplicon is likely to be associated with drug-resistance phenotype in multiple myeloma Title. American Journal of Pathology. 2004;July(165):71–81.

49. Zhang B, Gojo I, Fenton RG. Myeloid cell factor–1 is a critical survival factor for multiple myeloma. Blood [Internet]. 2002 Mar 15;99(6):1885–93. Available from: https://doi.org/10.1182/blood.V99.6.1885

50. Slomp A, Moesbergen LM, Gong J nan, Cuenca M, Von Dem Borne PA, Sonneveld P, et al. Multiple myeloma with 1q21 amplification is highly sensitive to MCL-1 targeting. Blood Adv [Internet]. 2019 Dec 23;3(24):4202–14. Available from: https://ashpublications.org/bloodadvances/article/3/24/4202/429970/Multiple-myeloma-with-1q21-amplification-is-highly

51. D'agostino M, Cairns DA, José Lahuerta J, Wester R, Bertsch U, Waage A, et al. Second Revision of the International Staging System (R2-ISS) for Overall Survival in Multiple Myeloma: A European Myeloma Network (EMN) Report Within the HARMONY Project [Internet]. J Clin Oncol. 2022. Available from: https://doi.org/10.

52. Boyd KD, Ross FM, Walker BA, Wardell CP, Tapper WJ, Chiecchio L, et al. Mapping of Chromosome 1p Deletions in Myeloma Identifies FAM46C at 1p12 and CDKN2C at 1p32.3 as Being Genes in Regions Associated with Adverse Survival. Clinical Cancer Research [Internet]. 2011 Dec 18;17(24):7776–84. Available from: https://doi.org/10.1158/1078-0432.CCR-11-1791

53. Menges CW, Altomare DA, Testa JR. FAS-Associated Factor 1 (FAF1): Diverse functions and implications for oncogenesis. Cell Cycle [Internet]. 2009 Aug 15;8(16):2528–34. Available from: https://doi.org/10.4161/cc.8.16.9280

54. Perrot A, Corre J, Avet-Loiseau H. Risk Stratification and Targets in Multiple Myeloma: From Genomics to the Bedside. American Society of Clinical Oncology Educational Book [Internet]. 2018 May;(38):675–80. Available from: https://ascopubs.org/doi/10.1200/EDBK_200879

55. Mroczek S, Chlebowska J, Kuliński TM, Gewartowska O, Gruchota J, Cysewski D, et al. The non-canonical poly(A) polymerase FAM46C acts as an onco-suppressor in multiple myeloma. Nat Commun [Internet]. 2017;8(1):619. Available from: https://doi.org/10.1038/s41467-017-00578-5

56. Leone PE, Walker BA, Jenner MW, Chiecchio L, Dagrada G, Protheroe RKM, et al. Deletions of CDKN2C in Multiple Myeloma: Biological and Clinical Implications.

Clinical Cancer Research [Internet]. 2008 Oct 1;14(19):6033–41. Available from: https://aacrjournals.org/clincancerres/article/14/19/6033/73040/Deletions-of-CDKN2C-in-Multiple-Myeloma-Biological

57. Avet-Loiseau H, Attal M, Moreau P, Charbonnel C, Garban F, Hulin C, et al. Genetic abnormalities and survival in multiple myeloma: the experience of the Intergroupe Francophone du Myélome. Blood [Internet]. 2007 Jan 5;109(8):3489–95. Available from: https://doi.org/10.1182/blood-2006-08-040410

58. Fonseca R, Blood E, Rue M, Harrington D, Oken MM, Kyle RA, et al. Clinical and biologic implications of recurrent genomic aberrations in myeloma. Blood [Internet]. 2003 Jun 1;101(11):4569–75. Available from: https://doi.org/10.1182/blood-2002-10-3017

59. Lode L, Eveillard M, Trichet V, Soussi T, Wuilleme S, Richebourg S, et al. Mutations in TP53 are exclusively associated with del(17p) in multiple myeloma. Haematologica [Internet]. 2010 Nov 1;95(11):1973–6. Available from: http://www.haematologica.org/cgi/doi/10.3324/haematol.2010.023697

60. Avet-Loiseau H, Gerson F, Magrangeas F, Minvielle S, Harousseau JL, Bataille R. Rearrangements of the c-myc oncogene are present in 15% of primary human multiple myeloma tumors. Blood [Internet]. 2001 Nov 15;98(10):3082–6. Available from: https://ashpublications.org/blood/article/98/10/3082/52990/Rearrangements-of-the-cmyc-oncogene-are-present-in

61. Bergsagel PL, Kuehl WM. Chromosome translocations in multiple myeloma. Oncogene [Internet]. 2001;20(40):5611–22. Available from: https://doi.org/10.1038/sj.onc.1204641

62. Hirano T, Ishihara K, Hibi M. Roles of STAT3 in mediating the cell growth, differentiation and survival signals relayed through the IL-6 family of cytokine receptors. Oncogene [Internet]. 2000;19(21):2548–56. Available from: https://doi.org/10.1038/sj.onc.1203551

63. Chappell SA, LeQuesne JPC, Paulin FEM, deSchoolmeester ML, Stoneley M, Soutar RL, et al. A mutation in the c-myc-IRES leads to enhanced internal ribosome entry in multiple myeloma: A novel mechanism of oncogene de-regulation. Oncogene [Internet]. 2000;19(38):4437–40. Available from: https://doi.org/10.1038/sj.onc.1203791

64. Shi Y, Frost PJ, Hoang BQ, Benavides A, Sharma S, Gera JF, et al. IL-6–Induced Stimulation of c- Myc Translation in Multiple Myeloma Cells Is Mediated by Myc Internal Ribosome Entry Site Function and the RNA-Binding Protein, hnRNP A1. Cancer Res [Internet]. 2008 Dec 15;68(24):10215–22. Available from: https://doi.org/10.1158/0008-5472.CAN-08-1066

65. Shi Y, Yang Y, Hoang B, Bardeleben C, Holmes B, Gera J, et al. Therapeutic potential of targeting IRES-dependent c-myc translation in multiple myeloma cells during ER stress. Oncogene [Internet]. 2016;35(8):1015–24. Available from: https://doi.org/10.1038/onc.2015.156

66. Walker BA, Boyle EM, Wardell CP, Murison A, Begum DB, Dahir NM, et al. Mutational Spectrum, Copy Number Changes, and Outcome: Results of a Sequencing Study of Patients With Newly Diagnosed Myeloma. Journal of Clinical Oncology [Internet]. 2015 Nov 20;33(33):3911–20. Available from: https://ascopubs.org/doi/10.1200/JCO.2014.59.1503

67. Hideshima T, Akiyama M, Hayashi T, Richardson P, Schlossman R, Chauhan D, et al. Targeting p38 MAPK inhibits multiple myeloma cell growth in the bone marrow milieu. Blood [Internet]. 2003 Jan 15;101(2):703–5. Available from: https://doi.org/10.1182/blood-2002-06-1874

68. Bolli N, Avet-Loiseau H, Wedge DC, Van Loo P, Alexandrov LB, Martincorena I, et al. Heterogeneity of genomic evolution and mutational profiles in multiple myeloma. Nat Commun [Internet]. 2014;5(1):2997. Available from: https://doi.org/10.1038/ncomms3997

69. Walker BA, Mavrommatis K, Wardell CP, Ashby TC, Bauer M, Davies FE, et al. Identification of novel mutational drivers reveals oncogene dependencies in multiple myeloma. Blood [Internet]. 2018 Aug 9;132(6):587–97. Available from: https://ashpublications.org/blood/article/132/6/587/39419/Identification-of-novel-mutational-drivers-reveals

70. Robinson S, Oliver A, Chevassut T, Newbury S. The 3' to 5' Exoribonuclease DIS3: From Structure and Mechanisms to Biological Functions and Role in Human Disease. Biomolecules [Internet]. 2015 Jul 17;5(3):1515–39. Available from: http://www.mdpi.com/2218-273X/5/3/1515

71. Todoerti K, Ronchetti D, Favasuli V, Maura F, Morabito F, Bolli N, et al. DIS3 mutations in multiple myeloma impact the transcriptional signature and clinical outcome. Haematologica [Internet]. 2021 May 6;107(4 SE-Articles):921–32. Available from: https://haematologica.org/article/view/haematol.2021.278342

72. Annunziata CM, Davis RE, Demchenko Y, Bellamy W, Gabrea A, Zhan F, et al. Frequent Engagement of the Classical and Alternative NF-κB Pathways by Diverse Genetic Abnormalities in Multiple Myeloma. Cancer Cell [Internet]. 2007 Aug;12(2):115–30. Available from: https://linkinghub.elsevier.com/retrieve/pii/S1535610807002036

73. Eckhert E, Hewitt R, Liedtke M. B-cell maturation antigen directed monoclonal antibody therapies for multiple myeloma. Immunotherapy [Internet]. 2019 May 16;11(9):801–11. Available from: https://doi.org/10.2217/imt-2018-0199

74. O'Connor BP, Raman VS, Erickson LD, Cook WJ, Weaver LK, Ahonen C, et al. BCMA Is Essential for the Survival of Long-lived Bone Marrow Plasma Cells . Journal of Experimental Medicine [Internet]. 2004 Jan 5;199(1):91–8. Available from: https://doi.org/10.1084/jem.20031330

75. Roos WP, Thomas AD, Kaina B. DNA damage and the balance between survival and death in cancer biology. Nat Rev Cancer [Internet]. 2016;16(1):20–33. Available from: https://doi.org/10.1038/nrc.2015.2

76. Herrero A, Rojas E, Misiewicz-Krzeminska I, Krzeminski P, Gutiérrez N. Molecular Mechanisms of p53 Deregulation in Cancer: An Overview in Multiple Myeloma. Int J

Mol Sci [Internet]. 2016 Nov 30;17(12):2003. Available from: http://www.mdpi.com/1422-0067/17/12/2003

77. Keller AD, Maniatis T. Identification and characterization of a novel repressor of beta-interferon gene expression. Genes Dev [Internet]. 1991 May;5(5):868–79. Available from: http://genesdev.cshlp.org/lookup/doi/10.1101/gad.5.5.868

78. Lin FR, Kuo HK, Ying HY, Yang FH, Lin KI. Induction of Apoptosis in Plasma Cells by B Lymphocyte–Induced Maturation Protein-1 Knockdown. Cancer Res [Internet]. 2007 Dec 18;67(24):11914–23. Available from: https://doi.org/10.1158/0008-5472.CAN-07-1868

79. Shaffer AL, Emre NCT, Lamy L, Ngo VN, Wright G, Xiao W, et al. IRF4 addiction in multiple myeloma. Nature [Internet]. 2008;454(7201):226–31. Available from: https://doi.org/10.1038/nature07064

80. Fink EC, Ebert BL. The novel mechanism of lenalidomide activity. Blood [Internet]. 2015 Nov 19;126(21):2366–9. Available from: https://doi.org/10.1182/blood-2015-07-567958

81. Jackson GH, Davies FE, Pawlyn C, Cairns DA, Striha A, Collett C, et al. Lenalidomide maintenance versus observation for patients with newly diagnosed multiple myeloma (Myeloma XI): a multicentre, open-label, randomised, phase 3 trial. Lancet Oncol [Internet]. 2019;20(1):57–73. Available from: https://www.sciencedirect.com/science/article/pii/S1470204518306879

82. Jenner MW, Pawlyn C, Davies FE, Menzies T, Hockaday A, Olivier C, et al. The addition of vorinostat to lenalidomide maintenance for patients with newly diagnosed multiple myeloma of all ages: results from ‘Myeloma <scp>XI’</scp> , a multicentre, open-label, randomised, phase III trial. Br J Haematol. 2023 Apr 21;201(2):267–79.

83. NICE TA[380]. Panobinostat for treating multiple myeloma after at least 2 previous treatments [Internet]. 2016 [cited 2022 Jul 23]. Available from: https://www.nice.org.uk/guidance/ta380

84. Walker BA, Wardell CP, Chiecchio L, Smith EM, Boyd KD, Neri A, et al. Aberrant global methylation patterns affect the molecular pathogenesis and prognosis of multiple myeloma. Blood [Internet]. 2011;117(2):553–62. Available from: https://www.sciencedirect.com/science/article/pii/S0006497120592033

85. Cyster JG. Homing of antibody secreting cells. Immunol Rev [Internet]. 2003 Aug 1;194(1):48–60. Available from: https://doi.org/10.1034/j.1600-065X.2003.00041.x

86. Kumar SK, Rajkumar V, Kyle RA, van Duin M, Sonneveld P, Mateos MV, et al. Multiple myeloma. Nat Rev Dis Primers [Internet]. 2017;3(1):17046. Available from: https://doi.org/10.1038/nrdp.2017.46

87. Ribatti D, Nico B, Vacca A. Importance of the bone marrow microenvironment in inducing the angiogenic response in multiple myeloma. Oncogene [Internet]. 2006;25(31):4257–66. Available from: https://doi.org/10.1038/sj.onc.1209456

88. Roodman GD. Pathogenesis of myeloma bone disease. Leukemia [Internet]. 2009;23(3):435–41. Available from: https://doi.org/10.1038/leu.2008.336

89. Zeman MK, Cimprich KA. Causes and consequences of replication stress. Nat Cell Biol [Internet]. 2014 Jan 24;16(1):2–9. Available from: http://www.nature.com/articles/ncb2897

90. Chatterjee N, Walker GC. Mechanisms of DNA damage, repair, and mutagenesis. Environ Mol Mutagen [Internet]. 2017 Jun;58(5):235–63. Available from: https://onlinelibrary.wiley.com/doi/10.1002/em.22087

91. Lips J, Kaina B. DNA double-strand breaks trigger apoptosis in p53-deficient fibroblasts. Carcinogenesis [Internet]. 2001 Apr;22(4):579–85. Available from: https://academic.oup.com/carcin/article-lookup/doi/10.1093/carcin/22.4.579

92. Shiloh Y, Ziv Y. The ATM protein kinase: regulating the cellular response to genotoxic stress, and more. Nat Rev Mol Cell Biol [Internet]. 2013 Apr 13;14(4):197–210. Available from: http://www.nature.com/articles/nrm3546

93. Mazouzi A, Velimezi G, Loizou JI. DNA replication stress: Causes, resolution and disease. Exp Cell Res [Internet]. 2014;329(1):85–93. Available from: https://www.sciencedirect.com/science/article/pii/S0014482714004352

94. Paull TT, Rogakou EP, Yamazaki V, Kirchgessner CU, Gellert M, Bonner WM. A critical role for histone H2AX in recruitment of repair factors to nuclear foci after DNA damage. Current Biology [Internet]. 2000 Aug;10(15):886–95. Available from: https://linkinghub.elsevier.com/retrieve/pii/S0960982200006102

95. Rogakou EP, Pilch DR, Orr AH, Ivanova VS, Bonner WM. DNA Double-stranded Breaks Induce Histone H2AX Phosphorylation on Serine 139. Journal of Biological Chemistry [Internet]. 1998 Mar;273(10):5858–68. Available from: https://linkinghub.elsevier.com/retrieve/pii/S0021925818678512

96. Bee L, Fabris S, Cherubini R, Mognato M, Celotti L. The Efficiency of Homologous Recombination and Non-Homologous End Joining Systems in Repairing Double-Strand Breaks during Cell Cycle Progression. Cotterill S, editor. PLoS One [Internet]. 2013 Jul 11;8(7):e69061. Available from: https://dx.plos.org/10.1371/journal.pone.0069061

97. Branzei D, Foiani M. Regulation of DNA repair throughout the cell cycle. Nat Rev Mol Cell Biol [Internet]. 2008 Apr 20;9(4):297–308. Available from: http://www.nature.com/articles/nrm2351

98. Herrero AB, San Miguel J, Gutierrez NC. Deregulation of DNA Double-Strand Break Repair in Multiple Myeloma: Implications for Genome Stability. Ricchetti M, editor. PLoS One [Internet]. 2015 Mar 19;10(3):e0121581. Available from: https://dx.plos.org/10.1371/journal.pone.0121581

99. Herrero AB, Gutiérrez NC. Targeting Ongoing DNA Damage in Multiple Myeloma: Effects of DNA Damage Response Inhibitors on Plasma Cell Survival. Front Oncol [Internet]. 2017 May 19;7. Available from: http://journal.frontiersin.org/article/10.3389/fonc.2017.00098/full

100. Shammas MA, Shmookler Reis RJ, Koley H, Batchu RB, Li C, Munshi NC. Dysfunctional homologous recombination mediates genomic instability and progression in myeloma. Blood [Internet]. 2009 Mar 5;113(10):2290–7. Available from: https://doi.org/10.1182/blood-2007-05-089193

101. Gourzones-Dmitriev C, Kassambara A, Sahota S, Rème T, Moreaux J, Bourquard P, et al. DNA repair pathways in human multiple myeloma. Cell Cycle [Internet]. 2013 Sep 28;12(17):2760–73. Available from: http://www.tandfonline.com/doi/abs/10.4161/cc.25951

102. Gkotzamanidou M, Terpos E, Bamia C, Munshi NC, Dimopoulos MA, Souliotis VL. DNA repair of myeloma plasma cells correlates with clinical outcome: the effect of the nonhomologous end-joining inhibitor SCR7. Blood [Internet]. 2016 Sep 1;128(9):1214–25. Available from: https://ashpublications.org/blood/article/128/9/1214/35794/DNA-repair-of-myeloma-plasma-cells-correlates-with

103. Gkotzamanidou M, Sfikakis PP, Kyrtopoulos SA, Bamia C, Dimopoulos MA, Souliotis VL. Chromatin structure, transcriptional activity and DNA repair efficiency affect the outcome of chemotherapy in multiple myeloma. Br J Cancer [Internet]. 2014 Sep 22;111(7):1293–304. Available from: http://www.nature.com/articles/bjc2014410

104. Pontano LL, Aggarwal P, Barbash O, Brown EJ, Bassing CH, Diehl JA. Genotoxic Stress-Induced Cyclin D1 Phosphorylation and Proteolysis Are Required for Genomic Stability. Mol Cell Biol [Internet]. 2008 Dec;28(23):7245–58. Available from: https://journals.asm.org/doi/10.1128/MCB.01085-08

105. Jirawatnotai S, Hu Y, Livingston DM, Sicinski P. Proteomic Identification of a Direct Role for Cyclin D1 in DNA Damage Repair. Cancer Res [Internet]. 2012 Sep 1;72(17):4289–93. Available from: https://aacrjournals.org/cancerres/article/72/17/4289/575960/Proteomic-Identification-of-a-Direct-Role-for

106. Shimura T, Kakuda S, Ochiai Y, Nakagawa H, Kuwahara Y, Takai Y, et al. Acquired radioresistance of human tumor cells by DNA-PK/AKT/GSK3β-mediated cyclin D1 overexpression. Oncogene [Internet]. 2010;29(34):4826–37. Available from: https://doi.org/10.1038/onc.2010.238

107. Milas L, Akimoto T, Hunter NR, Mason KA, Buchmiller L, Yamakawa M, et al. Relationship between cyclin D1 expression and poor radioresponse of murine carcinomas. International Journal of Radiation Oncology*Biology*Physics [Internet]. 2002 Feb;52(2):514–21. Available from: https://linkinghub.elsevier.com/retrieve/pii/S0360301601026931

108. Smith D, Mann D, Yong K. Cyclin D type does not influence cell cycle response to DNA damage caused by ionizing radiation in multiple myeloma tumours. Br J Haematol [Internet]. 2016 Jun 1;173(5):693–704. Available from: https://doi.org/10.1111/bjh.13982

109. Beltran E, Fresquet V, Martinez-Useros J, Richter-Larrea JA, Sagardoy A, Sesma I, et al. A cyclin-D1 interaction with BAX underlies its oncogenic role and potential as a therapeutic target in mantle cell lymphoma. Proceedings of the National Academy of Sciences [Internet]. 2011 Jul 26;108(30):12461–6. Available from: https://pnas.org/doi/full/10.1073/pnas.1018941108

110. Strasser A, Cory S, Adams JM. Deciphering the rules of programmed cell death to improve therapy of cancer and other diseases. EMBO J [Internet]. 2011 Sep

14;30(18):3667–83. Available from: http://emboj.embopress.org/cgi/doi/10.1038/emboj.2011.307

111. Souers AJ, Leverson JD, Boghaert ER, Ackler SL, Catron ND, Chen J, et al. ABT-199, a potent and selective BCL-2 inhibitor, achieves antitumor activity while sparing platelets. Nat Med [Internet]. 2013;19(2):202–8. Available from: https://doi.org/10.1038/nm.3048

112. Touzeau C, Dousset C, Le Gouill S, Sampath D, Leverson JD, Souers AJ, et al. The Bcl-2 specific BH3 mimetic ABT-199: a promising targeted therapy for t(11;14) multiple myeloma. Leukemia [Internet]. 2014 Jan 17;28(1):210–2. Available from: http://www.nature.com/articles/leu2013216

113. Touzeau C, Ryan J, Guerriero J, Moreau P, Chonghaile TN, Le Gouill S, et al. BH3 profiling identifies heterogeneous dependency on Bcl-2 family members in multiple myeloma and predicts sensitivity to BH3 mimetics. Leukemia [Internet]. 2016 Mar 15;30(3):761–4. Available from: https://www.nature.com/articles/leu2015184

114. Matulis SM, Gupta VA, Nooka AK, Hollen H V, Kaufman JL, Lonial S, et al. Dexamethasone treatment promotes Bcl-2 dependence in multiple myeloma resulting in sensitivity to venetoclax. Leukemia [Internet]. 2016 May 28;30(5):1086–93. Available from: https://www.nature.com/articles/leu2015350

115. Gong JN, Khong T, Segal D, Yao Y, Riffkin CD, Garnier JM, et al. Hierarchy for targeting prosurvival BCL2 family proteins in multiple myeloma: pivotal role of MCL1. Blood [Internet]. 2016 Oct 6;128(14):1834–44. Available from: https://ashpublications.org/blood/article/128/14/1834/35661/Hierarchy-for-targeting-prosurvival-BCL2-family

116. Kumar SK, Harrison SJ, Cavo M, de la Rubia J, Popat R, Gasparetto C, et al. Venetoclax or placebo in combination with bortezomib and dexamethasone in patients with relapsed or refractory multiple myeloma (BELLINI): a randomised, double-blind, multicentre, phase 3 trial. Lancet Oncol [Internet]. 2020 Dec;21(12):1630–42. Available from: https://linkinghub.elsevier.com/retrieve/pii/S1470204520305258

117. Ghobrial I. BELLINI: a renaissance for an era of precision therapy in multiple myeloma. Lancet Oncol [Internet]. 2020;21(12):1547–9. Available from: https://www.sciencedirect.com/science/article/pii/S1470204520305878

118. Sive J, Cuthill K, Hunter H, Kazmi M, Pratt G, Smith D, et al. Guidelines on the diagnosis, investigation and initial treatment of myeloma: a British Society for Haematology/UK Myeloma Forum Guideline. Br J Haematol [Internet]. 2021 Apr 1;193(2):245–68. Available from: https://doi.org/10.1111/bjh.17410

119. Kyle RA, Larson DR, Therneau TM, Dispenzieri A, Kumar S, Cerhan JR, et al. Long-Term Follow-up of Monoclonal Gammopathy of Undetermined Significance. New England Journal of Medicine [Internet]. 2018 Jan 18;378(3):241–9. Available from: http://www.nejm.org/doi/10.1056/NEJMoa1709974

120. Kyle RA, Vincent Rajkumar S. Monoclonal gammopathy of undetermined significance. Br J Haematol [Internet]. 2006 Sep;134(6):573–89. Available from: https://onlinelibrary.wiley.com/doi/10.1111/j.1365-2141.2006.06235.x

121. Leung N, Bridoux F, Hutchison CA, Nasr SH, Cockwell P, Fermand JP, et al. Monoclonal gammopathy of renal significance: when MGUS is no longer undetermined or insignificant. Blood [Internet]. 2012 Nov 22;120(22):4292–5. Available from: https://ashpublications.org/blood/article/120/22/4292/73069/Monoclonal-gammopathy-of-renal-significance-when

122. Fermand JP, Bridoux F, Dispenzieri A, Jaccard A, Kyle RA, Leung N, et al. Monoclonal gammopathy of clinical significance: a novel concept with therapeutic implications. Blood [Internet]. 2018 Oct 4;132(14):1478–85. Available from: https://ashpublications.org/blood/article/132/14/1478/39337/Monoclonal-gammopathy-of-clinical-significance-a

123. Bird J, Behrens J, Westin J, Turesson I, Drayson M, Beetham R, et al. UK Myeloma Forum (UKMF) and Nordic Myeloma Study Group (NMSG): guidelines for the investigation of newly detected M-proteins and the management of monoclonal gammopathy of undetermined significance (MGUS). Br J Haematol [Internet]. 2009 Oct 1;147(1):22–42. Available from: https://doi.org/10.1111/j.1365-2141.2009.07807.x

124. Rajkumar SV. Updated Diagnostic Criteria and Staging System for Multiple Myeloma. American Society of Clinical Oncology Educational Book [Internet]. 2016 May 1;(36):e418–23. Available from: https://doi.org/10.1200/EDBK_159009

125. Leach M, Drummond M, Doig A. Practical Flow Cytometry in Haematology Diagnosis [Internet]. Oxford: John Wiley & Sons; 2013. Available from: http://doi.wiley.com/10.1002/9781118487969

126. Bladé J, Cibeira MT, Rosiñol L. Bortezomib: A valuable new antineoplastic strategy in multiple myeloma. Acta Oncol (Madr) [Internet]. 2005 Jan 1;44(5):440–8. Available from: https://doi.org/10.1080/02841860510030002

127. Ito S. Proteasome Inhibitors for the Treatment of Multiple Myeloma. Cancers (Basel) [Internet]. 2020 Jan 22;12(2):265. Available from: https://www.mdpi.com/2072-6694/12/2/265

128. Boccadoro M, Morgan G, Cavenagh J. Preclinical evaluation of the proteasome inhibitor bortezomib in cancer therapy. Cancer Cell Int [Internet]. 2005 Dec 1;5(1):18. Available from: https://cancerci.biomedcentral.com/articles/10.1186/1475-2867-5-18

129. Obeng EA, Carlson LM, Gutman DM, Harrington WJ, Lee KP, Boise LH. Proteasome inhibitors induce a terminal unfolded protein response in multiple myeloma cells. Blood [Internet]. 2006 Jun 15;107(12):4907–16. Available from: https://ashpublications.org/blood/article/107/12/4907/129315/Proteasome-inhibitors-induce-a-terminal-unfolded

130. Dimopoulos MA, Moreau P, Terpos E, Mateos MV, Zweegman S, Cook G, et al. Multiple myeloma: EHA-ESMO Clinical Practice Guidelines for diagnosis, treatment and follow-up†. Annals of Oncology [Internet]. 2021 Mar;32(3):309–22. Available from: https://linkinghub.elsevier.com/retrieve/pii/S0923753420431692

131. Krönke J, Udeshi ND, Narla A, Grauman P, Hurst SN, McConkey M, et al. Lenalidomide Causes Selective Degradation of IKZF1 and IKZF3 in Multiple Myeloma Cells. Science (1979) [Internet]. 2014 Jan 17;343(6168):301–5. Available from: https://www.science.org/doi/10.1126/science.1244851

132. Quach H, Ritchie D, Stewart AK, Neeson P, Harrison S, Smyth MJ, et al. Mechanism of action of immunomodulatory drugs (IMiDS) in multiple myeloma. Leukemia [Internet]. 2010 Jan 12;24(1):22–32. Available from: https://www.nature.com/articles/leu2009236

133. Bjorklund CC, Kang J, Amatangelo M, Polonskaia A, Katz M, Chiu H, et al. Iberdomide (CC-220) is a potent cereblon E3 ligase modulator with antitumor and immunostimulatory activities in lenalidomide- and pomalidomide-resistant multiple myeloma cells with dysregulated CRBN. Leukemia [Internet]. 2020 Apr 12;34(4):1197–201. Available from: http://www.nature.com/articles/s41375-019-0620-8

134. ALEXANIAN R, BERGSAGEL DE, MIGLIORE PJ, VAUGHN WK, HOWE CD. Melphalan Therapy for Plasma Cell Myeloma. Blood [Internet]. 1968 Jan 1;31(1):1–10. Available from: https://doi.org/10.1182/blood.V31.1.1.1

135. Falco P, Bringhen S, Avonto I, Gay F, Morabito F, Boccadoro M, et al. Melphalan and its role in the management of patients with multiple myeloma. Expert Rev Anticancer Ther [Internet]. 2007 Jul 1;7(7):945–57. Available from: https://doi.org/10.1586/14737140.7.7.945

136. Schjesvold F, Oriol A. Current and Novel Alkylators in Multiple Myeloma. Cancers (Basel) [Internet]. 2021 May 18;13(10):2465. Available from: https://www.mdpi.com/2072-6694/13/10/2465

137. Lakshman A, Singh PP, Rajkumar SV, Dispenzieri A, Lacy MQ, Gertz MA, et al. Efficacy of VDT PACE-like regimens in treatment of relapsed/refractory multiple myeloma. Am J Hematol [Internet]. 2018 Feb;93(2):179–86. Available from: https://onlinelibrary.wiley.com/doi/10.1002/ajh.24954

138. Kikuchi J, Hori M, Iha H, Toyama-Sorimachi N, Hagiwara S, Kuroda Y, et al. Soluble SLAMF7 promotes the growth of myeloma cells via homophilic interaction with surface SLAMF7. Leukemia [Internet]. 2020 Jan 29;34(1):180–95. Available from: http://www.nature.com/articles/s41375-019-0525-6

139. Martin T, Usmani SZ, Berdeja JG, Agha M, Cohen AD, Hari P, et al. Ciltacabtagene Autoleucel, an Anti–B-cell Maturation Antigen Chimeric Antigen Receptor T-Cell Therapy, for Relapsed/Refractory Multiple Myeloma: CARTITUDE-1 2-Year Follow-Up. Journal of Clinical Oncology [Internet]. 2022 Jun 4;JCO.22.00842. Available from: https://doi.org/10.1200/JCO.22.00842

140. Lin Y, Martin TG, Usmani SZ, Berdeja JG, Jakubowiak AJ, Agha ME, et al. CARTITUDE-1 final results: Phase 1b/2 study of ciltacabtagene autoleucel in heavily pretreated patients with relapsed/refractory multiple myeloma. Journal of Clinical Oncology [Internet]. 2023 May 31;41(16_suppl):8009. Available from: https://doi.org/10.1200/JCO.2023.41.16_suppl.8009

141. Berdeja JG, Madduri D, Usmani SZ, Jakubowiak A, Agha M, Cohen AD, et al. Ciltacabtagene autoleucel, a B-cell maturation antigen-directed chimeric antigen receptor T-cell therapy in patients with relapsed or refractory multiple myeloma (CARTITUDE-1): a phase 1b/2 open-label study. The Lancet [Internet]. 2021;398(10297):314–24. Available from: https://www.sciencedirect.com/science/article/pii/S0140673621009338

142. San-Miguel J, Dhakal B, Yong K, Spencer A, Anguille S, Mateos MV, et al. Cilta-cel or Standard Care in Lenalidomide-Refractory Multiple Myeloma. New England Journal of Medicine [Internet]. 2023 Jun 5;389(4):335–47. Available from: https://doi.org/10.1056/NEJMoa2303379

143. Munshi NC, Anderson LD, Shah N, Madduri D, Berdeja J, Lonial S, et al. Idecabtagene Vicleucel in Relapsed and Refractory Multiple Myeloma. New England Journal of Medicine [Internet]. 2021 Feb 24;384(8):705–16. Available from: https://doi.org/10.1056/NEJMoa2024850

144. Rodriguez-Otero P, Ailawadhi S, Arnulf B, Patel K, Cavo M, Nooka AK, et al. Ide-cel or Standard Regimens in Relapsed and Refractory Multiple Myeloma. New England Journal of Medicine [Internet]. 2023 Feb 10;388(11):1002–14. Available from: https://doi.org/10.1056/NEJMoa2213614

145. Mailankody S, Devlin SM, Landa J, Nath K, Diamonte C, Carstens EJ, et al. GPRC5D-Targeted CAR T Cells for Myeloma. New England Journal of Medicine [Internet]. 2022 Sep 28;387(13):1196–206. Available from: https://doi.org/10.1056/NEJMoa2209900

146. Lonial S, Lee HC, Badros A, Trudel S, Nooka AK, Chari A, et al. Belantamab mafodotin for relapsed or refractory multiple myeloma (DREAMM-2): a two-arm, randomised, open-label, phase 2 study. Lancet Oncol [Internet]. 2020 Feb;21(2):207–21. Available from: https://linkinghub.elsevier.com/retrieve/pii/S1470204519307880

147. Usmani SZ, Terpos E, Janowski W, Quach H, West S, Williams D, et al. DREAMM-9: Phase III study of belantamab mafodotin plus VRd versus VRd alone in transplant-ineligible newly diagnosed multiple myeloma (TI NDMM). Journal of Clinical Oncology [Internet]. 2020 May 20;38(15_suppl):TPS8556–TPS8556. Available from: https://doi.org/10.1200/JCO.2020.38.15_suppl.TPS8556

148. Nooka AK, Cohen A, Lee HC, Badros AZ, Suvannasankha A, Callander N, et al. Single-Agent Belantamab Mafodotin in Patients with Relapsed or Refractory Multiple Myeloma: Final Analysis of the DREAMM-2 Trial. Blood. 2022 Nov 15;140(Supplement 1):7301–3.

149. Usmani SZ, Mielnik M, Byun JM, Alonso AA, Abdallah AOA, Garg M, et al. A phase 1 study of belantamab mafodotin in combination with standard of care in newly diagnosed multiple myeloma: An interim analysis of DREAMM-9. Journal of Clinical Oncology. 2023 Jun 1;41(16_suppl):8018–8018.

150. Weisel K, Hungria VT, Radinoff A, Delimpasi S, Mikala G, Masszi T, et al. A phase 3, open-label, randomized study to evaluate the efficacy and safety of single-agent belantamab mafodotin (belamaf) compared to pomalidomide plus low-dose dexamethasone (Pd) in patients (pts) with relapsed/refractory multiple myeloma

(RRMM): DREAMM-3. Journal of Clinical Oncology. 2023 Jun 1;41(16_suppl):8007–8007.

151. Moreau P, Garfall AL, van de Donk NWCJ, Nahi H, San-Miguel JF, Oriol A, et al. Teclistamab in Relapsed or Refractory Multiple Myeloma. New England Journal of Medicine [Internet]. 2022 Jun 5; Available from: http://www.nejm.org/doi/10.1056/NEJMoa2203478

152. Rodriguez-Otero P, Dholaria B, Askari E, Reece DE, van de Donk NWCJ, Chari A, et al. Subcutaneous Teclistamab in Combination with Daratumumab for the Treatment of Patients with Relapsed/Refractory Multiple Myeloma: Results from a Phase 1b Multicohort Study. Blood. 2021 Nov 5;138(Supplement 1):1647–1647.

153. Mateos MV, Bahlis NJ, Costa LJ, Perrot A, Pei L, Rubin ML, et al. MajesTEC-3: Randomized, phase 3 study of teclistamab plus daratumumab versus investigator's choice of daratumumab, pomalidomide, and dexamethasone or daratumumab, bortezomib, and dexamethasone in patients with relapsed/refractory multiple myeloma. Journal of Clinical Oncology. 2022 Jun 1;40(16_suppl):TPS8072–TPS8072.

154. Sebag M, Raje NS, Bahlis NJ, Costello C, Dholaria B, Solh M, et al. Elranatamab (PF-06863135), a B-Cell Maturation Antigen (BCMA) Targeted CD3-Engaging Bispecific Molecule, for Patients with Relapsed or Refractory Multiple Myeloma: Results from Magnetismm-1. Blood. 2021 Nov 5;138(Supplement 1):895–895.

155. Jakubowiak AJ, Bahlis NJ, Raje NS, Costello C, Dholaria BR, Solh MM, et al. Elranatamab, a BCMA-targeted T-cell redirecting immunotherapy, for patients with relapsed or refractory multiple myeloma: Updated results from MagnetisMM-1. Journal of Clinical Oncology. 2022 Jun 1;40(16_suppl):8014–8014.

156. Chari A, Touzeau C, Schinke C, Minnema MC, Berdeja J, Oriol A, et al. Talquetamab, a G Protein-Coupled Receptor Family C Group 5 Member D x CD3 Bispecific Antibody, in Patients with Relapsed/Refractory Multiple Myeloma (RRMM): Phase 1/2 Results from MonumenTAL-1. Blood. 2022 Nov 15;140(Supplement 1):384–7.

157. Cohen YC, Moreau P, Tolbert J, Qin X, Ma X, Vieyra D, et al. MonumenTAL-3: Phase 3 Trial of Talquetamab + Daratumumab ± Pomalidomide Versus Daratumumab + Pomalidomide + Dexamethasone in Relapsed/Refractory Multiple Myeloma Following ≥1 Prior Line of Therapy. Blood. 2022 Nov 15;140(Supplement 1):4418–9.

158. Bosch A, Frias Z. Radiotherapy in the treatment of multiple myeloma. International Journal of Radiation Oncology*Biology*Physics [Internet]. 1988;15(6):1363–9. Available from: https://www.sciencedirect.com/science/article/pii/0360301688902325

159. Cadet J, Ravanat JL, TavernaPorro M, Menoni H, Angelov D. Oxidatively generated complex DNA damage: Tandem and clustered lesions. Cancer Lett [Internet]. 2012 Dec;327(1–2):5–15. Available from: https://linkinghub.elsevier.com/retrieve/pii/S0304383512002534

160. Luedtke DA, Su Y, Liu S, Edwards H, Wang Y, Lin H, et al. Inhibition of XPO1 enhances cell death induced by ABT-199 in acute myeloid leukaemia via Mcl-1. J Cell Mol Med

[Internet]. 2018 Dec;22(12):6099–111. Available from: https://onlinelibrary.wiley.com/doi/10.1111/jcmm.13886

161. Gandhi UH, Senapedis W, Baloglu E, Unger TJ, Chari A, Vogl D, et al. Clinical Implications of Targeting XPO1-mediated Nuclear Export in Multiple Myeloma. Clin Lymphoma Myeloma Leuk [Internet]. 2018;18(5):335–45. Available from: https://www.sciencedirect.com/science/article/pii/S2152265017318815

162. Chari A, Vogl DT, Gavriatopoulou M, Nooka AK, Yee AJ, Huff CA, et al. Oral Selinexor–Dexamethasone for Triple-Class Refractory Multiple Myeloma. New England Journal of Medicine [Internet]. 2019 Aug 22;381(8):727–38. Available from: http://www.nejm.org/doi/10.1056/NEJMoa1903455

163. NICE TA796. Venetoclax for treating chronic lymphocytic leukaemia [Internet]. 2022 [cited 2022 Jul 26]. Available from: https://www.nice.org.uk/guidance/ta796/chapter/1-Recommendations

164. NICE TA765. Venetoclax with azacitidine for untreated acute myeloid leukaemia when intensive chemotherapy is unsuitable [Internet]. 2022 [cited 2022 Jul 26]. Available from: https://www.nice.org.uk/guidance/ta765

165. Greipp PR, Miguel JS, Durie BGM, Crowley JJ, Barlogie B, Bladé J, et al. International Staging System for Multiple Myeloma. Journal of Clinical Oncology [Internet]. 2005 May 20;23(15):3412–20. Available from: https://ascopubs.org/doi/10.1200/JCO.2005.04.242

166. Grundy M, Al-Kaisi F, Cull J, Williams C, Smith D, Seedhouse CH. A same-day assay predicts apoptotic response to combined BCL-2 and MCL-1 BH3-mimetic targeting in multiple myeloma cells. EJHaem [Internet]. 2021 Feb 20;2(1):40–7. Available from: https://onlinelibrary.wiley.com/doi/10.1002/jha2.133

167. Ostling O, Johanson KJ. Microelectrophoretic study of radiation-induced DNA damages in individual mammalian cells. Biochem Biophys Res Commun [Internet]. 1984 Aug;123(1):291–8. Available from: https://linkinghub.elsevier.com/retrieve/pii/0006291X8490411X

168. Fairbairn DW, Olive PL, O'Neill KL. The comet assay: a comprehensive review. Mutation Research/Reviews in Genetic Toxicology [Internet]. 1995 Feb;339(1):37–59. Available from: https://linkinghub.elsevier.com/retrieve/pii/0165111094000133

169. Collins AR. The Comet Assay for DNA Damage and Repair: Principles, Applications, and Limitations. Mol Biotechnol [Internet]. 2004;26(3):249–61. Available from: http://link.springer.com/10.1385/MB:26:3:249

170. Supiot S, Gouard S, Charrier J, Apostolidis C, Chatal JF, Barbet J, et al. Mechanisms of Cell Sensitization to α Radioimmunotherapy by Doxorubicin or Paclitaxel in Multiple Myeloma Cell Lines. Clinical Cancer Research [Internet]. 2005 Oct 1;11(19):7047s–52s. Available from: https://aacrjournals.org/clincancerres/article/11/19/7047s/190792/Mechanisms-of-Cell-Sensitization-to

171. Spanswick VJ, Craddock C, Sekhar M, Mahendra P, Shankaranarayana P, Hughes RG, et al. Repair of DNA interstrand crosslinks as a mechanism of clinical resistance to

melphalan in multiple myeloma. Blood [Internet]. 2002 Jul 1;100(1):224–9. Available from: https://ashpublications.org/blood/article/100/1/224/133970/Repair-of-DNA-interstrand-crosslinks-as-a

172. Turner JG, Dawson JL, Grant S, Shain KH, Dalton WS, Dai Y, et al. Treatment of acquired drug resistance in multiple myeloma by combination therapy with XPO1 and topoisomerase II inhibitors. J Hematol Oncol [Internet]. 2016 Dec 24;9(1):73. Available from: https://jhoonline.biomedcentral.com/articles/10.1186/s13045-016-0304-z

173. Kinner A, Wu W, Staudt C, Iliakis G. -H2AX in recognition and signaling of DNA double-strand breaks in the context of chromatin. Nucleic Acids Res [Internet]. 2008 Aug 21;36(17):5678–94. Available from: https://academic.oup.com/nar/article-lookup/doi/10.1093/nar/gkn550

174. Pilch DR, Sedelnikova OA, Redon C, Celeste A, Nussenzweig A, Bonner WM. Characteristics of γ-H2AX foci at DNA double-strand breaks sites. Biochemistry and Cell Biology [Internet]. 2003 Jun 1;81(3):123–9. Available from: http://www.nrcresearchpress.com/doi/10.1139/o03-042

175. Kiziltepe T, Hideshima T, Ishitsuka K, Ocio EM, Raje N, Catley L, et al. JS-K, a GST-activated nitric oxide generator, induces DNA double-strand breaks, activates DNA damage response pathways, and induces apoptosis in vitro and in vivo in human multiple myeloma cells. Blood [Internet]. 2007 Jul 15;110(2):709–18. Available from: https://ashpublications.org/blood/article/110/2/709/22953/JSK-a-GSTactivated-nitric-oxide-generator-induces

176. Ray A, Ravillah D, Das DS, Song Y, Nordström E, Gullbo J, et al. A novel alkylating agent Melflufen induces irreversible DNA damage and cytotoxicity in multiple myeloma cells. Br J Haematol [Internet]. 2016 Aug;174(3):397–409. Available from: https://onlinelibrary.wiley.com/doi/10.1111/bjh.14065

177. Clingen PH, Wu JYH, Miller J, Mistry N, Chin F, Wynne P, et al. Histone H2AX phosphorylation as a molecular pharmacological marker for DNA interstrand crosslink cancer chemotherapy. Biochem Pharmacol [Internet]. 2008 Jul;76(1):19–27. Available from: https://linkinghub.elsevier.com/retrieve/pii/S0006295208001986

178. Chou TC. Drug Combination Studies and Their Synergy Quantification Using the Chou-Talalay Method. Cancer Res [Internet]. 2010 Jan 15;70(2):440–6. Available from: https://aacrjournals.org/cancerres/article/70/2/440/559704/Drug-Combination-Studies-and-Their-Synergy

179. Liu Q, Yin X, Languino LR, Altieri DC. Evaluation of Drug Combination Effect Using a Bliss Independence Dose–Response Surface Model. Stat Biopharm Res. 2018 Apr 3;10(2):112–22.

180. Rampersad SN. Multiple Applications of Alamar Blue as an Indicator of Metabolic Function and Cellular Health in Cell Viability Bioassays. Sensors [Internet]. 2012 Sep 10;12(9):12347–60. Available from: http://www.mdpi.com/1424-8220/12/9/12347

181. Lonati L, Barbieri S, Guardamagna I, Ottolenghi A, Baiocco G. Radiation-induced cell cycle perturbations: a computational tool validated with flow-cytometry data. Sci Rep

[Internet]. 2021;11(1):925. Available from: https://doi.org/10.1038/s41598-020-79934-3

182. Santra MK, Wajapeyee N, Green MR. F-box protein FBXO31 mediates cyclin D1 degradation to induce G1 arrest after DNA damage. Nature [Internet]. 2009;459(7247):722–5. Available from: https://doi.org/10.1038/nature08011

183. Agami R, Bernards R. Distinct Initiation and Maintenance Mechanisms Cooperate to Induce G1 Cell Cycle Arrest in Response to DNA Damage. Cell [Internet]. 2000 Jul;102(1):55–66. Available from: https://linkinghub.elsevier.com/retrieve/pii/S0092867400000106

184. Araldi RP, de Melo TC, Mendes TB, de Sá Júnior PL, Nozima BHN, Ito ET, et al. Using the comet and micronucleus assays for genotoxicity studies: A review. Biomedicine & Pharmacotherapy [Internet]. 2015 May;72:74–82. Available from: https://linkinghub.elsevier.com/retrieve/pii/S0753332215000955

185. Olive PL, Banáth JP. The comet assay: a method to measure DNA damage in individual cells. Nat Protoc [Internet]. 2006;1(1):23–9. Available from: https://doi.org/10.1038/nprot.2006.5

186. Dolcet X, Llobet D, Pallares J, Matias-Guiu X. NF-kB in development and progression of human cancer. Virchows Archiv [Internet]. 2005;446(5):475–82. Available from: https://doi.org/10.1007/s00428-005-1264-9

187. Demchenko YN, Kuehl WM. A critical role for the NFkB pathway in multiple myeloma. Oncotarget [Internet]. 2010 May 31;1(1):59–68. Available from: https://www.oncotarget.com/lookup/doi/10.18632/oncotarget.109

188. Berenson JR, Ma HM, Vescio R. The role of nuclear factor-κb in the biology and treatment of multiple myeloma. Semin Oncol [Internet]. 2001;28(6):626–33. Available from: https://www.sciencedirect.com/science/article/pii/S0093775401900363

189. Ma MH, Yang HH, Parker K, Manyak S, Friedman JM, Altamirano C, et al. The Proteasome Inhibitor PS-341 Markedly Enhances Sensitivity of Multiple Myeloma Tumor Cells to Chemotherapeutic Agents1. Clinical Cancer Research. 2003 Mar 1;9(3):1136–44.

190. Gomez-Bougie P, Wuillème-Toumi S, Ménoret E, Trichet V, Robillard N, Philippe M, et al. Noxa Up-regulation and Mcl-1 Cleavage Are Associated to Apoptosis Induction by Bortezomib in Multiple Myeloma. Cancer Res [Internet]. 2007 Jun 1;67(11):5418–24. Available from: https://aacrjournals.org/cancerres/article/67/11/5418/533206/Noxa-Up-regulation-and-Mcl-1-Cleavage-Are

191. Qin JZ, Ziffra J, Stennett L, Bodner B, Bonish BK, Chaturvedi V, et al. Proteasome Inhibitors Trigger NOXA-Mediated Apoptosis in Melanoma and Myeloma Cells. Cancer Res [Internet]. 2005 Jul 15;65(14):6282–93. Available from: https://aacrjournals.org/cancerres/article/65/14/6282/518379/Proteasome-Inhibitors-Trigger-NOXA-Mediated

192. Rizzatti EG, Mora-Jensen H, Weniger MA, Gibellini F, Lee E, Daibata M, et al. Noxa mediates bortezomib induced apoptosis in both sensitive and intrinsically resistant

mantle cell lymphoma cells and this effect is independent of constitutive activity of the AKT and NF- kappa B pathways. Leuk Lymphoma [Internet]. 2008 Jan;49(4):798–808. Available from: http://www.tandfonline.com/doi/full/10.1080/10428190801910912

193. Ishii Y, Pirkmaier A, Alvarez J V., Frank DA, Keselman I, Logothetis D, et al. Cyclin D1 Overexpression and Response to Bortezomib Treatment in a Breast Cancer Model. JNCI: Journal of the National Cancer Institute [Internet]. 2006 Sep 6;98(17):1238–47. Available from: http://academic.oup.com/jnci/article/98/17/1238/2521761/Cyclin-D1-Overexpression-and-Response-to

194. An B, Goldfarb RH, Siman R, Dou QP. Novel dipeptidyl proteasome inhibitors overcome Bcl-2 protective function and selectively accumulate the cyclin-dependent kinase inhibitor p27 and induce apoptosis in transformed, but not normal, human fibroblasts. Cell Death Differ [Internet]. 1998;5(12):1062–75. Available from: https://doi.org/10.1038/sj.cdd.4400436

195. Lu G, Punj V, Chaudhary PM. Proteasome inhibitor Bortezomib induces cell-cycle arrest and apoptosis in cell lines derived from Ewing's sarcoma family of tumors and synergizes with TRAIL. Cancer Biol Ther [Internet]. 2008 Apr 27;7(4):603–8. Available from: http://www.tandfonline.com/doi/abs/10.4161/cbt.7.4.5564

196. Yang Z, Liu S, Zhu M, Zhang H, Wang J, Xu Q, et al. PS341 inhibits hepatocellular and colorectal cancer cells through the FOXO3/CTNNB1 signaling pathway. Sci Rep [Internet]. 2016;6(1):22090. Available from: https://doi.org/10.1038/srep22090

197. Goel A, Dispenzieri A, Greipp PR, Witzig TE, Mesa RA, Russell SJ. PS-341–mediated selective targeting of multiple myeloma cells by synergistic increase in ionizing radiation-induced apoptosis. Exp Hematol [Internet]. 2005 Jul;33(7):784–95. Available from: https://linkinghub.elsevier.com/retrieve/pii/S0301472X05001827

198. Russo SM, Tepper JE, Baldwin AS, Liu R, Adams J, Elliott P, et al. Enhancement of radiosensitivity by proteasome inhibition: Implications for a role of NF-κB. International Journal of Radiation Oncology*Biology*Physics [Internet]. 2001 May;50(1):183–93. Available from: https://linkinghub.elsevier.com/retrieve/pii/S0360301601014468

199. Kuroda Y, Sakai A, Tsuyama N, Katayama Y, Munemasa S, Okikawa Y, et al. Cyclin D1 Overexpression Increases Chemosensitivity Via Prolonged S-Phase and TRAIL Signal in Myeloma Cell. Blood [Internet]. 2007 Nov 16;110(11):3530–3530. Available from: https://ashpublications.org/blood/article/110/11/3530/75370/Cyclin-D1-Overexpression-Increases

200. Hideshima T, Richardson PG, Anderson KC. Mechanism of Action of Proteasome Inhibitors and Deacetylase Inhibitors and the Biological Basis of Synergy in Multiple Myeloma. Mol Cancer Ther [Internet]. 2011 Nov 1;10(11):2034–42. Available from: https://aacrjournals.org/mct/article/10/11/2034/91057/Mechanism-of-Action-of-Proteasome-Inhibitors-and

201. Thanh-Truc Ngo B, Felthaus J, Hein M, Follo M, Wider D, Ihorst G, et al. Monitoring bortezomib therapy in multiple myeloma: screening of cyclin D1, D2, and D3 via reliable real-time polymerase chain reaction and association with clinico-pathological

features and outcome. Leuk Lymphoma [Internet]. 2010 Sep 25;51(9):1632–42. Available from: http://www.tandfonline.com/doi/full/10.3109/10428194.2010.496014

202. Dhodapkar M V., Abe E, Theus A, Lacy M, Langford JK, Barlogie B, et al. Syndecan-1 Is a Multifunctional Regulator of Myeloma Pathobiology: Control of Tumor Cell Survival, Growth, and Bone Cell Differentiation. Blood [Internet]. 1998 Apr 15;91(8):2679–88. Available from: https://ashpublications.org/blood/article/91/8/2679/107643/Syndecan1-Is-a-Multifunctional-Regulator-of

203. Bustany S, Cahu J, Guardiola P, Sola B. Cyclin D1 sensitizes myeloma cells to endoplasmic reticulum stress-mediated apoptosis by activating the unfolded protein response pathway. BMC Cancer [Internet]. 2015 Dec 11;15(1):262. Available from: https://bmccancer.biomedcentral.com/articles/10.1186/s12885-015-1240-y

204. Carneiro BA, El-Deiry WS. Targeting apoptosis in cancer therapy. Nat Rev Clin Oncol [Internet]. 2020;17(7):395–417. Available from: https://doi.org/10.1038/s41571-020-0341-y

205. Singh R, Letai A, Sarosiek K. Regulation of apoptosis in health and disease: the balancing act of BCL-2 family proteins. Nat Rev Mol Cell Biol [Internet]. 2019;20(3):175–93. Available from: https://doi.org/10.1038/s41580-018-0089-8

206. Grundy M, Seedhouse C, Jones T, Elmi L, Hall M, Graham A, et al. Predicting effective pro-apoptotic anti-leukaemic drug combinations using co-operative dynamic BH3 profiling. Gartel AL, editor. PLoS One [Internet]. 2018 Jan 3;13(1):e0190682. Available from: https://dx.plos.org/10.1371/journal.pone.0190682

207. Derenne S, Monia B, Dean NM, Taylor JK, Rapp MJ, Harousseau JL, et al. Antisense strategy shows that Mcl-1 rather than Bcl-2 or Bcl-xL is an essential survival protein of human myeloma cells. Blood [Internet]. 2002 Jul 1;100(1):194–9. Available from: https://ashpublications.org/blood/article/100/1/194/133985/Antisense-strategy-shows-that-Mcl1-rather-than

208. Wei AH, Roberts AW, Spencer A, Rosenberg AS, Siegel D, Walter RB, et al. Targeting MCL-1 in hematologic malignancies: Rationale and progress. Blood Rev [Internet]. 2020 Nov;44:100672. Available from: https://linkinghub.elsevier.com/retrieve/pii/S0268960X20300229

209. Seiller C, Maiga S, Touzeau C, Bellanger C, Kervoëlen C, Descamps G, et al. Dual targeting of BCL2 and MCL1 rescues myeloma cells resistant to BCL2 and MCL1 inhibitors associated with the formation of BAX/BAK hetero-complexes. Cell Death Dis [Internet]. 2020;11(5):316. Available from: https://doi.org/10.1038/s41419-020-2505-1

210. Algarín EM, Díaz-Tejedor A, Mogollón P, Hernández-García S, Corchete LA, San-Segundo L, et al. Preclinical evaluation of the simultaneous inhibition of MCL-1 and BCL-2 with the combination of S63845 and venetoclax in multiple myeloma. Haematologica [Internet]. 2020 Mar;105(3):e116–20. Available from: http://www.haematologica.org/lookup/doi/10.3324/haematol.2018.212308

211. Ashkenazi A, Fairbrother WJ, Leverson JD, Souers AJ. From basic apoptosis discoveries to advanced selective BCL-2 family inhibitors. Nat Rev Drug Discov [Internet]. 2017;16(4):273–84. Available from: https://doi.org/10.1038/nrd.2016.253

212. Kotschy A, Szlavik Z, Murray J, Davidson J, Maragno AL, Le Toumelin-Braizat G, et al. The MCL1 inhibitor S63845 is tolerable and effective in diverse cancer models. Nature [Internet]. 2016;538(7626):477–82. Available from: https://doi.org/10.1038/nature19830

213. Wang X, Bathina M, Lynch J, Koss B, Calabrese C, Frase S, et al. Deletion of MCL-1 causes lethal cardiac failure and mitochondrial dysfunction. Genes Dev [Internet]. 2013 Jun 15;27(12):1351–64. Available from: http://genesdev.cshlp.org/lookup/doi/10.1101/gad.215855.113

214. Cleynen A, Samur M, Perrot A, Buisson L, Maheo S, Fulciniti M, et al. Variable BCL2/BCL2L1 ratio in multiple myeloma with t(11;14). Blood [Internet]. 2018 Dec 27;132(26):2778–80. Available from: https://ashpublications.org/blood/article/132/26/2778/39677/Variable-BCL2BCL2L1-ratio-in-multiple-myeloma-with

215. Kitadate A, Terao T, Narita K, Ikeda S, Takahashi Y, Tsushima T, et al. Multiple myeloma with t(11;14)-associated immature phenotype has lower CD38 expression and higher BCL2 dependence. Cancer Sci [Internet]. 2021 Sep 29;112(9):3645–54. Available from: https://onlinelibrary.wiley.com/doi/10.1111/cas.15073

216. Gomez-Bougie P, Maiga S, Tessoulin B, Bourcier J, Bonnet A, Rodriguez MS, et al. BH3-mimetic toolkit guides the respective use of BCL2 and MCL1 BH3-mimetics in myeloma treatment. Blood [Internet]. 2018 Dec 20;132(25):2656–69. Available from: https://ashpublications.org/blood/article/132/25/2656/39594/BH3mimetic-toolkit-guides-the-respective-use-of

217. Koehler BC, Scherr AL, Lorenz S, Elssner C, Kautz N, Welte S, et al. Pan-Bcl-2 Inhibitor Obatoclax Delays Cell Cycle Progression and Blocks Migration of Colorectal Cancer Cells. Gartel AL, editor. PLoS One [Internet]. 2014 Sep 5;9(9):e106571. Available from: https://dx.plos.org/10.1371/journal.pone.0106571

218. Or CH, Chang Y, Lin WC, Lee WC, Su HL, Cheung MW, et al. Obatoclax, a Pan-BCL-2 Inhibitor, Targets Cyclin D1 for Degradation to Induce Antiproliferation in Human Colorectal Carcinoma Cells. Int J Mol Sci [Internet]. 2016 Dec 27;18(1):44. Available from: http://www.mdpi.com/1422-0067/18/1/44

219. Ashimori N, Zeitlin BD, Zhang Z, Warner K, Turkienicz IM, Spalding AC, et al. TW-37, a small-molecule inhibitor of Bcl-2, mediates S-phase cell cycle arrest and suppresses head and neck tumor angiogenesis. Mol Cancer Ther [Internet]. 2009 Apr 1;8(4):893–903. Available from: https://aacrjournals.org/mct/article/8/4/893/93456/TW-37-a-small-molecule-inhibitor-of-Bcl-2-mediates

220. Tucker CA, Kapanen AI, Chikh G, Hoffman BG, Kyle AH, Wilson IM, et al. Silencing Bcl-2 in models of mantle cell lymphoma is associated with decreases in cyclin D1, nuclear factor-κB, p53, bax, and p27 levels. Mol Cancer Ther [Internet]. 2008 Apr 1;7(4):749–58. Available from:

https://aacrjournals.org/mct/article/7/4/749/93116/Silencing-Bcl-2-in-models-of-mantle-cell-lymphoma

221. Hao P, Yu J, Ward R, Liu Y, Hao Q, An S, et al. Eukaryotic translation initiation factors as promising targets in cancer therapy. Cell Communication and Signaling [Internet]. 2020;18(1):175. Available from: https://doi.org/10.1186/s12964-020-00607-9

222. Jia Y, Polunovsky V, Bitterman PB, Wagner CR. Cap-Dependent Translation Initiation Factor eIF4E: An Emerging Anticancer Drug Target. Med Res Rev [Internet]. 2012 Jul;32(4):786–814. Available from: https://onlinelibrary.wiley.com/doi/10.1002/med.21260

223. LÓPEZ-LASTRA M, RIVAS A, BARRÍA MI. Protein synthesis in eukaryotes: The growing biological relevance of cap-independent translation initiation. Biol Res [Internet]. 2005;38(2–3). Available from: http://www.scielo.cl/scielo.php?script=sci_arttext&pid=S0716-97602005000200003&lng=en&nrm=iso&tlng=en

224. Sharma DK, Bressler K, Patel H, Balasingam N, Thakor N. Role of Eukaryotic Initiation Factors during Cellular Stress and Cancer Progression. Himeno H, editor. J Nucleic Acids [Internet]. 2016;2016:8235121. Available from: https://doi.org/10.1155/2016/8235121

225. Baird TD, Wek RC. Eukaryotic Initiation Factor 2 Phosphorylation and Translational Control in Metabolism. Advances in Nutrition [Internet]. 2012 May 1;3(3):307–21. Available from: https://academic.oup.com/advances/article/3/3/307/4591529

226. Brewer JW, Hendershot LM, Sherr CJ, Diehl JA. Mammalian unfolded protein response inhibits cyclin D1 translation and cell-cycle progression. Proceedings of the National Academy of Sciences [Internet]. 1999 Jul 20;96(15):8505–10. Available from: https://pnas.org/doi/full/10.1073/pnas.96.15.8505

227. Schewe DM, Aguirre-Ghiso JA. Inhibition of eIF2α Dephosphorylation Maximizes Bortezomib Efficiency and Eliminates Quiescent Multiple Myeloma Cells Surviving Proteasome Inhibitor Therapy. Cancer Res [Internet]. 2009 Feb 15;69(4):1545–52. Available from: https://aacrjournals.org/cancerres/article/69/4/1545/552759/Inhibition-of-eIF2-Dephosphorylation-Maximizes

228. Burwick N, Zhang MY, de la Puente P, Azab AK, Hyun TS, Ruiz-Gutierrez M, et al. The eIF2-alpha kinase HRI is a novel therapeutic target in multiple myeloma. Leuk Res [Internet]. 2017 Apr;55:23–32. Available from: https://linkinghub.elsevier.com/retrieve/pii/S0145212617300061

229. Dytfeld D, Rosebeck S, Kandarpa M, Mayampurath A, Mellacheruvu D, Alonge MM, et al. Proteomic profiling of naïve multiple myeloma patient plasma cells identifies pathways associated with favourable response to bortezomib-based treatment regimens. Br J Haematol [Internet]. 2015 Jul;170(1):66–79. Available from: https://onlinelibrary.wiley.com/doi/10.1111/bjh.13394

230. Guo L, Chi Y, Xue J, Ma L, Shao Z, Wu J. Phosphorylated eIF2α predicts disease-free survival in triple-negative breast cancer patients. Sci Rep [Internet]. 2017;7(1):44674. Available from: https://doi.org/10.1038/srep44674

231. Burwick N, Delrow JJ, Shimamura A. Translational Profiling Reveals The eIF2 Kinase Pathway As a Mediator Of Dexamethasone Induced Apoptosis In Multiple Myeloma. Blood [Internet]. 2013 Nov 15;122(21):3104–3104. Available from: https://ashpublications.org/blood/article/122/21/3104/11725/Translational-Profiling-Reveals-The-eIF2-Kinase

232. Topisirovic I, Guzman ML, McConnell MJ, Licht JD, Culjkovic B, Neering SJ, et al. Aberrant Eukaryotic Translation Initiation Factor 4E-Dependent mRNA Transport Impedes Hematopoietic Differentiation and Contributes to Leukemogenesis. Mol Cell Biol [Internet]. 2003 Dec 15;23(24):8992–9002. Available from: https://journals.asm.org/doi/10.1128/MCB.23.24.8992-9002.2003

233. Yang S, Hewitt S, Steinberg S, Liewehr D, Swain S. Expression levels of eIF4E, VEGF, and cyclin D1, and correlation of eIF4E with VEGF and cyclin D1 in multi-tumor tissue microarray. Oncol Rep [Internet]. 2007 Feb 1; Available from: http://www.spandidos-publications.com/10.3892/or.17.2.281

234. Oridate N, Kim HJ, Xu X, Lotan R. Growth inhibition of head and neck squamous carcinoma cells by small interfering RNAs targeting eIF4E or cyclin D1 alone or combined with cisplatin. Cancer Biol Ther [Internet]. 2005 Mar 27;4(3):318–23. Available from: http://www.tandfonline.com/doi/abs/10.4161/cbt.4.3.1504

235. Culjkovic B, Topisirovic I, Skrabanek L, Ruiz-Gutierrez M, Borden KLB. eIF4E promotes nuclear export of cyclin D1 mRNAs via an element in the 3'UTR. Journal of Cell Biology [Internet]. 2005 Apr 25;169(2):245–56. Available from: https://rupress.org/jcb/article/169/2/245/51714/eIF4E-promotes-nuclear-export-of-cyclin-D1-mRNAs

236. Qin L, Guo J, Zheng Q, Zhang H. BAG2 structure, function and involvement in disease. Cell Mol Biol Lett [Internet]. 2016 Dec 20;21(1):18. Available from: http://cmbl.biomedcentral.com/articles/10.1186/s11658-016-0020-2

237. Zhang J, Lou X, Yang S, He S, Yang L, Liu M, et al. BAG2 is a target of the c-Myc gene and is involved in cellular senescence via the p21CIP1 pathway. Cancer Lett [Internet]. 2012 May;318(1):34–41. Available from: https://linkinghub.elsevier.com/retrieve/pii/S0304383511007348

238. Hong YC, Wang Z, Peng B, Xia LG, Lin LW, Xu ZL. BAG2 overexpression correlates with growth and poor prognosis of esophageal squamous cell carcinoma. Open Life Sci [Internet]. 2018 Dec 31;13(1):582–8. Available from: https://www.degruyter.com/document/doi/10.1515/biol-2018-0069/html

239. Zhang X, Zhang J, Liu Y, Li J, Tan J, Song Z. Bcl-2 Associated Athanogene 2 (BAG2) is Associated With Progression and Prognosis of Hepatocellular Carcinoma: A Bioinformatics-Based Analysis. Pathology and Oncology Research [Internet]. 2021 Apr 1;27. Available from: https://www.por-journal.com/articles/10.3389/pore.2021.594649/full

240. Wang F, Wang F, Zhang S, Xu X. MicroRNA-325 inhibits the proliferation and induces the apoptosis of T cell acute lymphoblastic leukemia cells in a BAG2-dependent manner. Exp Ther Med [Internet]. 2021 Apr 15;21(6):631. Available from: http://www.spandidos-publications.com/10.3892/etm.2021.10063

241. Vincenz L, Jäger R, O'Dwyer M, Samali A. Endoplasmic Reticulum Stress and the Unfolded Protein Response: Targeting the Achilles Heel of Multiple Myeloma. Mol Cancer Ther [Internet]. 2013 Jun 1;12(6):831–43. Available from: https://aacrjournals.org/mct/article/12/6/831/91696/Endoplasmic-Reticulum-Stress-and-the-Unfolded

242. Huang L, Wang Y, Bai J, Yang Y, Wang F, Feng Y, et al. Blockade of HSP70 by VER-155008 synergistically enhances bortezomib-induced cytotoxicity in multiple myeloma. Cell Stress Chaperones [Internet]. 2020;25(2):357–67. Available from: https://doi.org/10.1007/s12192-020-01078-0

243. Stankiewicz AR, Livingstone AM, Mohseni N, Mosser DD. Regulation of heat-induced apoptosis by Mcl-1 degradation and its inhibition by Hsp70. Cell Death Differ [Internet]. 2009;16(4):638–47. Available from: https://doi.org/10.1038/cdd.2008.189

244. Hu J, Dang N, Menu E, De Bryune E, Xu D, Van Camp B, et al. Activation of ATF4 mediates unwanted Mcl-1 accumulation by proteasome inhibition. Blood [Internet]. 2012 Jan 19;119(3):826–37. Available from: https://ashpublications.org/blood/article/119/3/826/135127/Activation-of-ATF4-mediates-unwanted-Mcl1

245. Aichem A, Groettrup M. The ubiquitin-like modifier FAT10 in cancer development. Int J Biochem Cell Biol [Internet]. 2016 Oct;79:451–61. Available from: https://linkinghub.elsevier.com/retrieve/pii/S1357272516301650

246. Hipp MS, Kalveram B, Raasi S, Groettrup M, Schmidtke G. FAT10, a Ubiquitin-Independent Signal for Proteasomal Degradation. Mol Cell Biol [Internet]. 2005 May;25(9):3483–91. Available from: https://journals.asm.org/doi/10.1128/MCB.25.9.3483-3491.2005

247. Gong P, Canaan A, Wang B, Leventhal J, Snyder A, Nair V, et al. The Ubiquitin-Like Protein FAT10 Mediates NF-κB Activation. Journal of the American Society of Nephrology [Internet]. 2010 Feb;21(2):316–26. Available from: https://jasn.asnjournals.org/lookup/doi/10.1681/ASN.2009050479

248. Choi Y, Kim JK, Yoo JY. NFκB and STAT3 synergistically activate the expression of FAT10, a gene counteracting the tumor suppressor p53. Mol Oncol [Internet]. 2014 May;8(3):642–55. Available from: http://doi.wiley.com/10.1016/j.molonc.2014.01.007

249. Zhang DW, Jeang KT, Lee CGL. p53 negatively regulates the expression of FAT10, a gene upregulated in various cancers. Oncogene [Internet]. 2006;25(16):2318–27. Available from: https://doi.org/10.1038/sj.onc.1209220

250. Feng Y, Chen X, Cassady K, Zou Z, Yang S, Wang Z, et al. The Role of mTOR Inhibitors in Hematologic Disease: From Bench to Bedside. Front Oncol [Internet]. 2021 Jan

8;10. Available from: https://www.frontiersin.org/articles/10.3389/fonc.2020.611690/full

251. Strömberg T, Dimberg A, Hammarberg A, Carlson K, Österborg A, Nilsson K, et al. Rapamycin sensitizes multiple myeloma cells to apoptosis induced by dexamethasone. Blood [Internet]. 2004 Apr 15;103(8):3138–47. Available from: https://ashpublications.org/blood/article/103/8/3138/18040/Rapamycin-sensitizes-multiple-myeloma-cells-to

252. Yan H, Frost P, Shi Y, Hoang B, Sharma S, Fisher M, et al. Mechanism by Which Mammalian Target of Rapamycin Inhibitors Sensitize Multiple Myeloma Cells to Dexamethasone-Induced Apoptosis. Cancer Res [Internet]. 2006 Feb 15;66(4):2305–13. Available from: https://aacrjournals.org/cancerres/article/66/4/2305/526649/Mechanism-by-Which-Mammalian-Target-of-Rapamycin

253. Peterson TR, Laplante M, Thoreen CC, Sancak Y, Kang SA, Kuehl WM, et al. DEPTOR Is an mTOR Inhibitor Frequently Overexpressed in Multiple Myeloma Cells and Required for Their Survival. Cell [Internet]. 2009 May;137(5):873–86. Available from: https://linkinghub.elsevier.com/retrieve/pii/S0092867409003894

254. Duffy MJ, O'Grady S, Tang M, Crown J. MYC as a target for cancer treatment. Cancer Treat Rev [Internet]. 2021 Mar;94:102154. Available from: https://linkinghub.elsevier.com/retrieve/pii/S0305737221000025

255. Dang C V. MYC on the Path to Cancer. Cell [Internet]. 2012 Mar;149(1):22–35. Available from: https://linkinghub.elsevier.com/retrieve/pii/S0092867412002966

256. Swerdlow S, Campo E, Harris N, Jaffe E, Pileri S, Stein H, et al. WHO Classification of Tumours of Haematopoietic and Lymphoid Tissues. 4th ed. 2015.

257. Chng WJ, Huang GF, Chung TH, Ng SB, Gonzalez-Paz N, Troska-Price T, et al. Clinical and biological implications of MYC activation: a common difference between MGUS and newly diagnosed multiple myeloma. Leukemia [Internet]. 2011 Jun 5;25(6):1026–35. Available from: https://www.nature.com/articles/leu201153

258. Franssen LE, Nijhof IS, Couto S, Levin MD, Bos GMJ, Broijl A, et al. Cereblon loss and up-regulation of c-Myc are associated with lenalidomide resistance in multiple myeloma patients. Haematologica [Internet]. 2018 Aug;103(8):e368–71. Available from: http://www.haematologica.org/lookup/doi/10.3324/haematol.2017.186601

259. Szabo AG, Gang AO, Pedersen MØ, Poulsen TS, Klausen TW, Nørgaard P. Overexpression of c-myc is associated with adverse clinical features and worse overall survival in multiple myeloma. Leuk Lymphoma [Internet]. 2016 Nov 31;57(11):2526–34. Available from: https://www.tandfonline.com/doi/full/10.1080/10428194.2016.1187275

260. Mura M, Hopkins TG, Michael T, Abd-Latip N, Weir J, Aboagye E, et al. LARP1 post-transcriptionally regulates mTOR and contributes to cancer progression. Oncogene [Internet]. 2015;34(39):5025–36. Available from: https://doi.org/10.1038/onc.2014.428

261. Hopkins TG, Mura M, Al-Ashtal HA, Lahr RM, Abd-Latip N, Sweeney K, et al. The RNA-binding protein LARP1 is a post-transcriptional regulator of survival and tumorigenesis in ovarian cancer. Nucleic Acids Res [Internet]. 2016 Feb 18;44(3):1227–46. Available from: https://academic.oup.com/nar/article-lookup/doi/10.1093/nar/gkv1515

262. Ye L, Lin S tao, Mi Y shuai, Liu Y, Ma Y, Sun H min, et al. Overexpression of LARP1 predicts poor prognosis of colorectal cancer and is expected to be a potential therapeutic target. Tumor Biology [Internet]. 2016;37(11):14585–94. Available from: https://doi.org/10.1007/s13277-016-5332-3

263. Xu Z, Xu J, Lu H, Lin B, Cai S, Guo J, et al. LARP1 is regulated by the XIST/miR-374a axis and functions as an oncogene in non-small cell lung carcinoma. Oncol Rep [Internet]. 2017 Oct 17; Available from: http://www.spandidos-publications.com/10.3892/or.2017.6040

264. Fonseca BD, Zakaria C, Jia JJ, Graber TE, Svitkin Y, Tahmasebi S, et al. La-related Protein 1 (LARP1) Represses Terminal Oligopyrimidine (TOP) mRNA Translation Downstream of mTOR Complex 1 (mTORC1). Journal of Biological Chemistry [Internet]. 2015 Jun;290(26):15996–6020. Available from: https://linkinghub.elsevier.com/retrieve/pii/S0021925820584330

265. Park S, Sim H, Lee K. Rapamycin-resistant and torin-sensitive mTOR signaling promotes the survival and proliferation of leukemic cells. BMB Rep [Internet]. 2016 Jan 31;49(1):63–8. Available from: http://koreascience.or.kr/journal/view.jsp?kj=E1MBB7&py=2016&vnc=v49n1&sp=63

266. Liu Q, Wang J, Kang SA, Thoreen CC, Hur W, Ahmed T, et al. Discovery of 9-(6-Aminopyridin-3-yl)-1-(3-(trifluoromethyl)phenyl)benzo[h][1,6]naphthyridin-2(1 H)-one (Torin2) as a Potent, Selective, and Orally Available Mammalian Target of Rapamycin (mTOR) Inhibitor for Treatment of Cancer. J Med Chem [Internet]. 2011 Mar 10;54(5):1473–80. Available from: https://pubs.acs.org/doi/10.1021/jm101520v

267. Simioni C, Cani A, Martelli AM, Zauli G, Tabellini G, McCubrey J, et al. Activity of the novel mTOR inhibitor Torin-2 in B-precursor acute lymphoblastic leukemia and its therapeutic potential to prevent Akt reactivation. Oncotarget [Internet]. 2014 Oct 30;5(20):10034–47. Available from: https://www.oncotarget.com/lookup/doi/10.18632/oncotarget.2490

268. Maiso P, Liu Y, Morgan B, Azab AK, Ren P, Martin MB, et al. Defining the role of TORC1/2 in multiple myeloma. Blood [Internet]. 2011 Dec 22;118(26):6860–70. Available from: https://ashpublications.org/blood/article/118/26/6860/29425/Defining-the-role-of-TORC12-in-multiple-myeloma

269. Longley DB, Harkin DP, Johnston PG. 5-Fluorouracil: mechanisms of action and clinical strategies. Nat Rev Cancer [Internet]. 2003;3(5):330–8. Available from: https://doi.org/10.1038/nrc1074

270. Vousden KH, Lu X. Live or let die: the cell's response to p53. Nat Rev Cancer [Internet]. 2002;2(8):594–604. Available from: https://doi.org/10.1038/nrc864

271. Ma Y, Zhang J, Wen L, Lin A. Membrane-lipid associated lncRNA: A new regulator in cancer signaling. Cancer Lett [Internet]. 2018 Apr;419:27–9. Available from: https://linkinghub.elsevier.com/retrieve/pii/S0304383518300302

272. Paraskevopoulou MD, Hatzigeorgiou AG. Analyzing MiRNA–LncRNA Interactions. In 2016. p. 271–86. Available from: http://link.springer.com/10.1007/978-1-4939-3378-5_21

273. Srikantan V, Zou Z, Petrovics G, Xu L, Augustus M, Davis L, et al. PCGEM1 , a prostate-specific gene, is overexpressed in prostate cancer. Proceedings of the National Academy of Sciences [Internet]. 2000 Oct 24;97(22):12216–21. Available from: https://pnas.org/doi/full/10.1073/pnas.97.22.12216

274. Liu H, He X, Li T, Qu Y, Xu L, Hou Y, et al. PCGEM1 promotes proliferation, migration and invasion in prostate cancer by sponging miR-506 to upregulate TRIAP1. BMC Urol [Internet]. 2022;22(1):14. Available from: https://doi.org/10.1186/s12894-022-00969-x

275. Liu C, Li H, Chu F, Zhou X, Xie R, Wei Q, et al. Long non-coding RNAs: Key regulators involved in metabolic reprogramming in cancer (Review). Oncol Rep [Internet]. 2021 Mar 8;45(5):54. Available from: http://www.spandidos-publications.com/10.3892/or.2021.8005

276. Wu Y, Wang H. LncRNA NEAT1 promotes dexamethasone resistance in multiple myeloma by targeting miR-193a/MCL1 pathway. J Biochem Mol Toxicol [Internet]. 2018 Jan;32(1):e22008. Available from: https://onlinelibrary.wiley.com/doi/10.1002/jbt.22008

277. Li Y, Wang X. The role of cullin4B in human cancers. Exp Hematol Oncol [Internet]. 2017;6(1):17. Available from: https://doi.org/10.1186/s40164-017-0077-2

278. Duan P jing, Zhao J hong, Xie L li. Cul4B promotes the progression of ovarian cancer by upregulating the expression of CDK2 and CyclinD1. J Ovarian Res [Internet]. 2020;13(1):76. Available from: https://doi.org/10.1186/s13048-020-00677-w

279. Wang S, Li Z, Gao S. Key regulators of sensitivity to immunomodulatory drugs in cancer treatment. Biomark Res [Internet]. 2021;9(1):43. Available from: https://doi.org/10.1186/s40364-021-00297-6

280. Hastings ML, Allemand E, Duelli DM, Myers MP, Krainer AR. Control of Pre-mRNA Splicing by the General Splicing Factors PUF60 and U2AF65. Valcarcel J, editor. PLoS One [Internet]. 2007 Jun 20;2(6):e538. Available from: https://dx.plos.org/10.1371/journal.pone.0000538

281. Long Q, Hua Y, He L, Zhang C, Sui S, Li Y, et al. Poly(U) binding splicing factor 60 promotes renal cell carcinoma growth by transcriptionally upregulating telomerase reverse transcriptase. Int J Biol Sci [Internet]. 2020;16(15):3002–17. Available from: http://www.ncbi.nlm.nih.gov/pubmed/33061812

282. Rahmutulla B, Matsushita K, Satoh M, Seimiya M, Tsuchida S, Kubo S, et al. Alternative splicing of FBP-interacting repressor coordinates c-Myc, P27Kip1/cyclinE and Ku86/XRCC5 expression as a molecular sensor for bleomycin-induced DNA

damage pathway. Oncotarget [Internet]. 2014 May 15;5(9):2404–17. Available from: https://www.oncotarget.com/lookup/doi/10.18632/oncotarget.1650

283. Matsushita K, Kitamura K, Rahmutulla B, Tanaka N, Ishige T, Satoh M, et al. Haploinsufficiency of the c-myc transcriptional repressor FIR, as a dominant negative-alternative splicing model, promoted p53-dependent T-cell acute lymphoblastic leukemia progression by activating Notch1. Oncotarget [Internet]. 2015 Mar 10;6(7):5102–17. Available from: http://www.ncbi.nlm.nih.gov/pubmed/25671302

284. Kobayashi S, Hoshino T, Hiwasa T, Satoh M, Rahmutulla B, Tsuchida S, et al. Anti-FIRs (PUF60) auto-antibodies are detected in the sera of early-stage colon cancer patients. Oncotarget [Internet]. 2016 Dec 13;7(50):82493–503. Available from: https://www.oncotarget.com/lookup/doi/10.18632/oncotarget.12696

285. Nawijn MC, Alendar A, Berns A. For better or for worse: the role of Pim oncogenes in tumorigenesis. Nat Rev Cancer [Internet]. 2011;11(1):23–34. Available from: https://doi.org/10.1038/nrc2986

286. Claudio JO, Masih-Khan E, Tang H, Gonçalves J, Voralia M, Li ZH, et al. A molecular compendium of genes expressed in multiple myeloma. Blood [Internet]. 2002 Sep 15;100(6):2175–86. Available from: https://ashpublications.org/blood/article/100/6/2175/16467/A-molecular-compendium-of-genes-expressed-in

287. Zhang Y, Wang Z, Li X, Magnuson NS. Pim kinase-dependent inhibition of c-Myc degradation. Oncogene [Internet]. 2008;27(35):4809–19. Available from: https://doi.org/10.1038/onc.2008.123

288. Fox CJ, Hammerman PS, Cinalli RM, Master SR, Chodosh LA, Thompson CB. The serine/threonine kinase Pim-2 is a transcriptionally regulated apoptotic inhibitor. Genes Dev [Internet]. 2003 Aug 1;17(15):1841–54. Available from: http://genesdev.cshlp.org/lookup/doi/10.1101/gad.1105003

289. Cervantes-Gomez F, Chen LS, Orlowski RZ, Gandhi V. Biological Effects of the Pim Kinase Inhibitor, SGI-1776, in Multiple Myeloma. Clin Lymphoma Myeloma Leuk [Internet]. 2013 Sep;13:S317–29. Available from: https://linkinghub.elsevier.com/retrieve/pii/S215226501300236X

290. Astex Pharmaceuticals. A Phase 1, Multicenter, Open-label, Dose-escalation Study of SGI-1776, a PIM Kinase Inhibitor, in Subjects With Relapsed/Refractory Leukemias [Internet]. [cited 2022 Aug 6]. Available from: https://clinicaltrials.gov/ct2/show/NCT01239108

291. Santo L, Ramachandran J, Cirstea DD, Eda H, Nemani N, Hideshima T, et al. Effect of the Pan-PIM Kinase Inhibitor, AZD1208, Alone and in Combination with Bortezomib in Multiple Myeloma. Blood [Internet]. 2014 Dec 6;124(21):5726–5726. Available from: https://ashpublications.org/blood/article/124/21/5726/101128/Effect-of-the-PanPIM-Kinase-Inhibitor-AZD1208

292. Keeton EK, McEachern K, Dillman KS, Palakurthi S, Cao Y, Grondine MR, et al. AZD1208, a potent and selective pan-Pim kinase inhibitor, demonstrates efficacy in preclinical models of acute myeloid leukemia. Blood [Internet]. 2014 Feb

6;123(6):905–13. Available from: https://ashpublications.org/blood/article/123/6/905/32601/AZD1208-a-potent-and-selective-panPim-kinase

293. Cortes J, Tamura K, DeAngelo DJ, de Bono J, Lorente D, Minden M, et al. Phase I studies of AZD1208, a proviral integration Moloney virus kinase inhibitor in solid and haematological cancers. Br J Cancer [Internet]. 2018;118(11):1425–33. Available from: https://doi.org/10.1038/s41416-018-0082-1

294. Lombardi L, Poretti G, Mattioli M, Fabris S, Agnelli L, Bicciato S, et al. Molecular characterization of human multiple myeloma cell lines by integrative genomics: Insights into the biology of the disease. Genes Chromosomes Cancer. 2007 Mar 14;46(3):226–38.

295. Ogden C. Discovering a predictive biomarker of venetoclax sensitivity and resistance in Multiple Myeloma. Nottingham University; 2000.